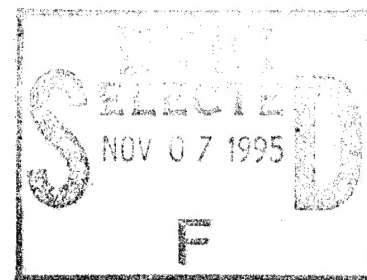
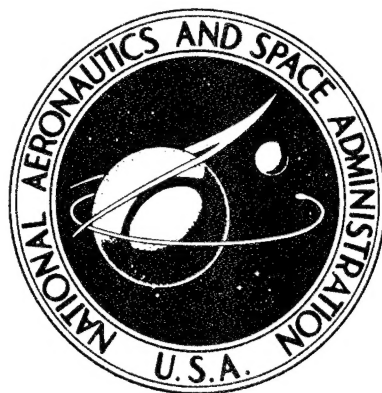


ADD 441254

NASA CR-132645



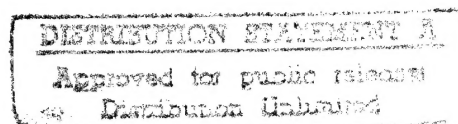
# BORON/ALUMINUM SKINS FOR THE DC-10 AFT PYLON

FINAL REPORT

by

S. Y. ELLIOTT

19951102 002



Prepared Under Contract NAS1 13029

McDonnell Douglas Corporation  
Douglas Aircraft Company  
3855 Lakewood Blvd  
Long Beach, California 90846

May 1975

for

Langley Research Center  
Hampton, Virginia 23366

NATIONAL AERONAUTICS AND SPACE ADMINISTRATION

DTIC QUALITY INSPECTED B

DEPARTMENT OF DEFENSE  
DEFENSE TECHNICAL EVALUATION CENTER  
ARLINGTON, VIRGINIA 22204-6145

PLASTIC 5078

\*MSG DI4 DROLS PROCESSING - LAST INPUT IGNORED

\*MSG DI4 DROLS PROCESSING-LAST INPUT IGNORED

-- 1 OF 2

\*\*\*DTIC DOES NOT HAVE THIS ITEM\*\*\*

-- 1 - AD NUMBER: D441254  
-- 5 - CORPORATE AUTHOR: MCDONNELL DOUGLAS CORP LONG BEACH CA DOUGLAS  
-- AIRCRAFT DIV  
-- 6 - UNCLASSIFIED TITLE: BORON/ALUMINUM SKINS FOR THE DC-10 AFT  
-- PYLON,  
-- 9 - DESCRIPTIVE NOTE: FINAL REPT., 28 FEB - 31 OCT 74,  
--10 - PERSONAL AUTHORS: ELLIOTT, S. Y.  
--11 - REPORT DATE: MAY , 1975  
--12 - PAGINATION: 137P  
--14 - REPORT NUMBER: N75-22314  
--15 - CONTRACT NUMBER: NAS-1-13029  
--18 - MONITOR ACRONYM: NASA  
--19 - MONITOR SERIES: CR-132645  
--20 - REPORT CLASSIFICATION: UNCLASSIFIED  
--22 - LIMITATIONS (ALPHA): APPROVED FOR PUBLIC RELEASE; DISTRIBUTION  
-- UNLIMITED. AVAILABILITY: NATIONAL TECHNICAL INFORMATION SERVICE,  
-- SPRINGFIELD, VA. 22161. N75-22314  
--33 - LIMITATION CODES: 1 24

--\*\*\*\*\*

-- 2 OF 2

\*\*\*DTIC DOES NOT HAVE THIS ITEM\*\*\*

-- 1 - AD NUMBER: D101440  
-- 5 - CORPORATE AUTHOR: MCDONNELL DOUGLAS CORP LONG BEACH CALIF DOUGLAS  
-- AIRCRAFT DIV  
-- 6 - UNCLASSIFIED TITLE: BORON/ALUMINUM SKINS FOR THE DC-10 AFT  
-- PYLON,  
-- 9 - DESCRIPTIVE NOTE: FINAL REPT. 28 FEB-31 OCT 74,  
--10 - PERSONAL AUTHORS: ELLIOTT,S. Y. ;  
--11 - REPORT DATE: MAY , 1975  
--12 - PAGINATION: 137P  
--14 - REPORT NUMBER: N75-22314  
--15 - CONTRACT NUMBER: NAS 1-13029  
--18 - MONITOR ACRONYM: NASA  
--19 - MONITOR SERIES: CR-132645  
--20 - REPORT CLASSIFICATION: UNCLASSIFIED  
--22 - LIMITATIONS (ALPHA): AVAILABILITY: NATIONAL TECHNICAL  
-- INFORMATION SERVICE, SPRINGFIELD, VA 22161/ORDER NO. N75-22314. (NO  
-- COPIES FURNISHED BY MCIC/DTIC.)  
--33 - LIMITATION CODES: 1

--\*\*\*\*\*

-- <<ENTER NEXT COMMAND>>

BORON/ALUMINUM SKINS  
FOR THE DC-10 AFT PYLON

FINAL REPORT

by

S.Y.ELLIOTT

Prepared under Contract NAS1-13029

McDonnell Douglas Corporation  
Douglas Aircraft Company  
3855 Lakewood Blvd  
Long Beach, California 90846

May 1975

for

Langley Research Center  
Hampton, Virginia 23366

NATIONAL AERONAUTICS AND SPACE ADMINISTRATION

Accession For	
NTIS CRA&I	<input checked="" type="checkbox"/>
DTIC TAB	<input type="checkbox"/>
Unannounced	<input type="checkbox"/>
Justification	
By ADD441254	
Distribution/	
Availability Codes	
Dist	Avail and/or Special
A-1	

## ABSTRACT

Four boron/aluminum aft pylon "boat tail" skins are designed and fabricated and three of them are installed on three DC-10 aircraft for a 5-year flight service demonstration test. The fourth skin is retained as a spare and all skins will be replaced at the end of the service period by their titanium counterparts. Inspection and tests of the exposed skins will establish the ability of the boron/aluminum composite to withstand long time flight service conditions, which include exposures to high temperatures, sonic fatigue, and flutter. The results of a preliminary testing program yield room temperature and elevated temperature data on the tension, compression, in-plane shear, interlaminar shear, bolt bearing, and tension fatigue properties of the oriented 11 ply boron/aluminum laminates and this information together with a stress analysis are used to obtain FAA approval. Present state-of-the-art technology (emphasizing low cost) was used in the fabrication of the skins and these are installed on the existing titanium substructure with the same number of the same sized mechanical fasteners as are used for the present titanium skins. The boron/aluminum skins measure approximately 20.32 x 170.18cm (8 x 67 inches) and are 2.032mm (0.080 inch) thick. Although maximum weight saving was not sought, the 1.56Kg (3.45 lb) weight of the constant thickness boron/aluminum skin is 26% less than the chemically milled titanium skin.

## FOREWORD

This report was prepared by the Douglas Aircraft Company (DAC), Long Beach, California of the McDonnell Douglas Corporation under the terms of contract NAS1-13029. It is the final report on this program and covers the work that was completed between 28 February and 31 October 1974. The program was sponsored by the National Astronautics and Space Administration's Langley Research Center, Hampton, Virginia. Dr. John G. Davis, Jr., was the technical monitor.

The following Douglas Aircraft Company personnel were the principal contributors to the program: Dr Steven Y. Elliott, technical director; T.W. Gladhill and E.R. Wogulis, specimen and component design; A. Cominsky, structural analysis; Dr T.L. Mackay, S.M. Weiman, R.W. Ross, R.L. Radecky, M.L. Marcoux, Materials, QC, NDT, and testing; R.T. Hartunian, tooling and manufacturing.

All numerical values used in measurements and calculations in this report are expressed in International (SI) System of Units. Equivalent US Customary Units are given in parentheses following the SI values.

## CONTENTS

	PAGE
INTRODUCTION AND SUMMARY	1
DESIGN STUDIES, MATERIALS, PROCESSING, AND FABRICATION	2
Design Criteria and Loads	3
Preliminary Design	4
Specimen Design	5
Specimen Fabrication	6
Definition of Manufacturing Procedures	8
COMPONENT DESIGN AND ANALYSIS	8
Component Design	8
Stress Analysis	9
DEMONSTRATION TESTS	14
Tension Tests	14
Compression Tests	20
Rail Shear Tests	23
Interlaminar Shear Tests	25
Bolt Bearing Tests	25
Tension Fatigue Tests	28
Summary of Demonstration Test Data	30
COMPONENT FABRICATION	30
Fabrication Plan	30
QC, and NDT	33
Composite Skin Fabrication and Installation	33
Cost Analysis	34
FLIGHT TESTS	35
Flight Service Demonstration Test	35
Skin Inspection and NDT	35
Skin Replacement	35
Skin Shipment to NASA	35
CONCLUSIONS	36
REFERENCES	37
APPENDIX A - Material Procurement Diffusion Bonded Boron/ Aluminum Composite Sheets	A1
APPENDIX B - DPS 3.67-67 Hole Preparation and Trimming of Boron/ Aluminum	B1
APPENDIX C - Fabrication Plan for Boron/Aluminum Aft Pylon Skin AVB7097-30	C1

# TABLES

	PAGE
1. Aerodynamic Loads on the Aft-Engine-Pylon Trailing Edge	3
2. Qualification and Demonstration Tests	15
3. Results of Tension Tests at Room Temperature 505K(450°F) and at Room Temperature after 1000 Hours Aging at 505K (450°F)	16
4. Modulus of Elasticity and Strain at Failure from Tension Tests at Room Temperature and at Room Temperature after Aging 1000 Hours at 505K (450°F)	19
5. Results of Compression Tests at Room Temperature, Elevated Temperature, and at Room Temperature after 1000 Hours Aging at 505K (450°F)	21
6. Modulus of Elasticity and Strain at Failure from Compression Tests at Room Temperature and at Room Temperature after Aging 1000 Hours at 505K (450°F)	22
7. Results of Rail Shear Tests at Room Temperature, Elevated Temperature, and at Room Temperature after 1000 Hours Aging at 505K (450°F)	24
8. Results of Interlaminar Shear Tests at Room Temperature, 505K (450°F), and at Room Temperature after 1000 hours Aging at 505K (450°F)	26
9. Results of Bolt Bearing Tests	27
10. Results of Fatigue Tests of 2.54cm(1.00 inch)Wide Tension Specimens with a 4.775mm(0.188 inch) Hole in the Center	29
11. Suggested Material Properties of Boron/Aluminum Composite with 90°,45°,90°,0°,-45°,0°,-45°,0°,90°,45°,90° Filament Orientation	31
12. Material Properties of Boron/Aluminum Composite with 90°,45°, 90°,0°,-45°,0°,-45°,0°,90°,45°,90° Filament Orientation with Commercially Pure Titanium	32

# FIGURES

	PAGE
1. DC-10 Tail Pylon	39
2. DC-10 Typical Mission Profile	40
3. Estimated Aerodynamic Loads on Aft-Engine-Pylon Trailing Edge	41
4. Estimated Acoustic Loads for 3-Engine Ground Runup at Take-off Thrust using JT9D-15 Engine (Aft Pylon Fairing)	42
5. Engine Fairing Temperature During Reverse Thrust	43
6. Specimen Assembly-Modified IITRI Tension Test	44
7. Specimen Assembly-Composite Honeycomb Sandwich Beam Test	45
8. Specimen Assembly-Composite Rail Shear Test	46
9. Specimen-Composite Interlaminar Shear Test	47
10. Composite Specimen-Bolt Bearing Test	48
11. Specimen-Composite Tensile Fatigue Test	49
12. Cutting Boron/Aluminum with Diamond Coated Wheel	50
13. Hole Produced by 0.635cm(0.250 in) Diameter Steel Drill	51
14. Hole Produced by 0.566cm(0.223 in) Diameter Steel Punch	52
15. Hole Produced by 0.566cm(0.223 in) Diameter Steel Punch Followed by 0.579cm(0.228 in) Diameter Steel Ream	53
16. Hole Produced by 0.635cm(0.250 in) Diameter Steel Punch Followed by 0.640cm(0.252 in) Diameter Diamond Ream	54
17. Drawing AVB7129-Rework-Lower Fairing Skin, Tail Pylon	55
18. Specimen 11 - Room Temperature Tension Stress Strain Curve	56
19. Specimen 11 - (3rd Run Only) Room Temperature Tension Stress-Strain Curve	57
20. Specimen 12 - Room Temperature Tension Stress-Strain Curve	58
21. Specimen 13 - Room Temperature Tension Stress-Strain Curve	59
22. Specimen 14 - Room Temperature Tension Stress-Strain Curve	60
23. Specimen 15 - Room Temperature Tension Stress-Strain Curve	61
24. Specimen 16 - Room Temperature Tension Stress-Strain Curve	62
25. Specimen 17 - Room Temperature Tension Stress-Strain Curve	63
26. Specimen 18 - Room Temperature Tension Stress-Strain Curve	64
27. Specimen 19 - Room Temperature Tension Stress-Strain Curve	65
28. Specimen 20 - Room Temperature Tension Stress-Strain Curve	66
29. Specimen 21 - Room Temperature Tension Stress-Strain Curve after 1000 Hours Aging at 505K (450°F)	67
30. Specimen 22 - Room Temperature Tension Stress-Strain Curve after 1000 Hours Aging at 505K (450°F)	68
31. Specimen 23 - Room Temperature Tension Stress-Strain Curve after 1000 Hours Aging at 505K (450°F)	69
32. Specimen 24 - Room Temperature Tension Stress-Strain Curve after 1000 Hours Aging at 505K (450°F)	70
33. Specimen 25 - Room Temperature Tension Stress-Strain Curve after 1000 Hours Aging at 505K (450°F)	71
34. Specimen 26 - Room Temperature Tension Stress-Strain Curve after 1000 Hours Aging at 505K (450°F)	72
35. Specimen 27 - Room Temperature Tension Stress-Strain Curve after 1000 Hours Aging at 505K (450°F)	73
36. Specimen 28 - Room Temperature Tension Stress-Strain Curve after 1000 Hours Aging at 505K (450°F)	74

37.	Specimen 29 - Room Temperature Tension Stress-Strain Curve after 1000 Hours Aging at 505K (450°F)	75
38.	Specimen 30 - Room Temperature Tension Stress-Strain Curve after 1000 Hours Aging at 505K (450°F)	76
39.	Schematic of Typical Tension Stress-Strain Curve	77
40.	Specimen 11 (Side #1) Poisson's Ratio vs Tension Stress	78
41.	Specimen 11 (Side #2) Poisson's Ratio vs Tension Stress	79
42.	Specimen 12 Poisson's Ratio vs Tension Stress	80
43.	Specimen 13 Poisson's Ratio vs Tension Stress	81
44.	Four-Point Bending Honeycomb Sandwich Compression Test	82
45.	Specimen 11 Room Temperature Compression Stress-Strain Curve	83
46.	Specimen 12 Room Temperature Compression Stress-Strain Curve	84
47.	Specimen 13 Room Temperature Compression Stress-Strain Curve	85
48.	A Tested and An Untested Room Temperature Honeycomb Sandwich Compression Specimen	86
49.	Specimen 14 Room Temperature Compression Stress-Strain Curve	87
50.	Specimen 15 Room Temperature Compression Stress-Strain Curve	88
51.	Specimen 16 Room Temperature Compression Stress-Strain Curve	89
52.	Specimen 17 Room Temperature Compression Stress-Strain Curve	90
53.	Specimen 18 Room Temperature Compression Stress-Strain Curve	91
54.	Specimen 19 Room Temperature Compression Stress-Strain Curve	92
55.	Specimen 20 Room Temperature Compression Stress-Strain Curve	93
56.	Compression Specimen Failure Surface	94
57.	Specimen 21 Room Temperature Compression Stress-Strain Curve after 1000 Hours Aging at 505K (450°F)	95
58.	Specimen 22 Room Temperature Compression Stress-Strain Curve after 1000 Hours Aging at 505K (450°F)	96
59.	Specimen 23 Room Temperature Compression Stress-Strain Curve after 1000 Hours Aging at 505K (450°F)	97
60.	Specimen 24 Room Temperature Compression Stress-Strain Curve after 1000 Hours Aging at 505K (450°F)	98
61.	Specimen 25 Room Temperature Compression Stress-Strain Curve after 1000 Hours Aging at 505K (450°F)	99
62.	Specimen 26 Room Temperature Compression Stress-Strain Curve after 1000 Hours Aging at 505K (450°F)	100
63.	Specimen 27 Room Temperature Compression Stress-Strain Curve after 1000 Hours Aging at 505K (450°F)	101
64.	Specimen 28 Room Temperature Compression Stress-Strain Curve after 1000 Hours Aging at 505K (450°F)	102
65.	Specimen 29 Room Temperature Compression Stress-Strain Curve after 1000 Hours Aging at 505K (450°F)	103

66.	Specimen 30 Room Temperature Compression Stress-Strain Curve after 1000 Hours Aging at 505K (450°F)	104
67.	Poisson's Ratio vs Compression Stress	105
68.	Failed Rail Shear Specimens	106
69.	Failed Rail Shear Specimen	107
70.	Shear Specimen Failure Surface	108
71.	Specimen 11 Room Temperature Rail Shear Stress-Strain Curve	109
72.	Specimen 12 Room Temperature Rail Shear Stress-Strain Curve	110
73.	Specimen 13 Room Temperature Rail Shear Stress-Strain Curve	111
74.	Mode of Failure of Bolt Bearing Specimen	112
75.	SEM Pictures of Bolt Bearing Specimen in the Vicinity of the Hi-Lok Bolt Head	113
76.	Constant Load Tensile Fatigue $R = .1$ (0/45/0/90/-45/90) <sub>s</sub> Loaded in 0° Direction 2.54cm (in) Wide Specimen with a 4.763mm (3/16-in) Diameter Hole in Its Center	114
77.	Failed Fatigue Specimen	115
78.	Fatigue Crack in Edge of Hole of Fatigue Specimen	116
79.	SEM Pictures of Fatigue Specimen 2 Tested Staticallly in Tension to Failure	117
80.	SEM Pictures of Fatigue Specimen 3. (failed on the 2,362,000th cycle of a Maximum Alternating Tensile Stress of 242.8MPa (35,222 psi)	118
81.	Fatigue Properties Comparison	119
82.	Surface Blemishes on Second Boron/Aluminum Aft Pylon Skin	120
83.	Boron/Aluminum Aft Pylon Skin-Edges and Corner Trimmed and Holes Punched	121
84.	Punching Holes in Boron/Aluminum Skin	122
85.	Installation of the Boron/Aluminum Skin Onto the Substructure	123
86.	Installation of the Aluminum Upper Skins Onto the Substructure	124

BORON/ALUMINUM SKINS  
FOR THE DC-10 AFT PYLON

By S.Y. ELLIOTT

Douglas Aircraft Company  
Long Beach, California 90846

INTRODUCTION AND SUMMARY

Structural applications of advanced metal matrix composites have received increasing attention during the past 10 years because of the excellent potential in weight savings and increased strength and stiffness at elevated temperatures. Most of these applications have been oriented toward military aircraft, jet engines, or space vehicles. A few of these applications have reached the flight test stage, but as yet no major structural component involving metal matrix composite has been exposed to the long-term continuous flight service operation that will be required for commercial aircraft.

An extended period of apprenticeship is highly desirable for every new structural material for proper assessment of its service performance. Because the utilization of commercial vehicles is consistently much greater than the military or space vehicles, it is possible to log considerably more flight hours on such a vehicle in a given time period. Introduction of advanced metal matrix filamentary composites into commercial aircraft would benefit military and space programs as well, because the larger potential market would reduce the cost of raw materials and the burden of other development and testing costs.

The selection of the DC-10 commercial aircraft was particularly appropriate as it is representative of the new generation of wide-bodied aircraft which will dominate the commercial scene for many years to come. The DC-10 is already in service with 22 airlines and its use will become even more widespread in the near future. Its immediate availability ensured a practical and realistic approach to the program.

This report describes a flight demonstration development program which will demonstrate the use of advanced metal matrix composite material. The program objective was to design, fabricate, and install boron/aluminum skins on three DC-10 aft pylon "boat tail" assemblies for flight service evaluation (Figure 1). The flight service demonstration of the completed assemblies commenced with the establishment of United Air Lines interface and after FAA approval.

The design philosophy was to substitute a 1.56kg(3.45 lb) boron/aluminum skin for a 2.111 kg(4.65 lb) titanium skin, using the existing titanium substructure with little alteration. Present state-of-the-art technology (emphasizing low cost) was used in the fabrication of the skins rather than new approaches.

The existing internal riveted rib-type construction was used. This approach resulted in a component which was as simple to fabricate and assemble as the existing design.

After the program was started, a number of the DC-10 domestic carriers, including United Air Lines, eliminated the use of the thrust reversers on the #2 engines during the landing operation. Elimination of this operation meant that the peak heating of the aft pylon boron/aluminum skin of up to 589K(600°F) during each landing would not occur, so that part of the anticipated high temperature operating environment would be different from that originally anticipated.

The program consisted of a 6-month effort which involved the development of the design, materials, processing, fabrication, and quality control verification of three components, and static and fatigue tests of specimens. Flight service demonstration testing of the three completed assemblies for a period of five years is scheduled to start in July 1975 and has involved securing FAA and commercial airline approval. A fourth boron/aluminum skin was fabricated and delivered to NASA Langley Research Center for storage and possible installation at a later date.

#### DESIGN STUDIES, MATERIALS, PROCESSING, AND FABRICATION

This section contains the design criteria, and external loads of the boron/aluminum panel for the DC-10 tail pylon (Figure 1). Preliminary design studies of the panel are discussed and the design and fabrication of the supporting data specimens are described. The definition of manufacturing procedures for the specimens and the production panels concludes this task.

##### Design Criteria and Loads

The boron/aluminum panel for the DC-10 aft pylon is little more than a skin fairing to reduce turbulence and aerodynamic drag. Four types of loads affect the design of this panel, ie;

1. Aerodynamic loads act normal to the surface of the panel. Airplane yaw conditions are critical (Reference 1).
2. Acoustic loads are maximum for the 3-engine ground run up at takeoff thrust.
3. Temperature variations over the surface of the panel produce thermally induced stresses. Maximum temperatures occur during landing with thrust reverser operation (Figure 2). If the thrust reverser is not used during landing, the maximum temperature during landing and up to 15 minutes after landing is between 339 and 367K (150 and 200°F).
4. Inertia loads are induced in the panel by flutter or resonance during flight.

The panel itself is secondary structure and is considered failsafe as its loss will in no way reduce the controllability of the aircraft.

The aerodynamic loads on the aft-engine-pylon trailing edge of the DC-10 for two design conditions are shown in Figure 3 (taken from Reference 1) and summarized in Table 1.

TABLE 1  
AERODYNAMIC LOADS ON THE AFT-ENGINE-PYLON  
TRAILING EDGE

CONDITION	Mach Number  M	Air Speed  V		Dynamic Pressure,  q		Rudder Angle-  $\delta_r$	Fuselage Angle of Attack $\alpha_F$	Fuselage Yaw Angle $\beta$
		KMEAS	KEAS	KPA	PSF			
1. Steady Side Slip. Flap Angle, $\delta_F=25^\circ$	0.33	407.66	220	7.85	164	13.5°	2°	13°
2. Max Dynamic Pressure, $2q$ where $q=V^2/2$	0.78	796.79	430	29.93	625	4°	0°	3.6°

NOTE: KMEAS = Kilometers per hour equivalent air speed  
KEAS = Knots equivalent air speed  
KPA = KiloPascals, or KiloNewtons per square meter  
PSI = Pounds per square foot

The maximum  $\beta q$  condition was also analyzed, but it resulted in less load than the maximum q condition and is therefore not presented. The results for the low-speed condition are presented to show the relative magnitude of loads between the low-speed and the high-speed conditions.

The load differential acting on the pylon may be applied to any thrust condition. (The load differential is considered independent of engine thrust level).

The aft-pylon load differentials are based on wind-tunnel test pressure data obtained on a 4.7% scale model DC-10 (LB-241C) in the North American Rockwell 213.36 x 335.28m (7 x 11 foot) low-speed wing tunnel (NAL 574), and on a 3.25% scale model DC-10 (LB-244B) in the Cornell Aeronautical Laboratory high-speed wind tunnel (CAL820-023).

The direction of loads is as viewed from the rear. Positive  $\delta_r$  is trailing edge left and positive  $\beta$  is airplane nose left. The loads may be applied uniformly over the aft-engine-nacelle pylon from FS2340 aft.

Limit aerodynamic loads will be multiplied by 1.5 to obtain design ultimate airloads.

The acoustic loading in the center portion of the boron/aluminum panel is shown in Figure 4.

The variation in skin temperature during landing with reverse thrust is shown in Figure 5. After the program was started, a number of the DC-10 domestic carriers, including United Air Lines, eliminated the use of the thrust reversers on the #2 engines during the landing operation. Elimination of this operation meant that the peak heating of the aft pylon boron/aluminum skin of up to 589K(600°F) during

each landing would not occur, so that part of the anticipated high temperature operating environment would be different from that originally anticipated. However, it has been determined that after each engine shutdown the rising hot air from the #2 engine heats the aft pylon skin to a temperature of up to 367K (200°F) for a period of about 15 minutes. On a hot day it is estimated that the temperature from this engine shutdown condition may reach 395K(250°F).

### Preliminary Design

The design of the lower skin of the aft pylon was directed toward complete interchangeability with the present metal structure and toward certification as a structural component suitable for use on a commercial aircraft in regular passenger carrying operations. The internal reinforcing substructure was not to be changed and only the outer skin segment would be changed from the present titanium to aluminum matrix/boron filament composite material. Because the titanium skin is 2.032mm (0.080 inch) thick, the number of boron filament layers was thereby established to be 11 (ie; 11 layers x 1.829mm/layer (0.0072 in/layer) = 2.012mm (0.0792 in)). The boron filaments were 1.422mm(0.0056 inch) in diameter and were required to meet the McDonnell Douglas specification (Reference 2). The aluminum matrix alloy was 6061. The finished sheet was furnished in the as-fabricated condition and required to meet the specification listed in Appendix A.

The present 2.032mm (0.080 inch) annealed skin measures approximately 20.32 x 170.18cm (8 x 67 inches) as shown in Figure 1 and has a slight curvature. Approximately 50 percent of the area of this skin is now chemically milled to a 1.016mm (0.04 inch) thickness leaving a scalloped doubler arrangement around its perimeter. For aerodynamic loading purposes, the 1.016mm(0.040 inch) thickness would have been adequate, but the 2.032mm(0.080 inch) perimeter thickness had to be added to prevent edge cracking as a result of a flutter condition and to provide sufficient thickness for the countersunk heads of monel rivet fasteners. Because it was not the objective of this program to demonstrate maximum weight savings, and because a similar scalloping of the boron/aluminum skin would have increased its fabricating cost substantially, it was left as a solid 2.032mm (0.080 inch) thick skin. Nevertheless, because of its lower density, its total weight was 26% less than the chemically milled titanium skin. It was proposed that a rectangular boron/aluminum skin slightly larger than 20.32 x 170.18 cm (8 x 67 inches) would be fabricated by a selected manufacturer and then machined to exact size.

The present mechanical fasteners include 33 titanium screws 4.762mm (3/16 inch diameter) flush tri-wing head along the top surface and 77 monel rivets 3.175, 3.972, and 4.762mm (1/8, 5/32, and 3/16 inch) flush head along the bottom and sides. The heads of these fasteners are countersunk for reduction of aerodynamic drag. Because drilling and countersinking holes in boron/aluminum is difficult and expensive, it was determined to eliminate the countersinks in the boron/aluminum by adding a thin external titanium strip along the bottom of the panel to contain the required countersinks and by using protruding fasteners with low head profiles across the top and down the sides. Preliminary riveting tests of drilled boron/aluminum strips revealed that the diametral growth of the required rivets when they were impacted was sufficient to split the composite. For this reason, rivets were completely eliminated and removable Hi-Lok screw fasteners were substituted. These threaded type mechanical fasteners have the additional advantage that when the boron/aluminum skins are replaced by the standard titanium skins after the 5-year flight service program, installation will be facilitated by elimination of drilling out monel rivets.

In another set of preliminary tests, it was determined that the fastener pull-out strength of boron/aluminum composite formed from 0°-90° oriented plies alone might be marginal for the application and, of course, much less than the similar fastener strength of titanium sheet. The three potential methods of increasing this property in boron/aluminum composite are: incorporating layers of thin titanium foils among the 0°-90° plies, incorporating layers of thin stainless steel woven screens, and incorporating +45° plies of boron filament layers among the 0°-90° plies. As a result of some preliminary laboratory tests it was determined that the third method was the most suitable and required no new fabricating developments or risks.

With the number of plies established at 11 and with the filament orientations established as 0°, 90°, +45°, the only remaining requirement was to select an orientation arrangement that was symmetrical about the neutral axis and which did not place two identically oriented layers together. This latter requirement was considered to be important from the standpoint of preventing fiber nesting and hence, permitting aluminum matrix squeeze out and possibly leading to undesirable fiber contact. The final fiber orientation selected as a result of the preliminary design effort therefore was:

90°, 45°, 90°, 0°, -45°, 0°, -45°, 0°, 90°, 45°, 90°

where the 0° direction was the long direction of the skin. The four 90° plies at the outside of this composite arrangement insured that the skin would have greater bending strength across the short direction of the pressure loaded plate and the remaining 0° and +45° layers were primarily needed to insure adequate fastener pull-out strength in all directions.

### Specimen Design

The demonstration test specimens, consisting of tension, compression, rail shear, interlaminar shear, bolt shear, and tensile fatigue specimens, were designed to help demonstrate the suitability of the boron/aluminum skin for its application to the DC-10 aft pylon.

1. The tension specimen (Z4941424), a modified IITRI design shown in Figure 6, used (as did all of the test specimens) a ply layup and thickness identical to the boron/aluminum aft pylon skin. Fiberglass phenolic was used for the tabs because it had good matching of thermal coefficients with boron/aluminum which assured a strain-free bond and a low modulus which reduced the tendency of the tabs to create a stress concentration in the grip area. Scarfing the tabs reduced peel stresses at the tip of the tab. The room temperature specimens were bonded with Hysol EA951, a "ductile" adhesive which allowed a more even distribution of shear stress in the bond than that of a "brittle" adhesive. Because ductile adhesives lose strength radically at temperatures above 367K(200°F), a high temperature adhesive, HT424, was chosen for the 505K (450°F) tests.
2. The honeycomb sandwich beam type of compression test (Figure 7) was chosen because it provided support for the specimen in compression and therefore helped insure a compression failure only instead of the buckling or brooming failure more likely to be encountered in an edge-

loaded compression test. The specimen had two different core types. The outer core was dense to support the high shear loads introduced by the four point loading, whereas the inner core which experienced no shear was lighter to lessen the interaction between the core and the boron/aluminum in the test region. The tension side of the beam was a steel sheet which minimized beam deflections when a high compressive load was developed in the boron/aluminum. The room temperature specimens were bonded with Metlbond 329 because the shear stresses in the bond line were already uniform so the ductility of Hysol EA951 was unnecessary. HT424 was used to bond the high temperature test specimens.

3. The rail shear specimen (Figure 8) was chosen for obtaining shear data because it used standard 2.032mm (0.080 inch) flat boron/aluminum sheet and produced relatively pure shear in the test section. The rails were tapered to provide uniform shear introduction into the specimen and were bonded to the boron/aluminum with Hysol EA951 for the room temperature tests and with HT424 for the 505K(450°F) tests.
4. The length of the interlaminar shear specimen (Figure 9) was chosen to accommodate a 8.128mm (0.32 inch) test span (determined from a span-to-depth ratio of 4 as specified in ASTM (D2344-72) for specimens with filament moduli greater than 31.05kPa ( $4.5 \times 10^6$  psi) with an overhang of 5.08mm (0.2 inch) on both ends of the span.
5. The bolt shear specimen (Figure 10) was designed to simulate the aft pylon where the boron/aluminum skin is fastened to 1.016mm (0.040 inch) thick titanium ribs by bolts--principally of 3.969 and 4.762mm (5/32 and 3/16 inch) diameters. The specimen made optimum use of the boron/aluminum test strip, testing it twice. First the specimen was pulled by both titanium strips until one joint failed, then the remaining joint was tested by gripping the failed end of the boron/aluminum. Thus, two data points were obtained from one specimen.
6. A center hole tensile fatigue specimen (Figure 11) was chosen to enable comparison of its fatigue data with similar existing data for titanium. Holes were punched into the specimens to study their effect on the strength and fatigue life of the laminate. This was of interest because the boron/aluminum aft pylon skin had many fastener holes and was in a fatigue environment. Steel tabs were chosen for strength. The hole through the steel tabs accommodated a pin which transferred the fatigue loading from the testing machine to the specimen. Hysol EA951 was used so that the shear in the bond would be distributed more evenly.

### Specimen Fabrication

The selection of a fabricator for the boron/aluminum composite panels for the specimens and skins was based on considerations of quality, capability, cost, and confidence. The company selected was Hamilton Standard of Windsor Locks, Connecticut, who are represented on the West coast by DWA (Dolowy Webb Associates) Composite Specialties, Inc. The purchase of all material for the specimen test program was based on a material procurement specification reproduced in Appendix A. The quality of the panels fabricated and received was determined by means of tensile

tests of specimens cut from the edges of each panel in both the 0° and 90° directions and by X-ray and C-scan type NDT inspections. All materials used for test specimens complied with the requirements of Appendix A.

When a new material is proposed for use on a commercial transport, FAA certification must be secured even though the material is only intended for a temporary flight test. Receipt of such certification involves the following steps:

1. A report is submitted to the local FAA office summarizing the steps which will be followed in securing FAA certification of the flight test. It contains a specimen test plan.
2. A material specification document is prepared and submitted to the FAA which is used to control the quality of the incoming materials.
3. Drawings of the qualification specimens which will be used to generate the required design data are prepared and submitted to the FAA.
4. A Testing and Development document is prepared by the Structural Design Engineering department and submitted to the Testing department authorizing the preparation of specimens and the conduction of the design data tests in accordance with the test plan.
5. The Testing department prepares a Development Release Order authorizing the Planning department to prepare the necessary planning papers.
6. The Planning department prepares a series of Fabricating Orders for each of the types of specimens describing in detail the sequential operations to be performed by each department in their preparation and testing.
7. As the specimens are fabricated, inspection reports guaranteeing that the specimens comply with the drawings and the Fabrication Orders are signed and submitted to the FAA.
8. As the specimens are tested, FAA inspectors and approved witnesses check the test machines, jigs, and procedures. Copies of all raw test data generated are submitted to the FAA.
9. When all the tests are completed, a report summarizing the results and analyzing their significance in the establishment of the adequacy of the material is prepared and submitted to the FAA.

Specimen fabrication primarily involved cutting the large panels into the proper sized rectangular strips using a rotating diamond coated wheel, Figure 12, punching holes as required into the composite with a hand operated punch tool, bonding reinforcing tabs or honeycomb cores with selected adhesives as described in the specimen drawings, and finally bonding strain gages to the surfaces of the test specimens as required. Each of these operations was performed in accordance with written procedural directions. No unsolvable problems were encountered and all specimens were eventually successfully completed and approved for testing.

## Definition of Manufacturing Procedures

A specification describing the cutting of boron/aluminum and the preparation of holes was written, approved, and published. Its title is DPS 3.67-67, Hole Preparation and Trimming of Boron/Aluminum, and a copy is included in Appendix B. Preliminary tests determined that the most suitable hole preparation method was punching followed by sufficient reaming to enlarge the holes to the exact desired size, if necessary. Figures 13 through 16, for example, show enlargements of four holes through boron/aluminum skins produced by four different techniques, ie;

- Figure 13 - Hole produced by 0.635cm (0.250 inch) diameter steel drill
- Figure 14 - Hole produced by 0.566cm (0.223 inch) diameter steel punch
- Figure 15 - Hole produced by 0.566cm (0.223 inch) diameter steel punch followed by 0.579cm (0.228 inch) diameter steel ream
- Figure 16 - Hole produced by 0.635cm (0.250 inch) diameter steel punch followed by 0.640cm (0.252 inch) diameter diamond ream

Of these four techniques, the first involving the steel drill alone showed unacceptable edge roughness, but the other three techniques all produced approximately similar quality holes. It was concluded, therefore, that since punching alone was the least expensive, it would be the preferred method and that additional reaming with either steel or diamond coated reamers would be performed, if needed, to enlarge the holes to the exact desired size.

It was also determined by laboratory testing that the boron fibers in boron/aluminum are attacked by the standard anodizing process that is usually employed to provide corrosion protection to aluminum in exterior structural applications. For this application, therefore, the alodine (chromate conversion) process, which does not attack boron fibers was selected as the boron/aluminum surface treatment. In addition, the inner surface of the skin would have to be epoxy primed and all mechanical fasteners installed with wet sealant.

## COMPONENT DESIGN AND ANALYSIS

This section contains a description of the component design and a stress analysis of the boron/aluminum skin. The result of the design effort was a complete engineering working drawing which replaced the present drawing of the titanium counterpart. The stress analysis followed from the Design Criteria and Loads and was also furnished to the FAA for their certification.

### Component Design

The boron/aluminum skin panel was designed to fulfill the same requirements as its titanium counterpart. It had the same external dimensions, including the same hole spacings and edge distances, differing only in that the boron/aluminum was not chemically milled. The 2.032mm (0.080 inch) thick annealed titanium sheet was chemically milled to 1.016mm (0.040 inch) over 50% of its area, leaving the effect of a scalloped doubler around its perimeter. The weight of the chemically milled titanium sheet was 2.111Kg (4.65 pounds), ie; 0.545Kg (1.20 pounds) more than the boron/aluminum skin, 1.566 Kg (3.45 pounds), even though the boron/aluminum skin occupied a larger, unmilled volume. Hence the weight saving provided in the substitution of the boron/aluminum skin for the titanium skin was 26%. The Rework Drawing (Dwg AVB7129) showing the installation of the boron/aluminum skin is shown in Figure 17.

The titanium skin was fastened to the pylon by a variety of fasteners, including bucked, flush-head rivets and flush-head bolts. It was undesirable to use bucked rivets in the boron/aluminum design because they expand and strain their holes, and promote crack formation in the boron/aluminum.

Flush-head fasteners were undesirable because their bearing area for bolt shear is less than that available from protruding head fasteners. Where flush-head bolts were used across the top of the titanium skin, pan-head bolts were substituted. Where flush, bucked rivets were used along the forward and aft edges of the titanium skin, protruding head, clearance fit Hi-Loks were substituted. Where flush, bucked rivets held the titanium skin to the rib beneath the seal, flush Hi-Loks, sunk into a titanium strip were substituted. The flush-head bolts attaching the seal retainers remained unchanged because they were countersunk into the retainers only. The result of these fastener substitutions was to eliminate countersinks in the boron/aluminum and bucked rivets from the design.

The selected orientation of plies in the boron/aluminum skin was ( $90^\circ, 45^\circ, 90^\circ, 0^\circ, -45^\circ, 0^\circ, 45^\circ, 0^\circ, 90^\circ, 45^\circ, 90^\circ$ ). The four plies in the  $90^\circ$  direction provided strength across the width of the skin panel and the  $\pm 45^\circ$  plies provided a higher bolt shear strength. The total number of plies (11) was dictated by the thickness of the titanium panel 2.032mm (0.080 inch) which was replaced since it was necessary that the boron/aluminum panel be flush with the surrounding structure.

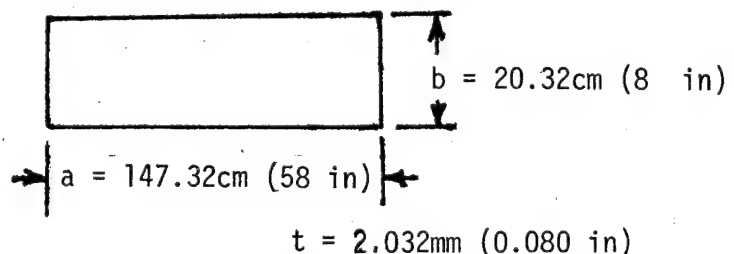
The processing specification (DPS 3.67-67) referenced on the drawing described the cutting and hole fabrication processes for the boron/aluminum skin and is the same as Appendix B of this report.

### Stress Analysis

The boron/aluminum composite panel was analyzed as a flat panel, acted upon by normal air pressure. The critical loads for the aft-engine-ylon trailing edge of the DC-10 occur for a maximum dynamic pressure,  $q$ , yaw condition designated as design condition number 2 in Figure 3. The question of satisfactory strength for acoustic loads and adequacy for flutter or resonance during flight was approached by determining that the boron/aluminum panel was stiffer than the original titanium panel (which has demonstrated satisfactory service for these considerations).

According to the lowest curve shown on the critical design condition 2 of Figure 3 (ie; Pylon Left Side corresponding to Fuselage Station 2363), the maximum limit air pressure is 3.59kPa (0.52 psi). Hence, the maximum ultimate air pressure is  $1.5 \times 3.59 = 5.38\text{kPa}$  ( $1.5 \times 0.52 = 0.78$  psi).

Although the left skin shown in Figure 1 was not rectangular, its average dimensions were approximated by a 147.32 x 20.32cm (58 x 8 inch) rectangular plate with a thickness of 2.032mm (0.080 inch). Assuming all edges simply supported the formula for the maximum bending stress in the center of a rectangular plate subjected to a normal pressure is taken from page 203 of Reference 3 for bending around the horizontal axis.



$$S_b = \frac{0.75wb^2}{t^2(1 + 1.61\alpha^3)} \quad (1)$$

where  $w$  = normal pressure, Pa (psi)  
 $b$  = shorter dimension, cm (in)  
 $a$  = longer dimension, cm (in)  
 $\alpha$  =  $b/a = 20.32/147.32 = (8/58) = 0.138$

Substituting appropriate values:

$$S_b = \frac{0.75 \times 5.378 \times (20.32)^2}{(0.2032)^2 [1 + 1.61(0.138)^3]} = 40.17 \text{ MPa} \quad (5825 \text{ psi})$$

From Reference 4 the formula for bending around the vertical axis is:

$$\begin{aligned} S_a &= \frac{wb^2(0.225 + 0.382\alpha^2 - 0.320\alpha^3)}{t^2} \quad (2) \\ &= \frac{5.378(20.32)^2(0.225 + 0.382(0.138)^2 - 0.320(0.138)^3)}{(0.2032)^2} \\ &= 12.45 \text{ MPa} \quad (1805 \text{ psi}) \end{aligned}$$

The other critical static stress condition checked was the magnitude of the skin stress in the vicinity of the mechanical fasteners. For this case the maximum bending stress at the center of the long edge of a rectangular plate with fixed edges and subjected to a normal air pressure is given by the following formula on page 205 of Reference 3:

$$\begin{aligned} S_b &= \frac{0.5wb^2}{t^2(1 + 0.623\alpha^6)} \quad (3) \\ &= \frac{0.5(5.378)(20.32)^2}{(0.2032)^2(1 + 0.623(0.138)^6)} = 26.89 \text{ MPa} \quad (3900 \text{ psi}) \end{aligned}$$

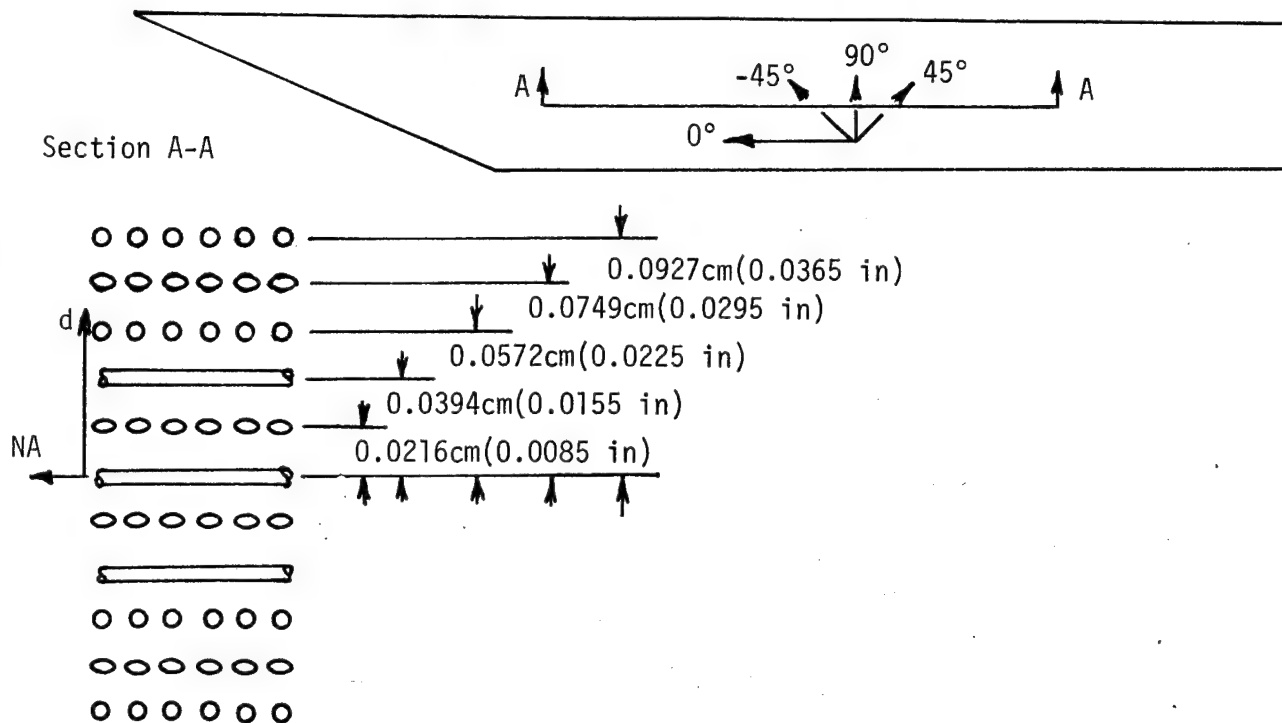
This is the stress that would exist if there were no fastener holes at the edge of the plate, but since there are 6.35mm (1/4 inch) diameter attachment holes at a pitch of 2.54cm (1 inch), the net bending stress is:

$$S_b = 26,890 \times \frac{2.54}{2.54 - 0.635} = 35.85 \text{ MPa} \quad (5200 \text{ psi})$$

Assuming a stress concentration factor for the hole of 3.0, the design stress was:

$$\text{Design } S_b = 3.0 \times 35,850 = 107.55 \text{ MPa} \quad (15,600 \text{ psi})$$

The stiffness of the boron/aluminum skin is calculated as follows:



PLY ORIENTATION	E		d		Ed <sup>2</sup>	
	GPa	PSI	cm	in	GN	lb
90°	221	32 x 10 <sup>6</sup>	0.0927	0.0365	1.896	42,600
45°	124	18.0	0.0749	0.0295	0.696	15,700
90°	221	32	0.0572	0.0225	0.722	16,200
0°	135	19.5	0.0394	0.0155	0.209	4,690
-45°	124	18.0	0.0216	0.0085	0.058	1,300
0°	135	19.5	0	0	0	0
-45°	124	18.0	-0.0216	-0.0085	0.058	1,300
0°	135	19.5	-0.0394	-0.0155	0.209	4,690
90°	221	32	-0.0572	-0.0225	0.722	16,200
45°	124	18	-0.0749	-0.0295	0.696	15,700
90°	221	32	-0.0927	-0.0365	1.896	42,600
				Σ	7.162	160,980

Panel thickness = 0.2032cm(0.080 in)

Thickness per ply,  $t = 0.2032 \div 11 = 0.0185\text{cm}(0.0073 \text{ in})$

Weight,  $W_{B/A} = \rho t = 2.72 \text{ gr/cm}^3(0.2032\text{cm}) = 0.553 \text{ gr/cm}^2(0.00785 \text{ lb/in}^2)$

Stiffness of boron/aluminum skin,  $(EI)_{B/A} = t \sum (Ed^2) = 0.0185(7.162)$

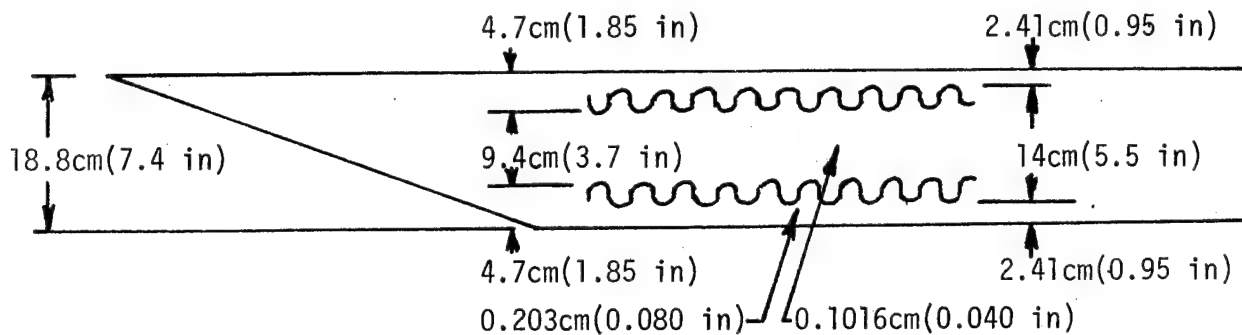
$= 0.001323\text{GNm}(1171 \text{ lb in})$

According to Appendix A the target ultimate tensile strength of the boron/aluminum composite skin in the 90° orientation is 503.3MPa(73,000 psi). Assuming a conservative 413,700MPa (60,000 psi) value for design purposes, the margin of safety is:

$$MS = \frac{F_{tu}}{S_b} - 1 = \frac{413.7}{107.6} - 1 = 2.85 \quad (4)$$

which is, of course, very adequate.

The adequacy of the boron/aluminum composite skin design for the flutter condition was determined by comparing its stiffness with that of the present chemically milled titanium skin shown below:



$$\begin{aligned} \text{Average thickness, } t &= \frac{1}{18.8} [18.8 \times 0.1016 + 2 \times 2.41 \times 0.1016 + (4.7 - 2.41)0.1016] \\ &= \frac{1}{18.8} [1.91 + 0.49 + 0.23] \\ &= 0.14 \text{ cm (0.0551 inch)} \end{aligned}$$

$$\text{Weight, } w_T = \rho t = 4.53 \text{ gr/cm}^3 \times 0.14 \text{ cm} = 0.634 \text{ gr/cm}^2 (0.009 \text{ lb/in}^2)$$

$$\text{Modulus of elasticity for titanium, } E_T = 110.3 \text{ GPa} (16 \times 10^6 \text{ psi})$$

$$\text{Moment of Inertia, } I_T = \frac{1}{12} (t)^3 = \frac{(0.14)^3}{12} = 2.286 \times 10^{-4} \text{ cm}^4 / \text{cm} (13.95 \times 10^{-6} \text{ in}^4 / \text{in})$$

$$\text{Stiffness of titanium skin } (EI)_T = 110.3 \text{ GPa} \times 2.286 \times 10^{-4} \text{ cm}^3$$

$$= 0.000252 \text{ GNm} (223.5 \text{ lb in})$$

The formula for natural frequency of a beam on two supports is given on page 379 of Reference 4 as:

$$f_i = K \sqrt{\frac{gEI}{wL^4}} \quad (5)$$

where K = Constant  
 $g = 980 \text{ cm/sec}^2 (386 \text{ in/sec}^2)$   
 $E = \text{Young's modulus, Pa (psi)}$   
 $I = \text{Moment of Inertia, cm}^4 (\text{in}^4)$   
 $w = \text{Weight of a Unit Length of Beam, Kg/in (lb/in)}$   
 $L = \text{Beam Length, cm (in)}$

For equivalent resistance to acoustic fatigue or panel flutter, the boron/aluminum panel should have an equal or greater natural frequency than the original titanium panel.

$$f_i (\text{titanium}) = f_i (\text{boron/aluminum})$$

$$K \sqrt{\frac{g E_T I_T}{w_T L_T^4}} = K \sqrt{\frac{g E_{B-A} I_{B-A}}{w_{B-A} L_{B-A}^4}}$$

$$\frac{E_T I_T}{w_T L_T^4} = \frac{E_{B-A} I_{B-A}}{w_{B-A} L_{B-A}^4}$$

minimum required stiffness of boron/aluminum skin is:

$$\begin{aligned} \text{min reqd } (EI)_{B-A} &= \frac{w_{B-A}}{w_T} \cdot \frac{L_{B-A}^4}{L_T^4} \cdot (EI)_T \\ &= \frac{0.553}{0.634} \times \left(\frac{18.8}{18.8}\right)^4 \times 0.000252 \\ &= 0.000220 \text{ GNm (195 lb in)} \end{aligned}$$

Since the calculated actual stiffness of the boron/aluminum skin is

$$\text{actual } (EI)_{B-A} = 0.001323 \text{ GNm (1171 lb in)}$$

the stiffness of boron/aluminum is approximately six times greater than required and hence, acoustic fatigue and/or panel flutter will not be a problem.

## DEMONSTRATION TESTS

The demonstration of the suitability of the boron/aluminum composite skin for the aft-pylon application relied primarily on specimen testing combined with the stress analysis. The specific types and numbers of tests and specimens are summarized in Table 2. These tests primarily involved tension, rail shear, interlaminar shear, and bolt bearing tests of specimens under various environments. In addition to these static type tests, dynamic tests were also conducted to determine tension fatigue properties of boron/aluminum composite specimens containing center holes. Metallographic and scanning electron microscope tests were made on selected failed specimens to study their mode of failure. All details describing the proposed tests were first summarized in a TEST PLAN, Reference 5, which was furnished to the FAA. The results of the tests were used to establish the initial stress levels and also to establish the strength requirements for the material specification.

### Tension Tests

The calculated tensile strengths of all tension specimens tested are summarized in Table 3. The 2.54cm (1-inch) wide by 25.4cm (10-inch) long parallel edge composite strips had all been reinforced at the ends by bonded 1.524mm (0.06 inch) thick and 7.62cm (3-inch) long fiberglass end tabs with a 2.54cm (1 inch) scarfed edge adjoining the test section. This method of protection from grip damage is quite satisfactory because in all but four tests the failures were well within the 10.16cm (4 inch) gage length section. Even in those four specimens where the failures were at, or near, the edge the calculated values were quite high. Comparing the average room temperature tensile strength of 565MPa (81,930 psi) with the 555MPa (80,562 psi) average obtained at room temperature after 1000 hours aging at 505K(450°F) and the 602MPa (87,300 psi) average obtained at 505K (450°F), it is seen that not only is very little strength lost by this material from long term aging at 505K(450°F), but it even becomes stronger when heated briefly at 505K(450°F) and then tested. The significance of this observation coupled with the test results of the interlaminar shear specimens is that although the aluminum matrix is softened and slightly weakened by 505K(450°F) temperature, it is still adequately strong to maintain laminate continuity and enable the unaffected boron filaments to predominately support tensile loads. Indeed, the increased ductility (and hence toughness) of the aluminum at 505K (450°F) may even be beneficial in reducing local stress concentrations or residual stresses and thereby lead to some tensile strength improvement at moderately elevated temperatures.

Stress-strain curves of tension specimens tested at room temperature are shown in Figures 18 through 28. Figures 18 through 21 were plotted with strain data obtained from strain gages, whereas Figures 23 through 28 were obtained using an extensometer. As a check on the uniformity of loading by the tension grips, the first strain gaged specimen had longitudinal strain gages on opposite faces. Figure 19 indicated that both gages gave nearly identical readings which demonstrated that the specimens were being loaded axially. In addition, to obtain Poisson's ratio, the first three specimens had transverse strain gages as well as longitudinal gages. Because extensometers are too delicate to survive the shock, they must be removed prior to failure of the specimen so the final portion of the stress-strain history is not measured. The dotted portions of the stress-strain curves of Figures 22 through 28, therefore indicate they have been obtained by extrapolation.

TABLE 2  
QUALIFICATION AND DEMONSTRATION TESTS

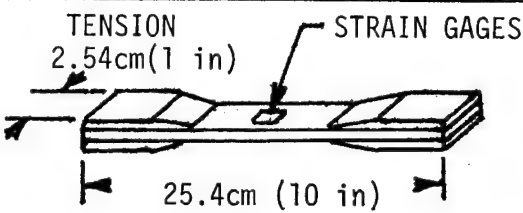
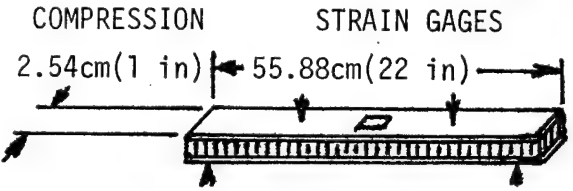
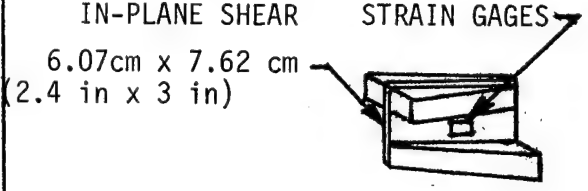

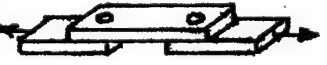



TYPE OF TEST	TEST TEMP ( K )	NO. OF SPECIMENS	MEASURED DATA
<p>TENSION</p>  <p>2.54cm (1 in)</p> <p>25.4cm (10 in)</p> <p>STRAIN GAGES</p>	<p>RT</p> <p>505</p> <p>RT after 1000 hrs at 505</p>	<p>10</p> <p>10</p> <p>10</p>	<p><math>F_{tu}, E_t, \nu, \epsilon_x</math></p> <p><math>F_{tu}</math></p> <p><math>F_{tu}</math></p>
<p>COMPRESSION</p>  <p>2.54cm (1 in)</p> <p>55.88cm (22 in)</p> <p>STRAIN GAGES</p>	<p>RT</p> <p>420 &amp; 505</p> <p>RT after 1000 hrs at 505</p>	<p>10</p> <p>10</p> <p>10</p>	<p><math>F_{cu}, E_c, \nu, \epsilon_x</math></p> <p><math>F_{cu}</math></p> <p><math>F_{cu}</math></p>
<p>IN-PLANE SHEAR</p>  <p>6.07cm x 7.62 cm (2.4 in x 3 in)</p> <p>STRAIN GAGES</p>	<p>RT</p> <p>367 to 505</p> <p>RT after 1000 hrs at 505</p>	<p>10</p> <p>10</p> <p>10</p>	<p><math>F_{su}, G</math></p> <p><math>F_{su}</math></p> <p><math>F_{su}</math></p>
<p>INTERLAMINAR SHEAR</p>  <p>0.635 x 3.048cm (0.25 x 1.2 in)</p>	<p>RT</p> <p>505</p> <p>RT after 1000 hrs at 505</p>	<p>10</p> <p>10</p> <p>10</p>	<p><math>F_{su}</math></p> <p><math>F_{su}</math></p> <p><math>F_{su}</math></p>
<p>BOLT SHEARING</p>  <p>2.85cm x 10.16cm (1.12 in x 4 in)</p> <p>2 Configurations</p>	<p>RT</p>	<p>20</p>	<p><math>P_u</math></p>
<p>METALLOGRAPHY</p> 		<p>3</p>	<p>BOND QUALITY AND UNIFORMITY, FILAMENT DISTRIBUTION AND DEGRADATION</p>
<p>SCANNING ELECTRON FRACTOGRAPHY (TO BE PERFORMED ON SELECTED FAILED SPECIMENS)</p> 		<p>5</p>	<p>BOND QUALITY</p>
<p>TENSION FATIGUE</p>  <p>P</p> <p>P</p>	<p>RT</p>	<p>10</p>	<p>CYCLES TO FAILURE</p>

TABLE 3

RESULTS OF TENSION TESTS AT ROOM TEMPERATURE 505K(450°F) AND  
AT ROOM TEMPERATURE AFTER 1000 HOURS AGING AT 505K (450°F)

(BORON/ALUMINUM-90°,45°,90°,0°,-45°,0°,-45°,0°,90°,45°,90°)

ULTIMATE TENSILE STRENGTH								
AT ROOM TEMP			AT 505K (450°F)			AT ROOM TEMP AFTER 1000 HRS AT 505K (450°F)		
SPEC NO	MPa	PSI	SPEC NO	MPa	PSI	SPEC NO	MPa	PSI
11	470.9	68,296	1	557.5	80,856	21	540.8	78,438
12	628.4	91,136	2	606.1	87,905	22	599.0	86,875
13	635.4	92,158	3	632.9	91,791	23	554.4	80,413
14	629.9	91,364	4	628.6	91,165	24	576.0	83,543*
15	623.7	90,463	5	626.8	90,909	25	563.1	81,665
16	546.6	79,276	6	631.2	91,551	26	555.9	80,625
17	528.7	76,683	7	623.9	90,486	27	529.9	76,851
18	495.5	71,859*	8	560.9	81,351	28	532.7	77,261*
19	517.8	75,094**	9	566.2	82,115	29	549.2	79,660
20	572.1	82,974	10	585.3	84,893	30	553.6	80,290
AVG	564.9	81,930		601.9	87,302		555.5	80,562
STD DEV	61.7	8,950		31.4	4,550		20.6	2,979

NOTE: \* Failure occurred at edge of scarfed end tab  
 \*\* Failure occurred at 3.18mm (1/8 in) within scarfed end tab

In testing Specimen 11 (Figure 18) the grips (which consisted of thick serrated steel plates clamped against the specimen with six bolts) slipped and the specimen had to be unloaded and the plate bolts tightened. This happened twice but the third time the bolts and grip plates held and the specimen was successfully tested to failure. When the stress-strain curve of Figure 18 was plotted however, it was observed that each time the specimen had been unloaded it retained a "permanent set" which was equal to about one-third of the maximum strain that had been reached prior to unloading. This behavior was checked again with Specimen 15 (Figure 23), Specimen 16 (Figure 24), Specimen 17 (Figure 25), and Specimen 18 (Figure 26). Finally in the case of Specimen 20 (Figure 28) the grips slipped once again and had to be tightened before the specimen could be loaded to failure. In these six specimens, the respective strains from which the specimens were unloaded varied from about 10 to 95% of the maximum strain at failure, but in each case the "permanent set" was approximately one-third of the strain prior to unloading.

Stress-strain curves of tension specimens tested at room temperature after 1000 hours aging at 505K (450°F) are shown in Figures 29 through 38. Strain readings were all obtained by means of an extensometer and therefore dotted line extensions of each curve indicate the approximate extrapolations to failure. As in the case of the previous room temperature tension tests, six of the specimens were unloaded prior to failure and then loaded again to determine whether the magnitude of the "permanent set" had been effected by the aging, ie; Specimen 23 (Figure 31), Specimen 24 (Figure 32), Specimen 25 (Figure 33), Specimen 26 (Figure 34), Specimen 27 (Figure 35), and Specimen 28 (Figure 36). In this group of six specimens each unloading occurred when the tensile stress reached 345MPa (50,000 psi) and the corresponding "permanent set" was consistently about one-quarter of the maximum strain reached prior to unloading. Because these specimens had not been unloaded completely (about 41.4MPa (6000 psi) stress remaining) the curves had to be extrapolated to zero stress to obtain an approximate strain at zero stress reading. Nevertheless, the smaller ratio of "permanent set" indicated that the 1000 hours aging at 505K (450°F) may have metallurgically effected the aluminum matrix and increased its resistance to incurring "permanent set".

Additional observation of the stress-strain curves of Figures 18 through 38 indicated that all curves followed a characteristic bilinear pattern with an initial slope or "primary modulus" which was relatively brief but about twice as large as the much more extensive subsequent slope or "secondary modulus". As illustrated in the schematic, Figure 39, when the specimen was unloaded and then reloaded prior to failure, the reloading curve essentially paralleled the higher initial slope up to the unloading point and then continued along the lower second slope. Although it is primarily speculative, a plausible explanation of this behavior has been devised as follows: "When boron aluminum composite with a multiple ply orientation including 0°, 90°, and +45° layers is cooled from its bonding temperature, the greater coefficient of contraction of the aluminum matrix leads to a residual stress condition where the compression in the 0° boron fibers is balanced by tension in the matrix. Upon initial loading, a complete rearrangement of residual and imposed stresses takes place with the boron compressive stresses reducing to zero and the aluminum tensile stresses rising higher. With the aluminum supporting an appreciable proportion of the load, the primary modulus is relatively high but because of the strain magnification in the matrix of the 90° fibers and because of the rotation of the +45° fibers in the direction of the tensile load, gradual micro-cracking and slipping of the matrix occurs which cannot be reversed completely when the specimen is unloaded. After the knee of the curve is passed, the aluminum matrix, which is now plastic, no longer picks up additional load and

the secondary slope or modulus is controlled primarily by the elastic elongation of the boron alone. If the specimen is unloaded prior to failure, it will exhibit a permanent set which indicates that the residual stresses are now reversed and the tension in the fibers is balanced by compression in the matrix. Furthermore, when the specimen is reloaded, the matrix contributes to supporting the load as long as some of its compression remains and hence the primary slope region is repeated and increased. But when the same stress is reached from which the specimen was previously unloaded, then the residual compression in the aluminum is completely reduced and again, the aluminum yields plastically, microcracks and 45° fiber alignment continue, and the stress-strain curve proceeds along the lower secondary modulus slope".

The primary and secondary slopes or moduli taken from the tensile specimens shown in Figures 18 through 38, together with the maximum strains obtained either from actual strain gage readings or extrapolated data are summarized in Table 4. It can be seen that the primary modulus is consistently about twice as high as the secondary modulus and that the ranges and averages of both moduli as well as the strain at failure was about the same in both groups of specimens. It was concluded that the 1000 hours aging at 505K (450°F), had no appreciable effect on the moduli or the maximum strains of the boron aluminum composite.

To obtain information on the Poisson's ratio of boron/aluminum composites tested in tension, both sides of specimen 11 had been instrumented with longitudinal and lateral strain gages. As previously discussed, specimen 11 slipped twice in the grips during the testing so it was loaded and unloaded three times as shown in Figure 18. During each run the calculated ratio of the lateral and longitudinal strain gage readings (ie; Poisson's ratio) varied from run to run, from one side to the other side and from the beginning of the run to the end of the run. These data have been plotted on Figures 40 and 41. Although there was considerable scatter in the calculated results, the trend that appeared was that during initial loading, the Poisson's ratio remained approximately constant at a value of about 0.20 as stress increased. Upon unloading and reloading, the rearrangement of the residual stress distribution in some way effected this trend so the Poisson's ratio started low and increased asymptotically to the same value of about 0.20 as stress increased. As the stresses at which unloading increased, the initial value of Poisson's ratio decreased proportionally. Specimens 12 and 13 were instrumented with longitudinal and lateral strain gages (on one side only) and the calculated Poisson's ratio curves are shown in Figures 42 and 43. Again there was considerable scatter but the results were consistent with the first loading of Specimen 11 in that Poisson's ratio did not vary much from the 0.20 as stress increased.

TABLE 4

MODULUS OF ELASTICITY AND STRAIN AT FAILURE FROM  
TENSION TESTS AT ROOM TEMPERATURE AND AT ROOM  
TEMPERATURE AFTER AGING 1000 HOURS AT 505K(450°F)  
(BORON/ALUMINUM-90°, 45°, 90°, 0°, -45°, 0°,  
-45°, 0°, 90°, 45°, 90°)

(SPECIMENS LOADED IN 90° DIRECTION)

SPEC NO.	AGING AT 505 (450°F)  HOURS	PRIMARY MODULUS		SECONDARY MODULUS		STRAIN AT FAILURE
		$\frac{GN}{m^2}$	PSI	$\frac{GN}{m^2}$	PSI	
11	0	151.0	21.9x10 <sup>6</sup>	79.3	11.5x10 <sup>6</sup>	0.0052
12	0	153.8	22.3	89.6	13.0	0.0059
13	0	129.6	18.8	80.0	11.6	0.0072
14	0	193.7	28.1	88.3	12.8	0.0072
15	0	137.9	20.0	83.4	12.1	0.0071
16	0	151.7	22.0	84.1	12.2	0.0061
17	0	166.9	24.2	82.0	11.9	0.0057
18	0	151.0	21.9	86.9	12.6	0.0053
19	0	163.4	23.7	87.6	12.7	0.0055
20	0	163.7	23.6	86.9	12.6	0.0061
AVG		156.3	22.7	84.8	12.3	0.0061
STD DEV		17.3	2.5	3.6	0.5	0.0008
21	1000	142.0	20.6	84.1	12.2	0.0062
22	1000	134.4	19.5	80.0	11.6	0.0071
23	1000	137.9	20.0	84.1	12.2	0.0063
24	1000	126.9	18.4	84.1	12.2	0.0067
25	1000	162.0	23.5	84.1	12.2	0.0065
26	1000	141.3	20.5	83.4	12.1	0.0066
27	1000	129.6	18.8	84.1	12.2	0.0061
28	1000	182.0	26.4	86.9	12.6	0.0060
29	1000	156.5	22.7	84.8	12.3	0.0062
30	1000	142.0	20.6	86.2	12.5	0.0060
AVG		145.5	21.1	84.2	12.2	0.0064
STD DEV		16.8	2.4	1.8	0.3	0.0004

## Compression Tests

The first three room temperature compression specimens were strain-gaged and loaded in a four point bending (Figure 44). Their stress-strain plots are shown in Figures 45, 46, and 47. A tested and an untested compression specimen are shown together in Figure 48.

The first specimen was tested four times before it failed because the limits set on the strain recording instruments were exceeded three times. Each time a strain limit was exceeded the specimen was brought back to zero load and the strain instrumentation adjusted before resuming the test. When the strain limit was exceeded the strain reading was lost, so the magnitude of permanent set at zero load was also lost. Therefore, the graph of specimen #11 plotted all four runs as starting from zero longitudinal strain. The presence of permanent set in specimen 11 can be surmised from the graph of specimen 12's response to multiple loadings, Figure 46. Having determined the maximum strain settings for the instrumentation from specimen 11, specimen 12 was loaded up to 521 MPa (75,525 psi), then unloaded to 174 MPa (25,175 psi), loaded to 1041 MPa (151,050 psi), unloaded back to 174 MPa (25,175 psi), loaded to 1388 MPa (201,400 psi), unloaded back to 174 MPa (25,175 psi), then finally loaded to failure at 1875 MPa (271,890 psi). It is apparent that most of the permanent set occurred in the first loading amounting to 0.0024 cm/cm, or 12.5% of the total strain to failure. As with the tension specimens, the modulus varied with load, higher near zero stress and lower at higher stresses.

The stress-strain plots of the remaining seven room temperature compression specimens are shown in Figures 49 through 55. The strain data for these specimens was obtained with an extensometer rather than with strain gages. Apparently the two strain measuring techniques are not equivalent because the slopes, or moduli, determined from the stress-strain curves of the former were about 25% greater than those of the latter. The calculated compression strengths of all room temperature specimens tested are summarized in Table 5, and the primary and secondary moduli together with the maximum strain gage readings are summarized in Table 6. Comparing the tension and compression tests data obtained from strain gaged specimens listed in Tables 3, 4, 5, and 6, the compression strengths and strains at failure are more than three times greater, the primary moduli are approximately 9% less, the secondary moduli are approximately 12% greater. The ratio of primary to secondary moduli for tension and compression tests is 1.75 and 1.40, respectively. Observation of the failed compression specimens (Figure 56) indicated that when failure occurred it was very catastrophic with a massive combination of crushing and shearing of the aluminum matrix and buckling of the filaments.

The results of the room temperature tests of the 10 specimens aged at 505K (450°F) for 1000 hours are also shown in Tables 5 and 6. The averages reflect a slight decrease in moduli, compression strengths, and strain at failure from the room temperature tests, but only on the order of 3 to 10%. The stress-strain curves for the 1000 hour-aged specimens are shown in Figures 57 to 66.

The 10 elevated temperature specimens were originally to be tested at 505K (450°F), but after the first five experienced adhesive failures at that temperature, the test temperature was lowered to 422K (300°F). As can be seen in Table 5, the 422K (300°F) temperature raised the adhesive strength somewhat, but not sufficiently to produce a consistently good boron/aluminum failure. The calculated stresses for the boron/aluminum (when the adhesive failed) are still quite

TABLE 5  
RESULTS OF COMPRESSION TESTS AT ROOM TEMPERATURE, ELEVATED TEMPERATURE,  
AND AT ROOM TEMPERATURE AFTER 1000 HOURS AGING AT 505K (450°F)  
(BORON/ALUMINUM - 90°, 45°, 90°, 0°, -45°, 0°, -45°, 0°, 90°, 45°, 90°)

ULTIMATE COMPRESSION STRENGTH IN 90° DIRECTION												
AT ROOM TEMPERATURE				AT ELEVATED TEMPERATURE				AT ROOM TEMPERATURE AFTER AGING 1000 HOURS AT 505K (450°F)				
SPEC NO	MPa	PSI	FAILURE MODE	SPEC NO	TEST TEMP	MPa	PSI	FAILURE MODE	SPEC NO	MPa	PSI	FAILURE MODE
11	1868.3	270,974	1	1	505K (450°F)	1076.0	156,064	4	21	1704.4	247,207	1
12	1874.6	271,890	1	2	↓	911.0	132,128	5	22	1524.9	221,163	2
13	1900.6	275,660	1	3		860.4	124,787	5	23	1542.7	223,755	4
14	1850.9	268,454	1	4	↓	940.4	136,402	5	24	1444.9	209,564	3
15	1920.8	275,977	1	5		836.2	121,280	5	25	1845.4	267,652	1
16	1726.0	250,339	1	6	422K (300°F)	1025.3	148,704	4	26	1261.4	182,946	2
17	1576.7*	228,683*	4	7	↓	1095.3	158,858	4	27	1922.0	278,763	1
18	1767.9	256,415	2	8		1207.5	175,126	5	28	1855.2	269,070	2
19	1902.0	275,862	1	9	↓	1207.0	175,063	2	29	1669.7	242,176	1
20	1973.8	286,270	2	10		1126.3	163,358	5	30	1862.0	270,056	1
AVG	1865.0	270,204		AVG	505K	924.8	134,130		AVG	1663.3	241,235	
STD DEV	76.4	10,866				93.9	13,626			216.3	31,371	
				AVG	422K	1132.3	164,221					
STD DEV						77.6	11,256					

NOTES: \* Data not used in calculation of average

FAILURE MODE 1 - Compression Failure of B/A1 between Load Points 3 - B/A1 failure outside of Load Points  
2 - B/A1 failure at Load Point 4 - Adhesive failure under B/A1 Face  
5 - Adhesive failure under Steel Face

TABLE 6

MODULUS OF ELASTICITY AND STRAIN AT FAILURE FROM  
COMPRESSION TESTS AT ROOM TEMPERATURE AND AT ROOM  
TEMPERATURE AFTER AGING 1000 HOURS AT 505K(450°F)

(BORON/ALUMINUM-90°,45°,90°,0°,-45°,0°,-45°,0°,  
90°,45°,90°)

(SPECIMENS LOADED IN 90° DIRECTION)

SPEC NO	AGING AT 505K (450°F) HOURS	PRIMARY MODULUS		SECONDARY MODULUS		STRAIN AT FAILURE
		GPa	PSI	GPa	PSI	
11	0	145.5	21.1x10 <sup>6</sup>	91.7	13.3x10 <sup>6</sup>	0.0190
12	0	131.7	19.1	94.5	13.7	0.0191
13	0	120.7	17.5	97.9	14.2	0.0191
14	0	116.5	16.9	80.7	11.7	0.0216
15	0	106.2	15.4	82.7	12.0	0.0217
16	0	102.0	14.8	81.4	11.8	0.0202
17	0	104.8	15.3	82.7	12.0	0.0174
18	0	104.2	15.4	78.6	11.4	0.0198
19	0	106.9	15.5	80.7	11.7	0.0216
20	0	102.0	14.8	78.6	11.4	0.0227
AVG		114.1	16.6	85.0	12.3	0.0202
STD DEV		14.7	2.1	7.0	1.0	0.0016
21	1000	106.2	15.4x10 <sup>6</sup>	83.4	12.1x10 <sup>6</sup>	0.0188
22	1000	94.5	13.7	75.8	11.0	0.0176
23	1000	102.7	14.9	82.7	12.0	0.0170
24	1000	95.8	13.9	77.9	11.3	0.0164
25	1000	111.7	16.2	83.4	12.1	0.0204
26	1000	109.6	15.9	82.7	12.0	0.0133
27	1000	95.8	13.9	79.3	11.5	0.0202
28	1000	96.5	14.0	82.7	12.0	0.0212
29	1000	102.0	14.8	81.4	11.8	0.0189
30	1000	106.9	15.5	79.3	11.5	0.0215
AVG		102.2	14.8	80.9	11.7	0.0185
STD DEV		6.3	0.9	2.6	3.8	0.0025

high compared to the tension strength, averaging 924.8MPa (134,130 psi) for the 505K (450°F) compression tests and 1132MPa (164,221 psi) for the 422K(300°F) compression tests.

To obtain information on the Poisson's ratio of the boron aluminum composites tested in compression specimens 11, 12, and 13 were instrumented with longitudinal and lateral strain gages. This data is shown in Figure 67. As in the case of most of the tensile Poisson's ratio curves shown in Figures 40, 41, 42, and 43, some of the compression Poisson's ratio curves were obtained after the specimens had been loaded and unloaded several times prior to plotting of the data. Although there was considerable difference between the curves of the three specimens, the trend (as with the tension Poisson's ratio curves) that appeared was that during initial loading the Poisson's ratio started low and increased asymptotically to a constant value. Whereas this value was about 0.2 in the case of the tension Poisson curves, it was considerably higher (ie; from 0.29 to 0.34) in the case of the compression Poisson curves.

### Rail Shear Tests

The room and elevated temperature rail shear specimen test results are given in Table 7. It was found that the elevated temperature adhesive, HT424, was good only for about 9.65Pa (1400 psi) shear at 505 K (450°F), so the steel rails sheared off before the boron/aluminum failed. Knowing that the adhesive's strength would increase with lower temperatures, the sixth specimen was tested at 422 K (300°F). Since the adhesive still failed before the boron/aluminum (although at a higher adhesive stress than at 505 K (450°F)), the test temperature was lowered to 394 K (250°F). Although the adhesive shear strength again improved, it still was insufficient to fail the boron/aluminum, so the test temperature was reduced to 367 K (200°F), and a boron/aluminum failure was achieved with two of the remaining three specimens at that temperature. Figure 68 shows two specimens, 8 and 10. Specimen 10 is on the left and is typical of the specimens with adhesive failure. #8, on the right, displays the failure of the boron/aluminum. A close-up of 8 is shown in Figure 69. This failure apparently traversed along one rail bondline edge and then jumped to the other edge along a 45° plane at about the middle of the specimen. It, too, is typical of those specimens which failed in the boron/aluminum. SEM observation of the failure surface along the bondline edge (Figure 70) indicated that the 0° and 90° fibers failed in shear whereas some of the 45° fibers failed in tension at the interface between the fibers and the aluminum matrix.

The room temperature rail shear specimens using a different adhesive, Hysol EA951, all failed the boron/aluminum. The average boron/aluminum shear stress at failure was 338.7MPa (49,131 psi). The first three specimens tested were strain-gaged and their stress-strain curves are shown in Figures 71-73. The shear modulus at higher stresses is seen to be approximately 17.2 GPa ( $2.5 \times 10^6$  psi), and at lower stresses to be about 41.4 GPa ( $6 \times 10^6$  psi).

The primary and secondary slopes or moduli taken from the shear specimens shown in Figures 71 through 73 together with the maximum strains are summarized in Table 8. As with the tensile test results summarized in Table 4, the primary moduli were approximately twice as high as the secondary moduli. The magnitude of the shear moduli, however, were only about a quarter of the respective tensile moduli.

To determine whether unloading before failure in shear resulted in a similar "permanent set" as in the case of the tension and compression, one of the specimens (#13) was unloaded before failure and reloaded again. This permanent set was approximately one quarter of the shear strain prior to unloading.

TABLE 7

RESULTS OF RAIL SHEAR TESTS AT ROOM TEMPERATURE, ELEVATED TEMPERATURE AND AT ROOM TEMPERATURE AFTER 1000 HOURS AT 505 K (450°F)

(BORON/ALUMINUM-90°, 45°, 90°, 0°, -45°, 0°, 45°, 0°, 90°, 45°, 90°)

(SPECIMENS LOADED PARALLEL TO 90° DIRECTION)

U L T I M A T E   R A I L   S H E A R   S T R E N G T H									
AT ROOM TEMPERATURE			AT ELEVATED TEMPERATURE				AT ROOM TEMP AFTER AGING 1000 HRS AT 505 K (450°F)		
SPEC NO.	MPa	PSI	SPEC NO.	TEST TEMP	MPa	PSI	SPEC NO.	MPa	PSI
1	294.1	42,658	11	505 K	216.3	31,371*	21	282.4	40,964
2	302.3	43,849	12	(450°F)	219.1	31,781*	22	289.5	41,986
3	380.3	55,158	13	↓	228.2	33,097*	23	307.6	44,614
4	300.8	43,625	14		230.3	33,401*	24	289.6	42,002
5	361.2	52,390	15	↓	199.1	28,875*	25	362.3	52,552
6	342.7	49,702	16	422 K (300°F)	250.9	36,391*	26	284.0	41,194
7	359.1	52,083	17	394 K (250°F)	271.6	39,395*	299.8	299.8	43,487
8	362.5	52,579	18	367 K (200°F)	285.2	41,362	28	301.6	43,737
9	376.2	54,563	19	↓	299.6	43,448	29	274.6	39,826
10	308.2	44,706	20	↓	247.3	35,874*	30	269.2	39,047
AVG	338.7	49,131	AVG	367 K (200°F)	292.4	42,405	AVG	296.1	42,941
STD DEV	33.9	4,911			10.2	1,475		26.2	3,797

\* Cohesive failure of adhesive; boron/aluminum did not fail,  
Data not used in calculation of average

### Interlaminar Shear Tests

Table 8 summarizes the results of the room temperature interlaminar shear tests. Specimens #1 and #2 were tested with the testing jig set at a span of 8.13mm (0.32 inch) which is representative of a 4 to 1 span to thickness ratio. Because both specimens failed in tension rather than interlaminar shear, the jig was adjusted to its minimum span of 6.35mm (0.25 inch) which is representative of a 3 to 1 span to thickness ratio. Most of the remaining specimens failed at slightly higher loads, but the failures were still all tensile rather than interlaminar shear. It was concluded that because the specimens were so thin and because the fiber orientations were varied rather than unidirectional, it would not be possible to induce an interlaminar shear failure prior to tensile failure. Consequently, the shear stresses reported in Table 8 are on the low bound. Nevertheless, the magnitudes of the calculated stresses reported were appropriately high and were in the range of values normal for unidirectional boron/aluminum composites.

Table 8 also summarizes the results of the interlaminar shear tests at 505K (450°F) and at room temperature after the specimens had been aged 1000 hours at 505K (450°F). As in the case of the room temperature tests, all specimens failed in tension rather than interlaminar shear, even though the span was kept at the minimum 6.35mm (0.25 inch). Comparison of the average interlaminar shear strength values of Table 8 indicate that the reductions from room temperature strengths were modest, ie; about 20% after 1000 hours aging at 505K(450°F) and about 30% while at 505K (450°F).

### Bolt Bearing Tests

The bolt bearing test specimen, as shown in Figure 9, consisted of a 2.86cm (1 1/8 inch) wide by 10.16cm (4 inch) long strip of 2.03mm (0.08 inch) thick boron/aluminum mechanically fastened to two strips of 2.86cm (1 1/8 inch) wide by 10.16cm (4 inch) long by 1.02mm (0.04 inch) thick titanium. This specimen was gripped and pulled in tension until one of the two fastened ends failed, after which the remaining two fastened pieces were regripped and pulled in tension until the other fastened end failed. Two different fastener sizes and types were tested, ie; 3.97 and 4.76mm (5/32 and 3/16 inch) titanium Hi-Loks. The 20 results of the 10 specimens tested are summarized in Table 9. The first fastener failure load of each of the specimens was designated as "A" and the second as "B". Test scatter of similar specimens was low and the preloading that the "B" laps received when the "A" laps failed did not seem to reduce their values. The average failure load of the 3.972mm (5/32 inch) Hi-Lok fastened specimens was 636.5N (1431 pounds) and the corresponding average failure load of the 4.762mm (3/16 inch) Hi-Lok fastened specimens was 7,353N (1653 pounds). The typical mode of failure of most of the specimens is illustrated in Figure 74. When the ultimate load was reached, two tension cracks simultaneously started at location "A". This increasing crack length rapidly raised the tensile stress at location "B" until a second crack started in a direction perpendicular to the first two cracks. When the specimens finally failed, the two square corners around the hole were completely torn from the specimen ends and the Hi-Lok fastener had been pulled out.

TABLE 8

RESULTS OF INTERLAMINAR SHEAR TESTS AT ROOM TEMPERATURE, 505K (450°F), AND AT ROOM TEMPERATURE AFTER 1000 HOURS AGING AT 505K (450°F)

(BORON/ALUMINUM-90°,45°,90°,0°,-45°,0°,-45°,0°,90°,45°,90°)

INTERLAMINAR SHEAR STRENGTH (1)								
AT ROOM TEMPERATURE			AT 505K (450°F)			AT ROOM TEMP AFTER 1000 HRS AT 505K (450°F)		
SPEC NO.	MPa	PSI	SPEC NO.	MPa	PSI	SPEC NO.	MPa	PSI
1	123.3(2)	17,878(2)	11	91.1	13,214	21	107.6	15,611
2	121.1(2)	17,568(2)	12	81.9	11,879	22	110.3	16,000
3	127.2(3)	18,449(3)	13	89.4	12,961	23	105.0	15,228
4	132.0	19,152	14	88.5	12,830	24	105.3	15,278
5	132.3	19,195	15	89.7	13,009	25	99.9	14,494
6	132.7	19,242	16	89.7	13,005	26	98.7	14,313
7	132.6	19,236	17	86.5	12,547	27	103.2	14,965
8	124.4	18,048	18	88.1	12,785	28	103.7	15,036
9	122.0	17,692	19	82.6	11,974	29	94.9	13,759
10	131.7	19,098	20	88.5	12,841	30	107.4	15,584
AVG	129.4(4)	18,764(4)	AVG	87.6	12,705	AVG	103.6	15,027
STD DEV	4.3	616		3.2	446		4.6	675

- NOTES: (1) Shear stress was calculated from formula,  $F_s = 0.75 P/wt$   
 (2) For these two tests, the simple beam span was 8.128mm(0.32 in)  
 (3) For specimens #3 to #30 inclusive, the simple beam span was reduced to 6.35mm(0.25 in), which was the minimum obtainable with available equipment  
 (4) This average interlaminar shear stress is for specimen #3 through #10 only

TABLE 9  
RESULTS OF BOLT BEARING TESTS

SPEC NO.	TITANIUM HI-LOK SIZE		FAILURE LOAD	
	mm	in	N	lb
1A	3.97	5/32	6343	1426
1B	↓	↓	6583	1480
2A			6263	1408
2B			6236	1402
3A			6405	1440
3B			6389	1436
4A			6343	1426
4B			6485	1458
5A			6085	1368
5B			6512	1464
AVG			6364	1431
STD DEV			146	33
6A	4.76	3/16	7117	1600
6B	↓	↓	7206	1620
7A			7633	1716
7B			7784	1750
8A			7579	1704
8B			7330	1648
9A			7482	1682
9B			7562	1700
10A			7277	1636
10B			7001	1574
AVG			7397	1663
STD DEV			250	56

Additional examination of the failed specimens indicated that because single lap joints undergo considerable bending at the fastener by the time they fail, the head of the Hi-Lok fastener left a severe dent in the surface of the boron/aluminum composite. Scanning electron microscope (SEM) pictures (Figure 75) of this area demonstrated that the denting produced severe crushing damage of the surface layers of filaments.

To obtain a comparison of the bolt bearing strength of boron/aluminum composite with that of titanium, two of the undamaged strips of titanium were bolted together with a 4.762mm (3/16 inch) titanium Hi-Lok and then pulled until failure occurred. The failure load for the 1.016mm (0.04 inch) thick titanium strip specimen was 7517N (1690 pounds). This value compared closely with the 7397 (1663 pounds) average for the boron/aluminum specimens with the same fastener but of course the titanium was only half as thick as the boron/aluminum.

#### Tension Fatigue Tests

Tension fatigue tests were conducted on boron aluminum specimens which were 2.54cm (1.00 inch) wide and contained a 4.775mm (0.188 inch) hole in their centers. The R value (ie; minimum stress to maximum stress ratio) for all specimens was 0.1. Two of the specimens were tested statically in tension to obtain the first point on the S-N fatigue curve and the strengths of these together with the cycled test data are summarized in Table 10 and Figure 76. At a stress of 242.8MPa (35,222 psi), which represented 66.6 percent of the 364.5MPa (52,867 psi) average of the statically tested specimens, the number of cycles to failure exceeded the desired  $10^6$  cycle limit and hence this stress was determined to be the "fatigue strength" of the material. One of these two specimens reached 3,139,000 cycles before failure occurred (in the bonded steel extension plates, Figure 77). All the other specimens failed in tension at the minimum cross-sectional area in the vicinity of the hole. It was interesting to observe that in all of the specimens cracks appeared at the edges of the hole even after a relatively low number of cycles, but after progressing only about 0.794mm (1/32 inch), a second pair of cracks opened up, as shown in Figure 78, in a direction parallel to the load and grew progressively longer until catastrophic failure occurred when the cracks again turned perpendicular to the load.

It was theorized that the cracks perpendicular to the loading direction occurred first because of the local damage to the longitudinal fibers just under the surface, at the edges of the holes produced by the hole punching process, ie; see Figures 13, 14, 15, and 16. Subsequent fatigue loading then produced cracks parallel to the loading direction in the aluminum because of differential straining between those boron fibers, which were broken and hence supported no tensile load, and those that were not broken and hence produced a high stress concentrated load.

SEM photos were taken of the fractured surface of Specimen 2 which was tested statically to failure (Figure 79) and the fractured surface of Specimen 3 (Figure 80) which was cycled 2,362,000 times at a maximum alternating tensile stress of 242.8MPa (35,222 psi). Whereas the former showed clean, sharp, splits across filaments as well as the matrix, the latter showed a fragmented, worn, surface at the edges of the hole as the cracks gradually spread from fiber to fiber.

TABLE 10

RESULTS OF FATIGUE TESTS OF 2.54cm (1.00 inch) WIDE  
TENSION SPECIMENS WITH A 4.775mm (0.188 inch) HOLE  
IN THE CENTER

SPECIMENS LOADED IN 0° DIRECTION

BORON/ALUMINUM 90°, 45°, 90°, 0°, -45°, 0°, -45°, 0°, 90°,  
45°, 90°

SPEC NO.	STRESS		CYCLES TO FAILURE
	MPa	PSI	
1	365.8	53,058	Tested statically to failure
2	363.2	52,676	Tested statically to failure
3	242.8	35,222	2,362,000
4	242.8	35,222	3,139,000 *
5	291.6	42,300	210,000
6	291.6	42,300	178,000
7	328.2	47,600	300
8	311.6	45,200	59,000
9	273.7	39,700	453,000
10	255.1	37,000	394,000

\* Failed in Grip at Bearing Hole

## Summary of Demonstration Test Data

Table 11 contains the minimum values of the demonstration tests summarized in this section and has therefore been labeled "Suggested Material Properties".

The original aft pylon skin panel was made of commercially pure titanium (annealed with  $F_{tu} = 551.6\text{MPa}$  (80,000 psi)). Table 12 gives a comparison between the material properties for this titanium derived from Mil-Hdbk-5B and the results of Table 11 for the particular substituted boron/aluminum composite.

Figure 81 gives a comparison of the fatigue properties for commercially pure titanium (annealed with  $F_{tu} = 551.6\text{MPa}$  (80,000 psi)) derived from the fatigue properties of Ti-8Al-1Mo-1V titanium taken from Mil-Hdbk-5B and the fatigue properties of the particular substituted boron/aluminum composite.

## COMPONENT FABRICATION

This section contains the description of the fabrication of the boron/aluminum skin components, their assembly onto the substructure, and the associated quality control and non-destructive testing that was exercised to ensure the quality of the components. From records of the time and material expended, a cost analysis of the fabrication of the four boron/aluminum component skins was conducted and a comparison made with the existing titanium skins. Of the four boron/aluminum skins received, three were used for flight service demonstration tests and the fourth was delivered to NASA Langley Research Center for storage and possible installation at a later date.

### Fabrication Plan

After the fabrication developments described in Section II and the component design drawings described in Section III were completed, the Fabrication Plan (included as Appendix C) was prepared. This plan contained the exact details of the fabrication of the skins as well as the punching, trimming, and

TABLE 11  
SUGGESTED MATERIAL PROPERTIES OF  
BORON/ALUMINUM COMPOSITE WITH 90°,  
45°, 90°, 0°, -45°, 0°, -45°, 0°,  
90°, 45°, 90° FILAMENT ORIENTATION (a)

MATERIAL PROPERTY	ROOM TEMPERATURE		AT 505K (450°F)		AT ROOM TEMP AFTER 1000 HRS AT 505K	
	MPa	PSI	MPa	PSI	MPa	PSI
$F_{tu}$	470.9	68,296	557.5	80,856	529.9	76,851
$F_{cy}$	1726.0	250,339	836.2	121,280	1704.4	247,207
$F_{su}$ (In-Plane)	294.1	42,658	>230.3	>33,401	269.2	39,047
$F_{su}$ (Inter-laminar)	>122.0	>17,692	>81.9	>11,879	>94.9	>13,759
$F_{bru}$ 4.76mm (3/16 in)	723.5	104,933	-	-	-	-
TENSION FATIGUE STRENGTH K = 2.52	242.8	35,222	-	-	-	-

(a) All properties except fatigue were measured in the 90° direction. Fatigue specimens were loaded in the 0° direction.

TABLE 12

MATERIAL PROPERTIES OF BORON/ALUMINUM COMPOSITE WITH  
 90°, 45°, 90°, 0°, -45°, 0°, -45°, 0°, 90°, 45°, 90°  
 FILAMENT ORIENTATION COMPARED WITH COMMERCIAL PURE  
 TITANIUM

(PROPERTIES MEASURED IN 90° DIRECTION)

MATERIAL PROPERTY	BORON/ALUMINUM COMPOSITE			COMMERCIAL PURE TITANIUM		
	ROOM TEMP		AT 505 K (450°F)	ROOM TEMP		AT 505K (450°F)
	MPa	PSI	MPa	MPa	PSI	PSI
$F_{tu}$	470.9	68,296	557.5	551.6	80,000	43,200
$F_{cy}$	1726.0	250,339	836.2	482.6	70,000	31,500
$F_{su}$ (In-Plane)	294.1	42,658	> 230.3	289.6	42,000	24,800
$F_{su}$ (Interlaminar)	> 122.0	> 17,692	> 81.9	289.6	42,000	24,800
$F_{bru}$ 4.76mm (3/16 in)	710.2	103,000	-	827.4	120,000	72,000
$E_x^{tu}$	79,300 to 193,700	$11.5 \times 10^6$ to $28.1 \times 10^6$	-	106,869	$15.5 \times 10^6$	-
$E_x^{cu}$	78,600 to 145,500	$11.4 \times 10^6$ to $21.1 \times 10^6$	-	110,316	$16.0 \times 10^6$	-
G	17,099 to 42,265	$2.48 \times 10^6$ to $6.13 \times 10^6$	-	44,816	$6.5 \times 10^6$	-

mechanical fastener installation of the skins onto the internal structure. This plan and the drawing were in turn translated by planning engineers into Fabrication Orders which were detailed, step-by-step instruction sheets to be followed by the assigned production technician and approved at each step by the cognizant engineer. As changes evolved after the Fabrication Orders were written, Engineering Orders were prepared instructing and authorizing the changes so the Fabrication Orders, at all times, were kept current.

#### QC and NDT

When the first two boron/aluminum skins were received and visually inspected, it was determined that one was acceptable but that the other had numerous surface blemishes on both sides (Figure 82). This had been caused, according to the supplier, by a reaction between a graphite release agent left on the part during its trimming and the liquid coolant used during cutting. In spite of its cosmetic appearance, however, this panel's tension test QC results were entirely satisfactory and no premature specimen failures were initiated by the surface blemishes. Initially, it was planned that the fabricator, Hamilton Standard, would supply another panel to replace the blemished one, but because the aft pylon production schedule could not be delayed and the replacement skin schedule could not be accelerated, the rejection of this skin by Inspection was overruled by its acceptance by Engineering and it was used for the production of the second aft pylon skin.

Both skins had been ultrasonically C-scan inspected by means of the process described in Appendix A. Although the blemished panel had no voids, some voids were detected in one corner of the unblemished panel. Fortunately, it was possible to so orient this panel that these voids were entirely removed when the diagonal cut across the corner (Figure 83) was made and so it too was accepted for production of the first aft pylon skin.

When the third boron/aluminum skin was received, its appearance and ultrasonic C-scan NDT results were satisfactory, but Hamilton Standard had reported that their QC tension tests of specimens cut from the panel were low in the 90° layup direction, ie; 379.2MPa (55,000 psi) instead of the 503.3MPa (73,000 psi) target property specified in the procurement document Appendix A. To check Hamilton Standard's claim that the low results were attributable to poor specimen quality (the material for the tests being taken from the edge of the panel) and that the rest of the panel was satisfactory, additional specimens were fabricated and tested by Douglas. When these specimen strengths met the target tensile strength of Appendix A, this panel was accepted for production of the third aft pylon skin.

When the fourth panel was received, its NDT and QC results satisfactorily met the requirements of Appendix A, and it was accepted for production as the spare fourth aft pylon skin for NASA's retention.

#### Composite Skin Fabrication and Installation

After each of the four skins were accepted for production, they were cut to the correct outline and their holes were located and punched (Figure 84) in

accordance with the Manufacturing Plan outlined in Appendix C, and the trimming and hole preparation processes described in Appendix B. Both surfaces were alodined and the interior surface was painted with FR epoxy primer. Each skin was then given to the production department where its holes were used as a template to drill the holes in the substructure. After installing the boron/aluminum skin onto the substructure (Figure 85), the remaining aluminum skins were also added (Figure 86). When the entire aft pylon was fabricated, it was delivered to the paint shop where it was cleaned and its aluminum skins were painted with the United Airlines characteristic blue and white colors. In accordance with the painting drawing, since the engine exhaust and heat would scorch and discolor the lower titanium panels, these are normally left unpainted and hence, the boron/aluminum substitutes were also left unpainted. To preclude the possibility that during their five year service, the boron/aluminum skins might be damaged, discarded, and replaced by United Airlines service personnel, both sides were lettered with the words "BORON/ALUMINUM COMPOSITE PROPERTY

OF DOUGLAS AIRCRAFT COMPANY, IF  
DAMAGED, NOTIFY NEAREST DOUGLAS  
REPRESENTATIVE FOR DISPOSITION".

#### COST ANALYSIS

Direct labor manhours actually expended for the fabrication of each of the three boron/aluminum composite aft pylon skins were as follows:

- |                          |                    |
|--------------------------|--------------------|
| 1. Trimming and cutting  | - 8 manhours       |
| 2. Punching holes        | - 6 manhours       |
| 3. Alodining and priming | - 2 manhours       |
| 4. Inspection            | - <u>1 manhour</u> |

Total 17 manhours

Because this total does not include the cost of direct labor supervisory and other support personnel, it is customary to multiply it by a factor of 1.8 to obtain the true total manhour cost, ie;

$$17 \times 1.8 = 30.6 \text{ manhours}$$

This total is obviously very high, even for the first to the third new part. However, it was not an object of this program to develop low cost fabricating approaches or to emphasize cost competitiveness between boron/aluminum composites and titanium. This total cost should therefore not be considered as representative of typical fabrication costs of other similar applications. Furthermore, as a simple flat skin with a number of holes, it does not represent a particularly sophisticated application from which much extrapolation can be made to the prediction of costs of more complicated metal composite structures.

At \$496/Kg (\$225/lb) each of the as received blanks of boron/aluminum weighing 2.125Kg (4.68 lb) cost \$1,053. This material cost included tensile specimen QC testing and C-scan ultrasonic NDT testing. When machined to final dimensions, the boron/aluminum skin weighed 1.566Kg (3.45 lb). Hence, the

actual finished material cost was

$$\$1053 \div 1.566\text{Kg} = \$672/\text{Kg} \text{ or}$$

$$\$1053 \div 3.45 \text{ lbs} = \$305/\text{lb}$$

This actual material cost is also very high and no possibility of any reasonable comparison with similar costs of finished titanium skins exists.

## FLIGHT TESTS

This section briefly describes the flight service demonstration testing that will follow in June 1975, after delivery of the three (3) particular DC-10 aircraft to United Airlines that include the three (3) boron/aluminum composite aft pylon skins.

### 1. Flight Service Demonstration Tests

These tests will include the installation, periodic inspection, flight testing, removal and replacement of the three aft pylon boron/aluminum skins with the present titanium skins. With the delivery of the three DC-10 aircraft into flight service in July 1975, the scheduled five-year demonstration test will continue until July 1980.

### 2. Skin Inspection and NDT

During the five-year flight service demonstration period, yearly visual inspections of the three boron/aluminum skins will be conducted at the participating airline's maintenance facilities. These in-service checks will be scheduled to coincide with the regularly scheduled maintenance checks. Of particular concern will be the inspection of possible delaminations, fatigue cracks, evidences of erosion, corrosion, or overheating.

### 3. Skin Replacement

At the conclusion of the five-year period of exposure, Douglas will arrange for the removal of the three boron/aluminum skins and the replacement of the original titanium skins.

### 4. Skin Shipment to NASA

After visual and non-destructive inspection by Douglas, the three exposed boron/aluminum skins will be shipped to NASA Langley for further examination and any other desired testing.

## CONCLUSIONS

1. The structural adequacy of the boron/aluminum skin panel was demonstrated by the satisfactory results of the structural tests designed to simulate operating environmental extremes for the aft pylon of the DC-10 aircraft. The performances of the boron/aluminum material in compression and in fatigue were particularly noteworthy.
2. Based on the fabrication of the specimens and the four skin panels, the fabrication methods developed were shown to be suitable for the intended application. From a manufacturing standpoint, the methods of fabricating flat skins have sufficient growth potential to apply to larger and more complicated aircraft structural areas.
3. Although the saving of weight was not an objective of the program, the substitution of a boron/aluminum skin panel for a similar sized titanium panel resulted in a weight saving of 26%. No attempt was made to develop tooling or fabrication techniques that would result in lower costs. As a result, the manufacturing and material costs for boron/aluminum were not comparable in a complementary manner with those for titanium.
4. Examination of tension, compression, and shear data of cross-ply boron/aluminum specimens indicated considerable nonlinearity in its stress/strain curves and the retention of significant "permanent set" when it had been loaded and unloaded. Since such nonlinearity and permanent set is undesirable from a structural application standpoint, it is recommended that suitable material and fabrication approaches be developed to reduce this inelastic behavior.

#### REFERENCES

1. MDC J0717, VOL II, Section 3C - Aerodynamic Data for Stress Analysis-Models DC-10-20, and DC-10-30 Jet Transport.
2. McDonnell Douglas Material Specification MMS-583, Class C.
3. A J Roark, Formulas for Stress and Strain, McGraw-Hill, 3rd Edition, 1954.
4. A H Church, Mechanical Vibrations, John Wiley and Sons, 2nd Edition, 1957.
5. MDC J6541, DC-10 Boron/Aluminum Aft Pylon Boat-tail Panel-Test Plan.

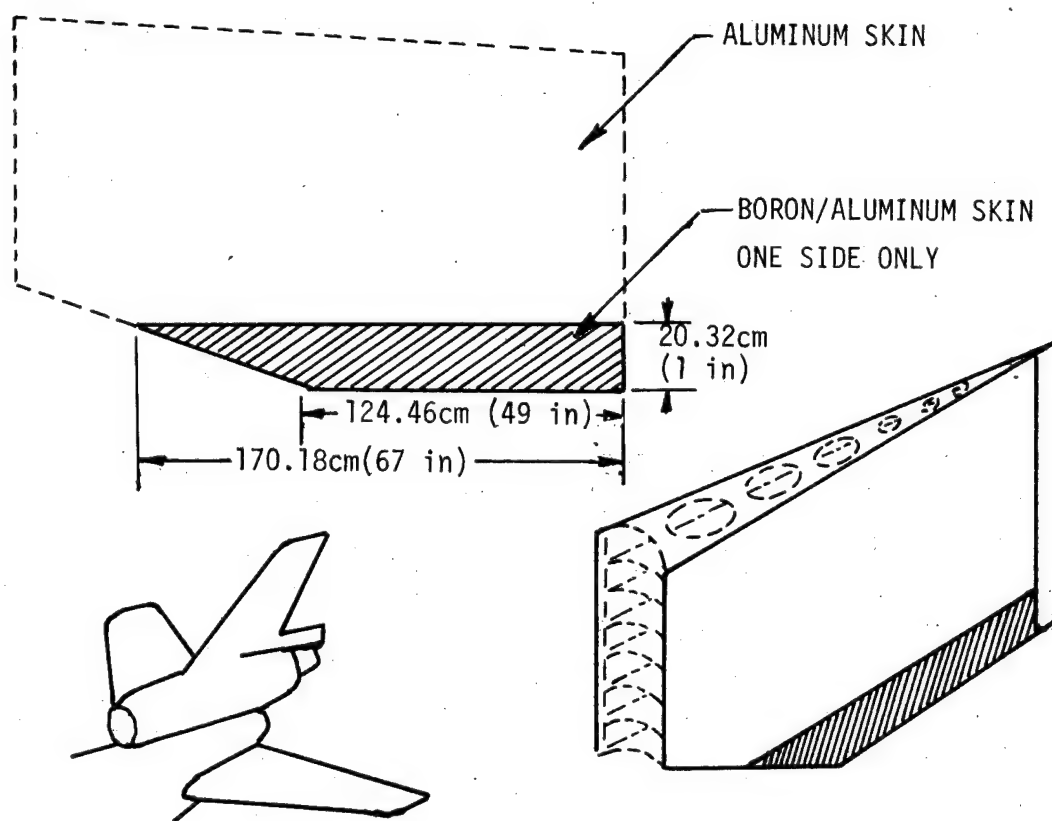


Figure 1. DC-10 Tail Pylon

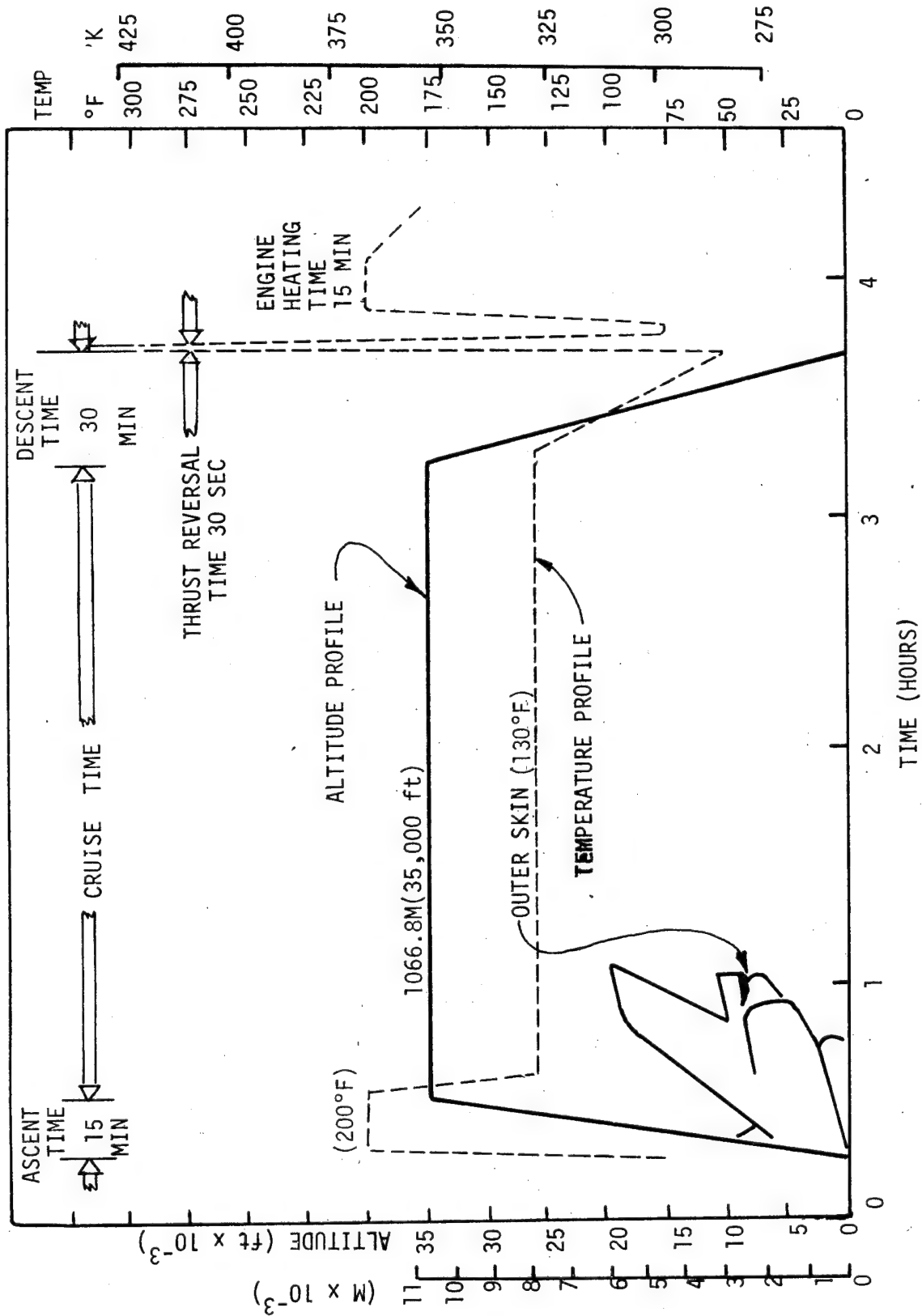


Figure 2. DC-10 Typical Mission Profile

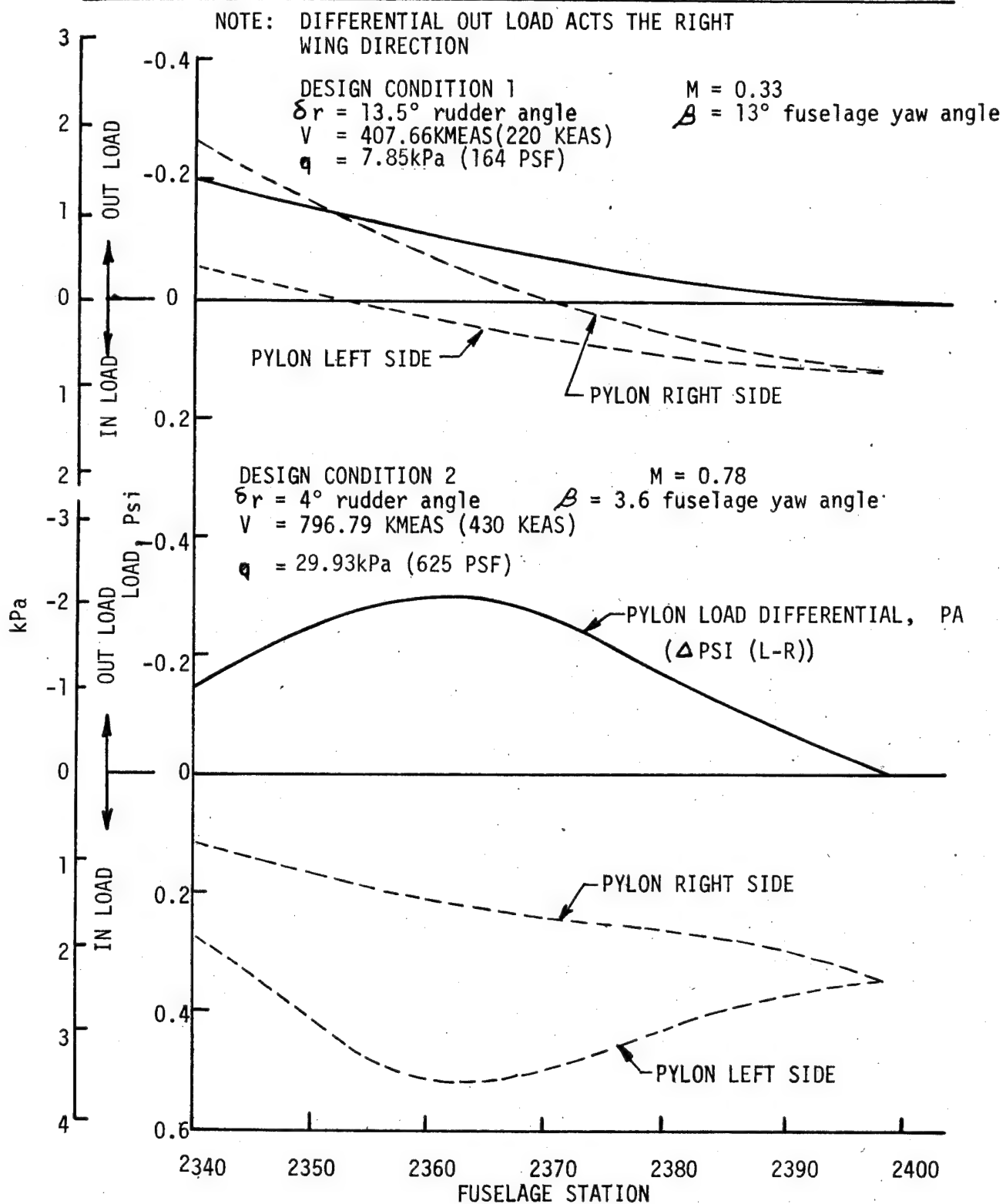


Figure 3. Estimated Aerodynamic Loads on Aft-Engine-Pylon Trailing Edge

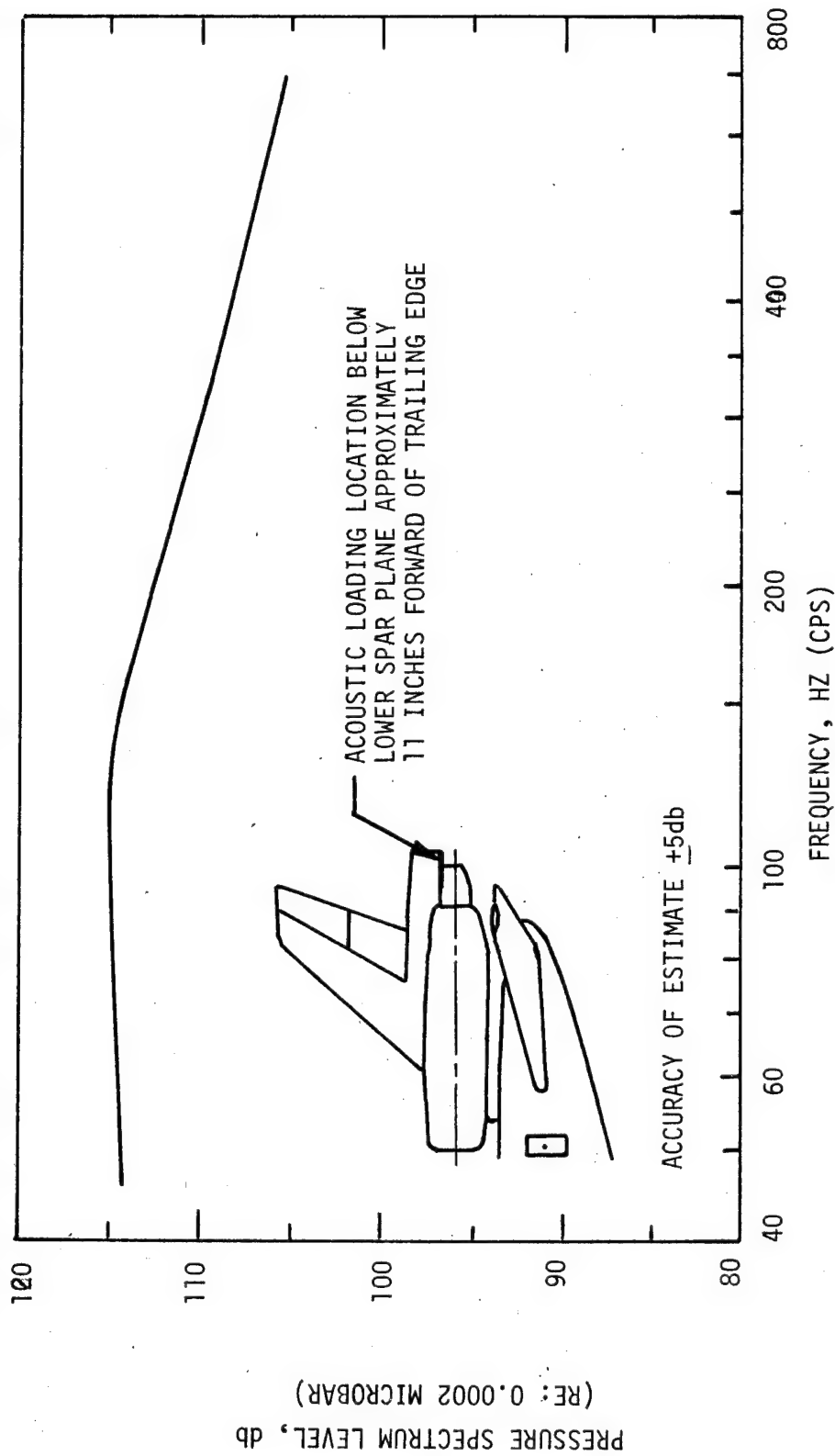


Figure 4. Estimated Acoustic Loads for 3-engine Ground Runup at Takeoff Thrust Using JT9D-15 Engines (Aft Pylon Fairing)

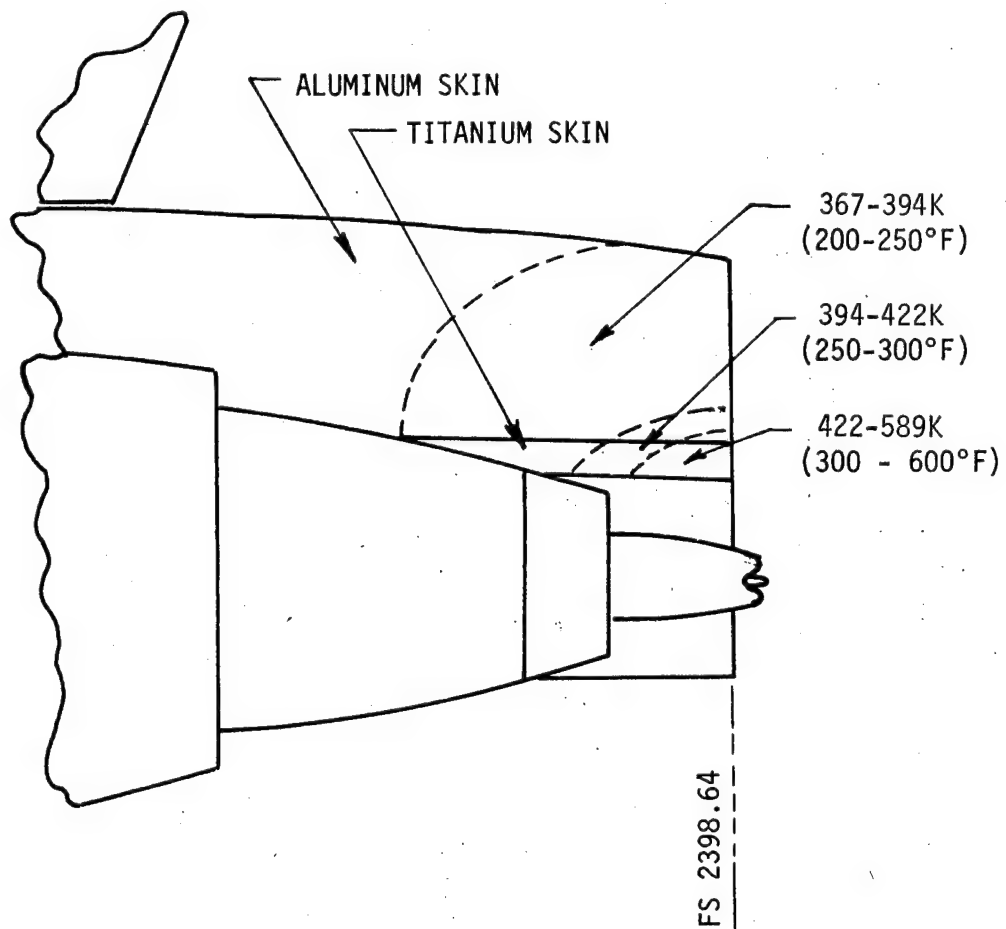
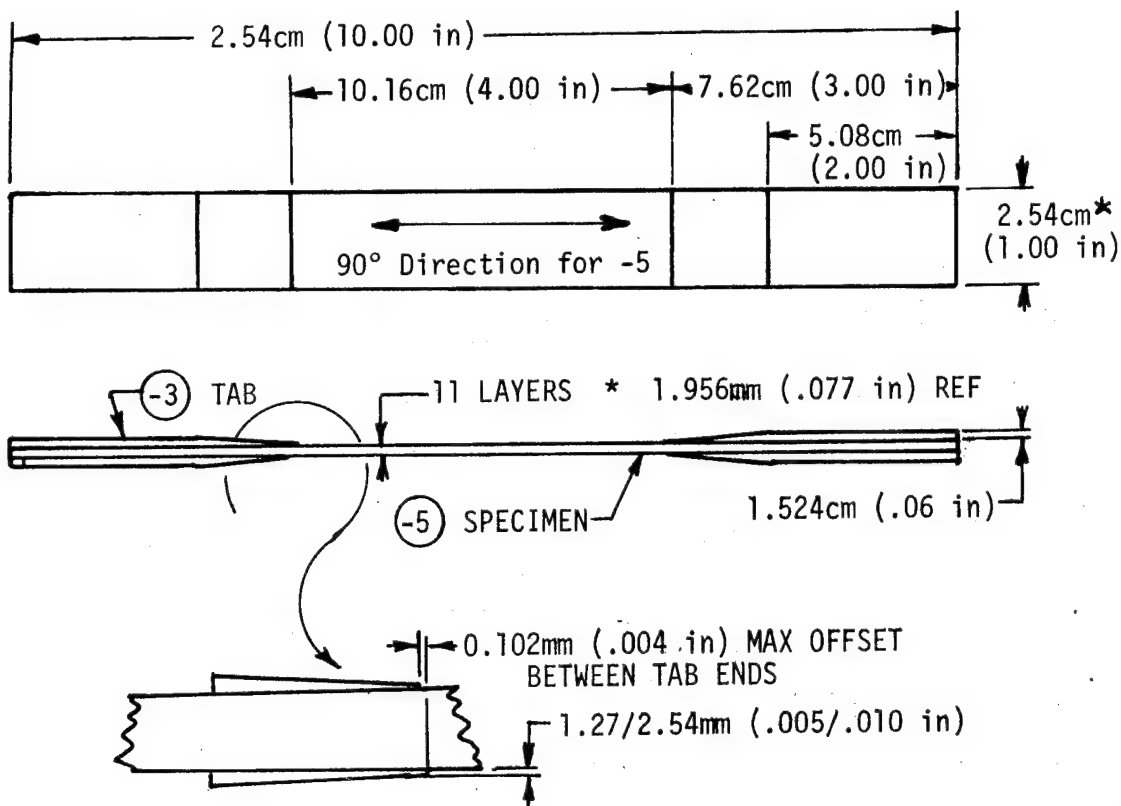


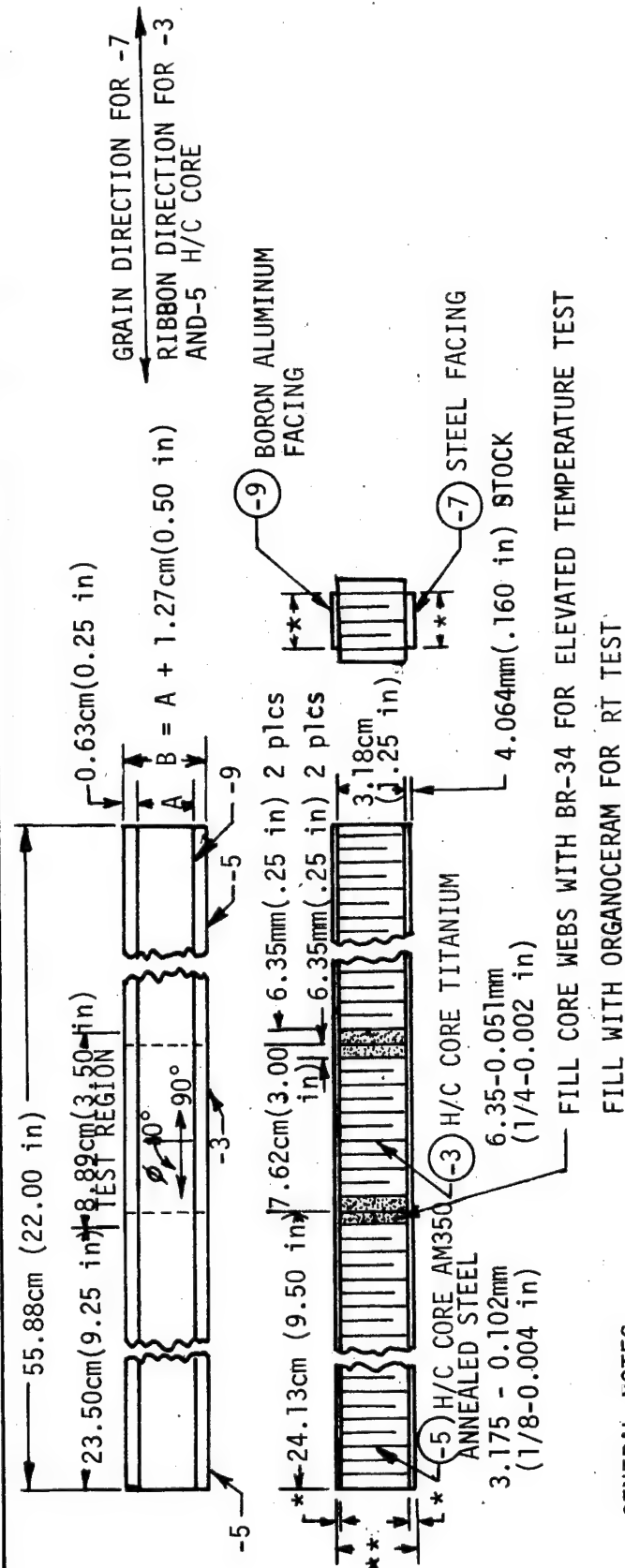
Figure 5. Engine Fairing Temperature During Reverse Thrust



#### GENERAL NOTES

1. ORIENTATION OF -3 TAB TO BE IN THE 0°, 90° DIRECTION
2. BOND -3 BI-DIRECTIONAL PHENOLIC GLASS LAMINATE TABS TO -5 SPECIMEN WITH HT424 FOR ELEVATED TEMPERATURE TEST WITH HYSOL EA951 FOR RT TEST
3. DIMENSIONS NOTED THUS (\*) TO BE TAKEN IN TEST SECTION AND RECORDED BEFORE TEST
4. FABRICATION STANDARDS PER APPENDIX B
5. FABRICATE BORON/ALUMINUM PER APPENDIX A

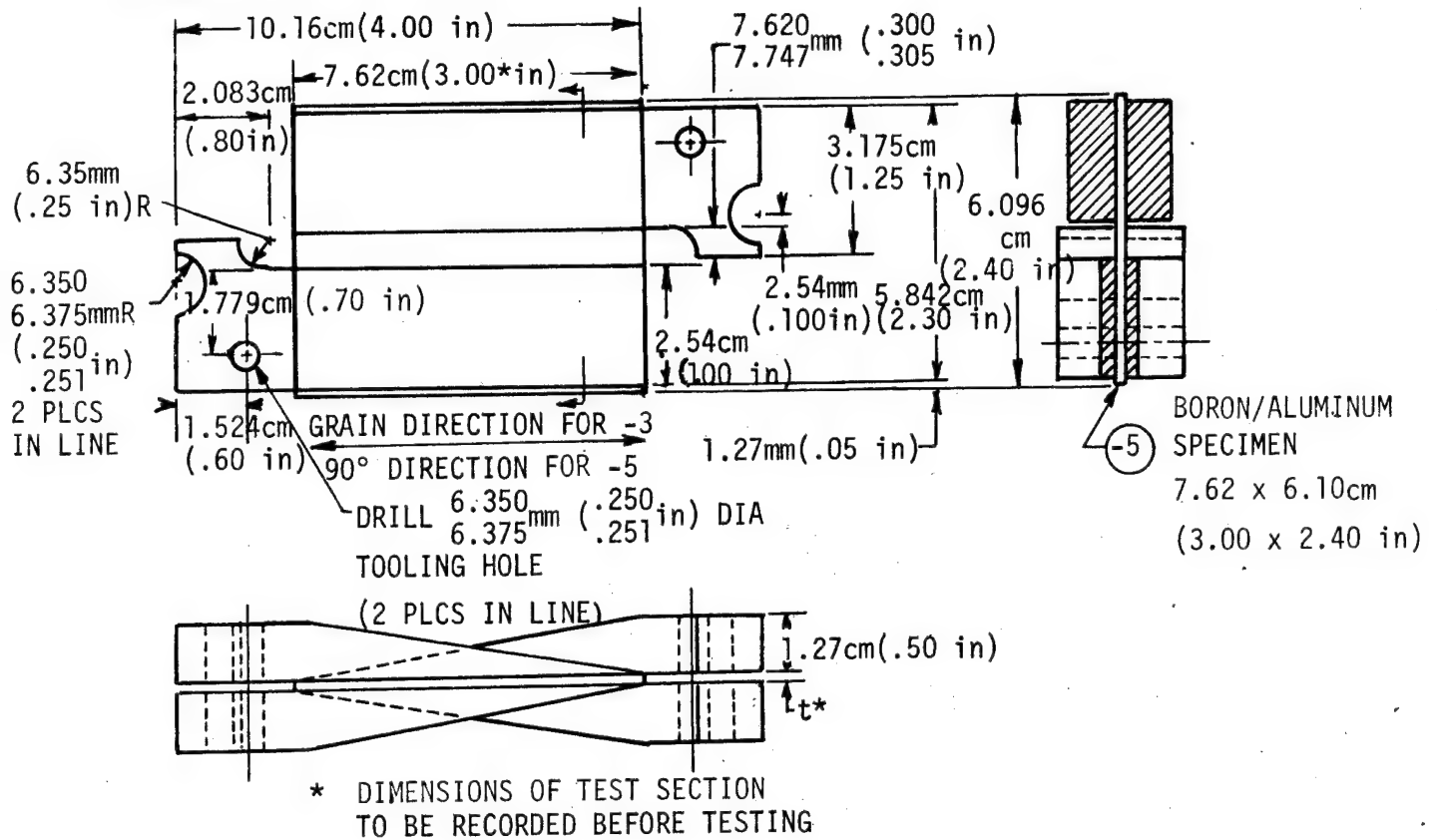
Figure 6. Specimen Assembly - Modified IITRI Tension Test



#### GENERAL NOTES:

1. FABRICATE BORON/ALUMINUM PER APPENDIX A
2. HT TR -7 SHEET 4340 STEEL FACING 125-145 KSI
3. FABRICATION STANDARDS PER APPENDIX B
4. DIMENSIONS NOTED THUS (\*) TO BE RECORDED BEFORE BONDING. DIMENSIONS NOTED THUS (\*\*) TO BE RECORDED BEFORE TESTING. DIMENSIONS ARE TO BE TAKEN IN TEST REGION.
5. BOND -3 and -5 TO -7 AND -9 WITH HT424 FOR ELEVATED TEMPERATURE TEST WITH METLBOND 329 FOR RT TEST

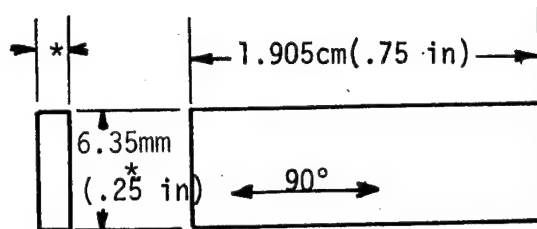
Figure 7. Specimen Assembly - Composite Honeycomb Sandwich Beam Test



#### GENERAL NOTES:

1. FABRICATE BORON/ALUMINUM PER APPENDIX A
2. FABRICATION STANDARDS APPENDIX B
3. BOND -3 AND -4 RAILS TO -5 SPECIMEN WITH HT424 FOR ELEVATED TEMPERATURE TEST WITH METLBOND 329 for RT TEST
4. MARK -3 AND -4 RAILS A AND B AS SHOWN TO INDICATE MATCHED PAIRS.
5. TOOLING FIXTURE REQUIRED DURING BONDING TO MAINTAIN DISTANCE BETWEEN -3 AND -4 RAILS AND TO LOCATE MATCHED PAIRS OF -3 AND -4 RAILS.
6. FABRICATE -3 AND -4 RAILS FROM 4130 STEEL PLATE

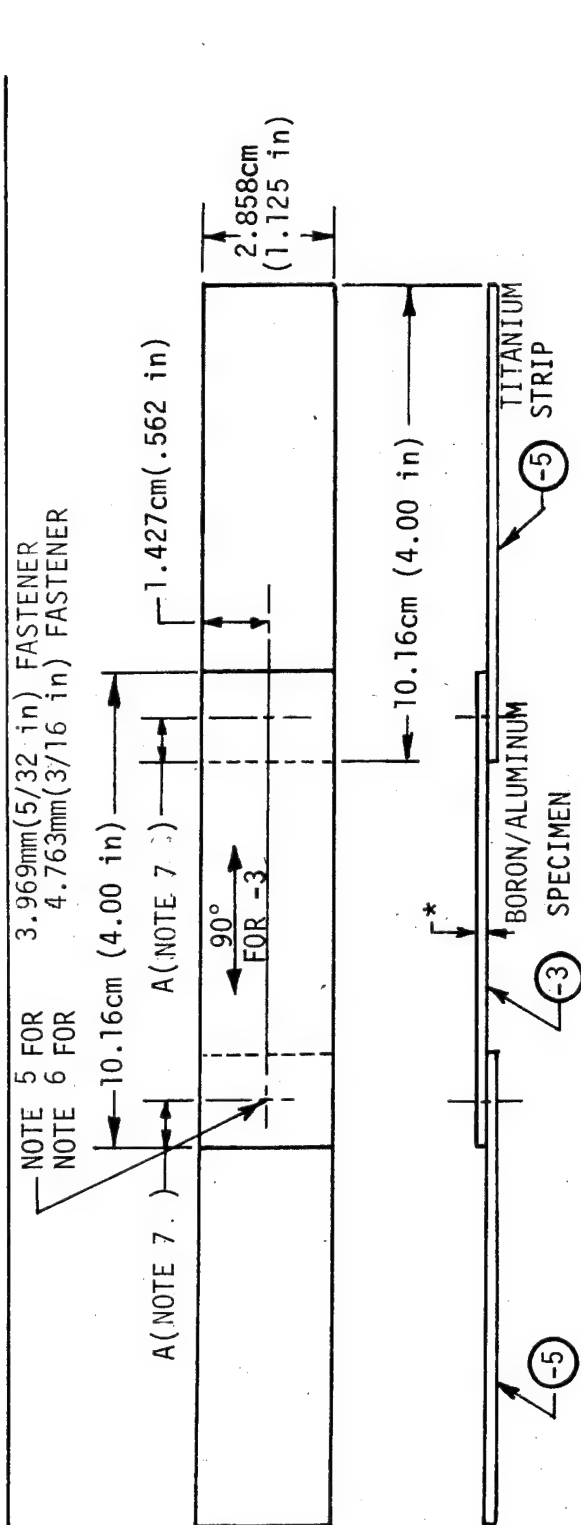
Figure 8. Specimen Assembly-Composite Rail Shear Test



#### GENERAL NOTES

1. FABRICATION STANDARDS PER APPENDIX B
2. DIMENSIONS NOTED THUS (\*) TO BE RECORDED BEFORE TEST.
3. FABRICATE PER APPENDIX A

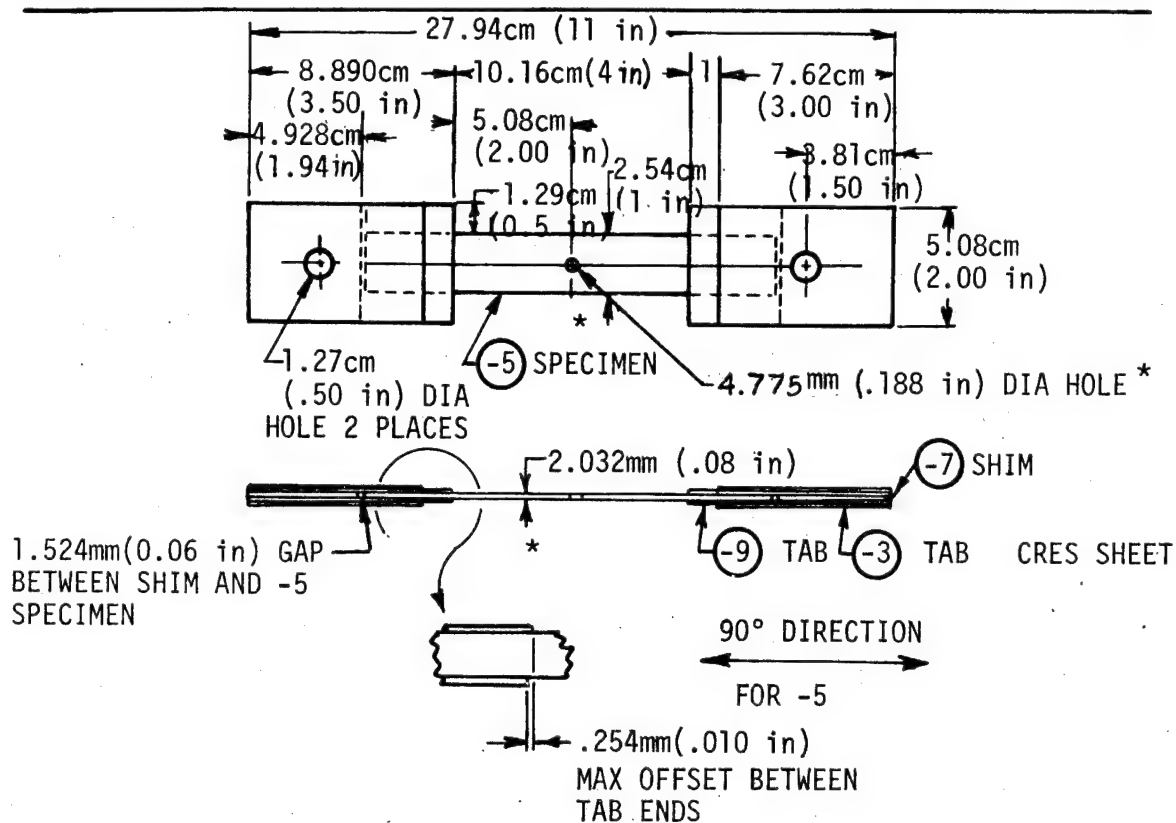
Figure 9. Specimen - Composite Interlaminar Shear Test



## GENERAL NOTES:

1. FABRICATION STANDARDS PER APPENDIX B
2. DIMENSIONS NOTED THUS (\*) TO BE RECORDED BEFORE TESTING.
3. INSTALL HI-LOKS PER S7933651-11
4. FABRICATE BORON/ALUMINUM PER APPENDIX A
5. HTL334-6-2 HI-LOK WITH MS21043-3 NUT AND AN960C10 WASHER
6. 3.518mm (.1385 in) DIA HOLE. BREAK EDGE PER S7933654-11. PUNCH HOLE UNDERSIZE AND REAM TO FIT.
7. HLT334-4-2 HI-LOK WITH MS21043-06 NUT AND AN960C6 WASHER.
8. DIMENSION A is 0.793cm (0.312 in) FOR 3.969mm(5/32 in) FASTENER AND 1.113cm(0.438 in) FOR 4.763mm(3/16 in) FASTENER

Figure 10. Composite Specimen - Bolt Bearing Test



GENERAL NOTES:

1. DIMENSIONS NOTED THUS (\*) TO BE RECORDED BEFORE TEST.
2. FABRICATION STANDARDS PER APPENDIX B
3. BOND -9 TABS TO -3 TABS AND TO -5 SPECIMEN AND -7 SHIMS WITH HYSOL EA951 ADHESIVE.
4. FABRICATE BORON/ALUMINUM PER APPENDIX A
5. HOLES SHOWN ON CENTERLINE TO BE WITHIN .096mm (.003 in) EITHER SIDE OF THE CENTERLINE.

Figure 11 Specimen-Composite Tensile Fatigue Test

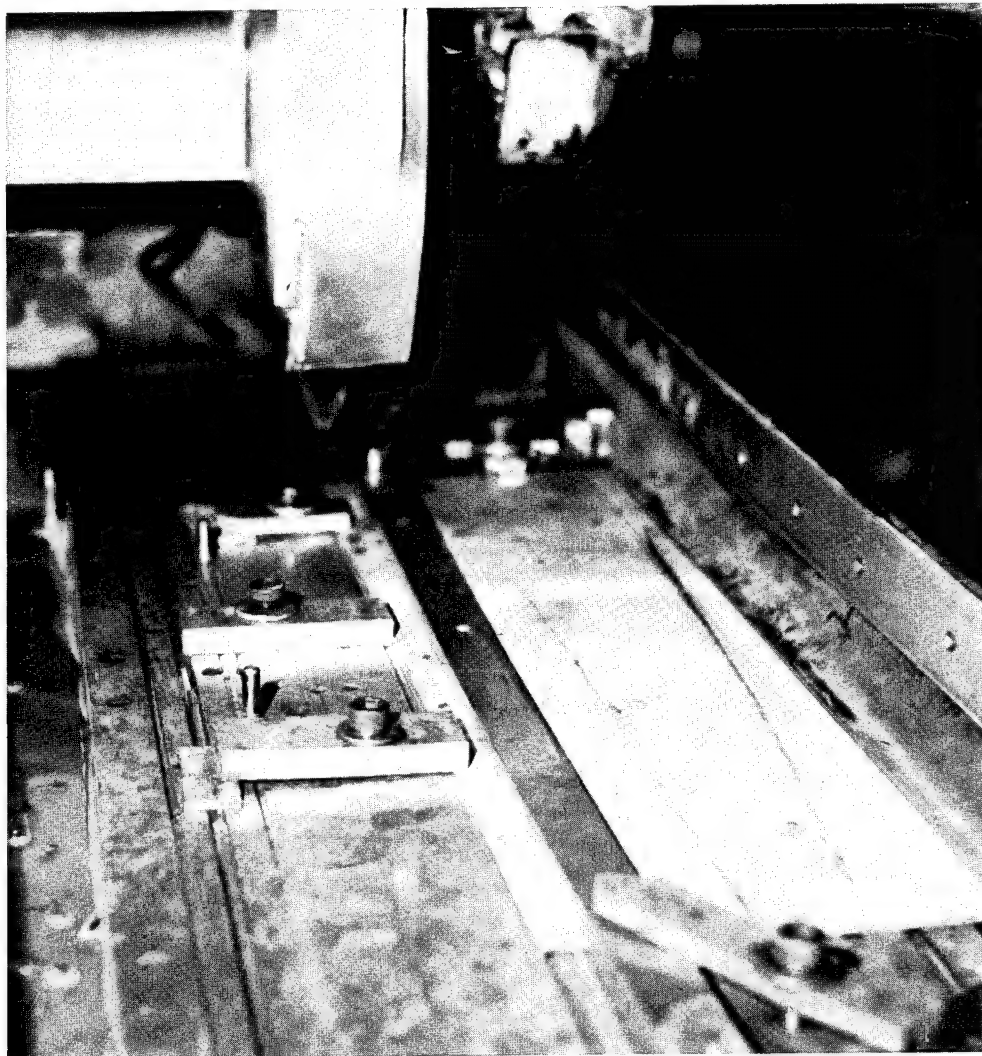
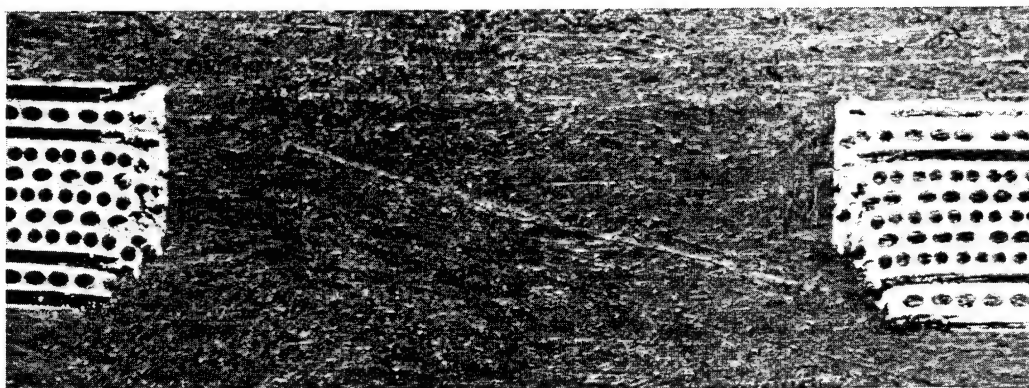


Figure 12 Cutting Boron/Aluminum with Diamond Coated Wheel

---



14.75 x

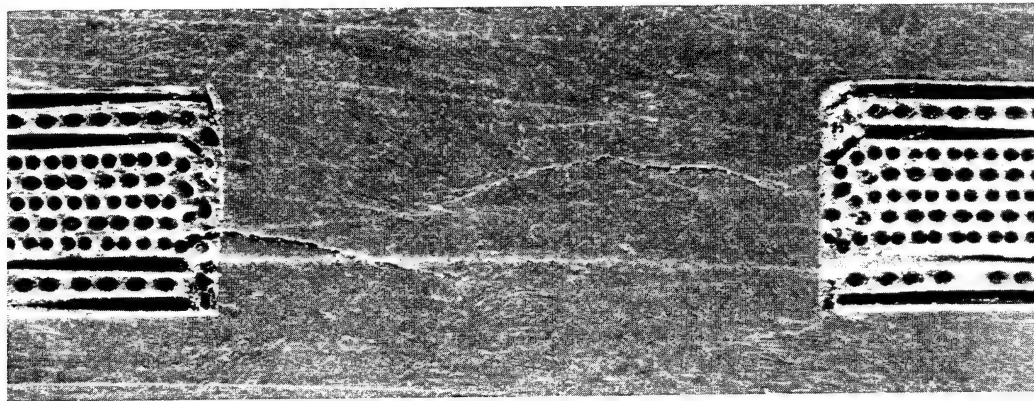


40 x

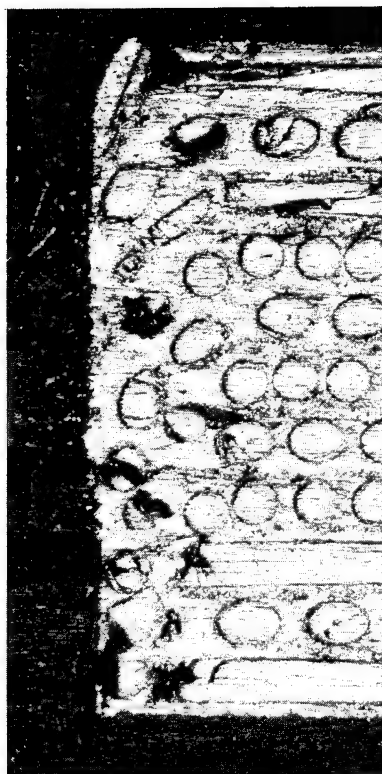


8.4 x

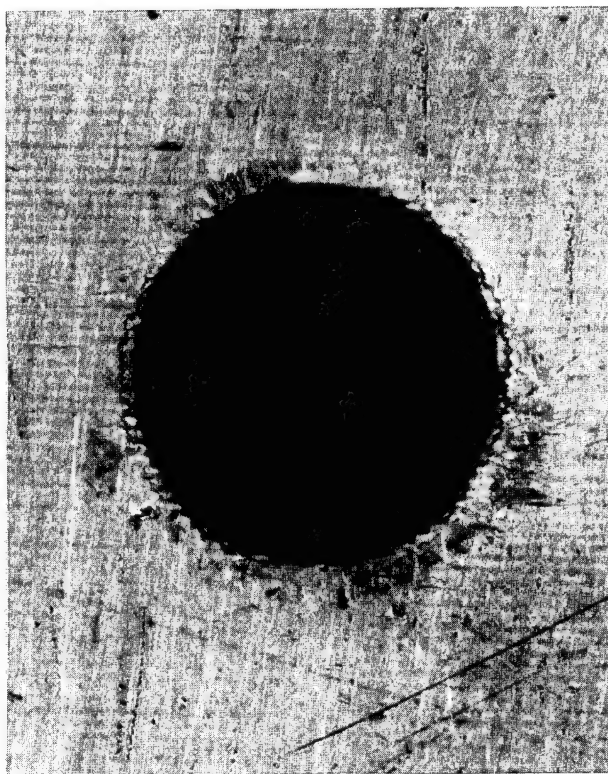
Figure 13 Hole Produced by 6.350mm(0.250 in) Diameter Steel Drill



14.75 x

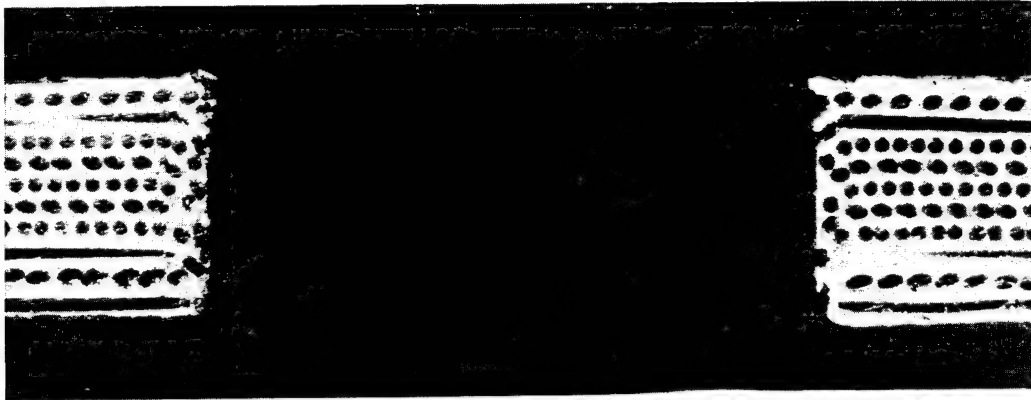


40 x



8.4 x

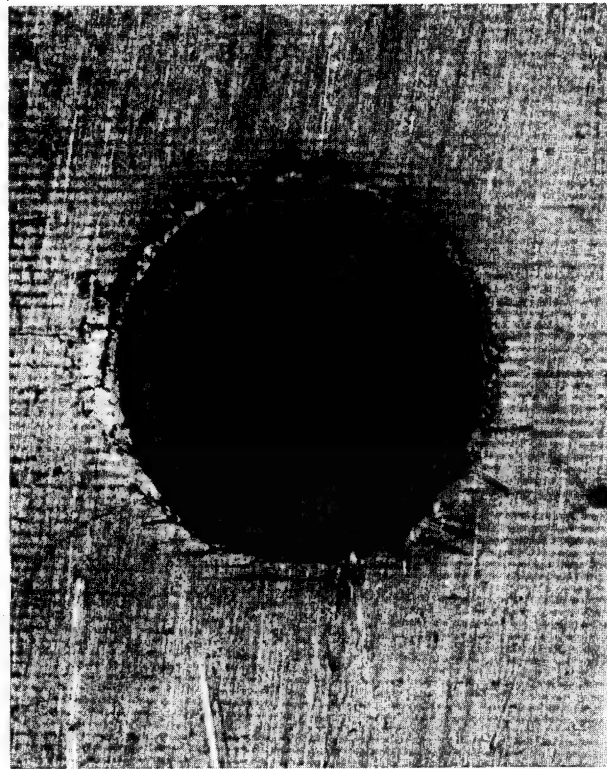
Figure 14 Hole Produced by 5.664mm (0.223 in) Diameter Steel Punch



14.75 x



40 x

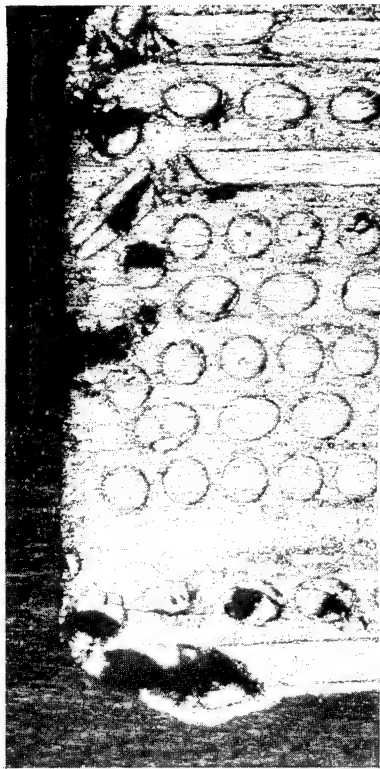


8.4 x

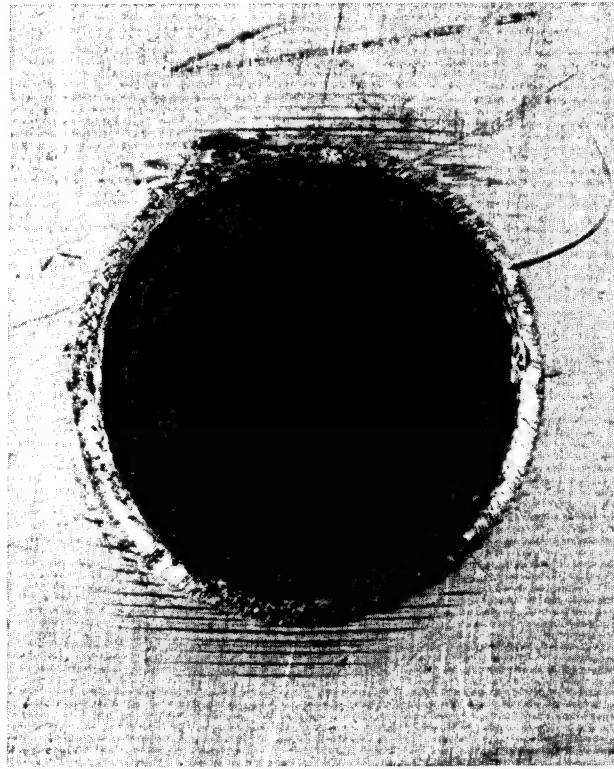
Figure 15 Hole Produced by 5.664cm (0.223 in) Diameter Steel Punch  
Followed by 5.791mm (.228 in) Diameter Steel Ream



14.75 x



40 x

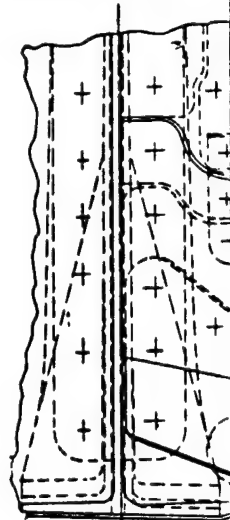


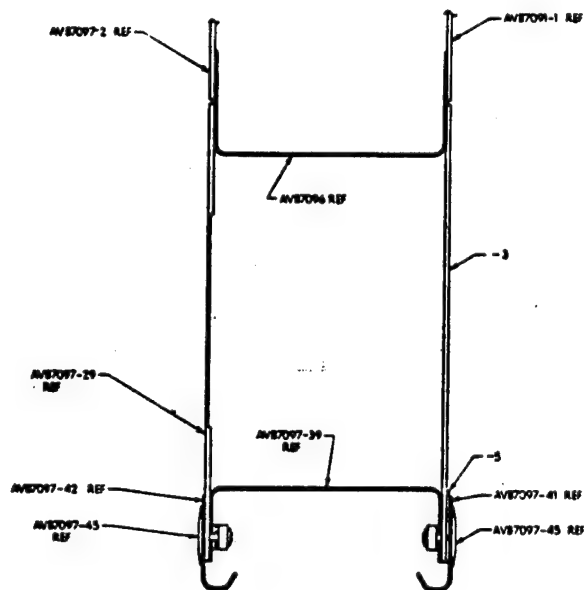
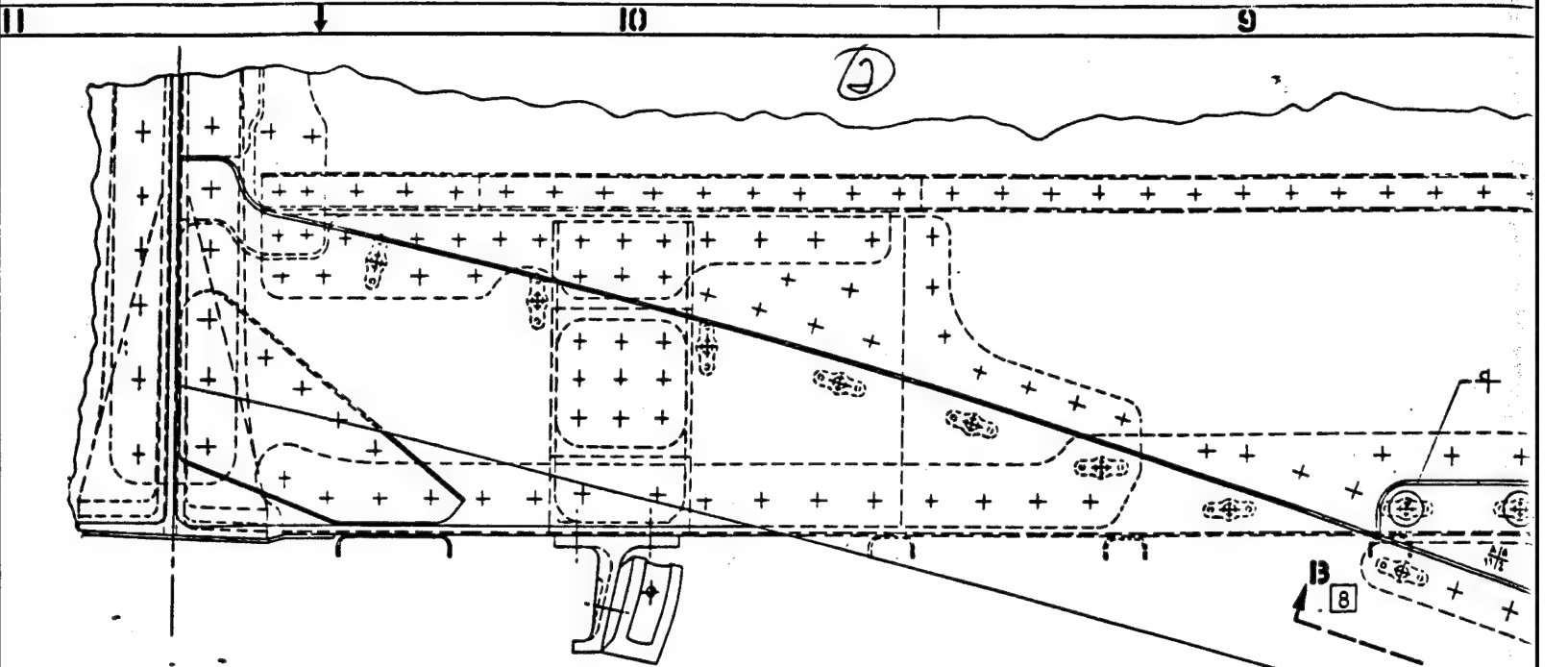
8.4 x

Figure 16 Hole Produced by 6.350mm(0.250 in) Diameter Steel Punch  
Followed by 6.401mm(0.252 in) Diameter Diamond Ream

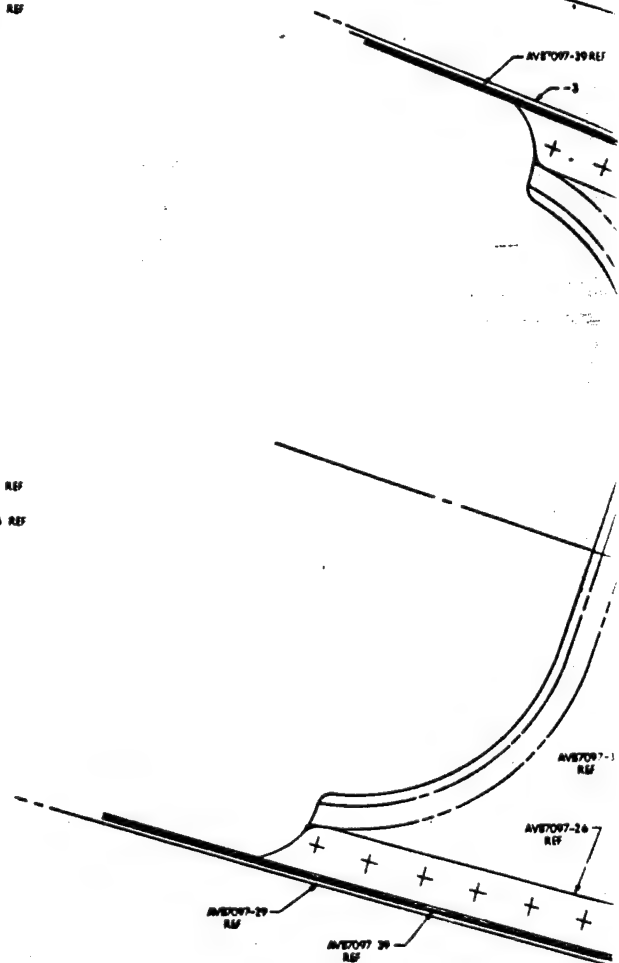
12

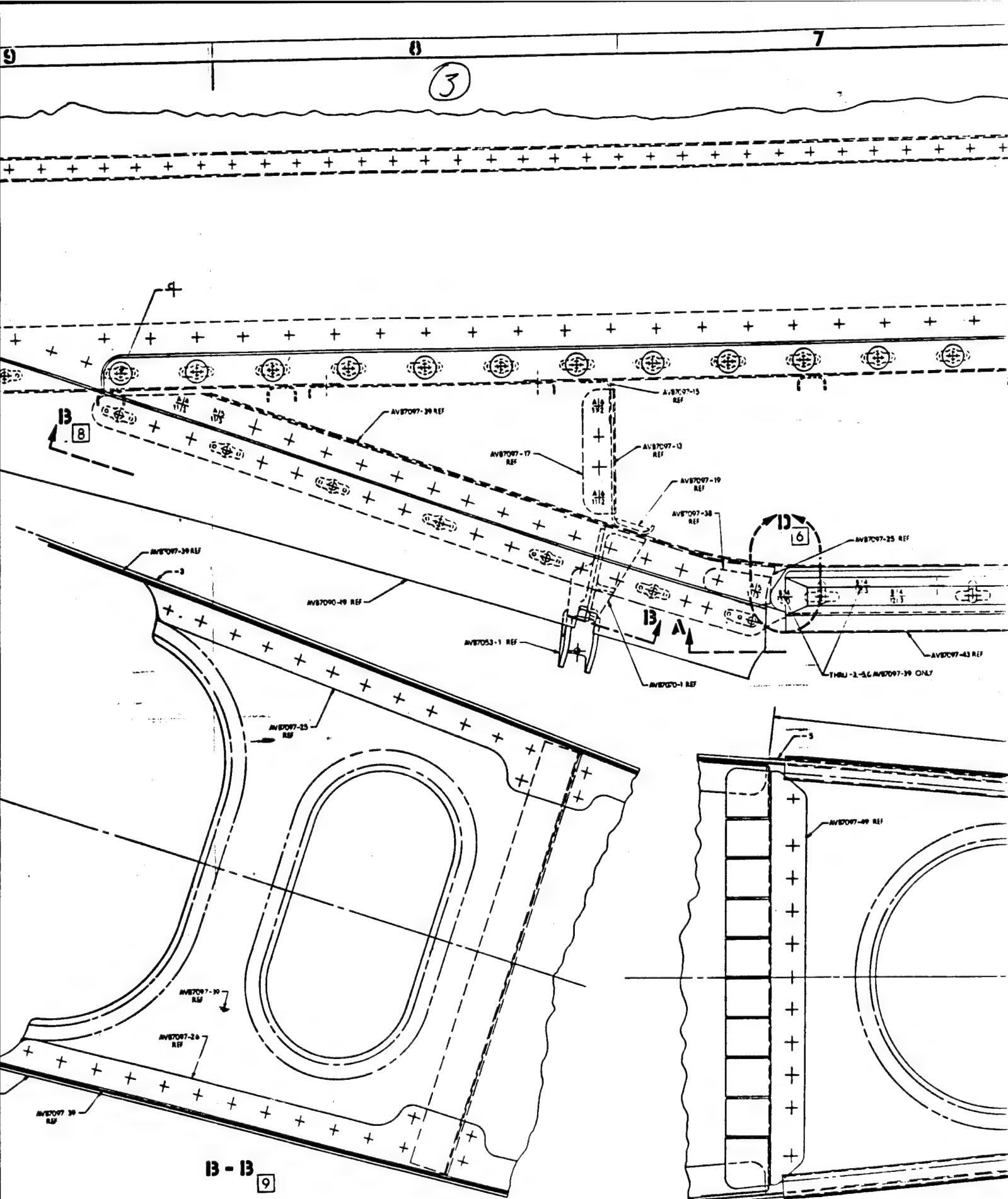
11



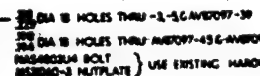


C - C 4





④





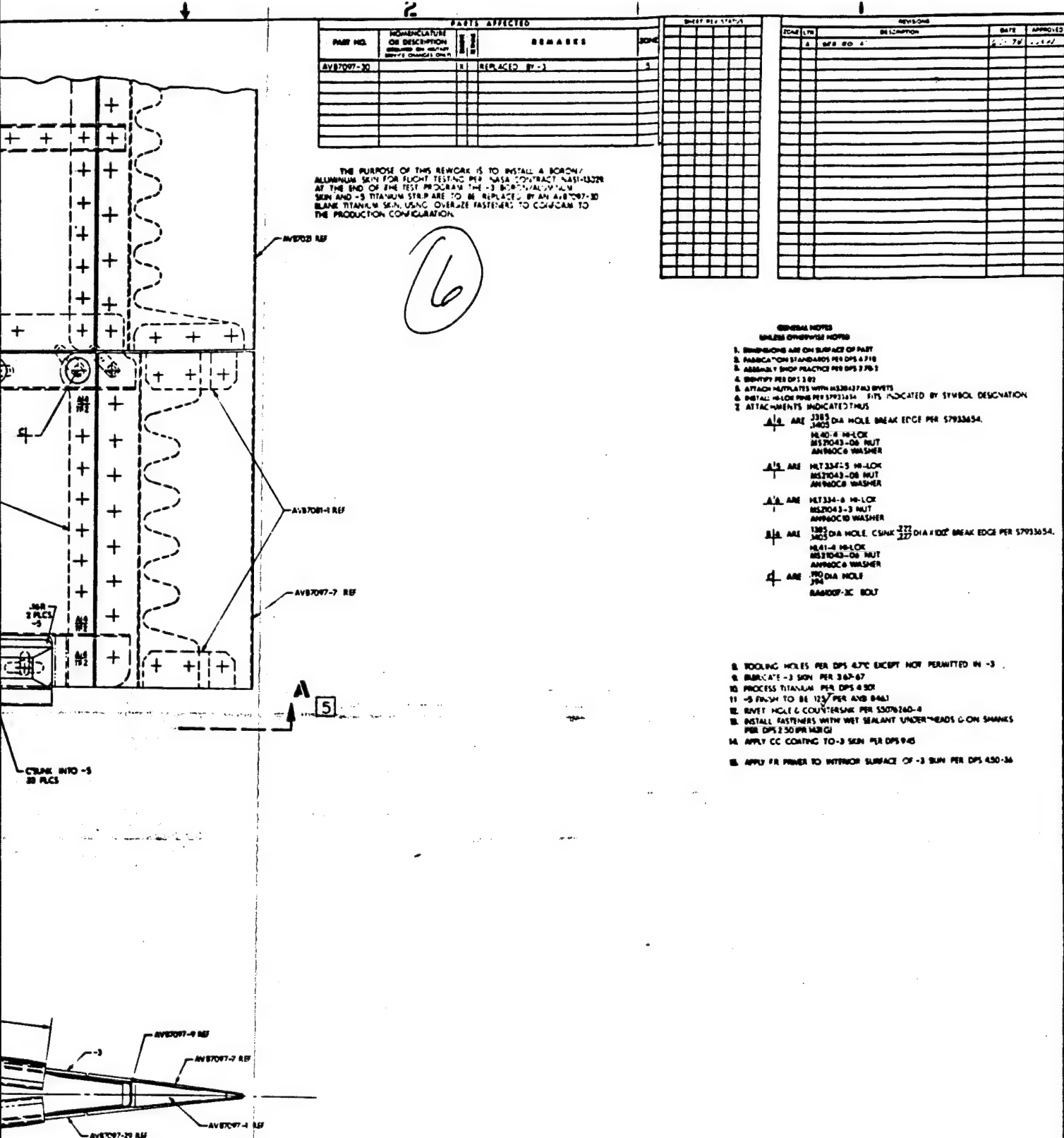


Figure 17 Drawing AVB7129-Rework Lower Fairing Skin, Tail Pylon

BY REPAIR PARTS LIST		DOUGLAS AIRCRAFT COMPANY	
DATE: 10/1/77	BY: J. J. J.	DATE: 10/1/77	BY: J. J. J.
REWORK-LOWER FAIRING SKIN, TAIL PYLON		REWORK DRAWING	
J 88277		AVB7129	
SCALE: 1/1		SHEET 1 OF 1	

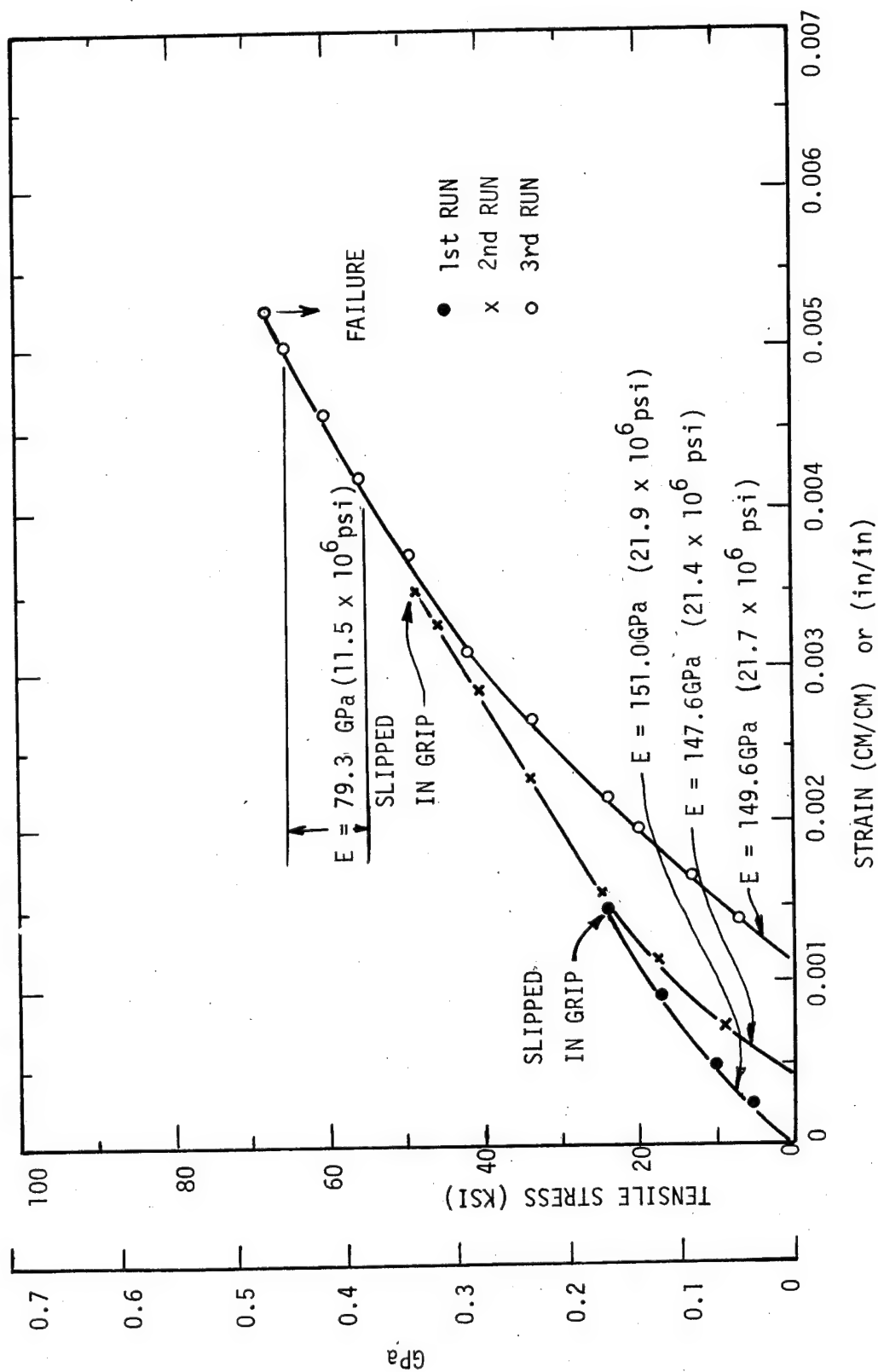


Figure 18 Specimen 11 - Room Temperature Tension Stress/Strain Curve

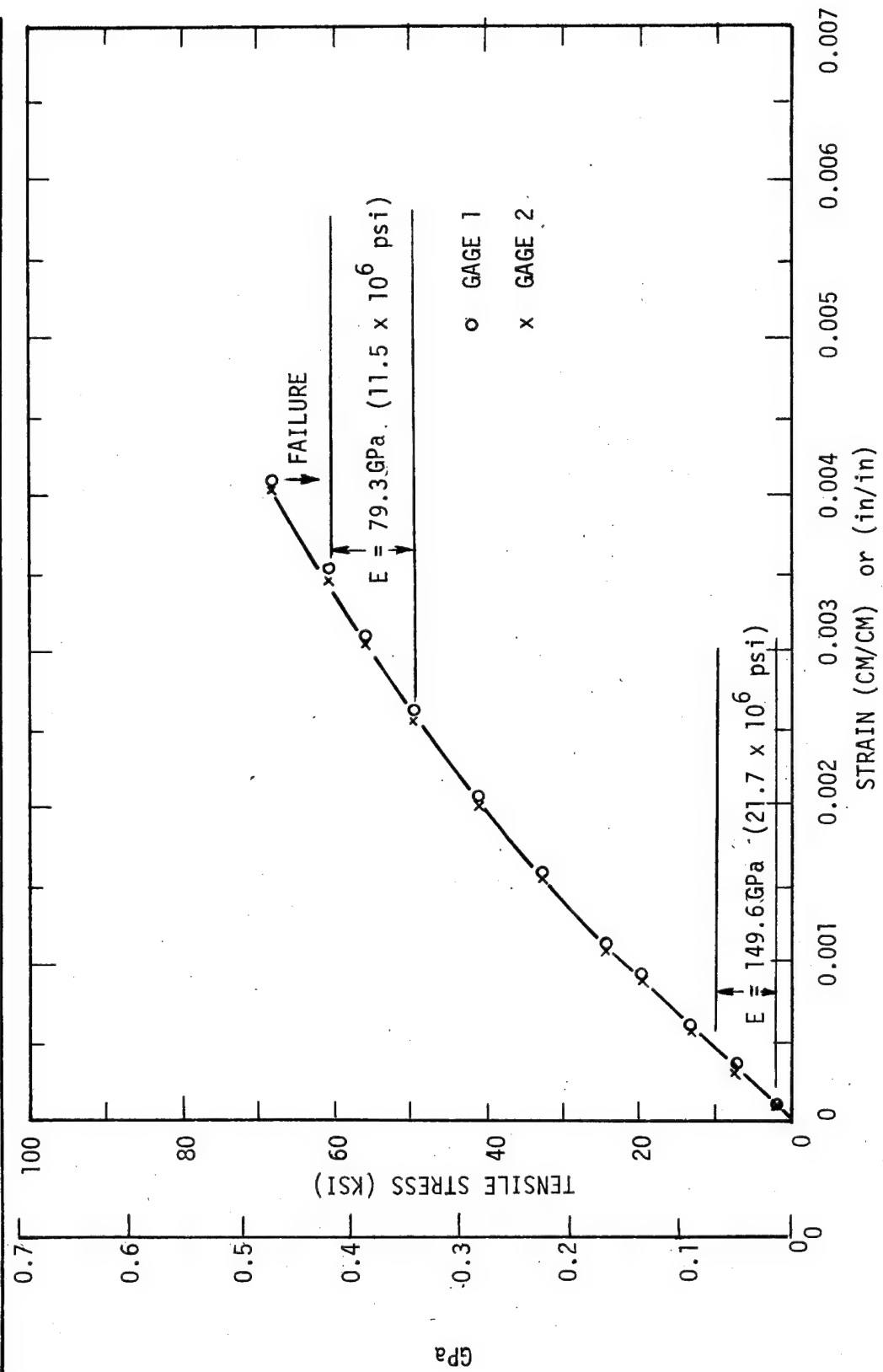


Figure 19 - Specimen 11 - (3rd Run Only) Room Temperature Tension Stress/Strain Curve

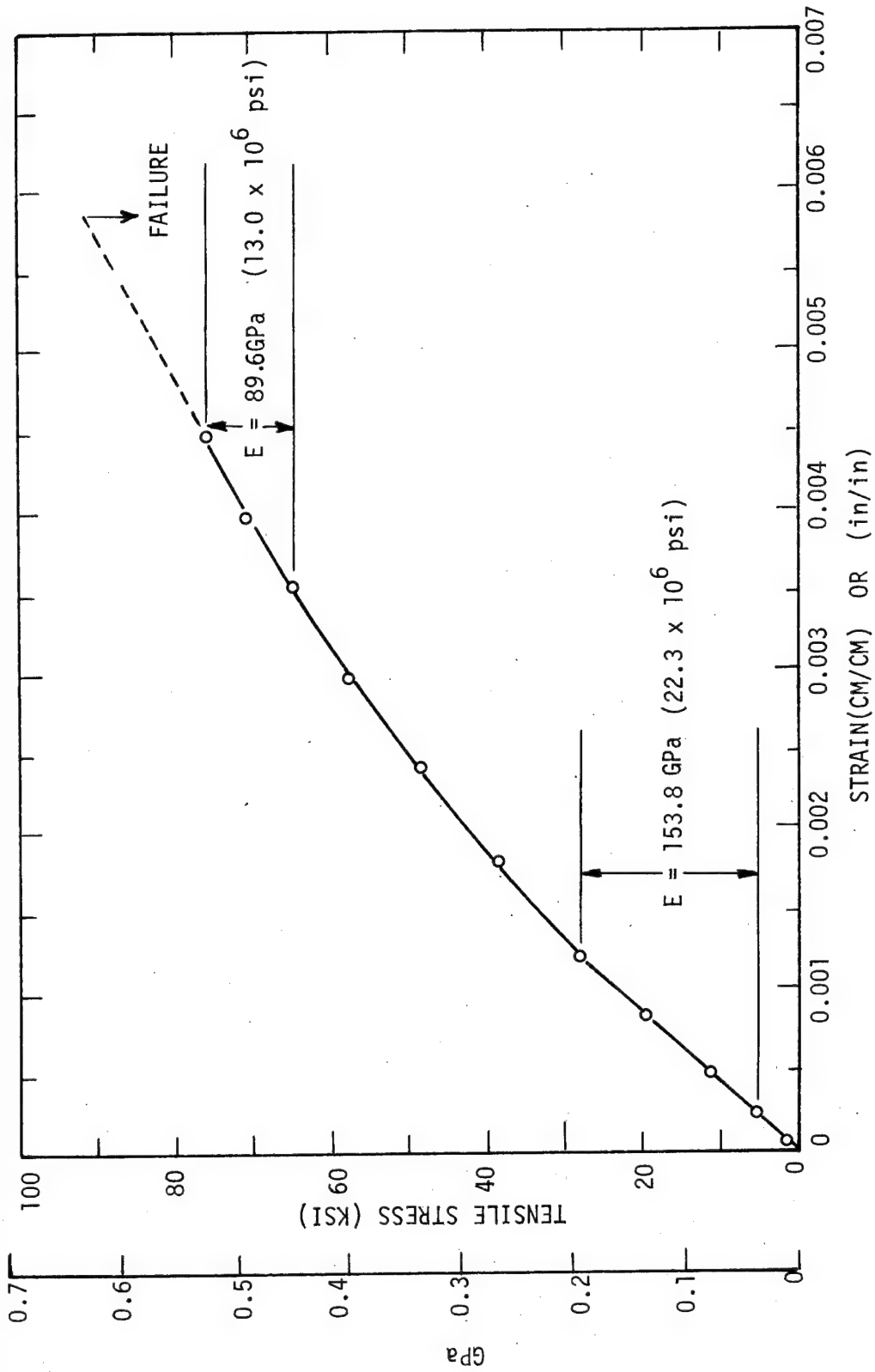


Figure 20 - Specimen 12 - Room Temperature Tension Stress/Strain Curve

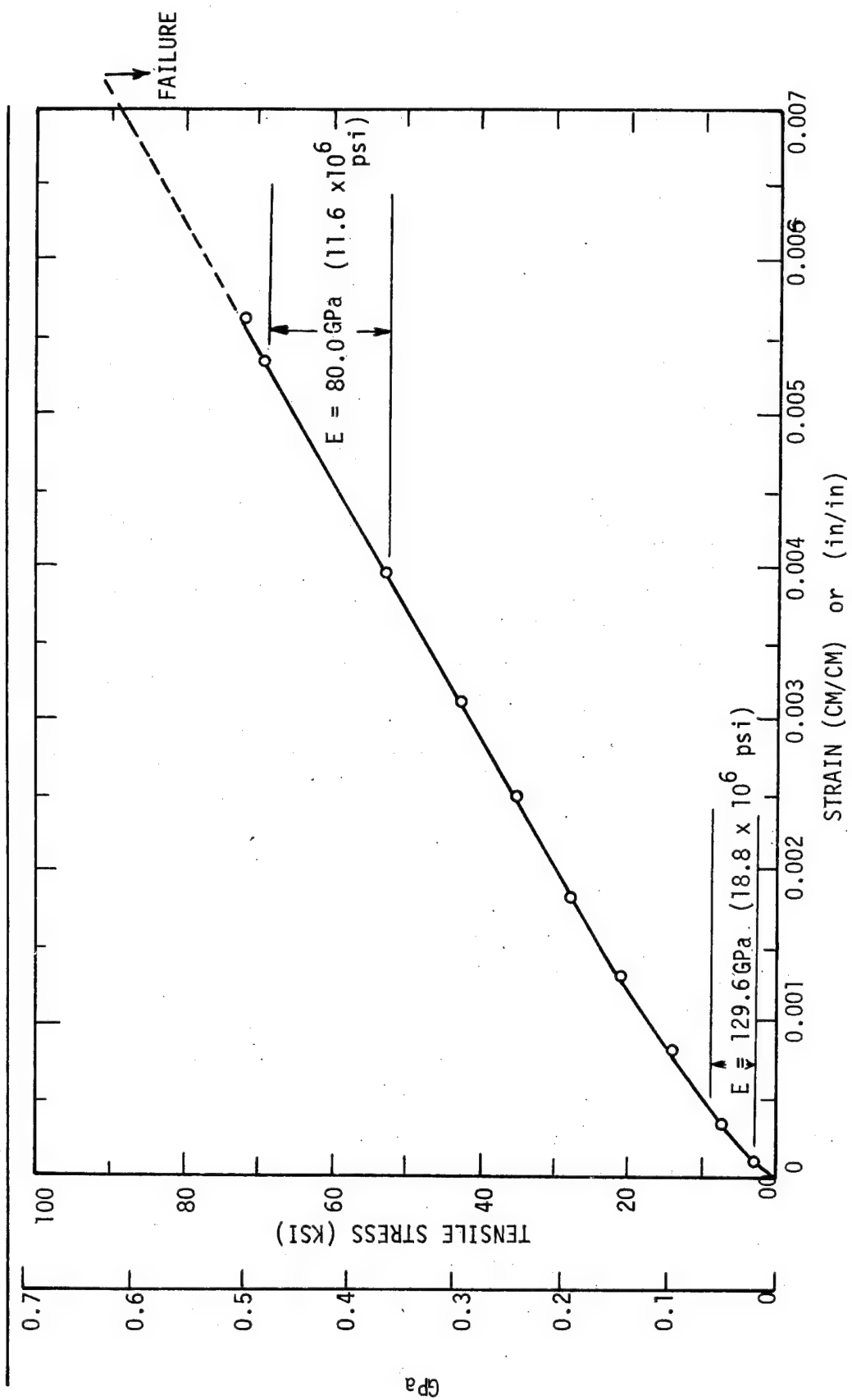


Figure 21 Specimen 13 - Room Temperature Tension Stress/Strain Curve

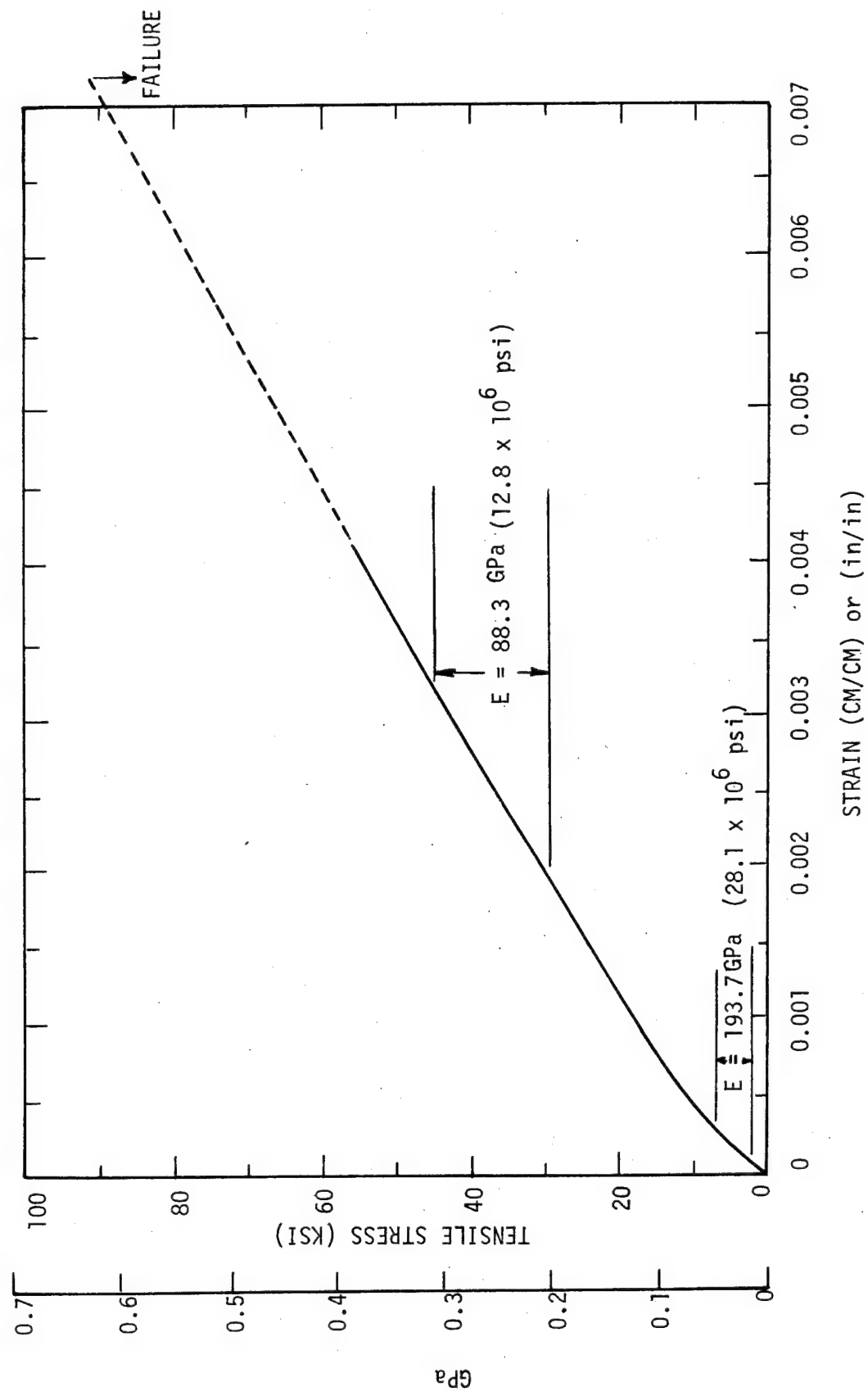


Figure 22 - Specimen 14 - Room Temperature Tension Stress/Strain Curve

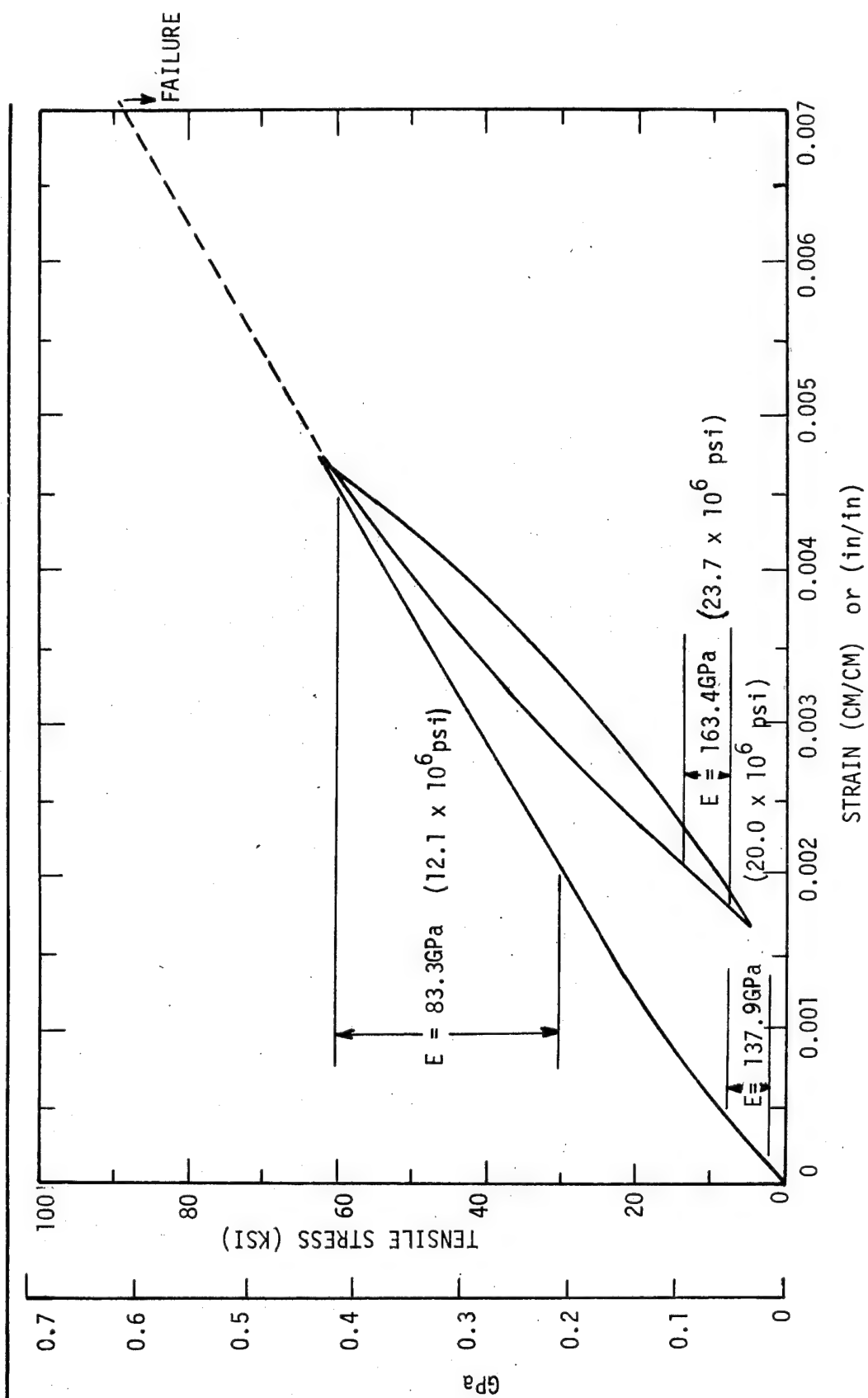


Figure 23 Specimen 15 - Room Temperature Tension Stress/Strain Curve

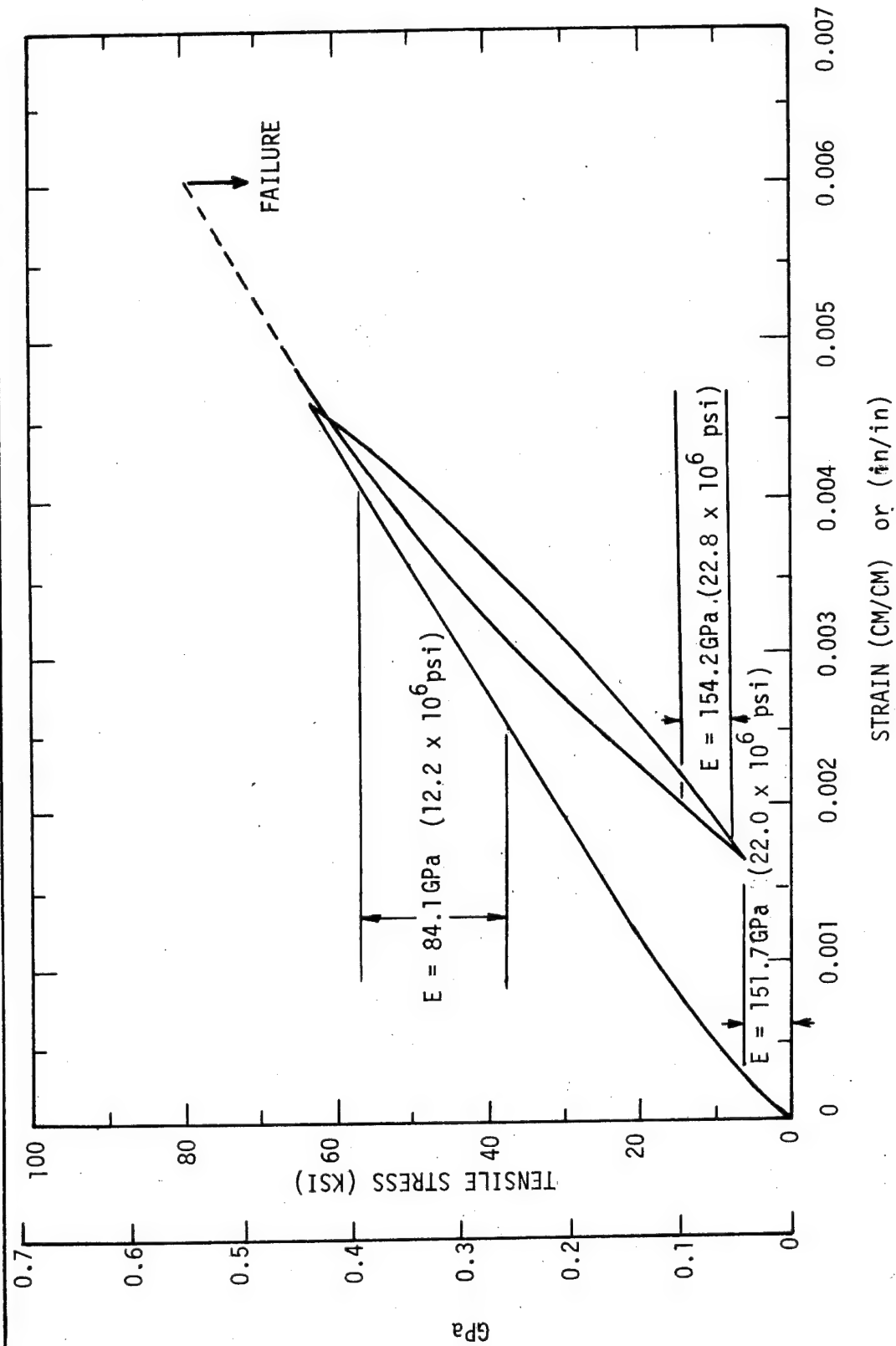


Figure 24 Specimen 16 - Room Temperature Tension Stress/Strain Curve

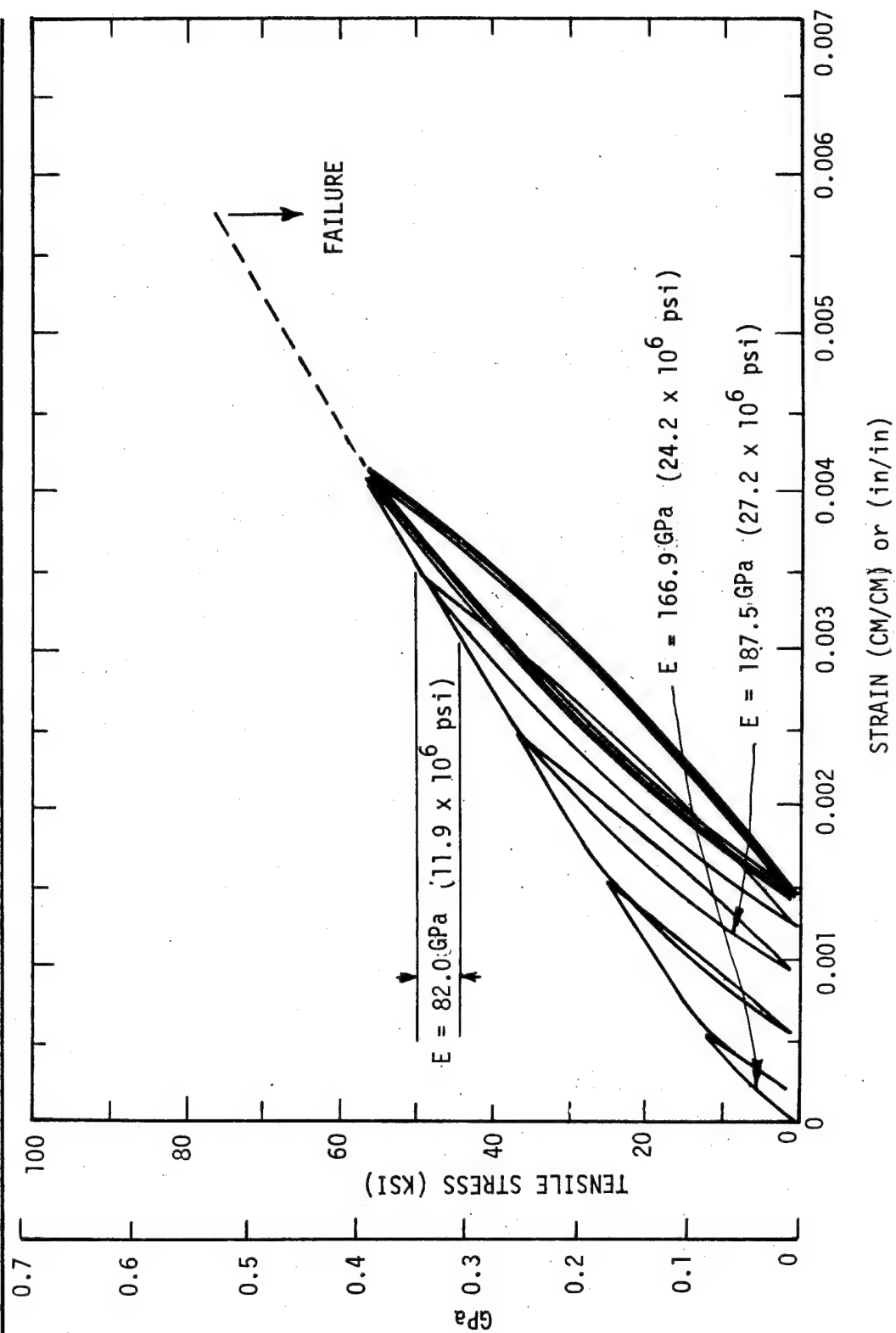


Figure 25 Specimen -17 - Room Temperature Tension Stress/Strain Curve

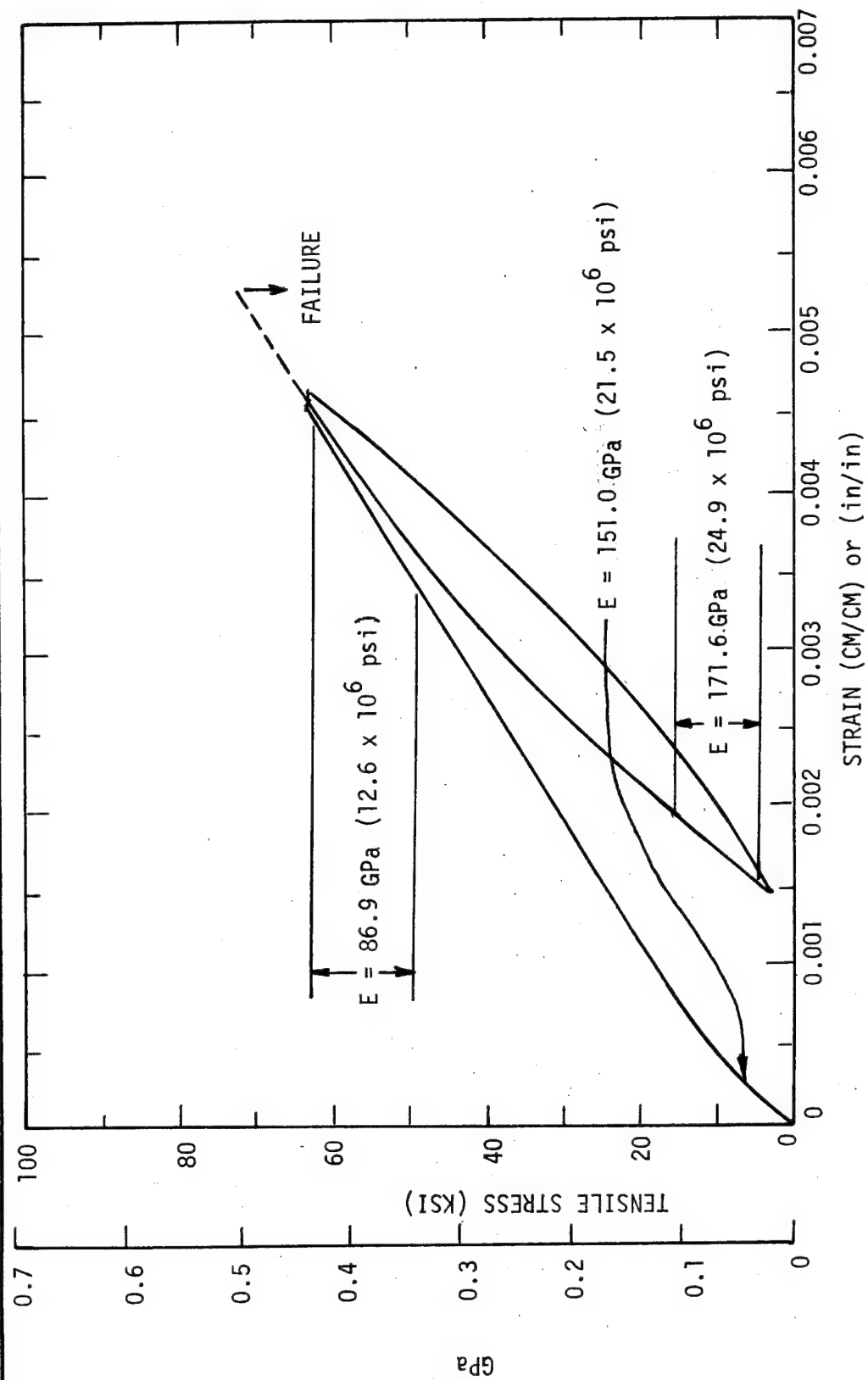


Figure 26 Specimen 18 - Room Temperature Tension Stress/Strain Curve

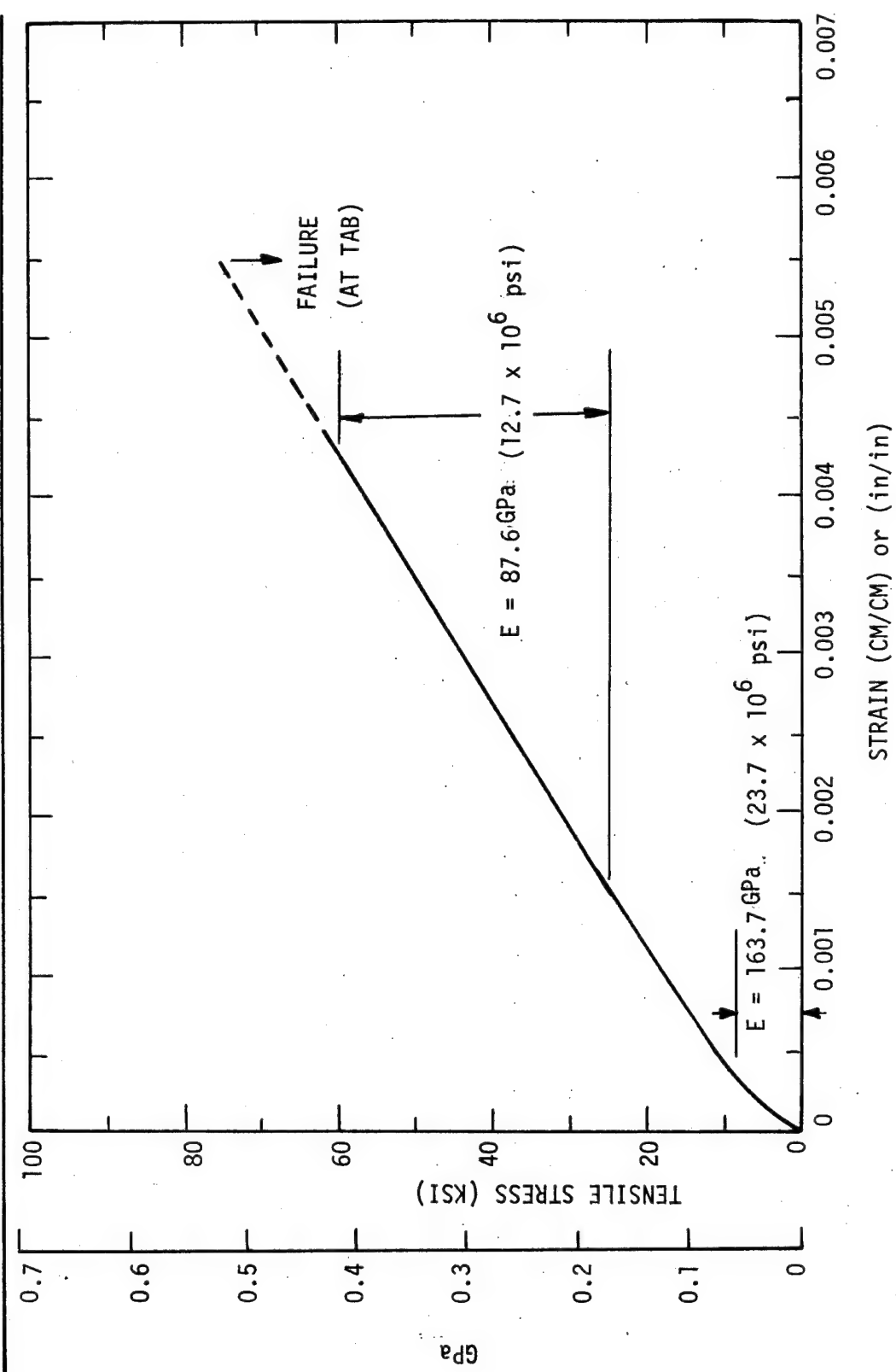


Figure 27 Specimen 19 - Room Temperature Tension Stress/Strain Curve

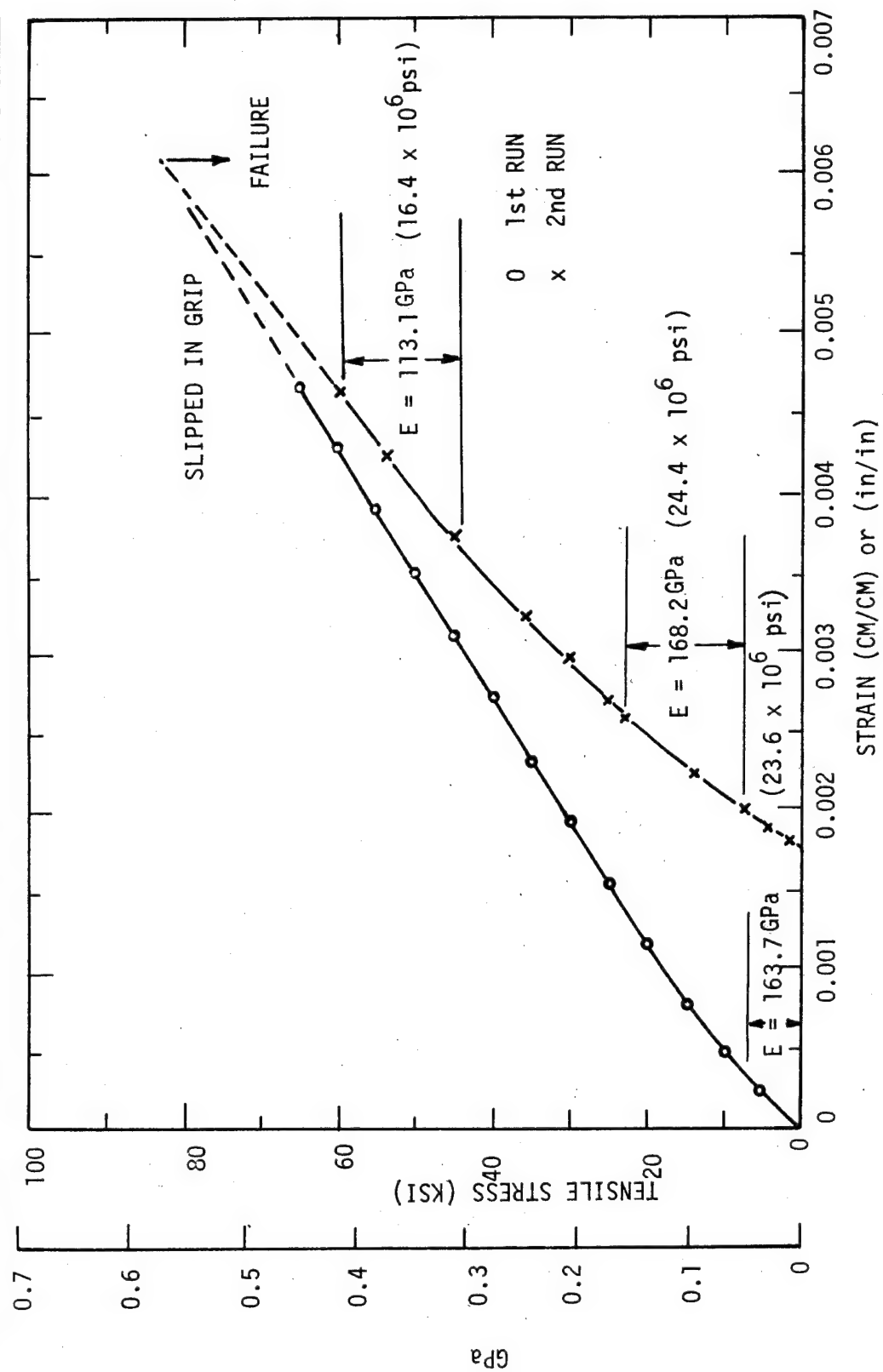


Figure 28 Specimen 20 - Room Temperature Tension Stress/Strain Curve

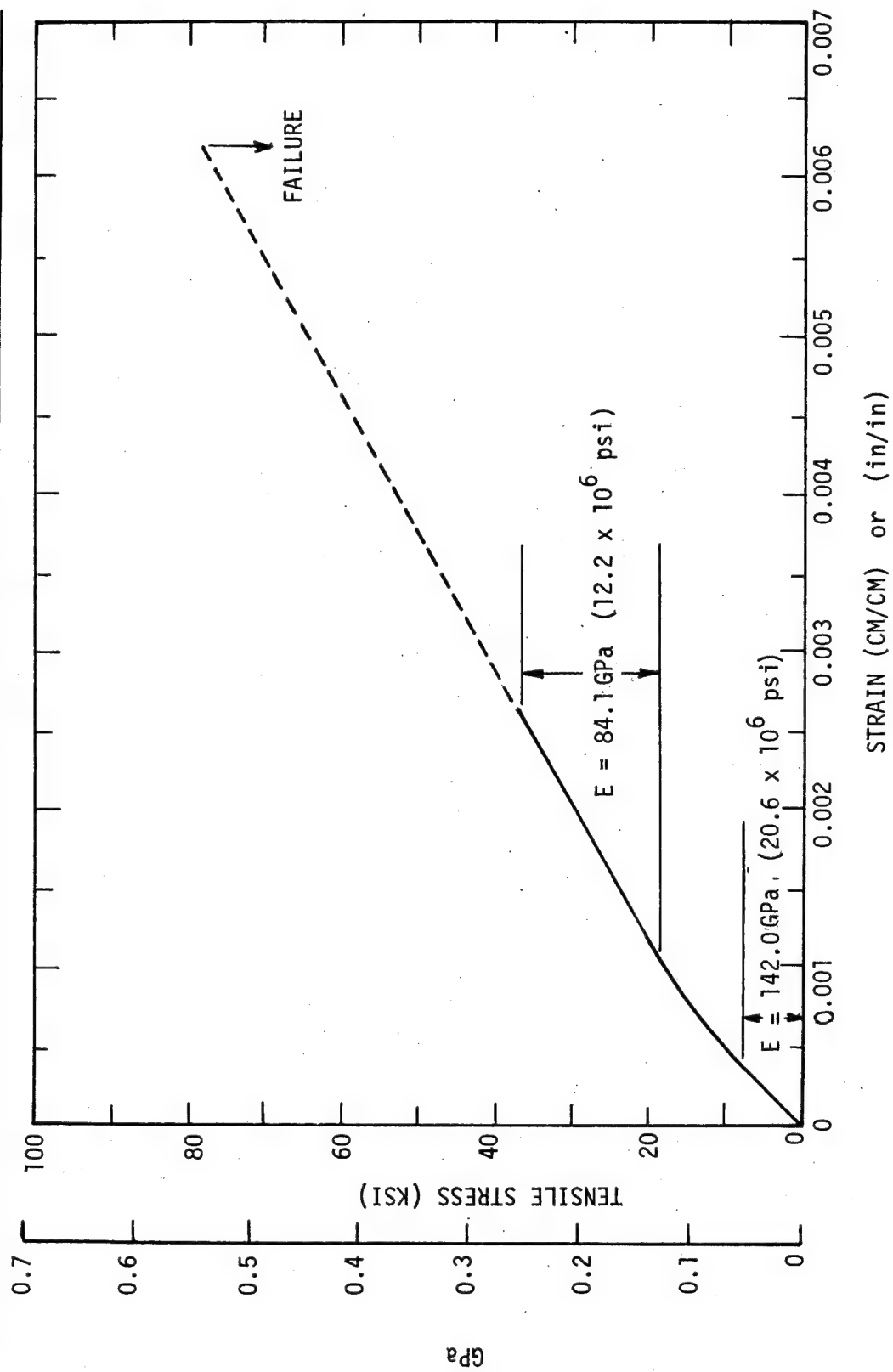


Figure 29 Specimen 21 - Room Temperature Tension Stress/Strain Curve after 1000 Hours Aging at 505K(450°F)

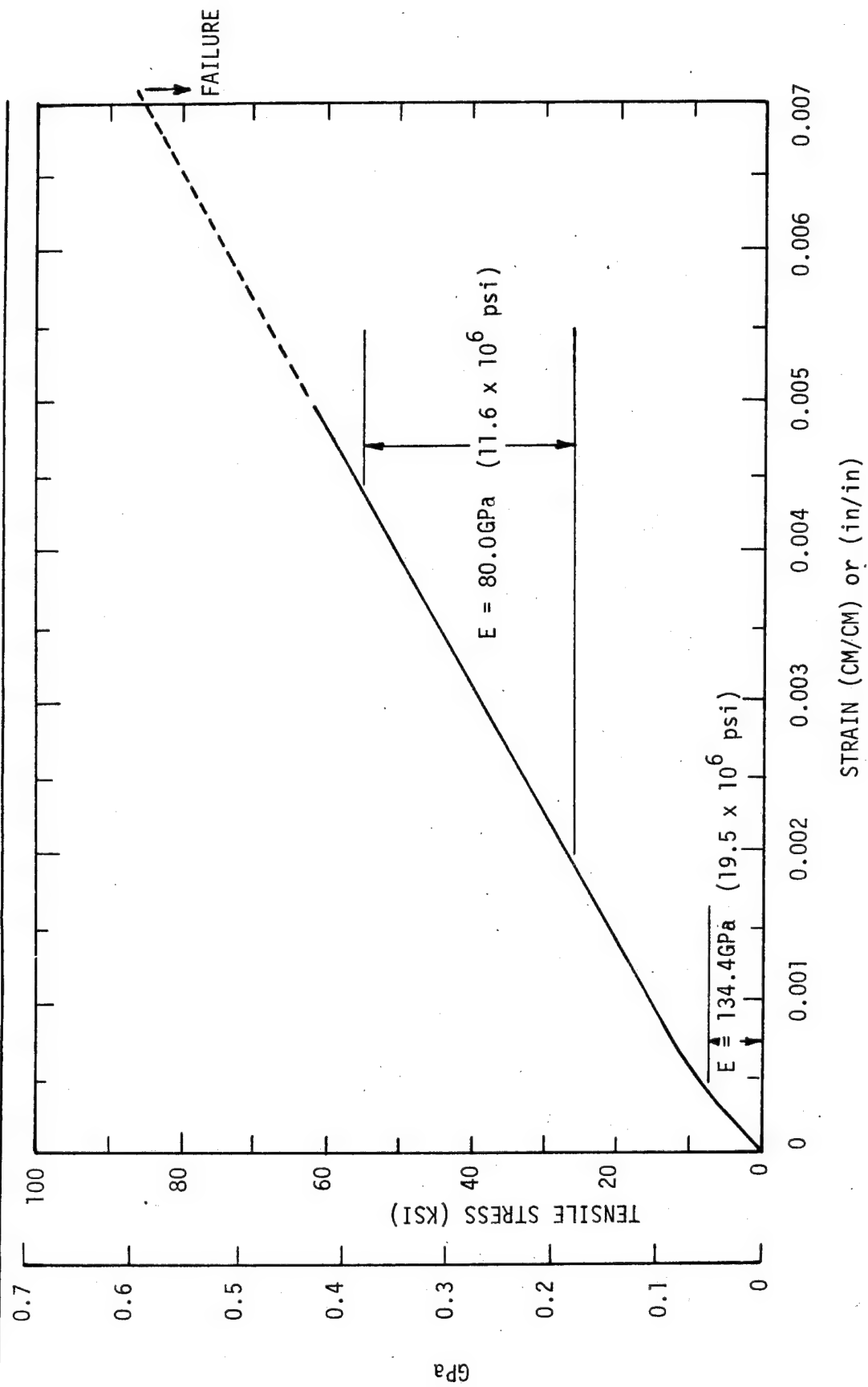


Figure 30 Specimen 22 - Room Temperature Tension Stress/Strain Curve after 1000 Hours Aging at 505K(450°F)

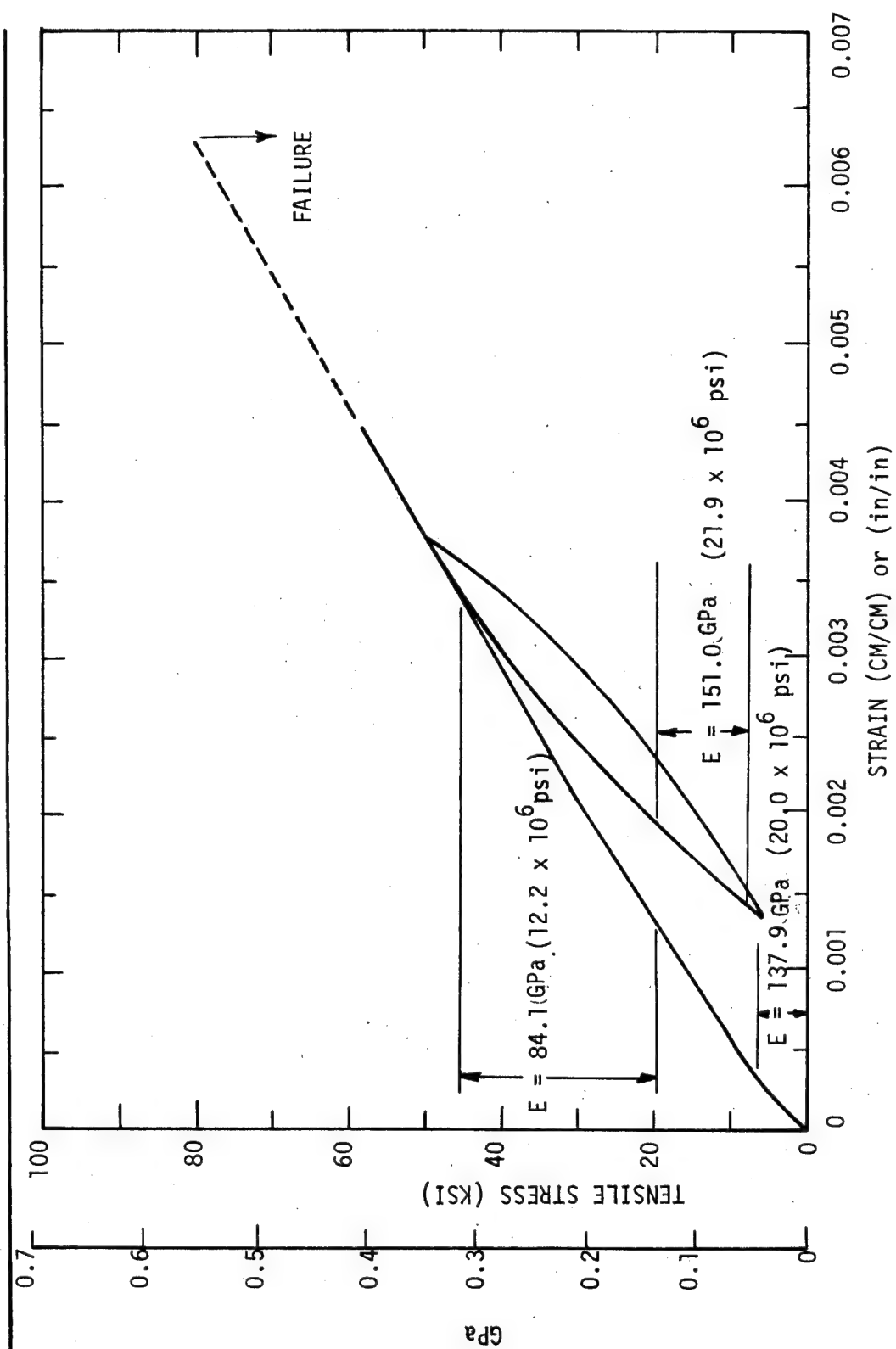


Figure 31 Specimen 23 - Room Temperature Tension Stress/Strain Curve after 1000 Hours Aging at 505K(450°F)

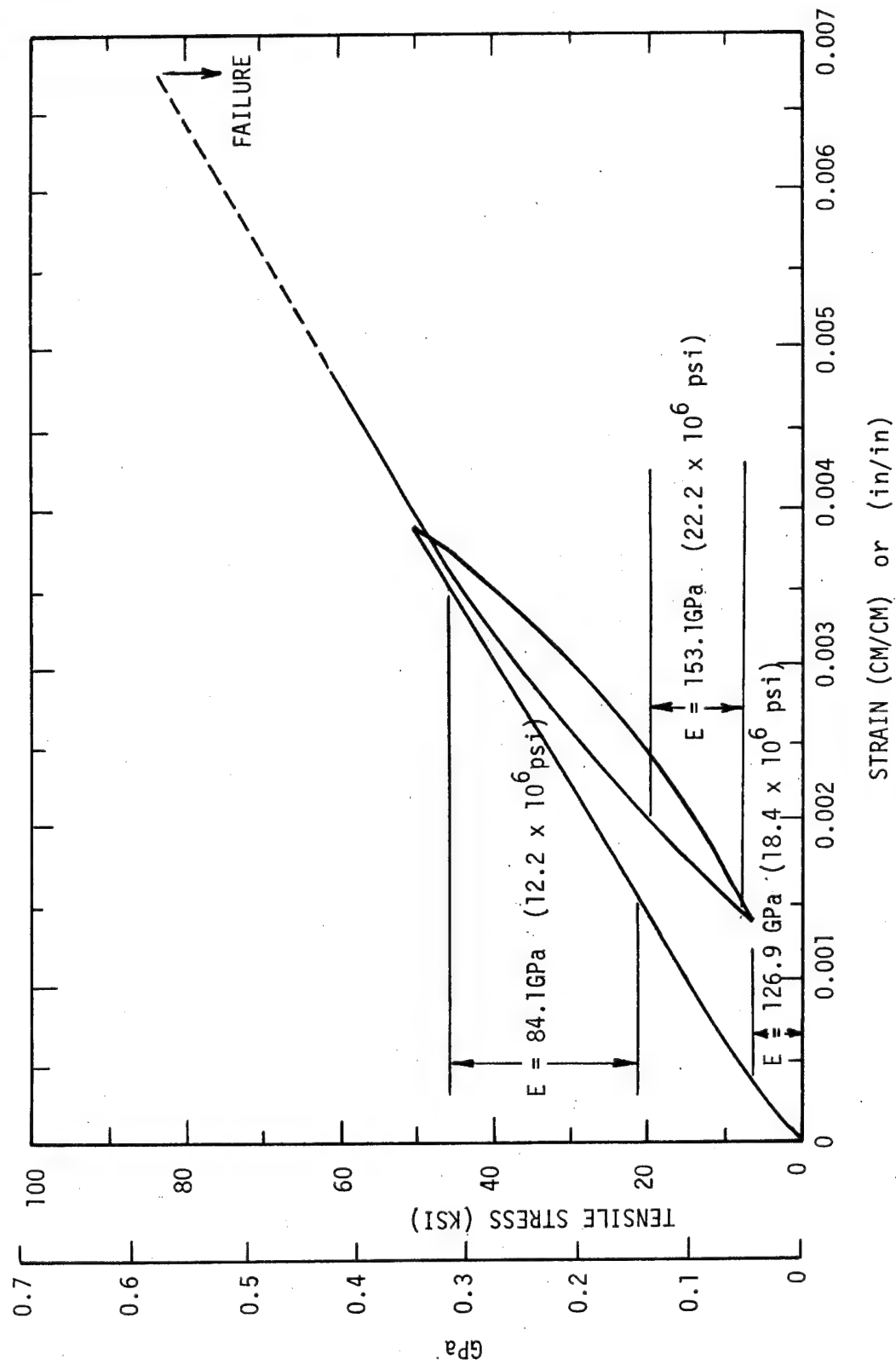


Figure 32 Specimen 24 - Room Temperature Tension Stress/Strain Curve after 1000 Hours Aging at 505K(450°F)

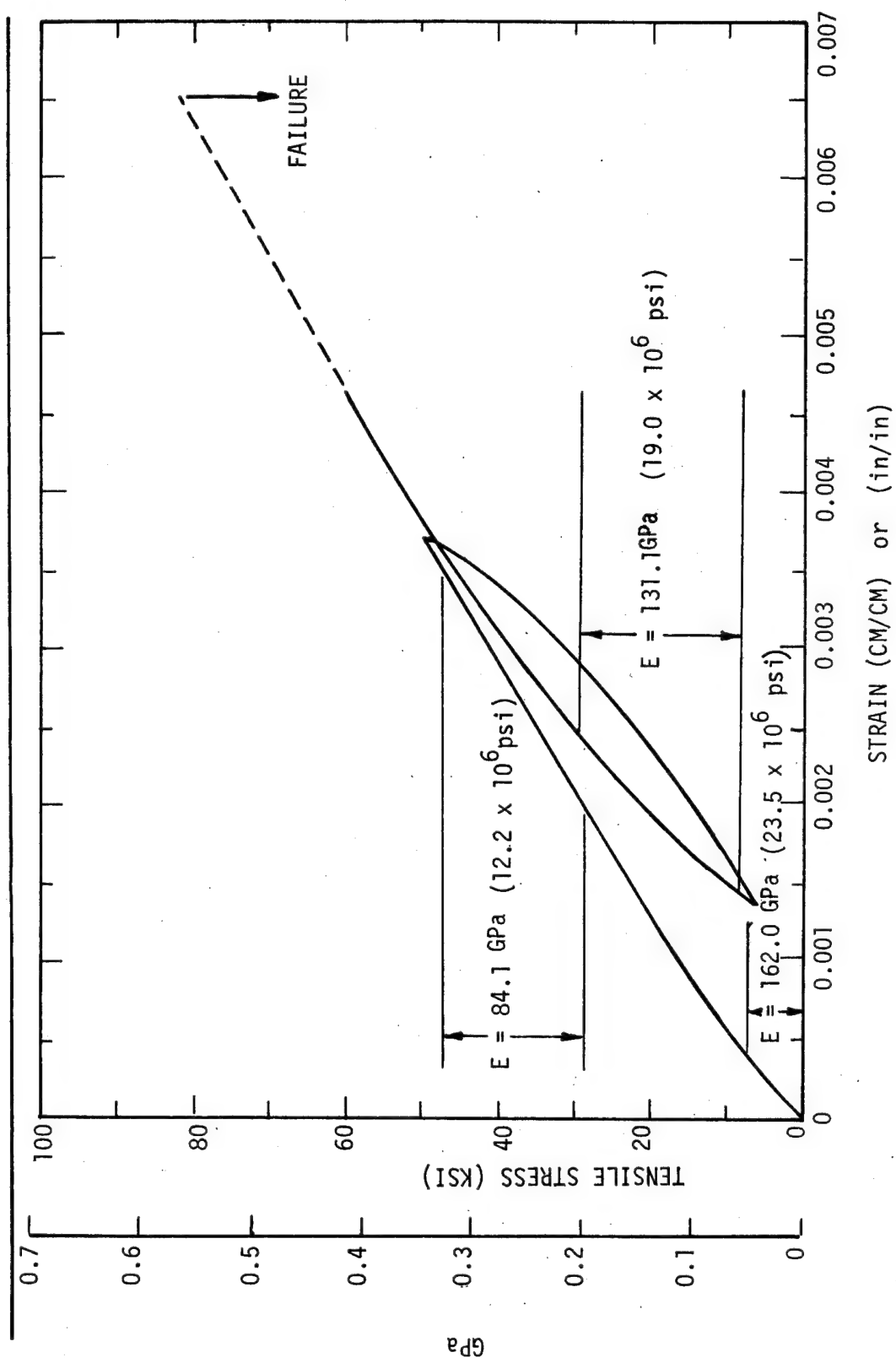


Figure 33 Specimen 25 - Room Temperature Tension Stress/Strain Curve after 1000 Hours Aging at 505K(450°F)

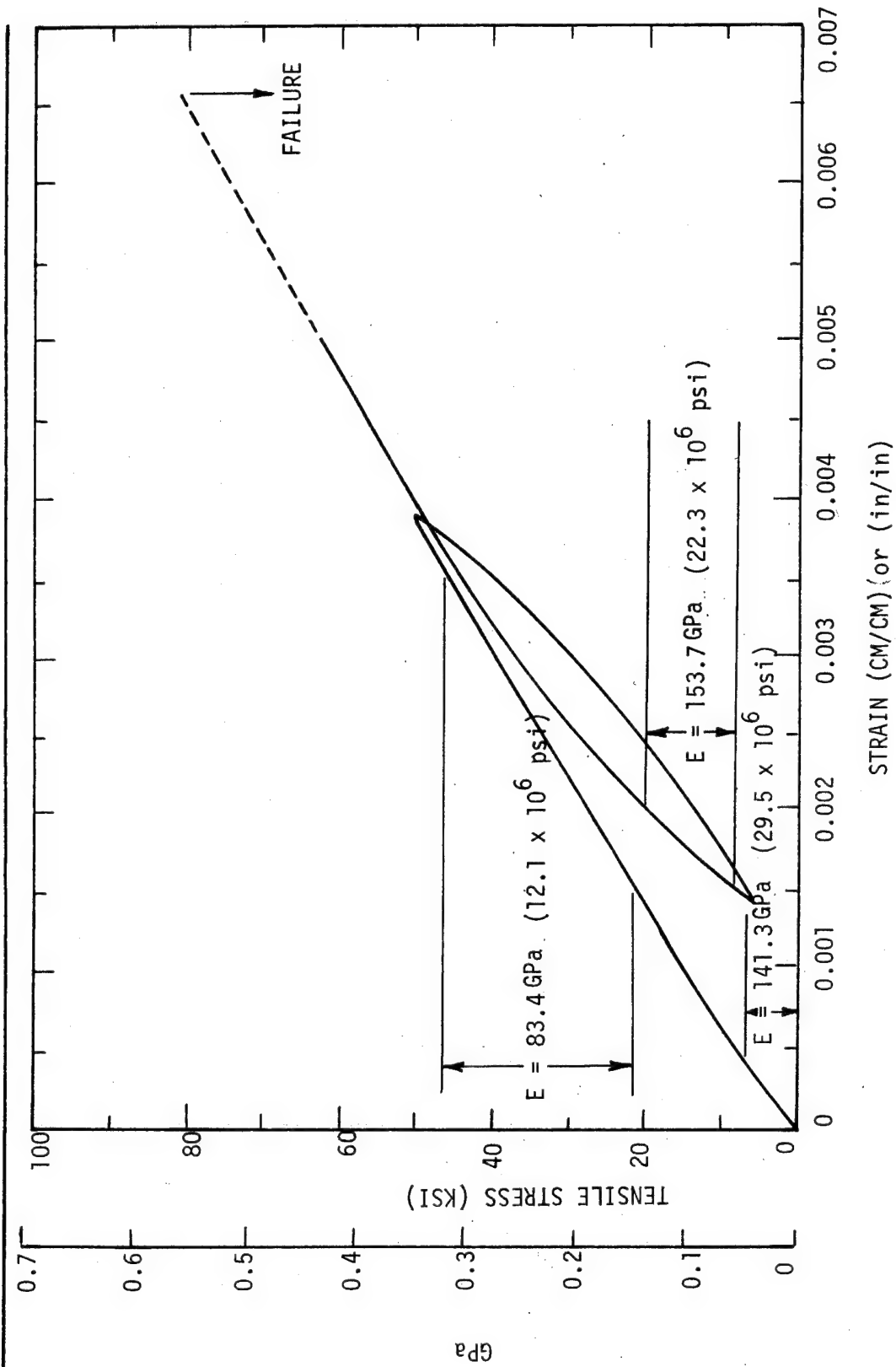


Figure 34 Specimen 26 - Room Temperature Tension Stress/Strain Curve after 1000 Hours Aging at 505K(450°F)

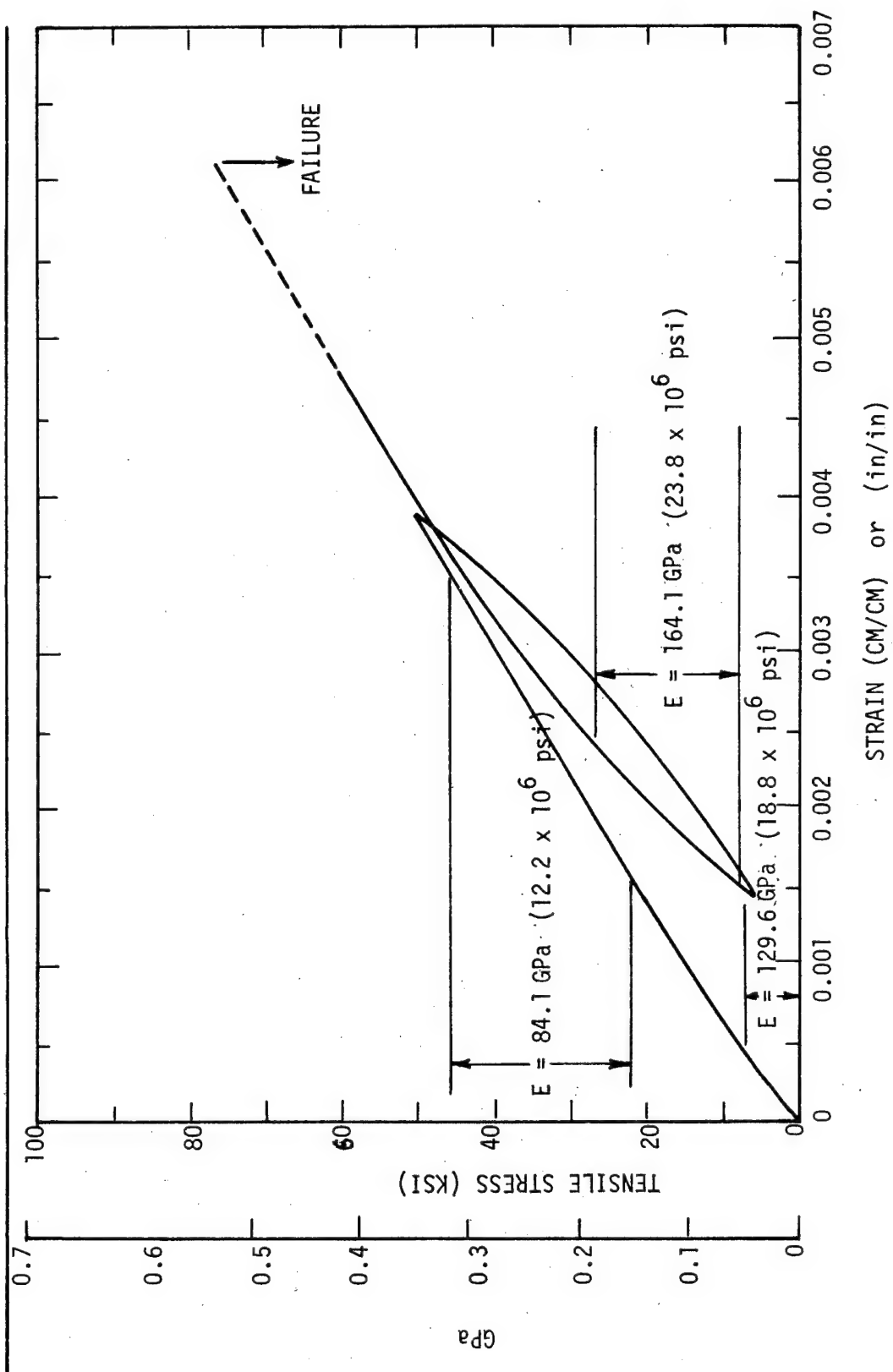


Figure 35 Specimen 27 - Room Temperature Tension Stress/Strain Curve after 1000 Hours Aging at 505K(450°F)

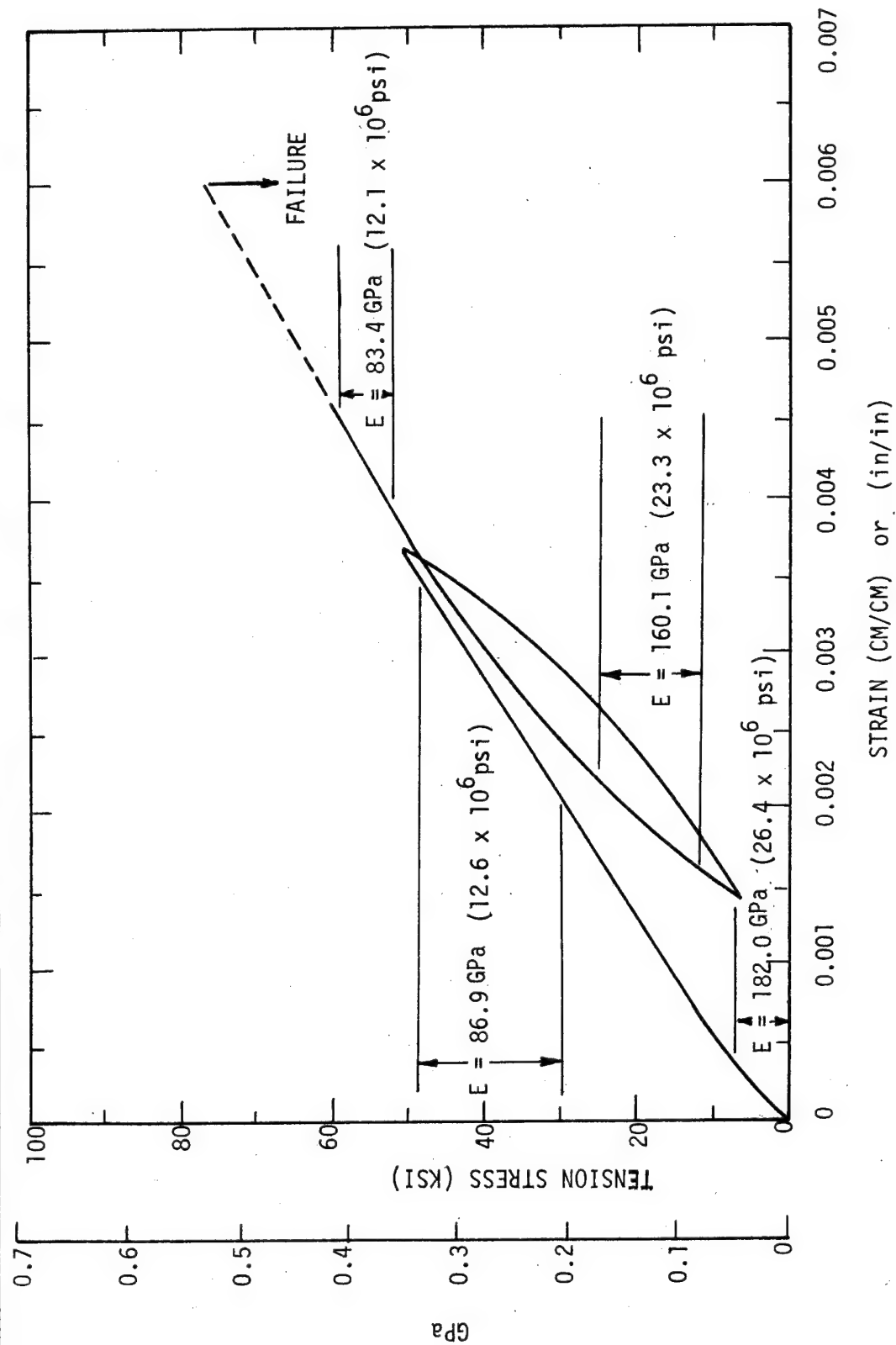


Figure 36 Specimen 28 - Room Temperature Tension Stress/Strain Curve after 1000 Hours Aging at 505K(450°F)

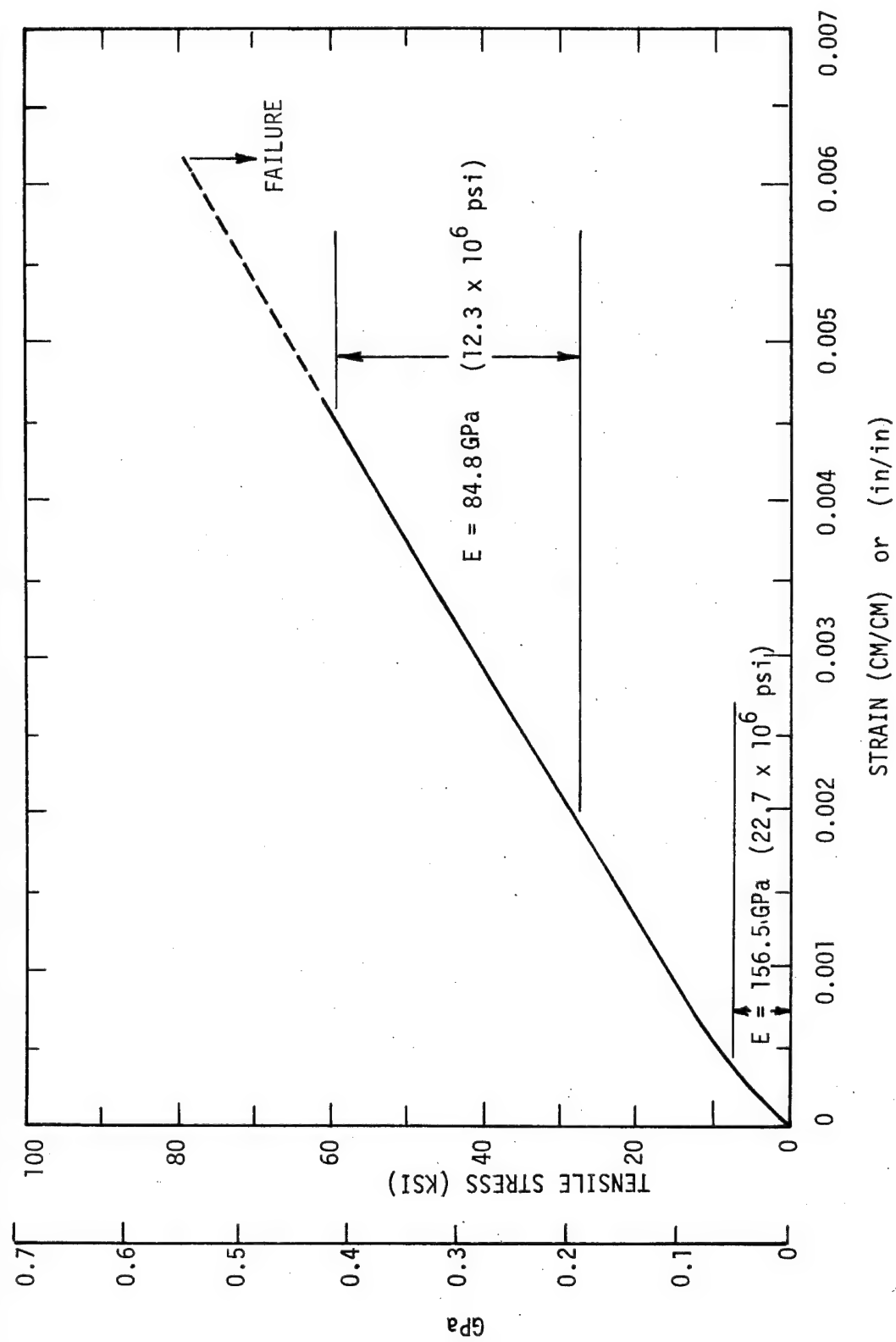


Figure 37 Specimen 29 - Room Temperature Tension Stress/Strain Curve after 1000 Hours Aging at 505K(450°F)

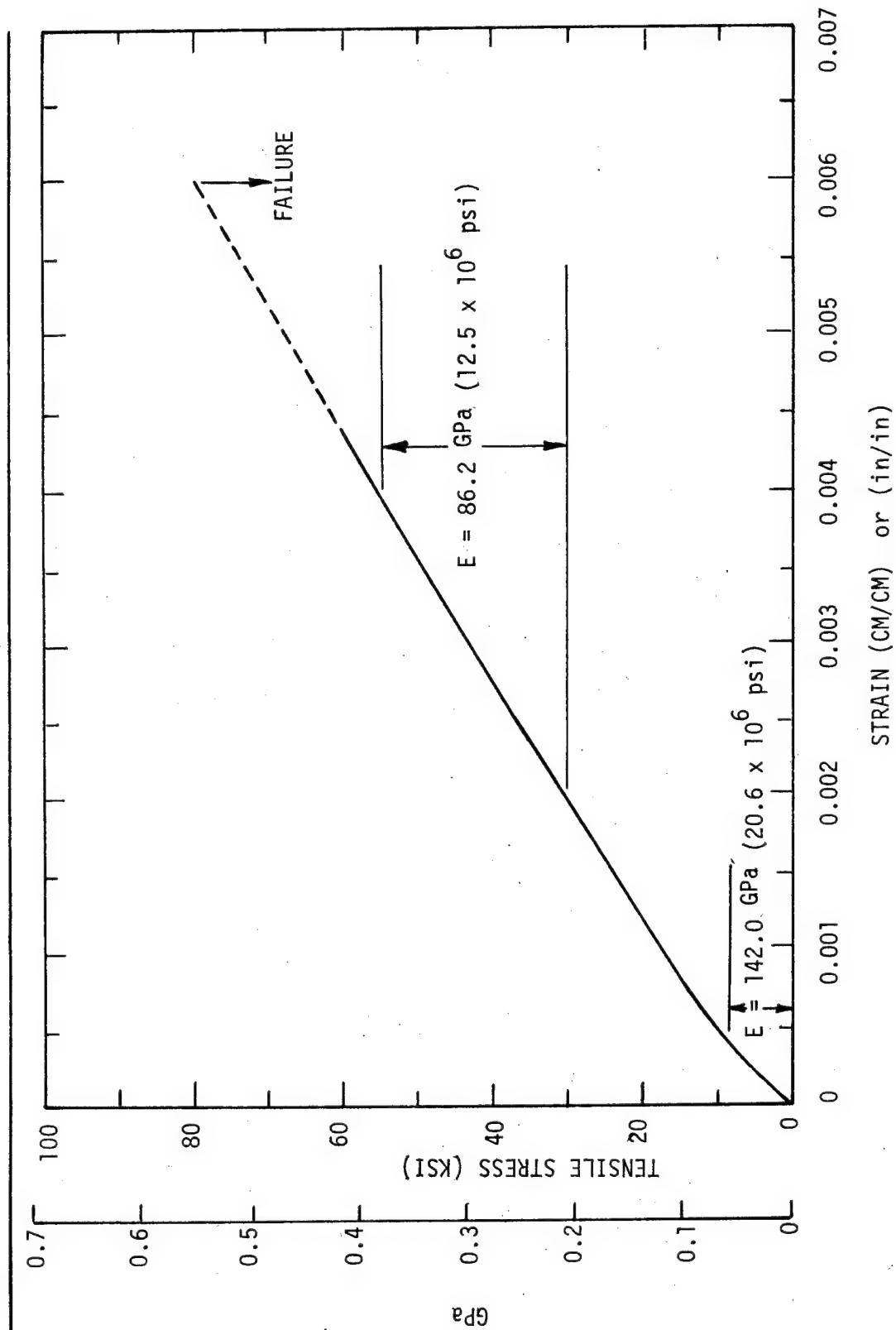


Figure 38 Specimen 30 - Room Temperature Tension Stress/Strain Curve after 1000 Hours Aging at 505K(450°F)

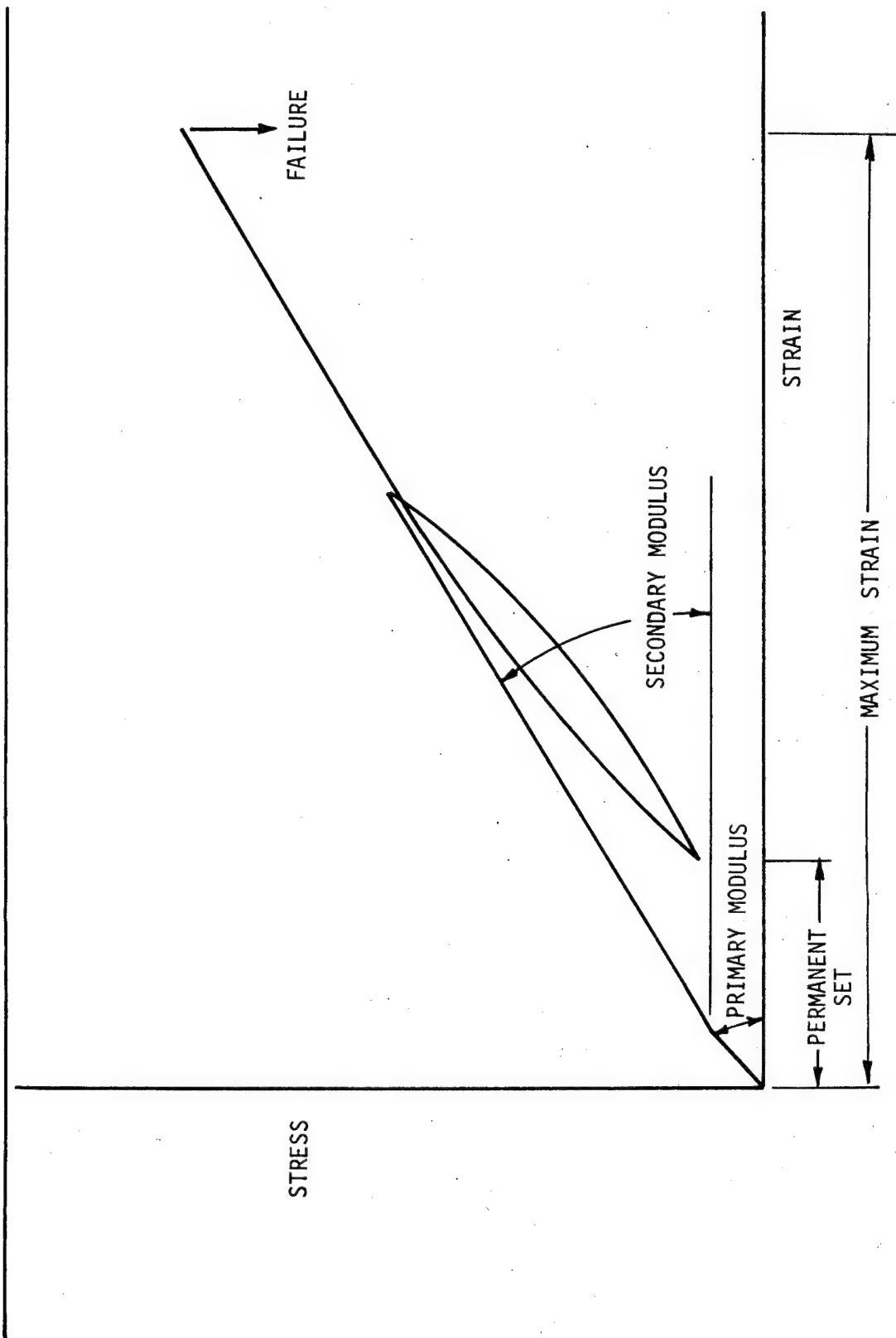


Figure 39 Schematic of Typical Tension Stress/Strain Curve

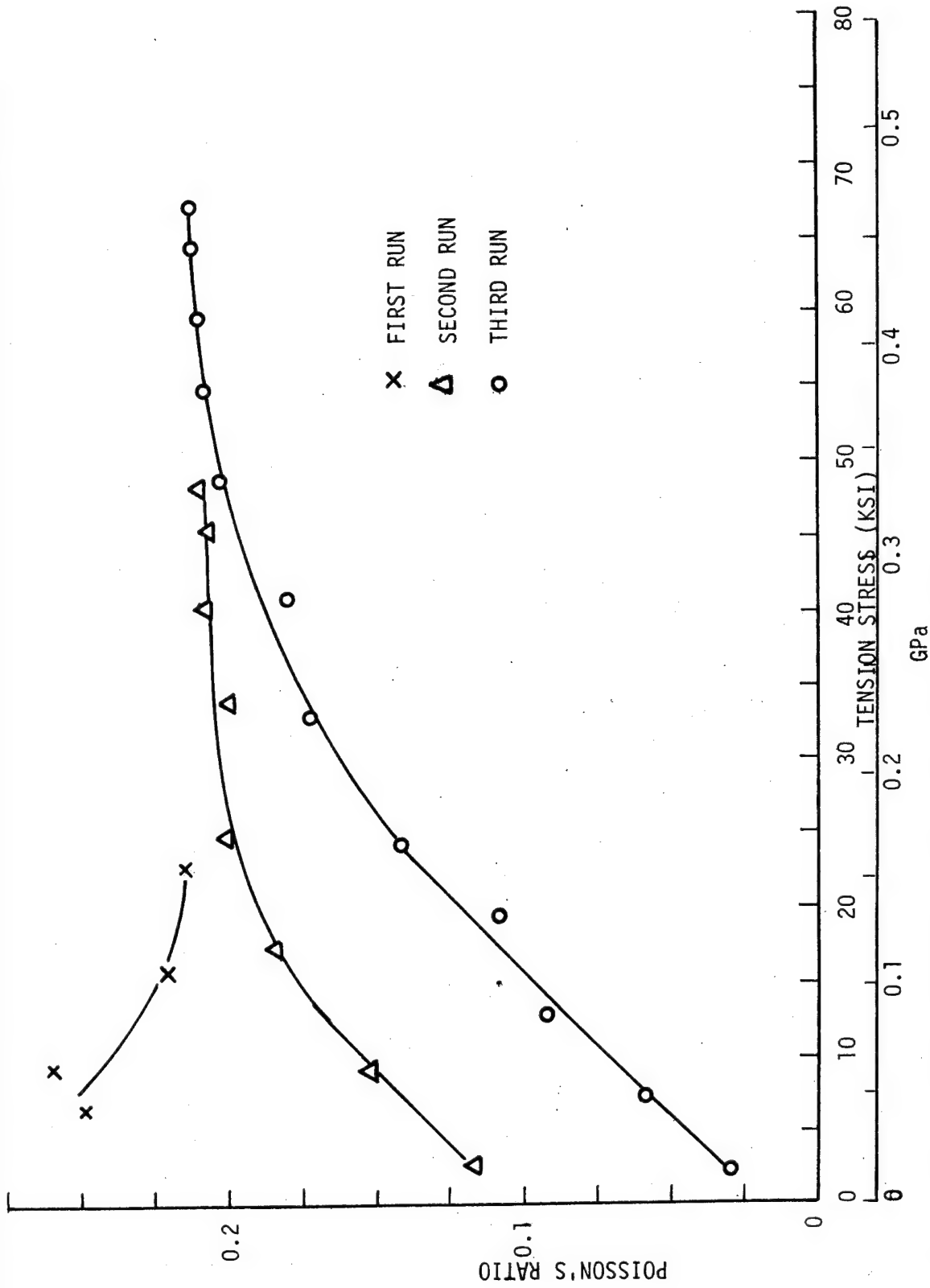


Figure 40 Specimen 11 (Side #1) Poisson's Ratio Vs Tension Stress

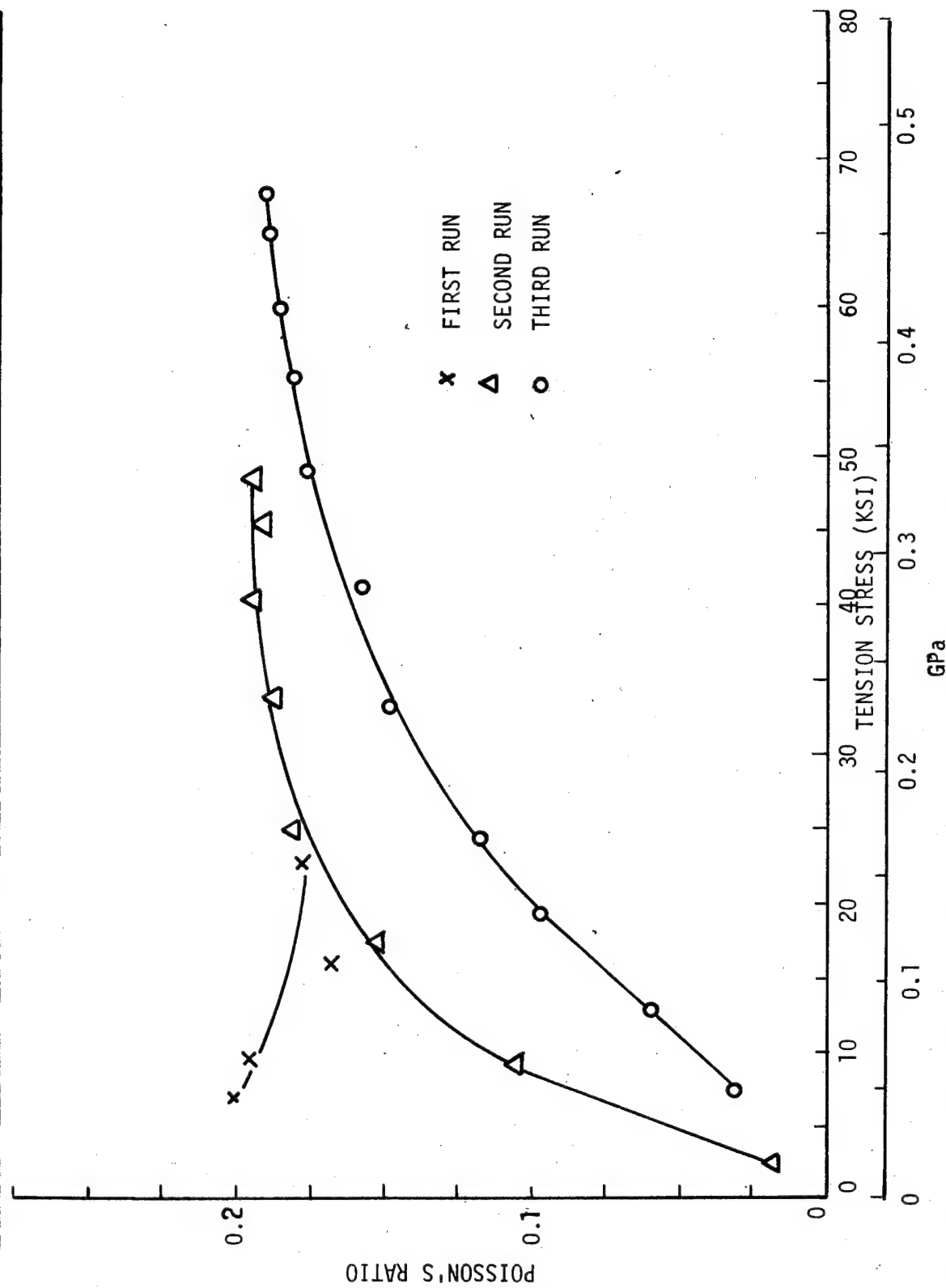


Figure 41 Specimen 11 (Side #2) Poisson's Ratio Vs Tension Stress

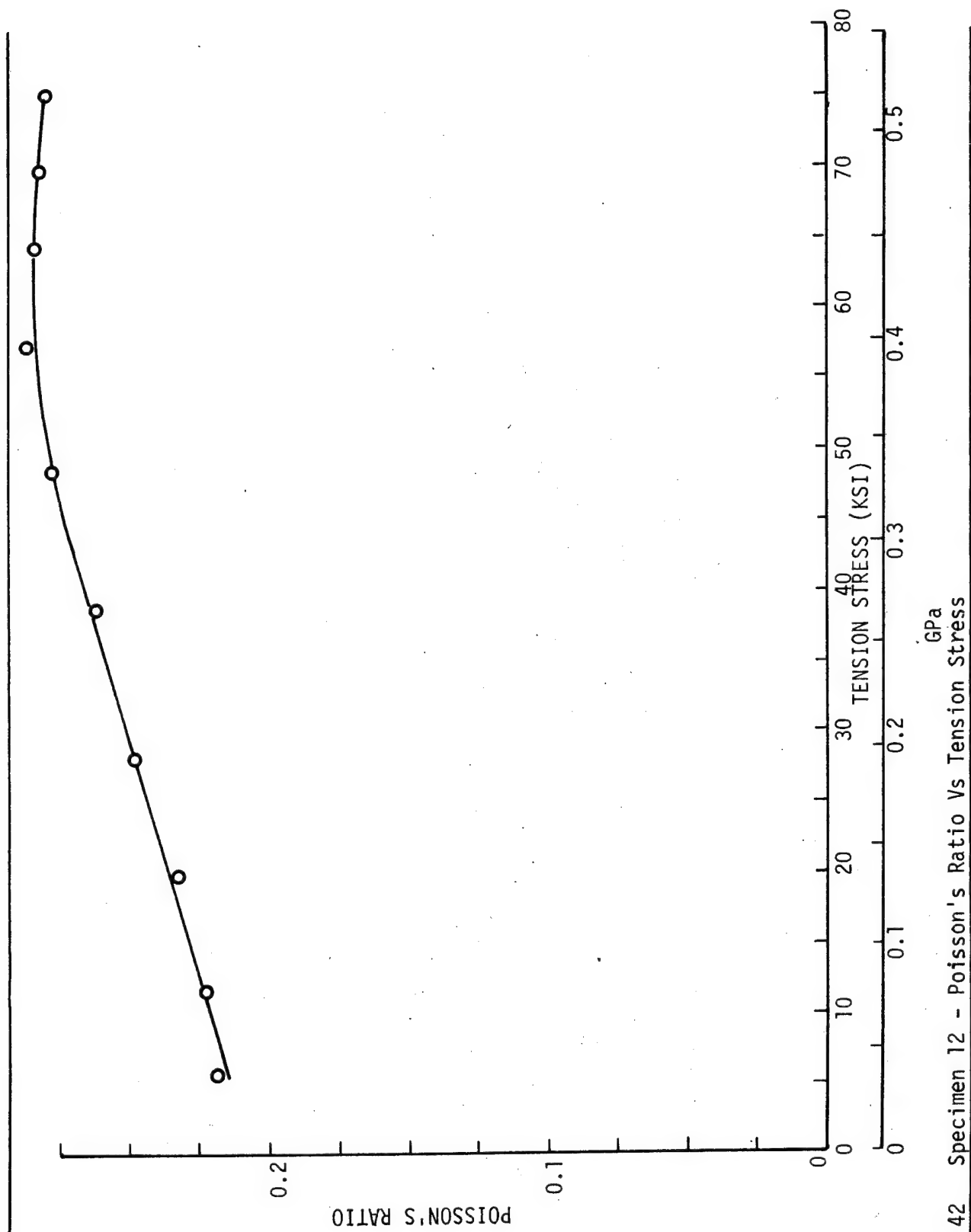


Figure 42 Specimen 12 - Poisson's Ratio Vs Tension Stress

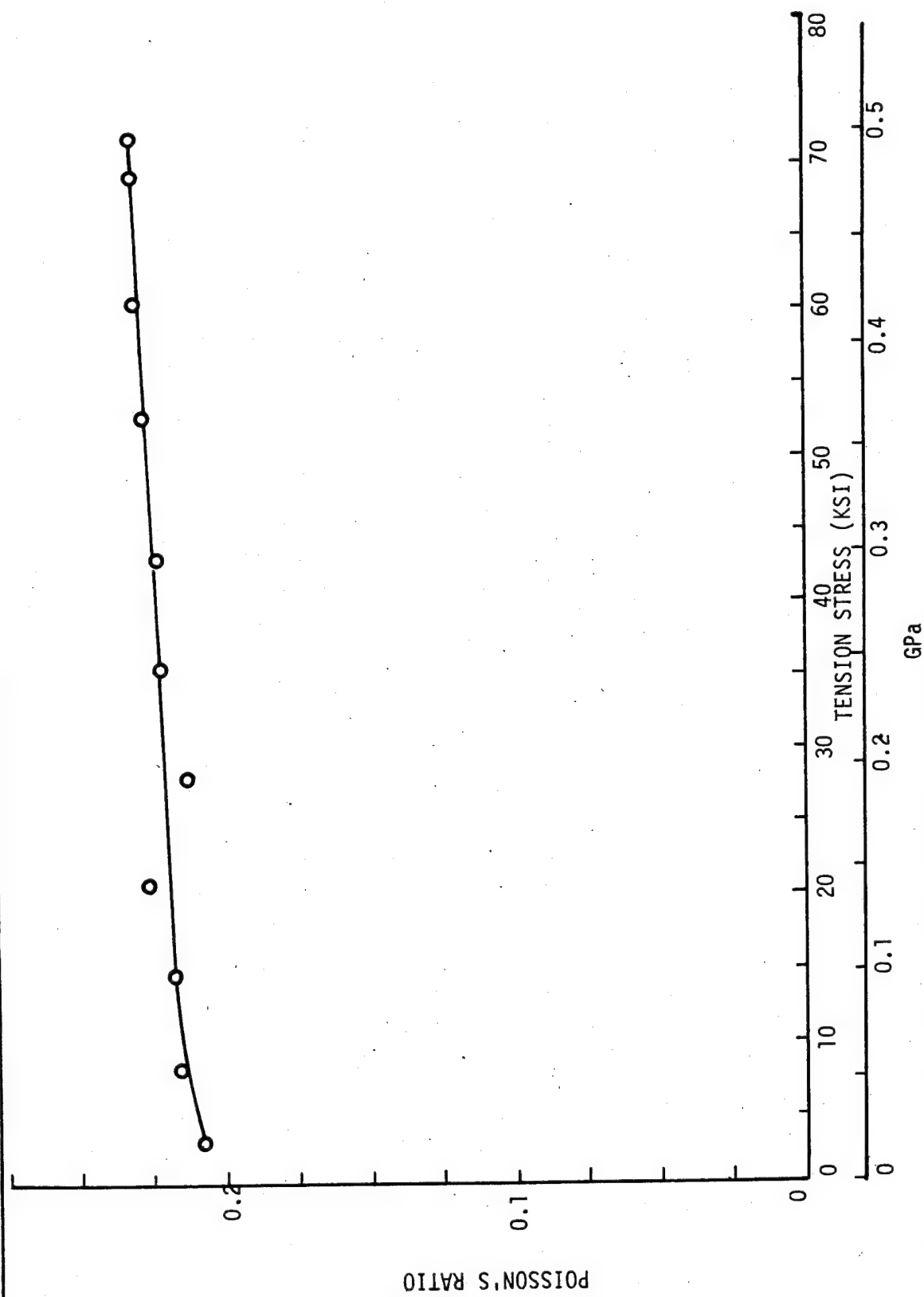


Figure 43 Specimen 13 - Poisson's Ratio Vs Tension Stress

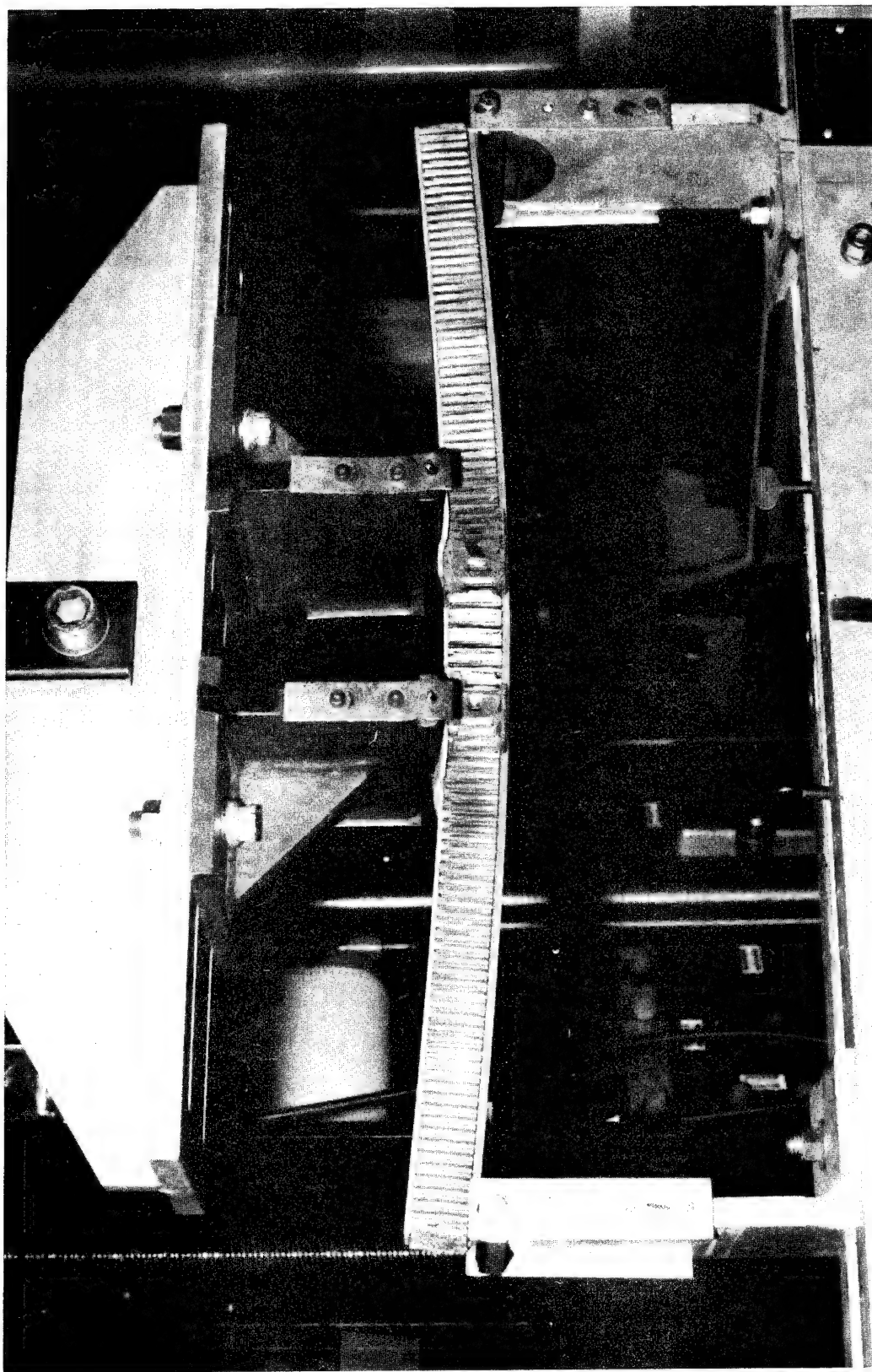


Figure 44 Four Point Bending Honeycomb Sandwich Compression Test

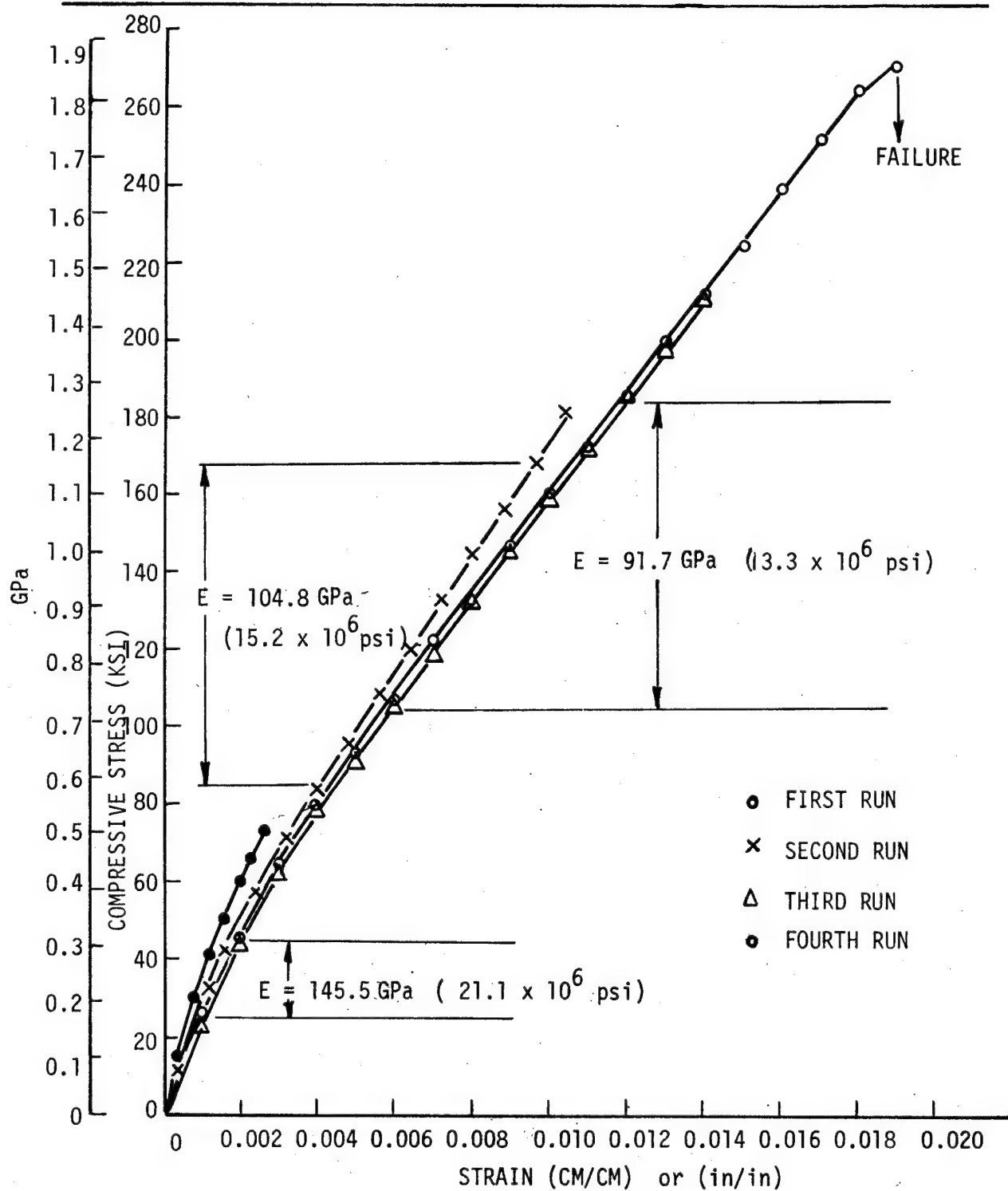


Figure 45 Specimen 11 - Room Temperature Compression Stress/Strain Curve

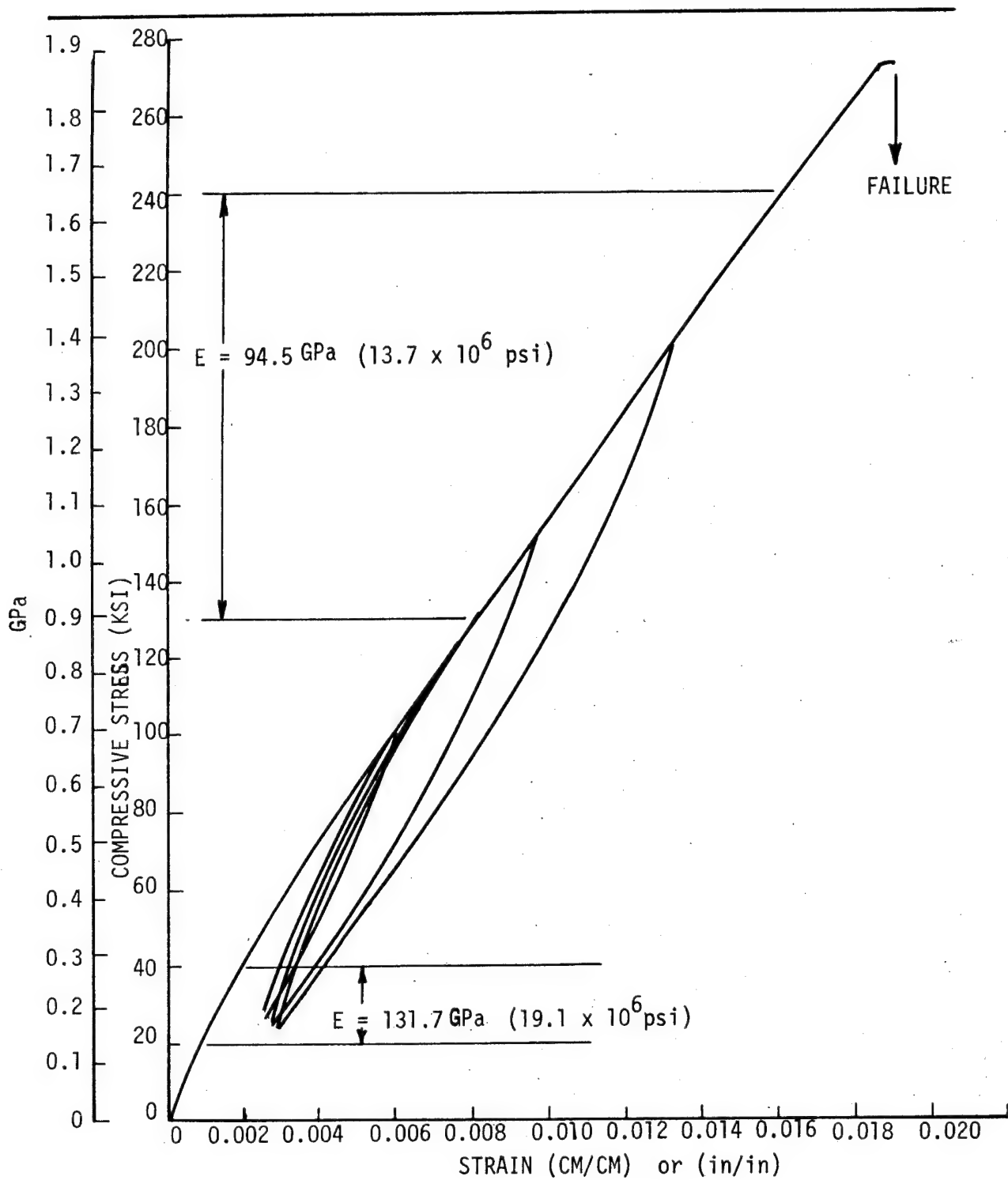


Figure 46 Specimen 12 - Room Temperature Compression Stress/Strain Curve

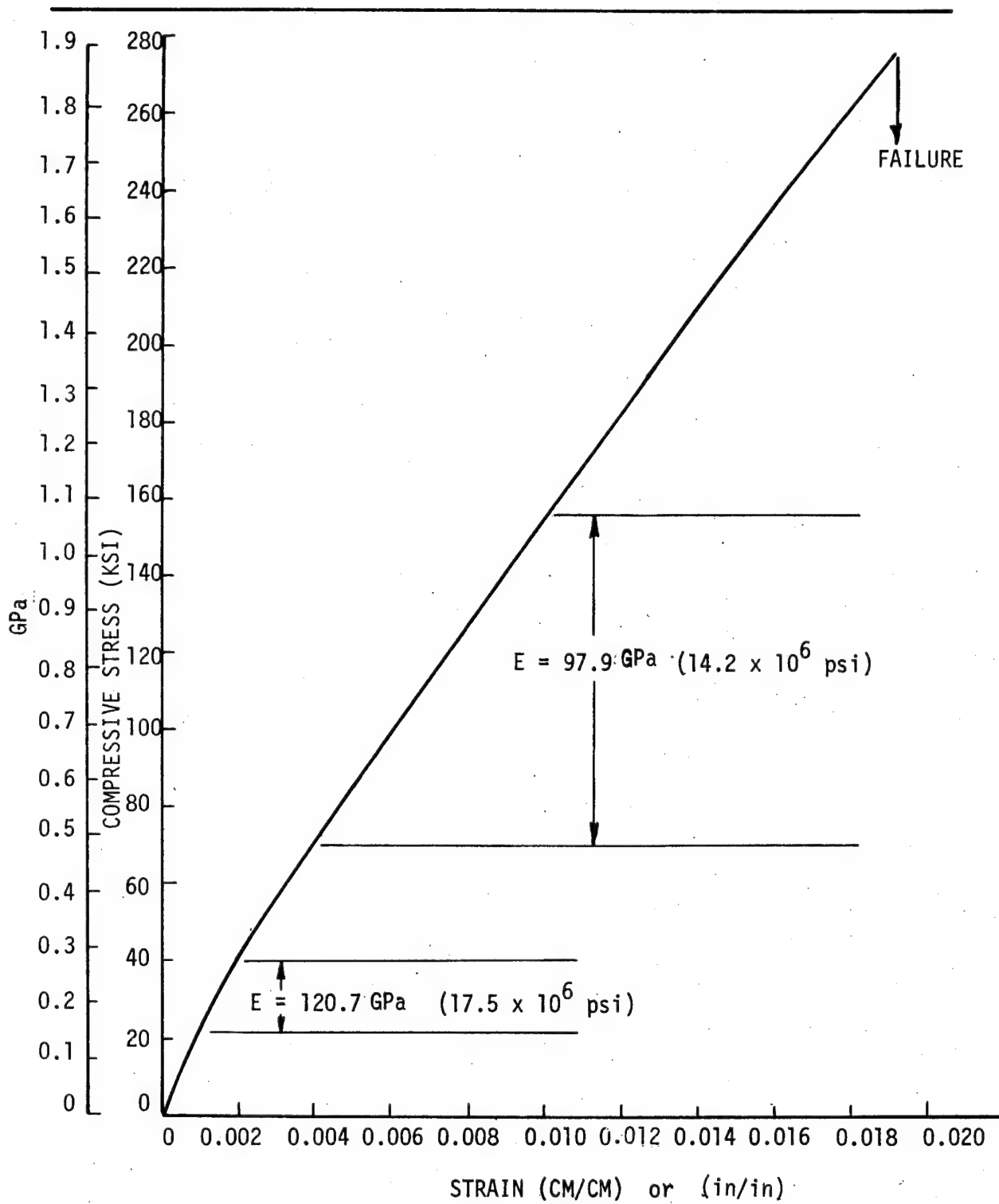


Figure 47 Specimen 13 - Room Temperature Compression Stress/Strain Curve

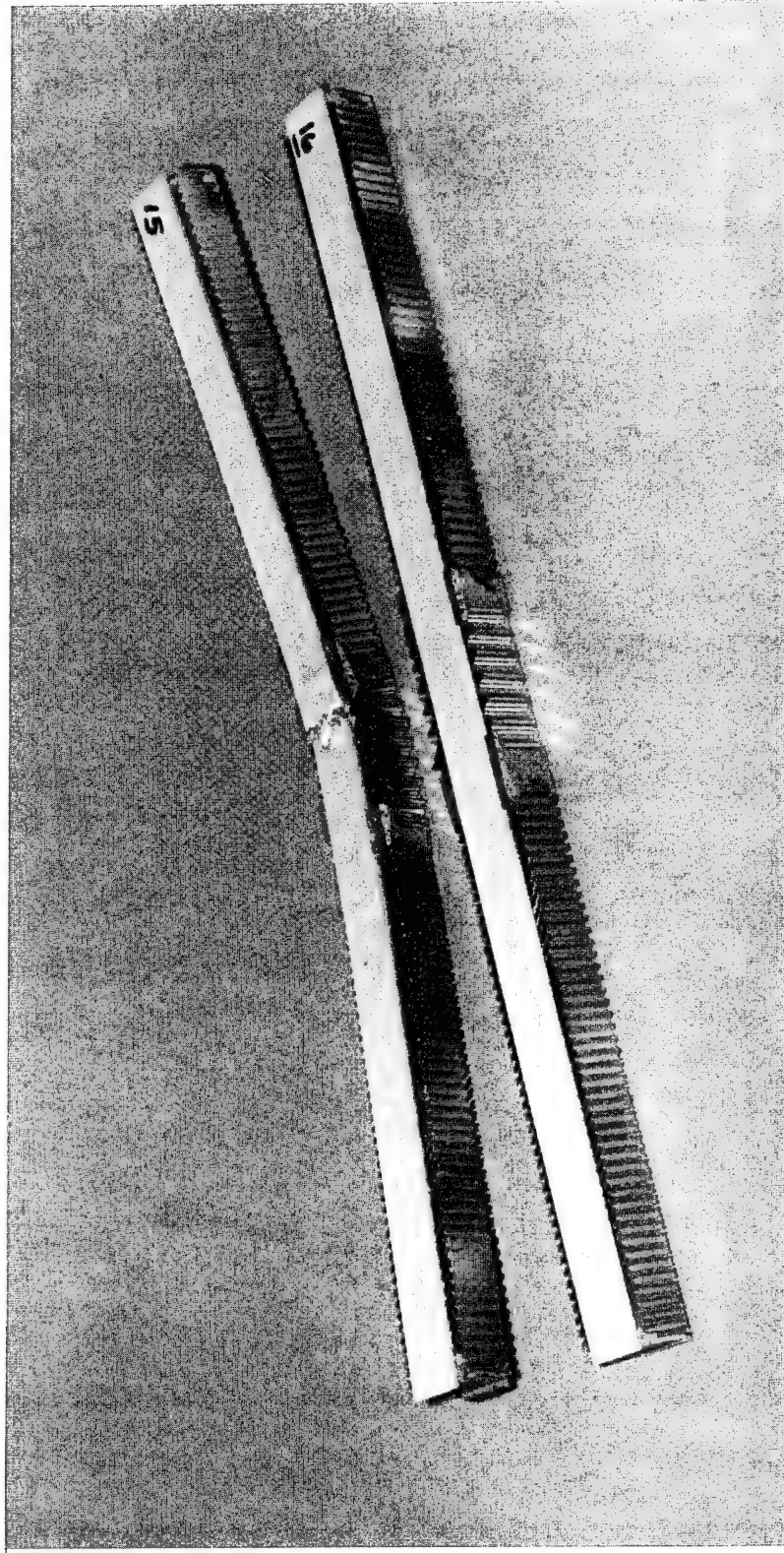


Figure 48 A Tested and An Untested Room Temperature Honeycomb Sandwich Compression Specimen

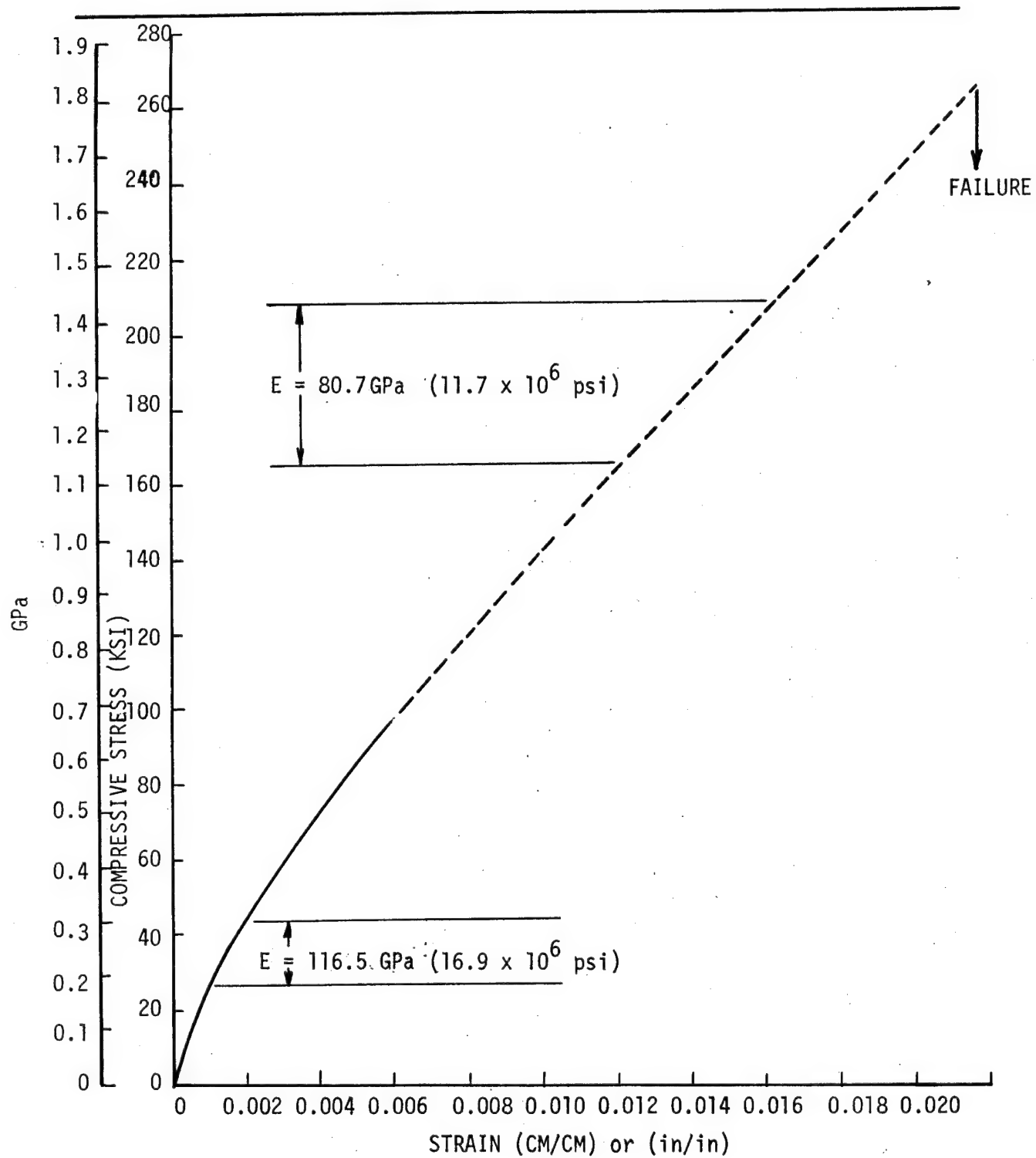


Figure 49 Specimen 14 - Room Temperature Compression Stress/Strain Curve

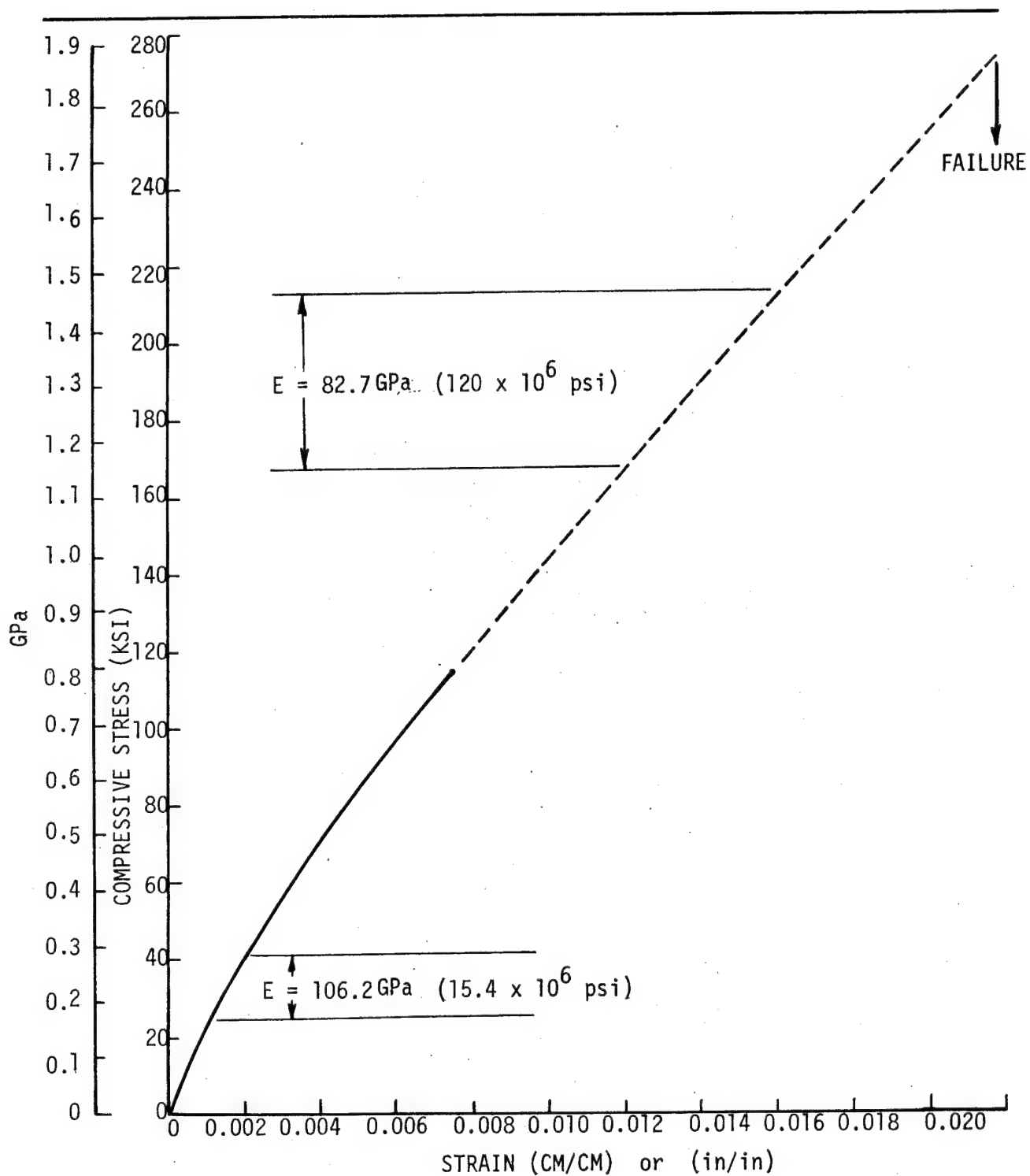


Figure 50 Specimen 15 - Room Temperature Compression Stress/Strain Curve

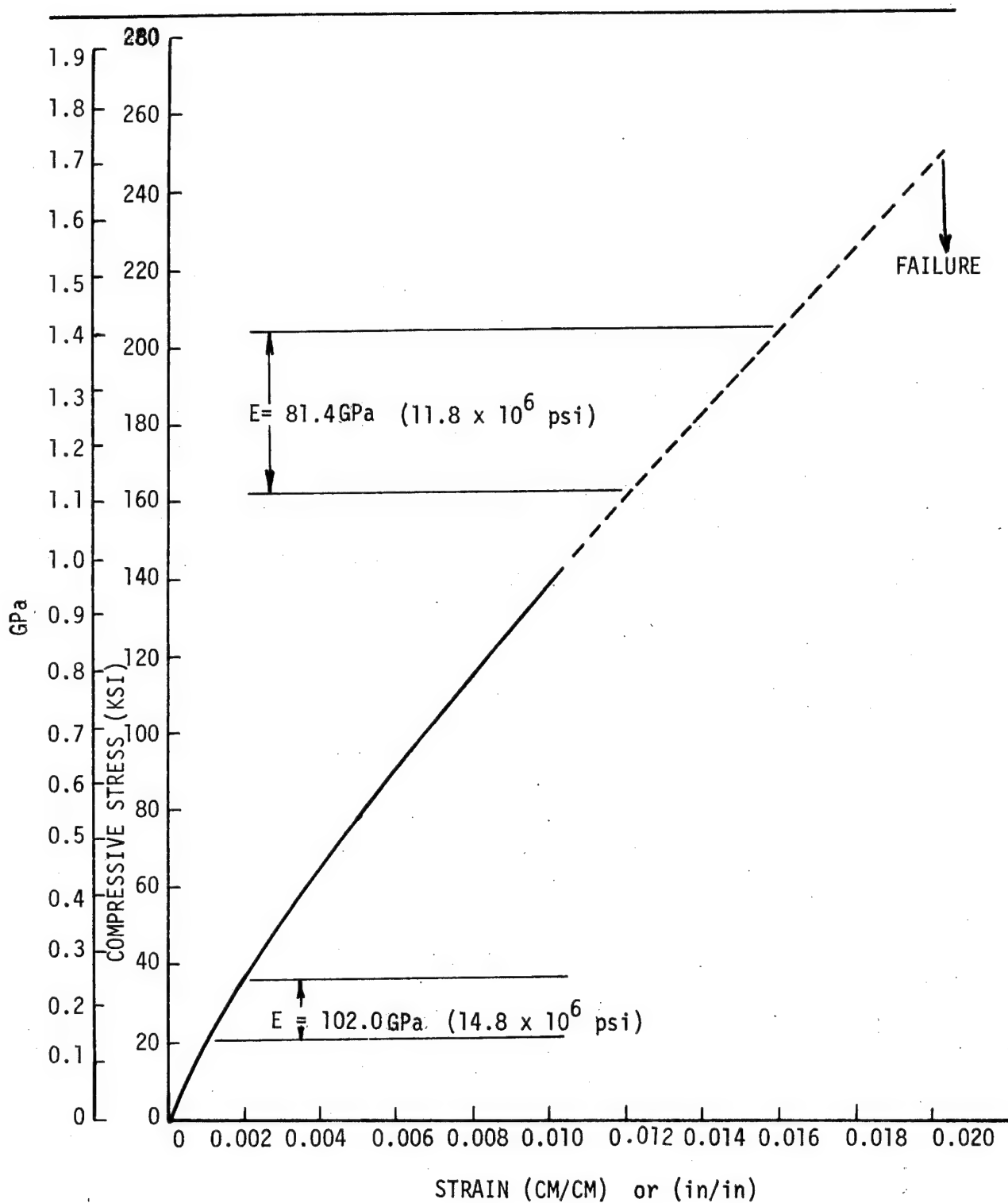


Figure 51 Specimen 16 - Room Temperature Compression Stress/Strain Curve

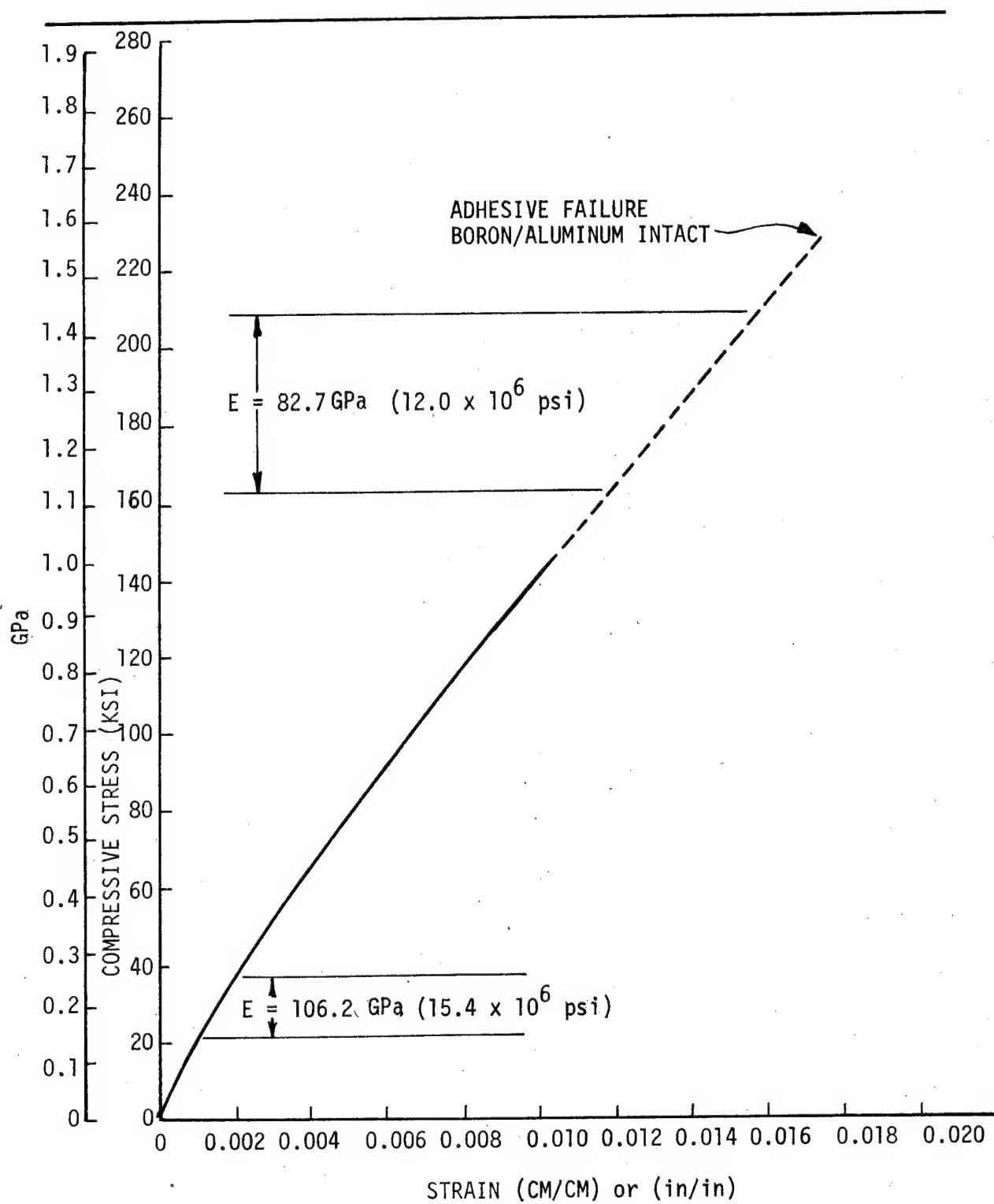


Figure 52 Specimen 17 - Room Temperature Compression Stress/Strain Curve

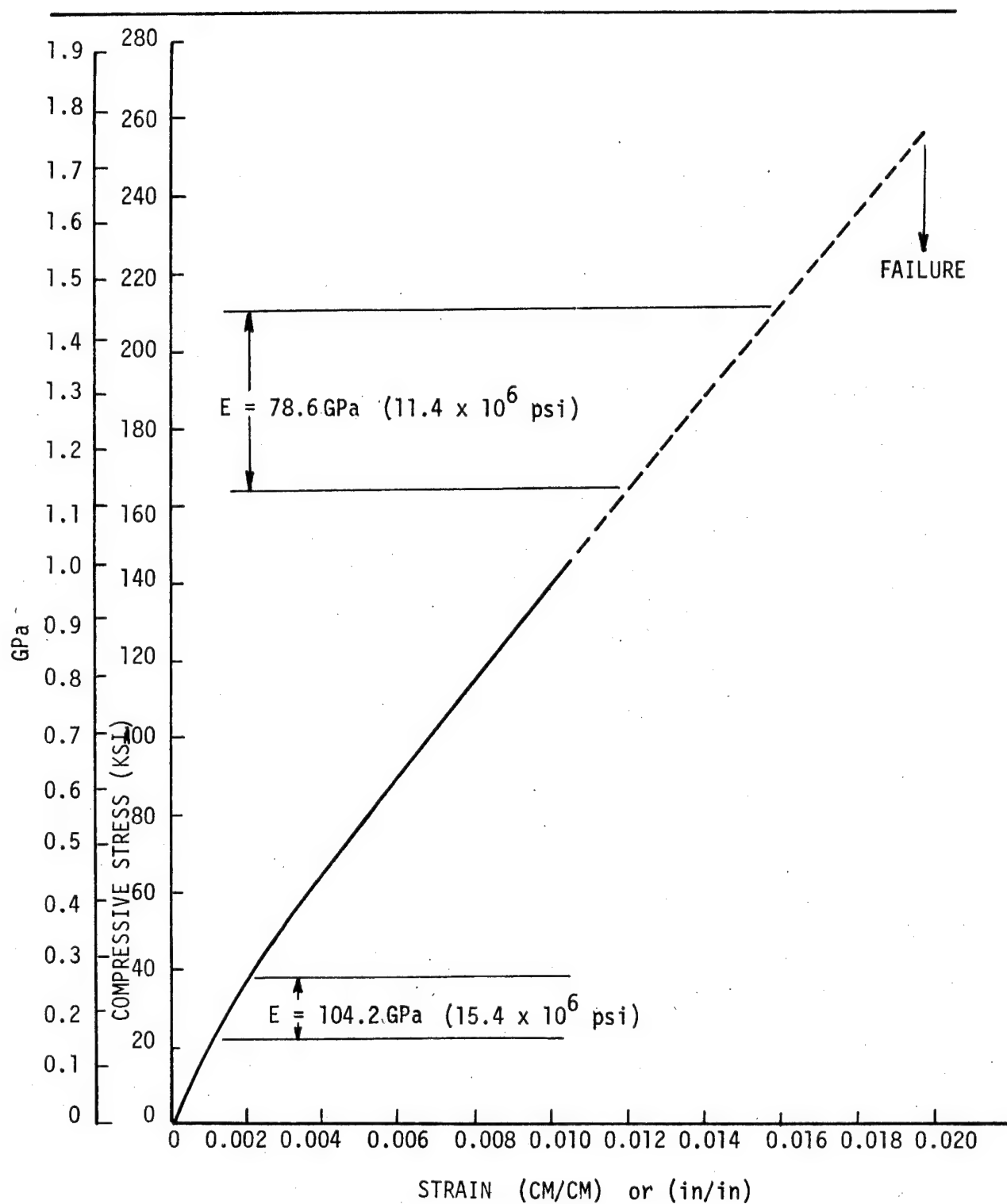


Figure 53 Specimen 18 - Room Temperature Compression Stress/Strain Curve

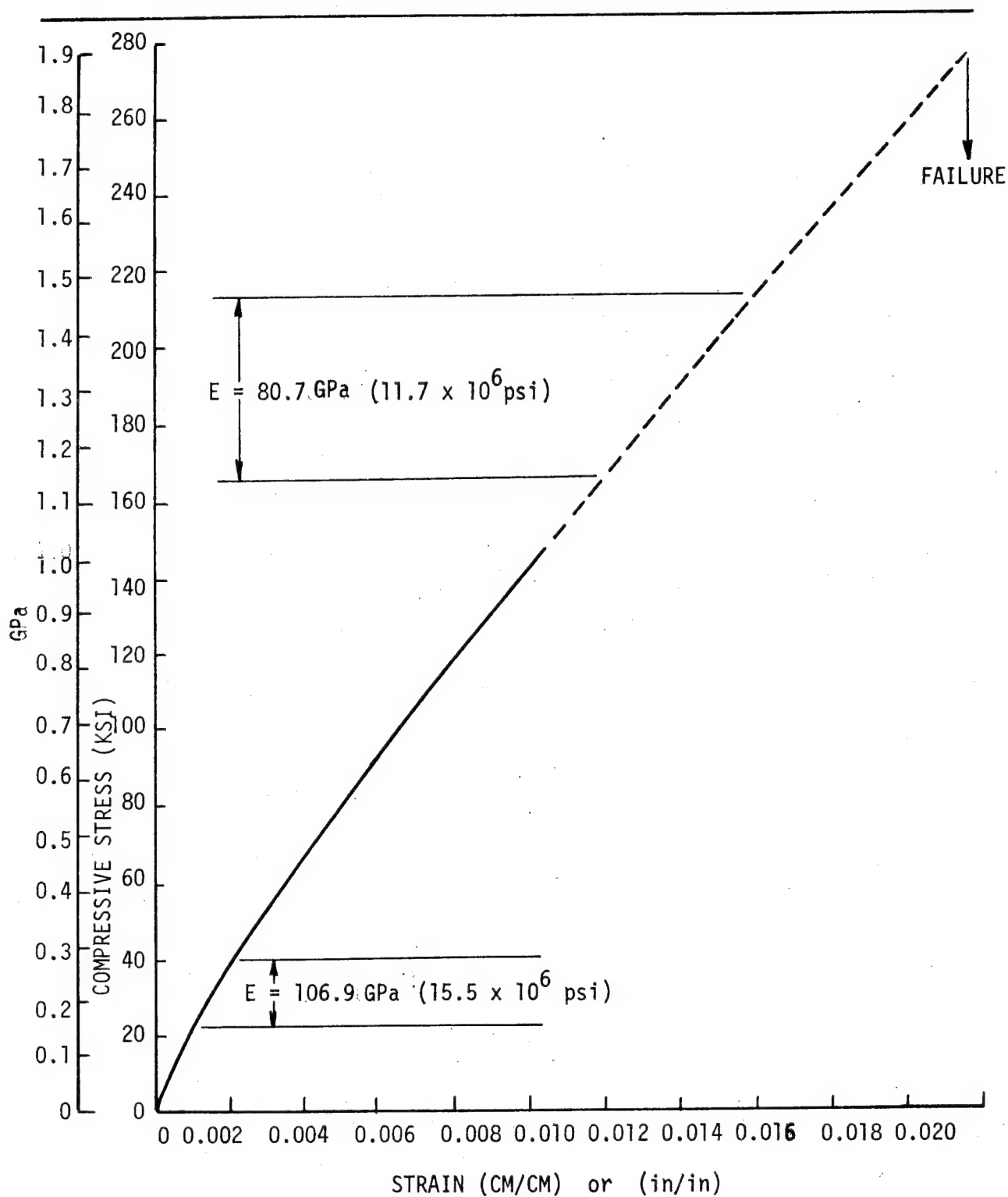


Figure 54 Specimen 19 - Room Temperature Compression Stress/Strain Curve

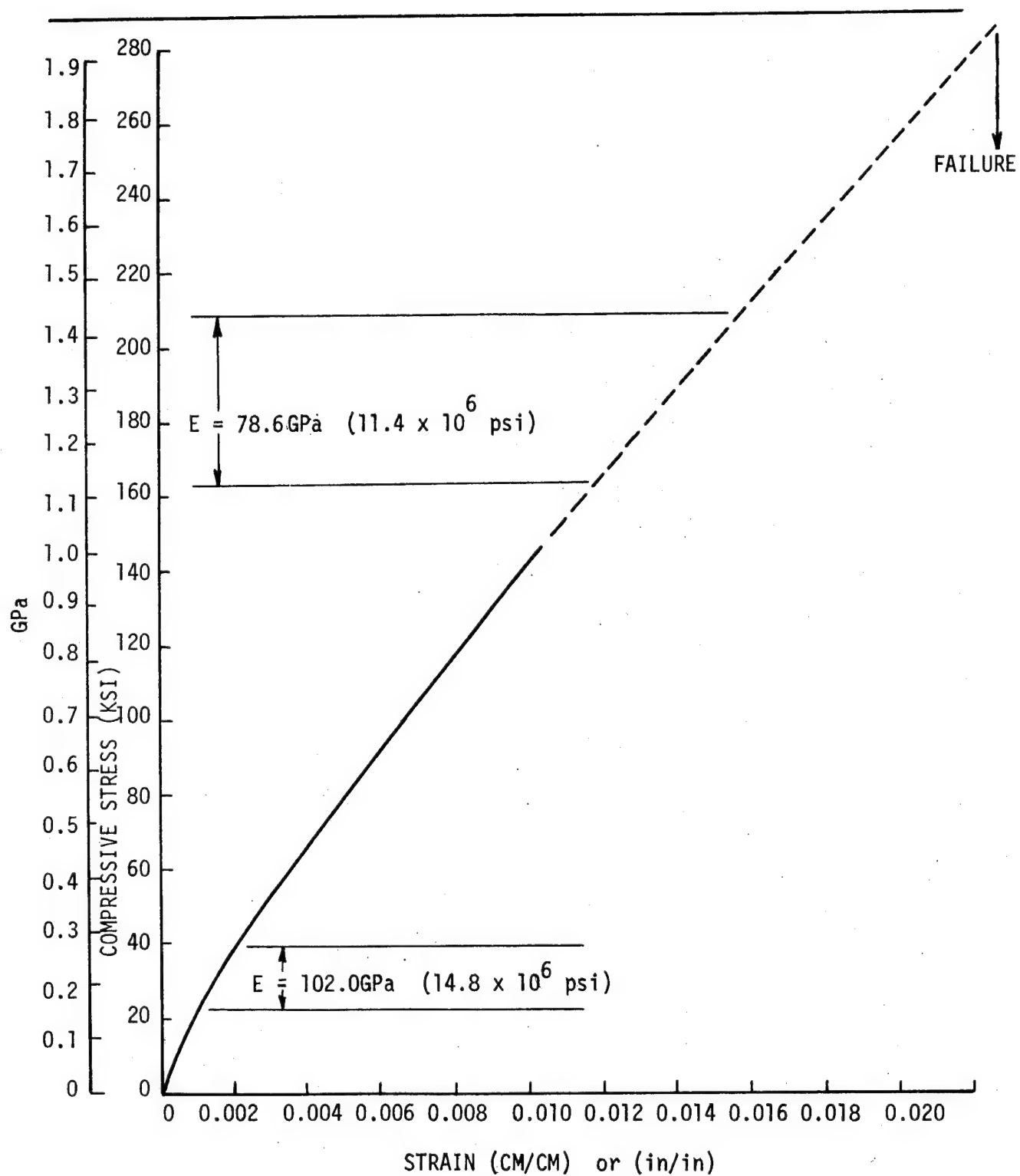
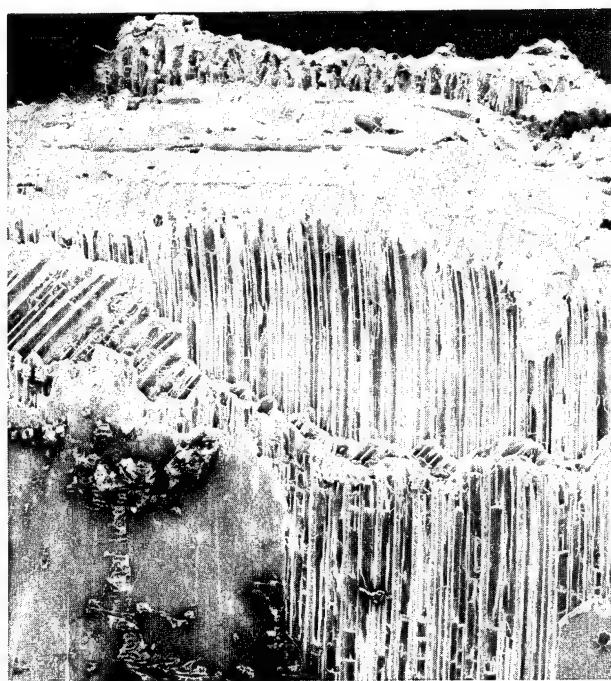


Figure 55 Specimen 20 - Room Temperature Compression Stress/Strain Curve



19 x



10 x

Figure 56    Compression Specimen Failure Surface

---

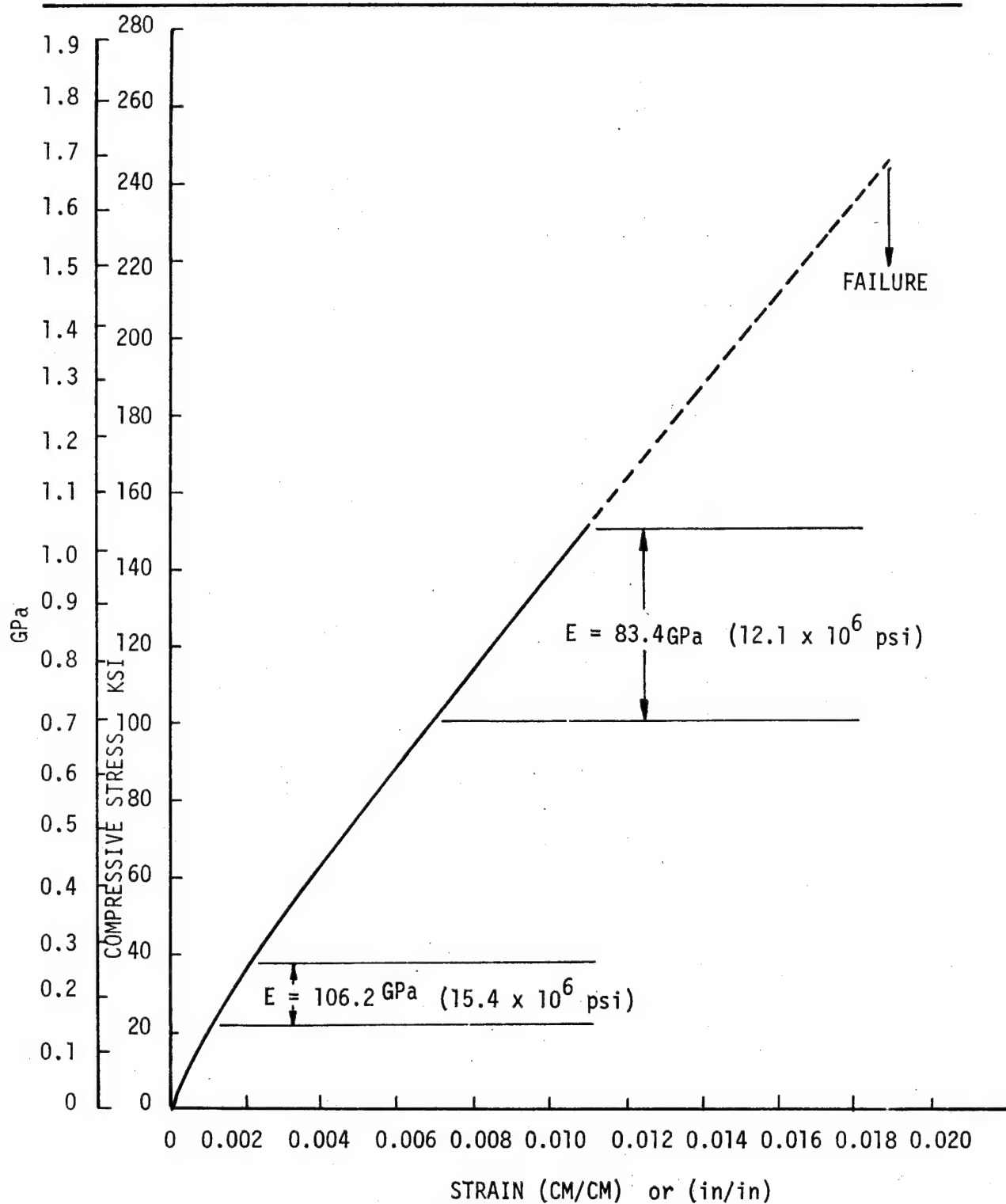


Figure 57 Specimen 21 - Room Temperature Compression Stress-Strain Curve after 1000 Hours at 505K(450°F)

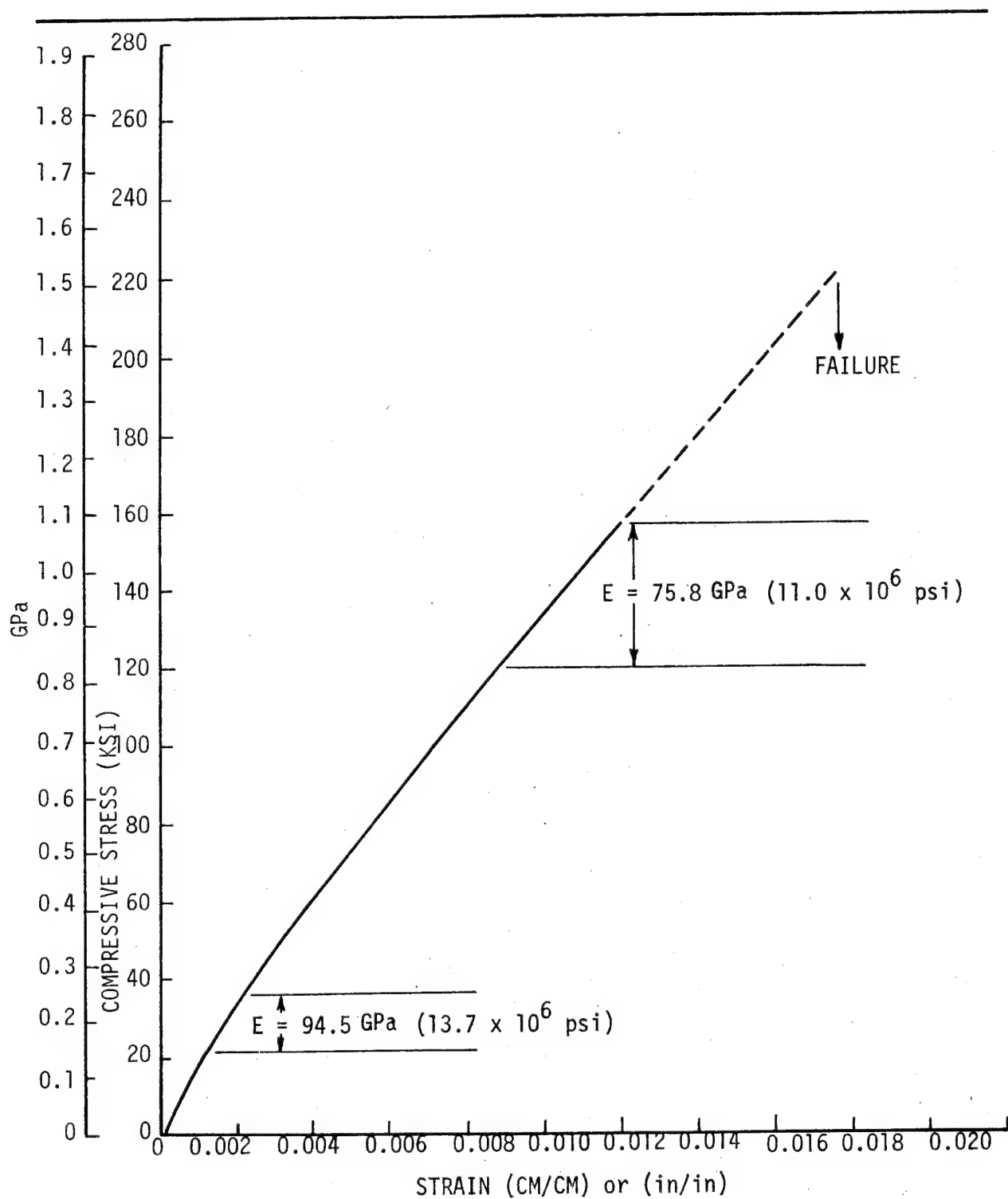


Figure 58 Specimen 22 - Room Temperature Compression Stress/Strain Curve after 1000 Hours at 505K(450°F)

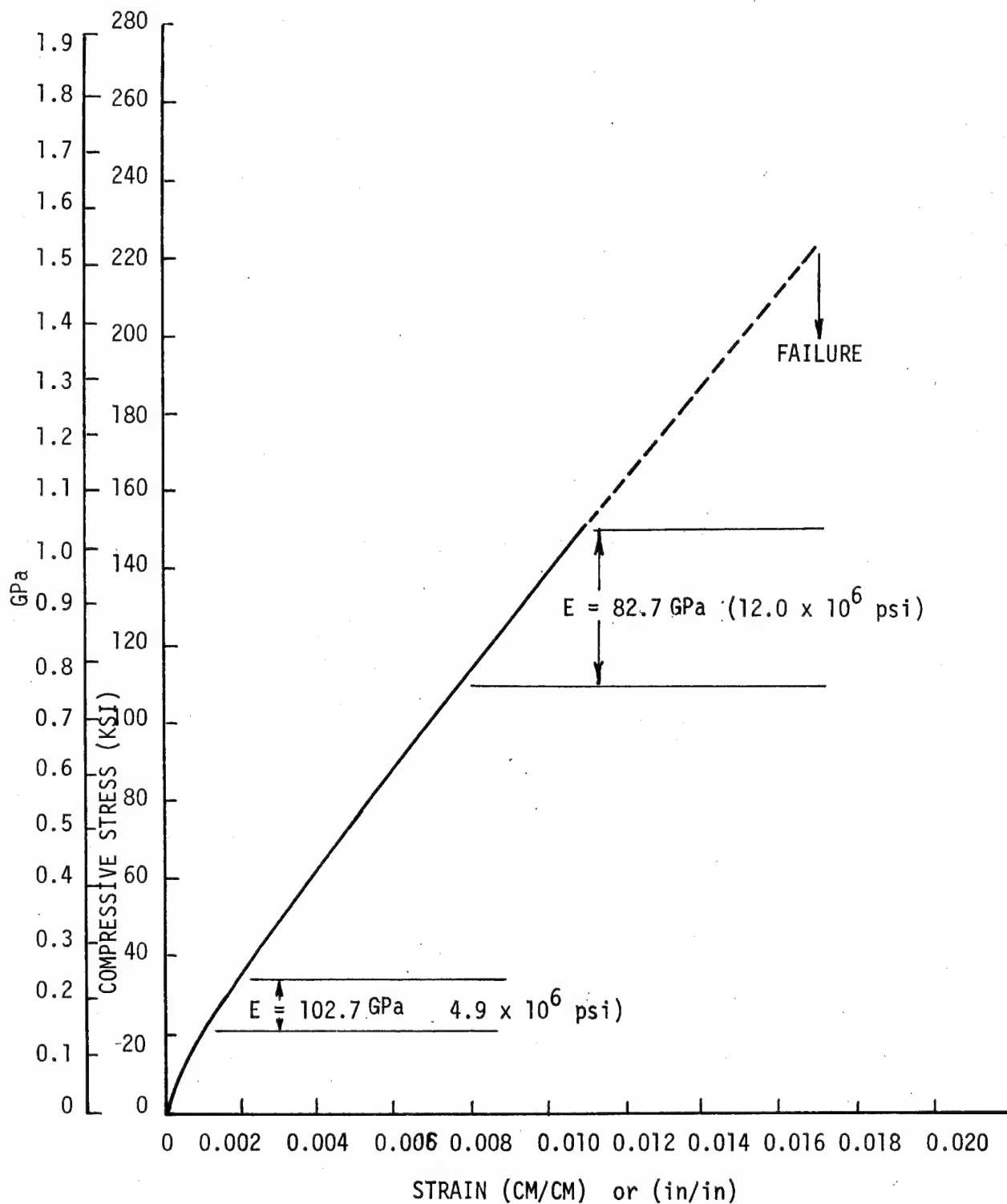


Figure 59 Specimen 23 - Room Temperature Compression Stress/Strain Curve after 1000 Hours at 505K(450°F)

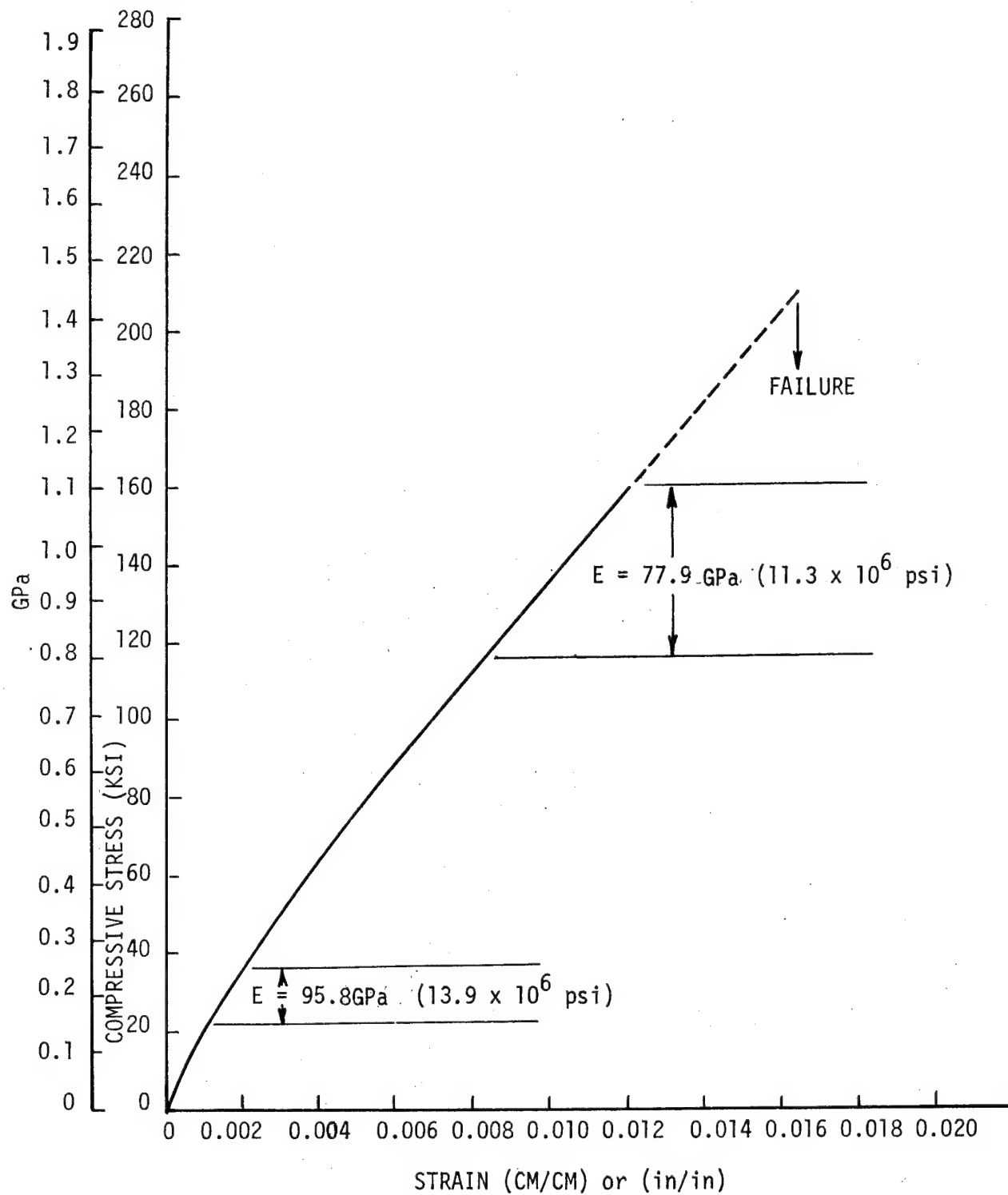


Figure 60 Specimen 24 - Room Temperature Compression Stress/Strain Curve after 1000 Hours at 505K(450°F)

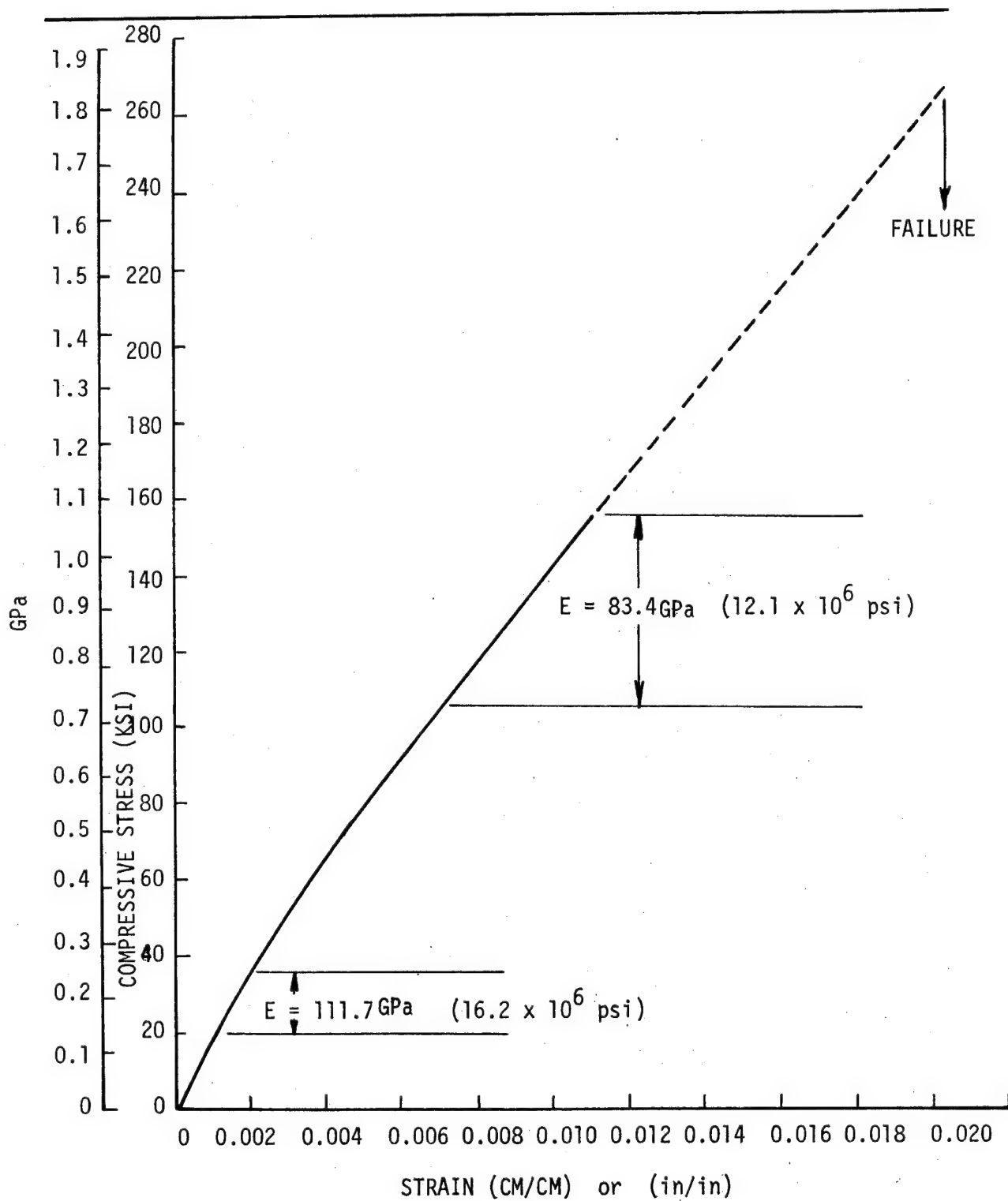


Figure 61 Specimen 25 - Room Temperature Compression Stress/Strain Curve after 1000 Hours at 505K(450°F)

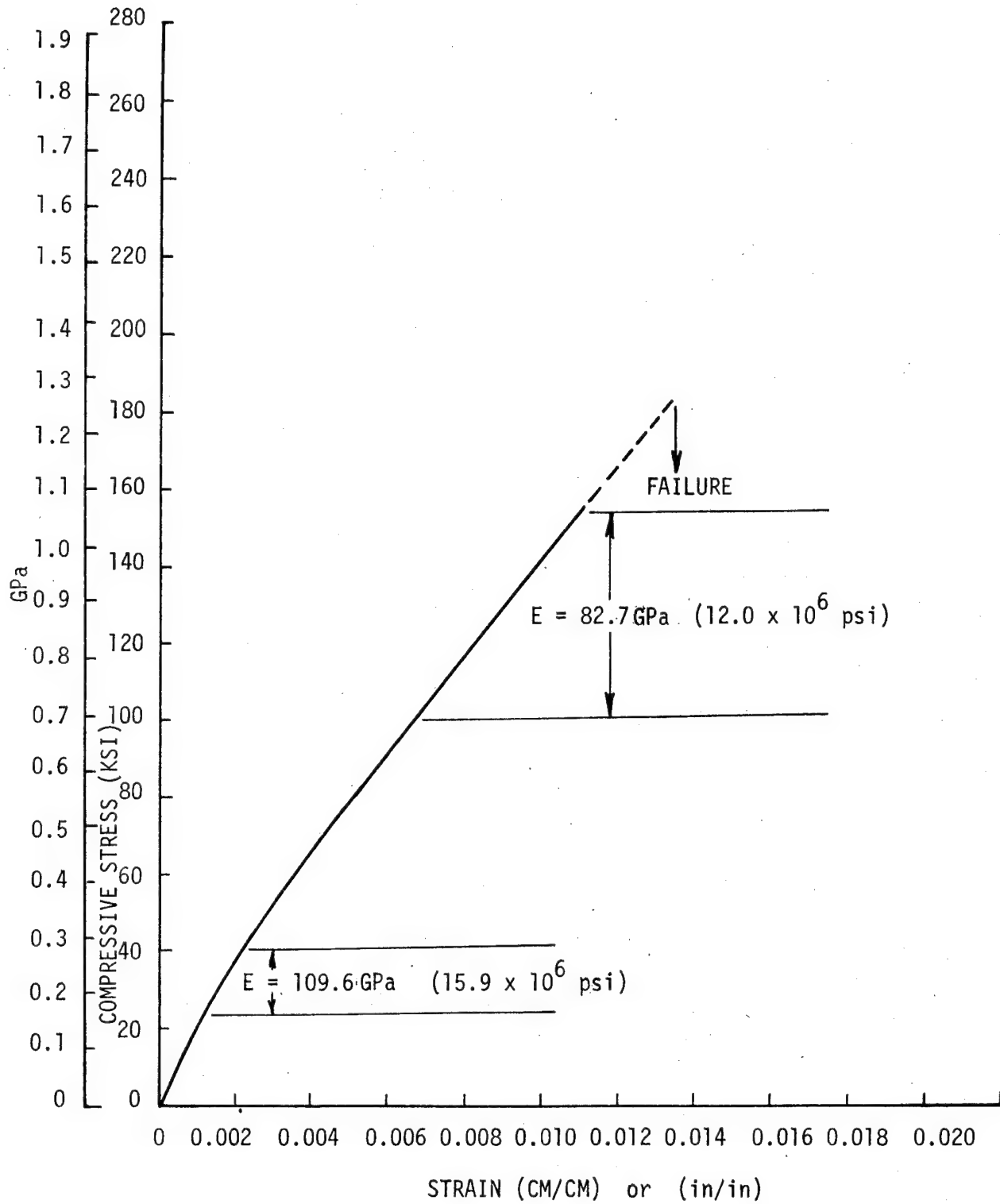


Figure 62 Specimen 26 - Room Temperature Compression Stress/Strain Curve after 1000 Hours at 505K(450°F)

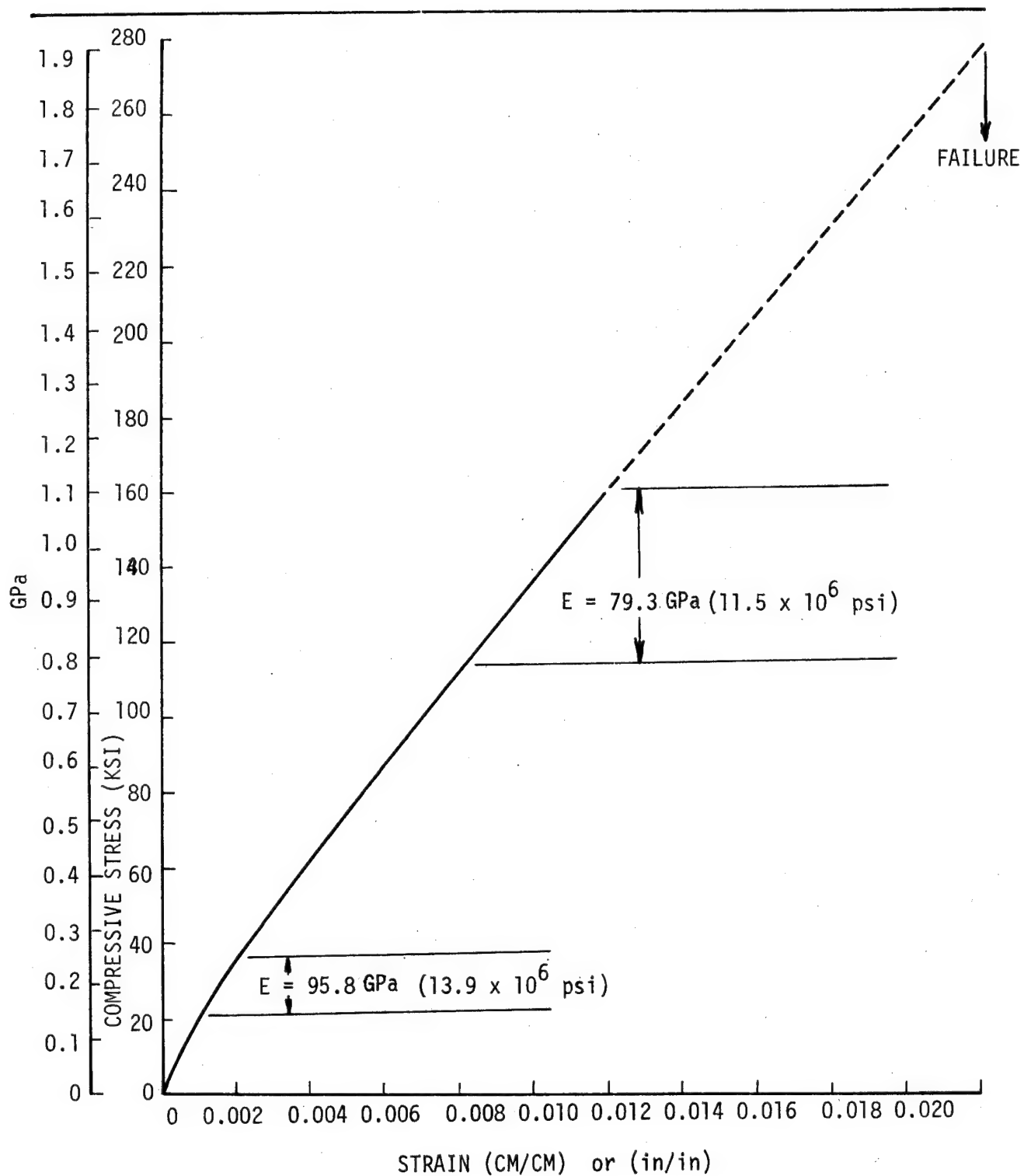


Figure 63 Specimen 27 - Room Temperature Compression Stress/Strain Curve after 1000 Hours at 505K(450°F)

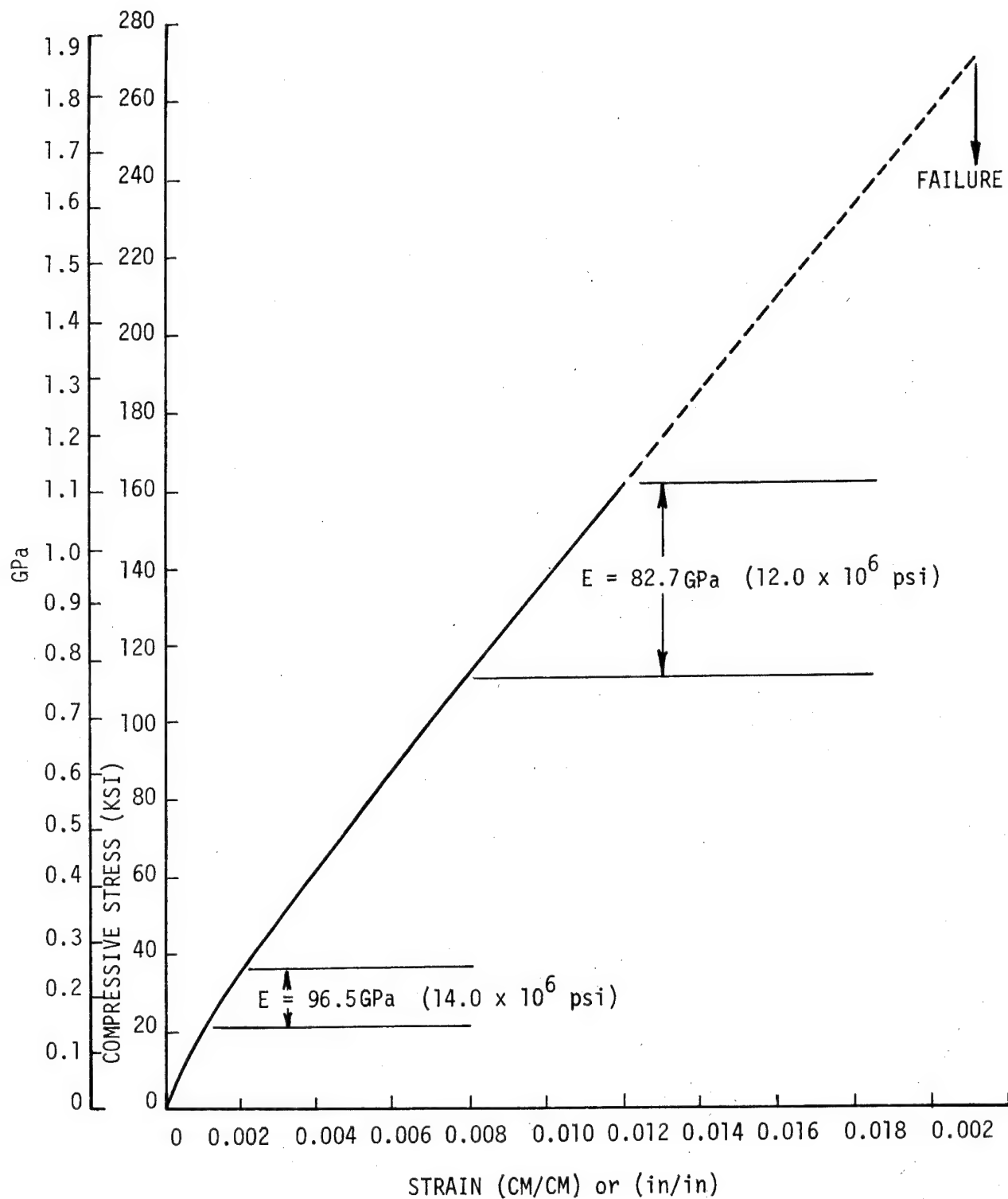


Figure 64 Specimen 28 - Room Temperature Compression Stress/Strain Curve after 1000 Hours at 505K(450°F)

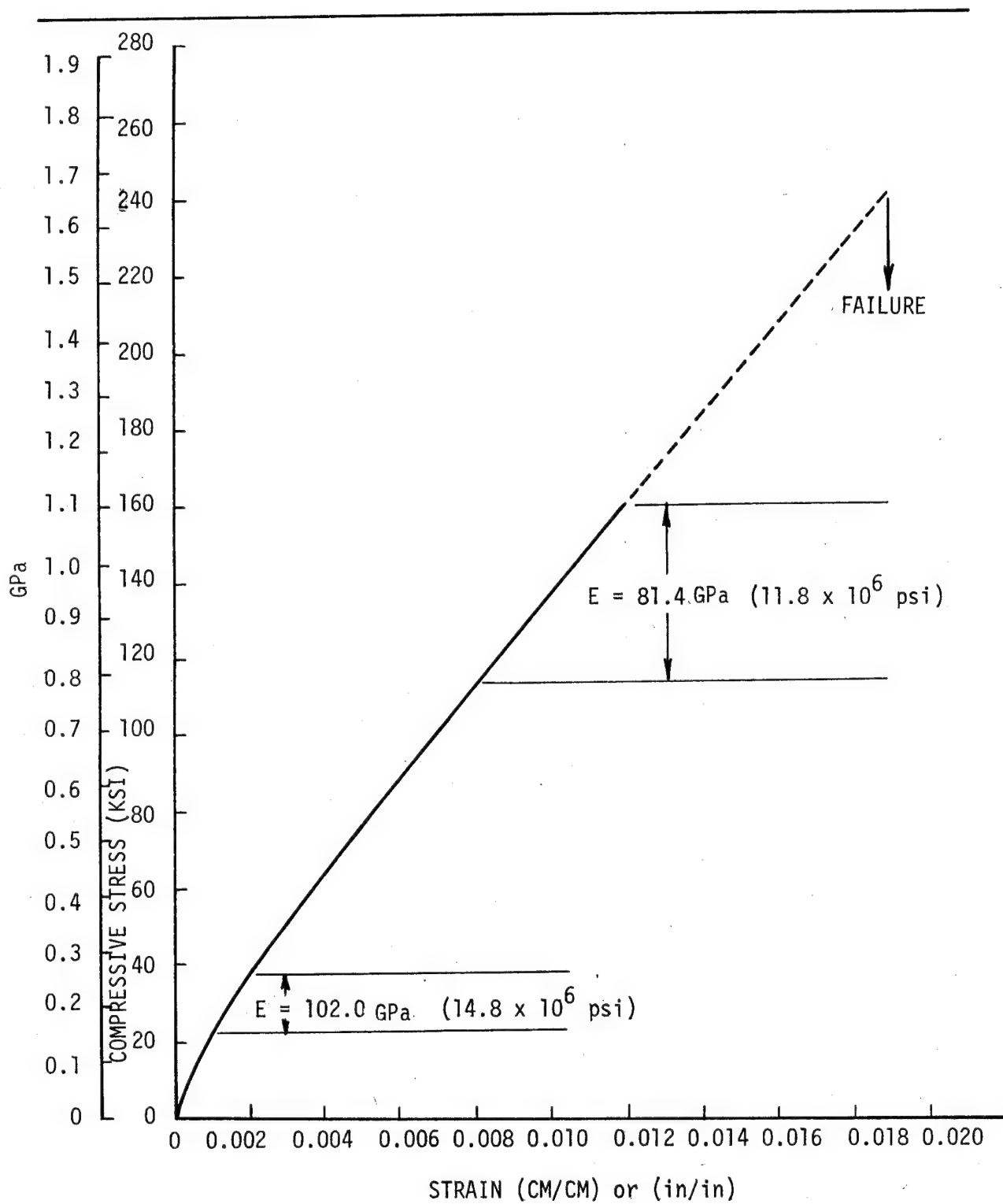


Figure 65 Specimen 29 - Room Temperature Compression Stress/Strain Curve after 1000 Hours at 505K(450°F)

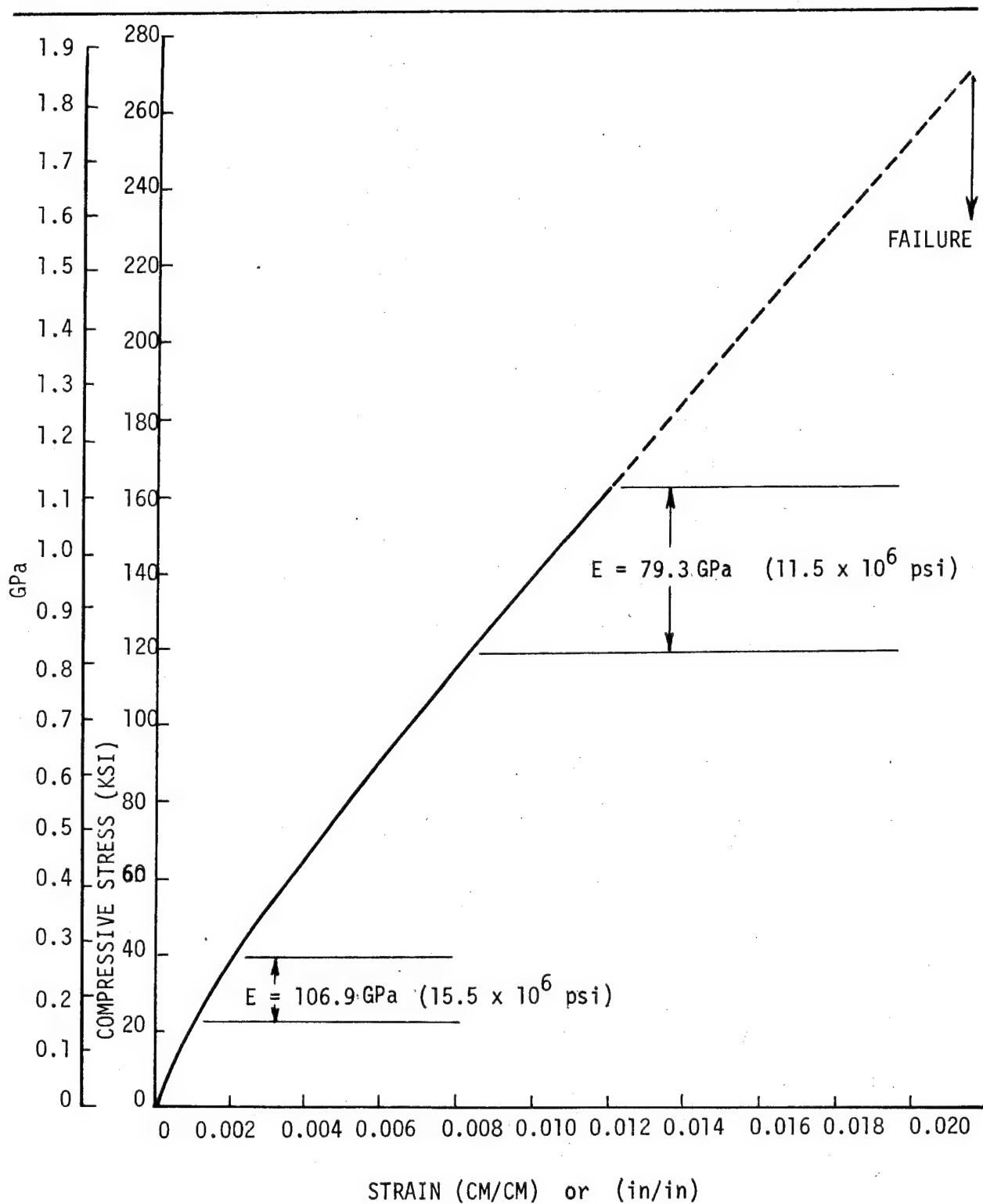


Figure 66 Specimen 30 - Room Temperature Compression Stress/Strain Curve after 1000 Hours at 505K(450°F)

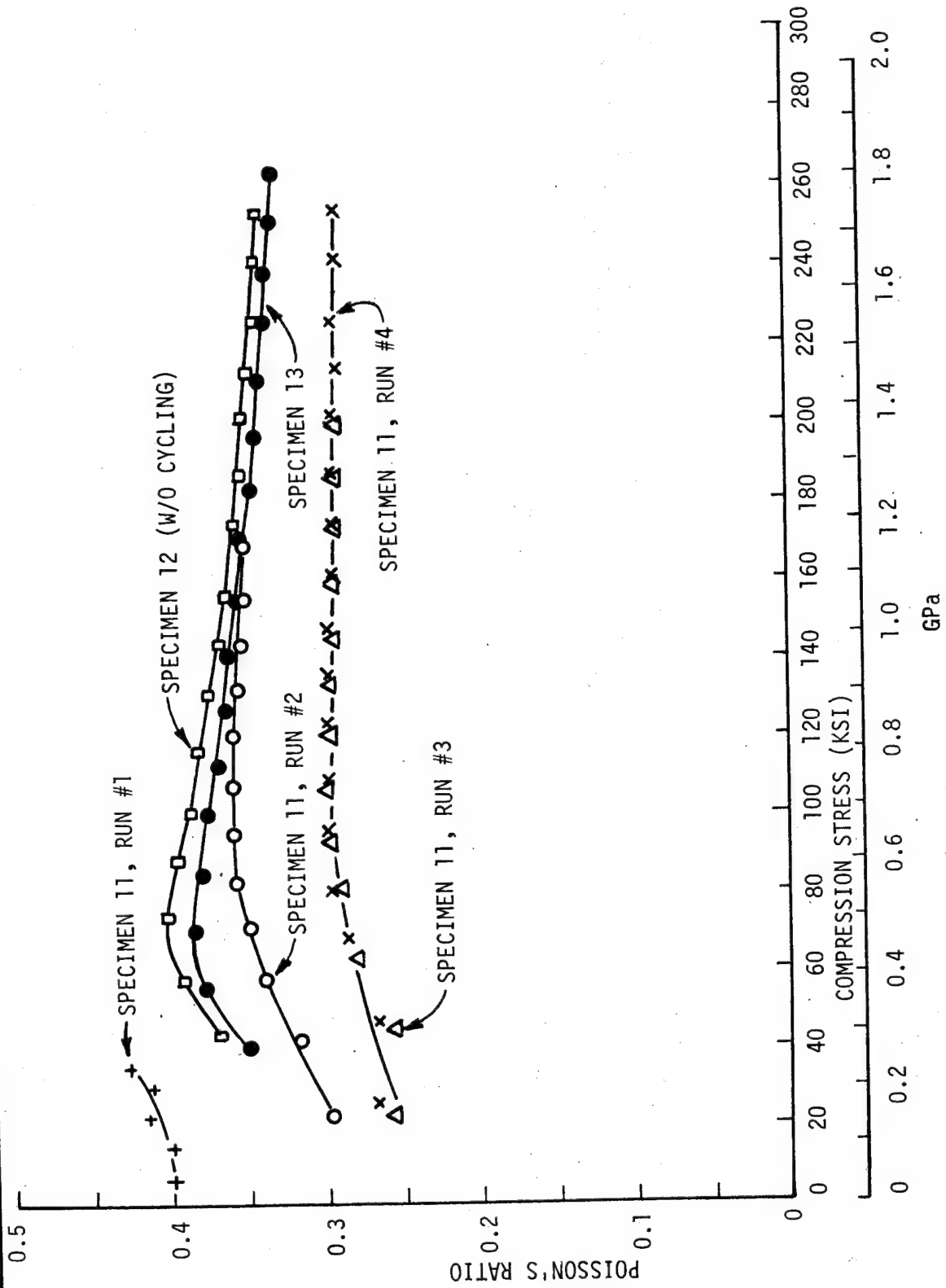
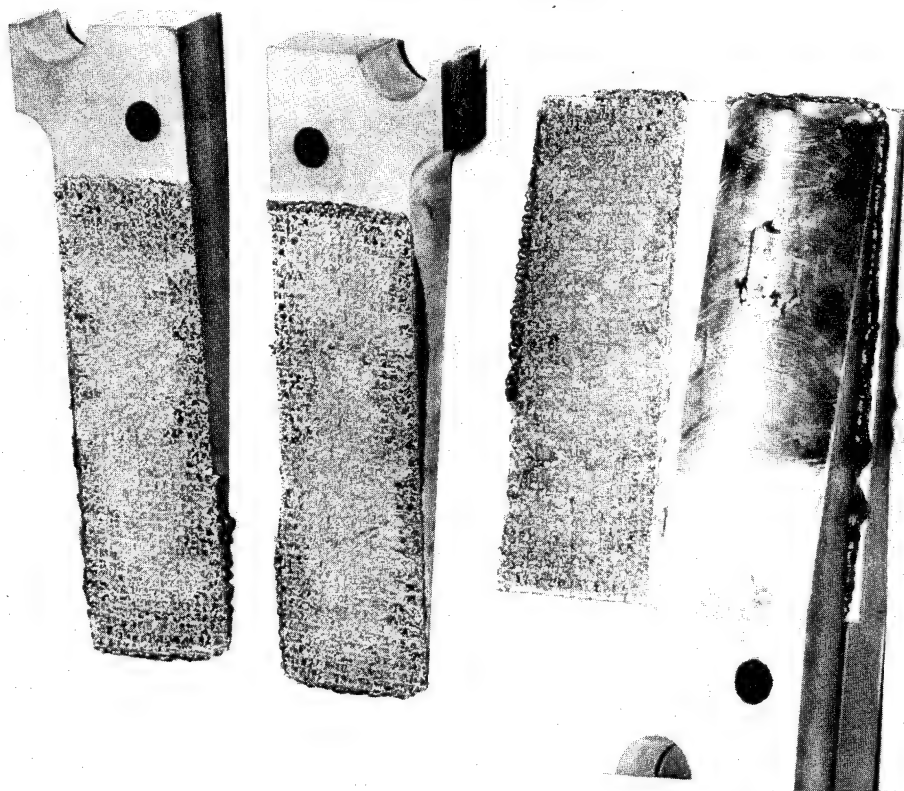
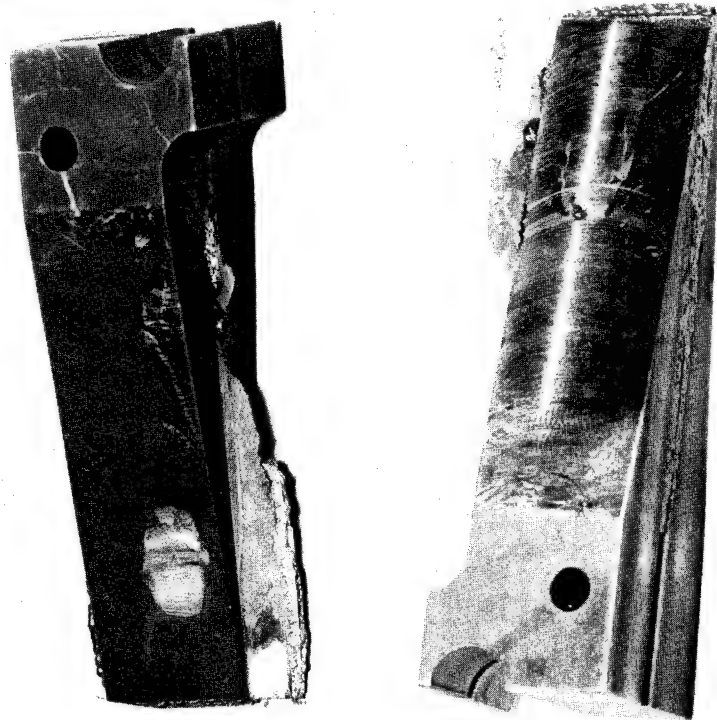


Figure 67 Poisson's Ratio Vs Compression Stress



SPECIMEN #10



SPECIMEN #8

Figure 68 Failed Rail Shear Specimens

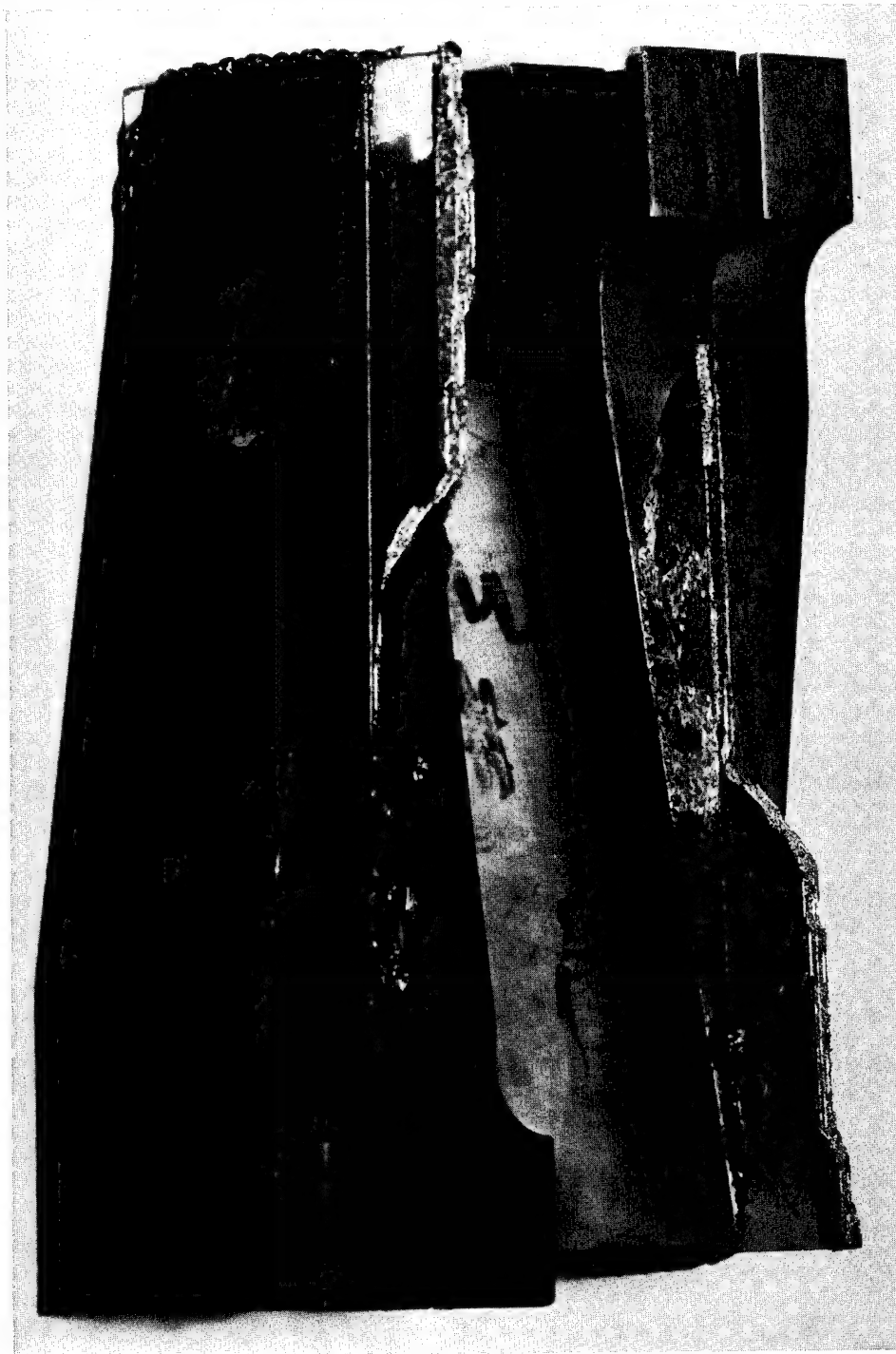
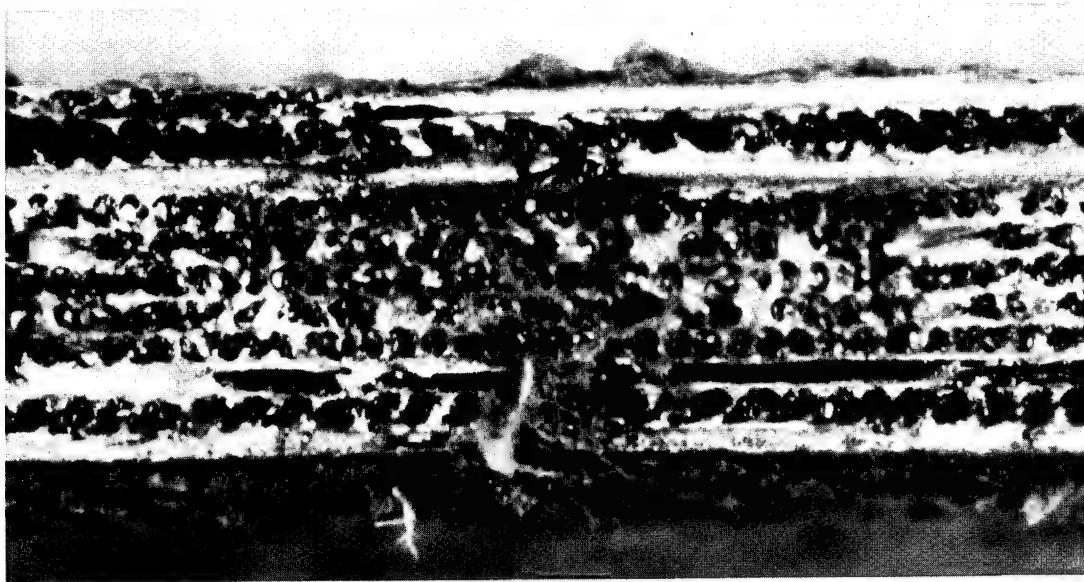
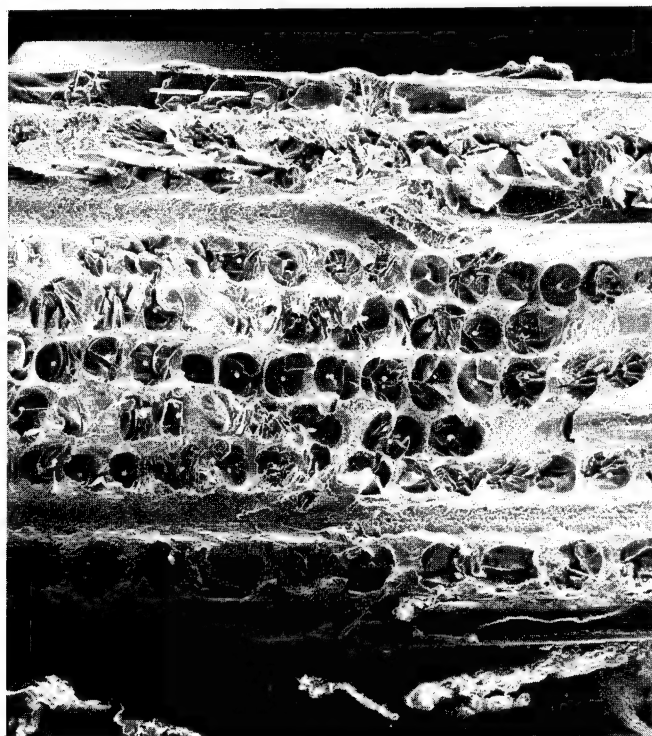


Figure 69 Failed Rail Shear Specimen

---



21 x



34 x

Figure 70 Shear Specimen Failure Surface

---

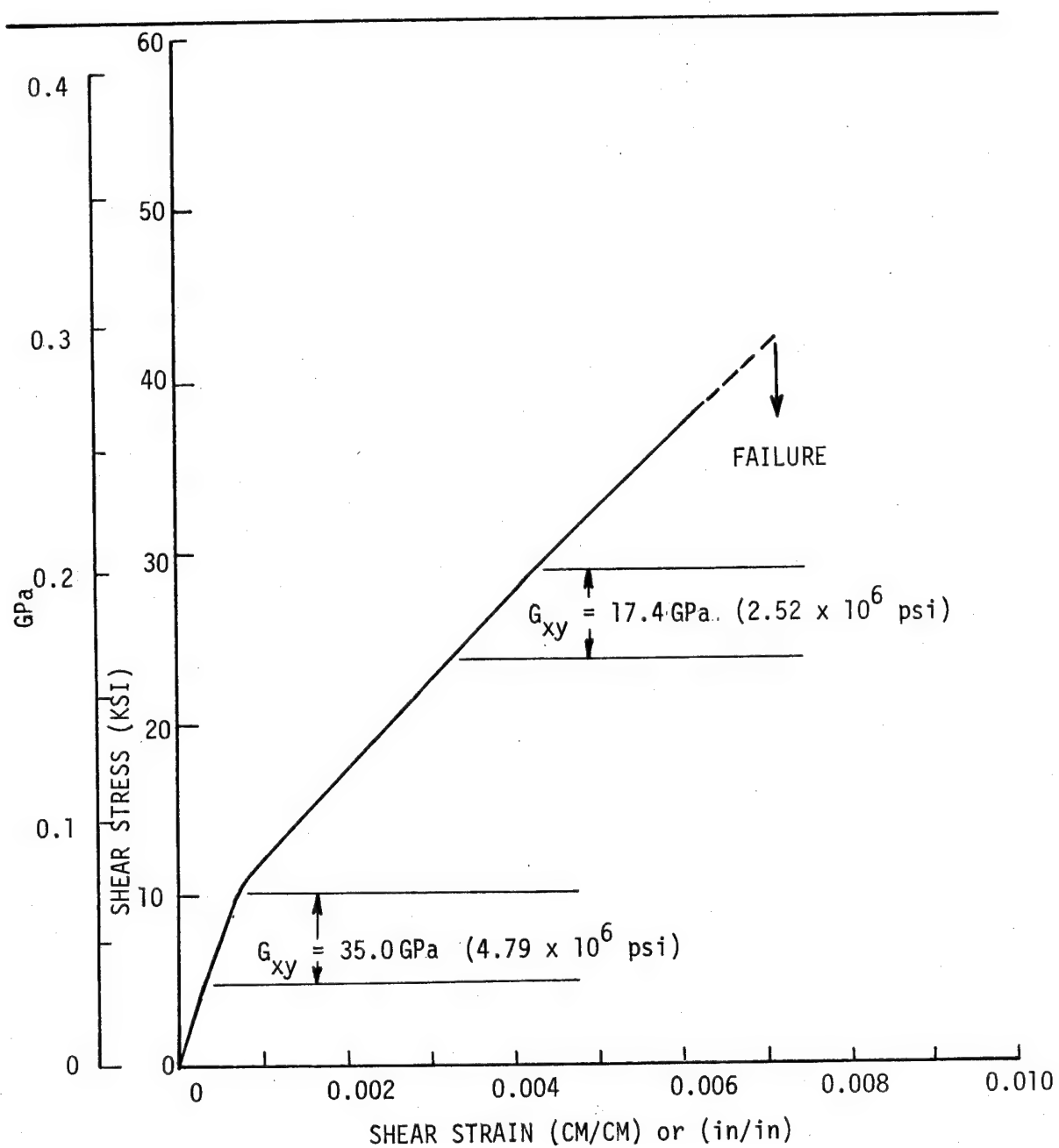


Figure 71 Specimen 11 - Room Temperature Rail Shear Stress/Strain Curve

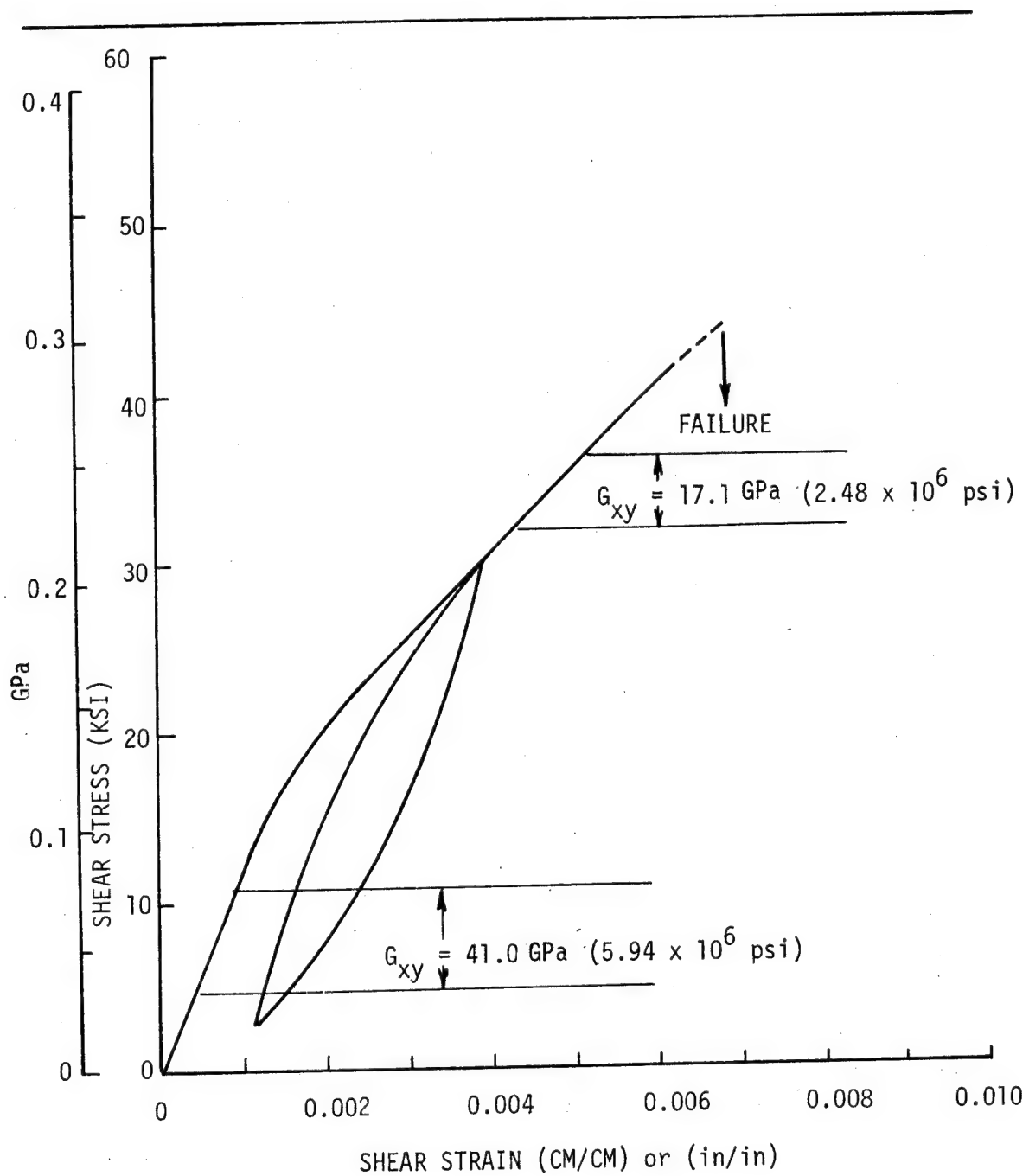


Figure 72 Specimen 12 - Room Temperature Rail Shear Stress/Strain Curve

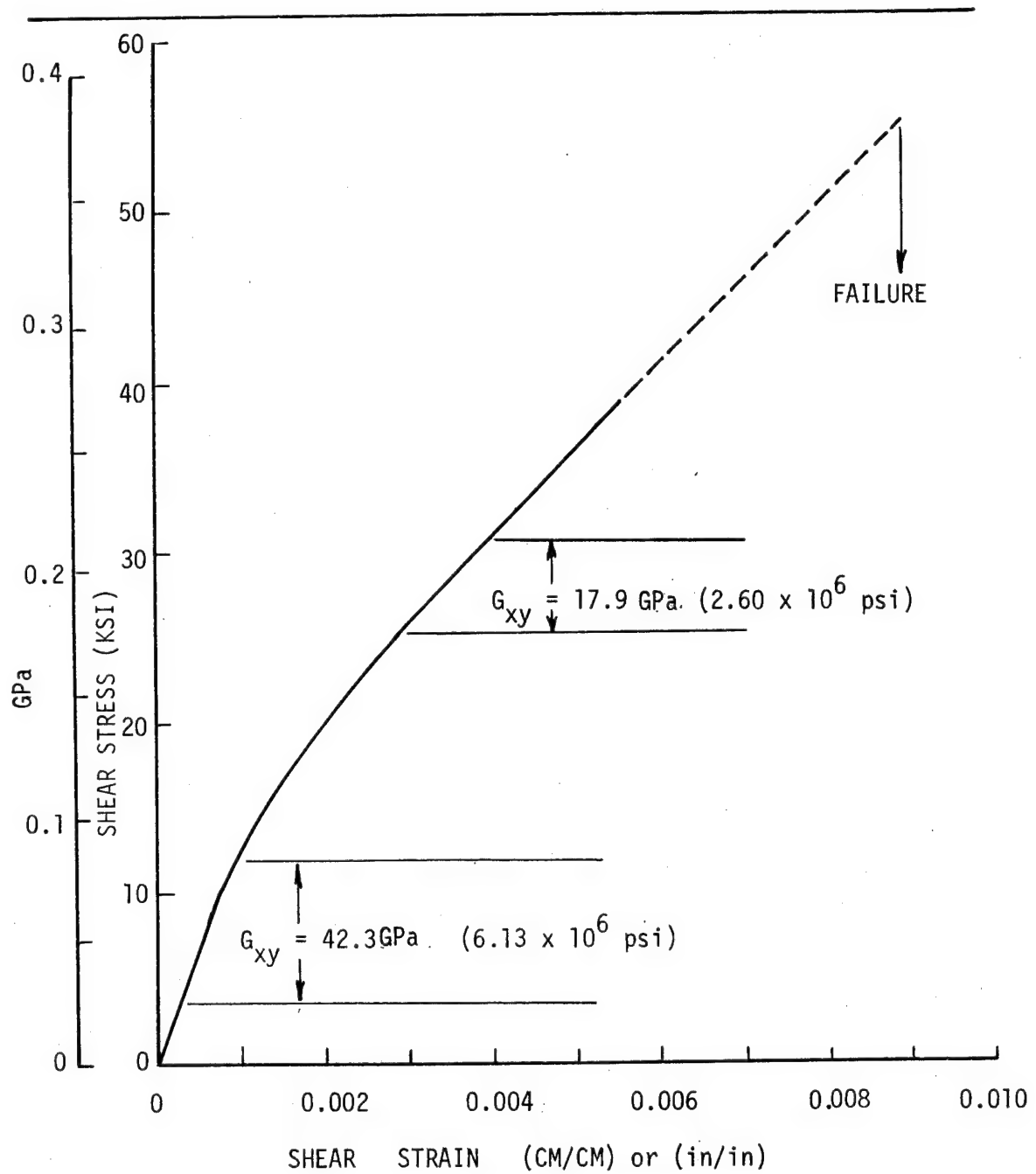


Figure 73 Specimen 13 - Room Temperature Rail Shear Stress/Strain Curve

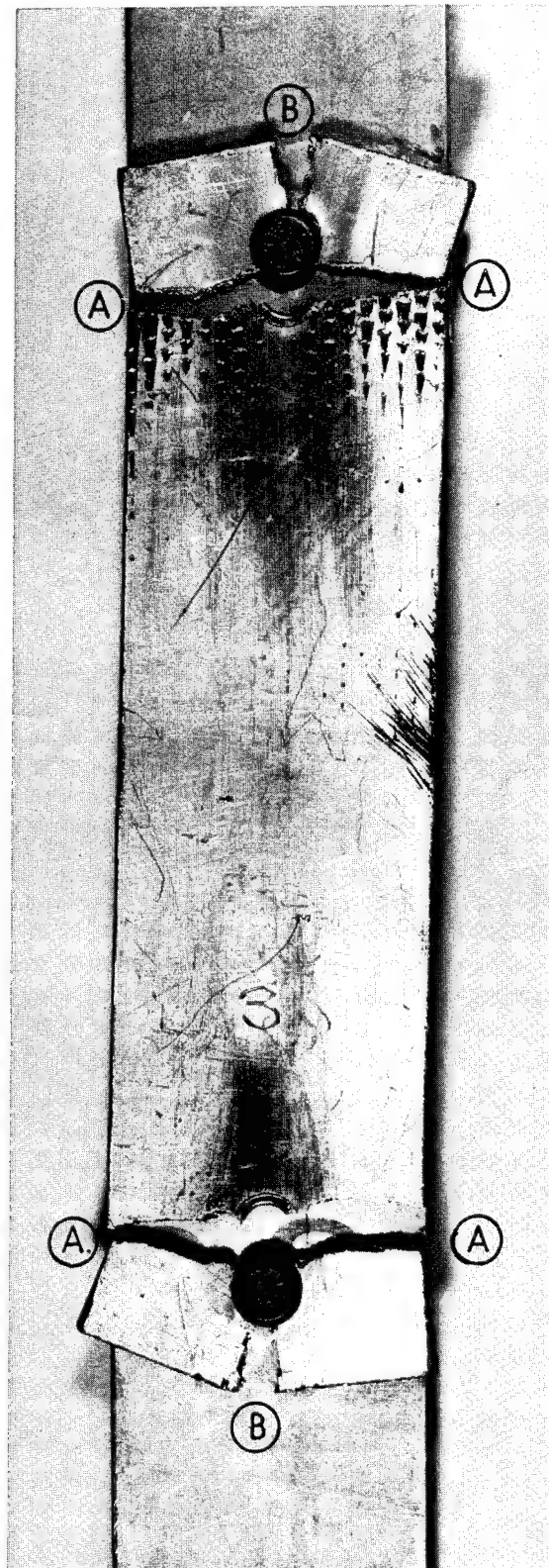


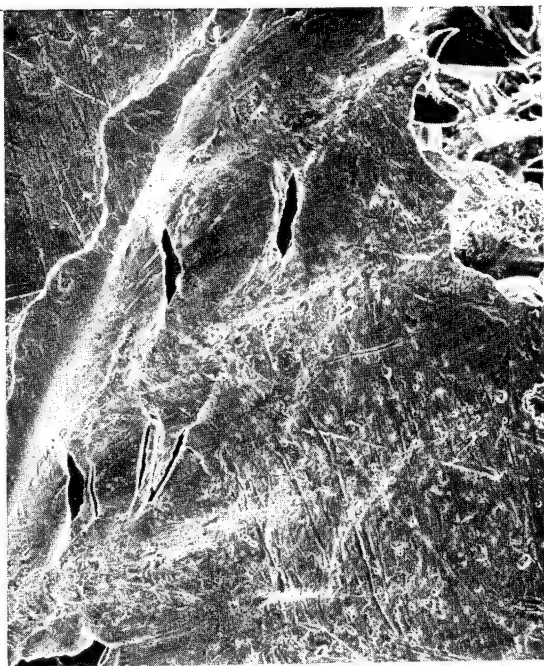
Figure 74 Mode of Failure of Bolt Bearing Specimen



18.5 x



20 x



100 x



200 x

Figure 75 SEM Pictures of Bolt Bearing Specimen

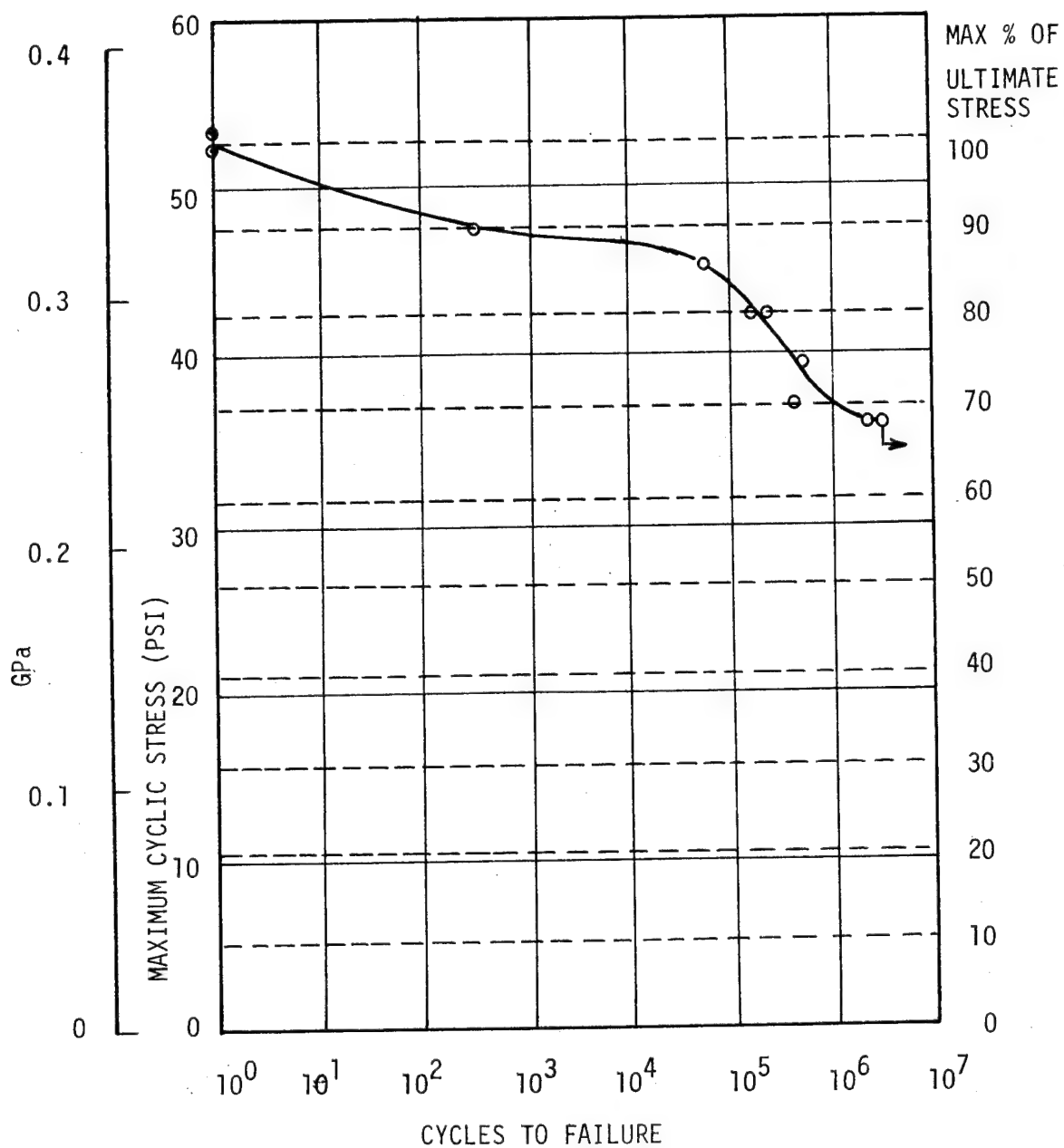
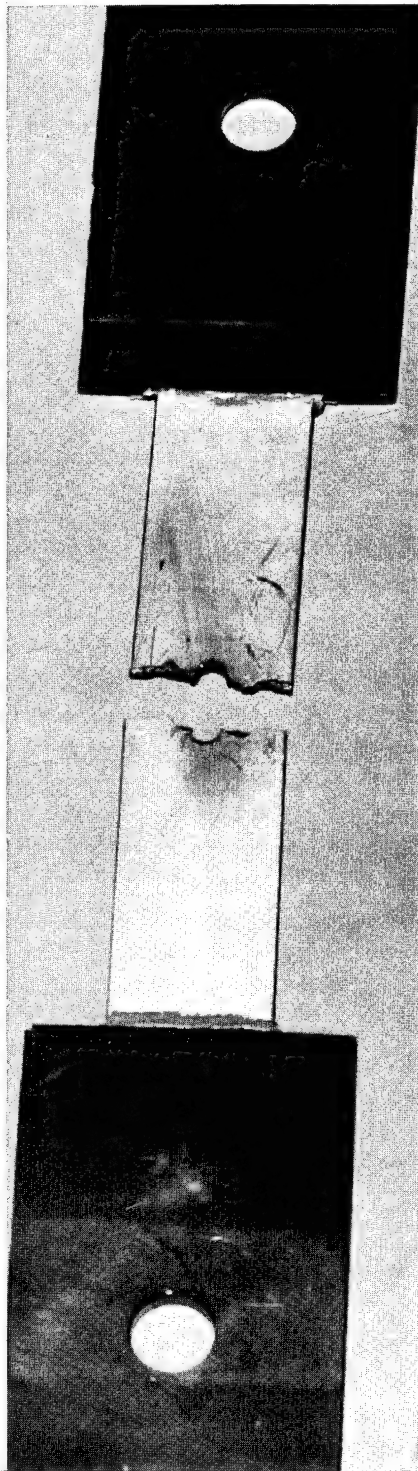
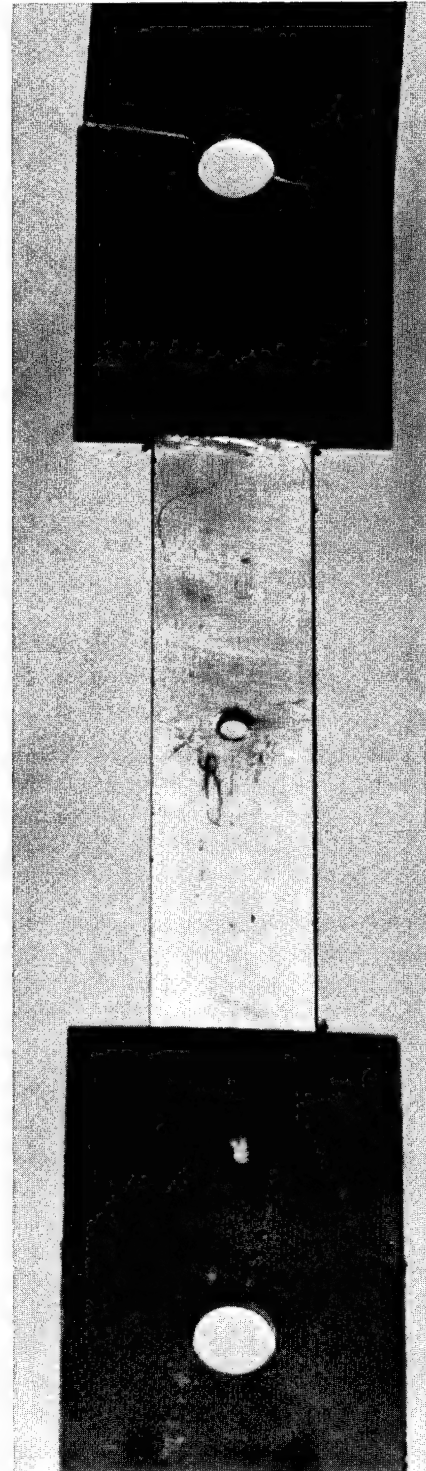


Figure 76 Constant Load Tensile Fatigue,  $R = .1(0/45/0/90/-45/90)_S$  Loaded in  $0^\circ$  Direction 2.54cm(1 in) Wide Specimen with a 4.763mm (3/16 in) Diameter Hole in Its Center

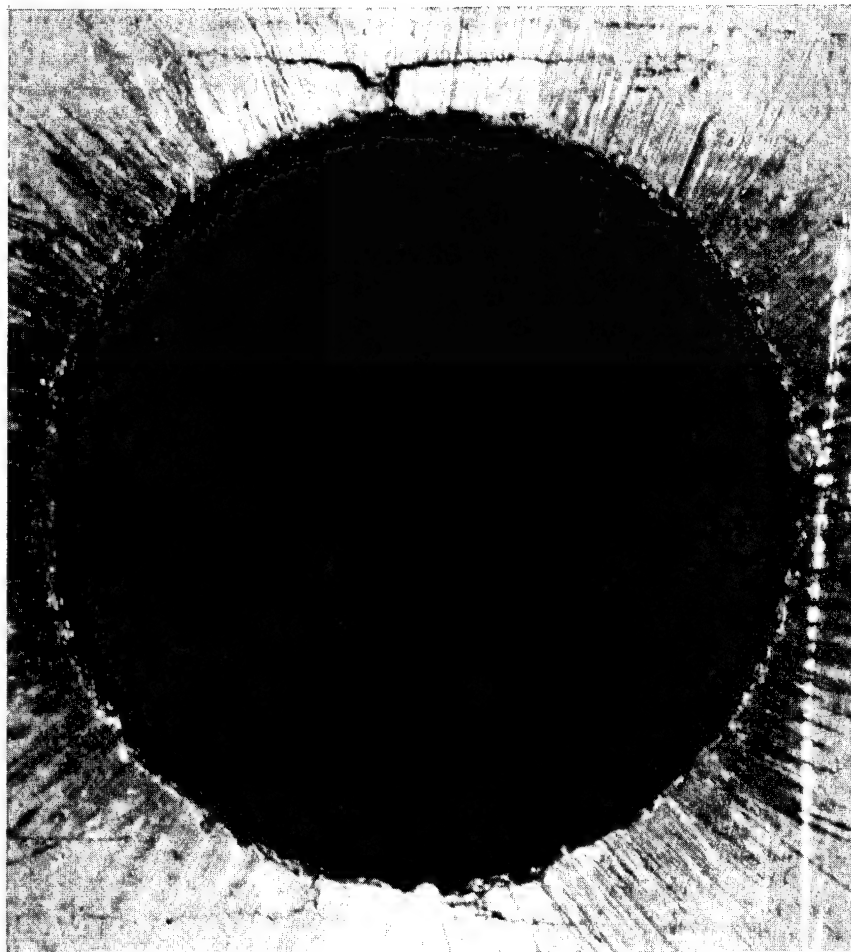


#3 Failed at 2,362,000 Cycles

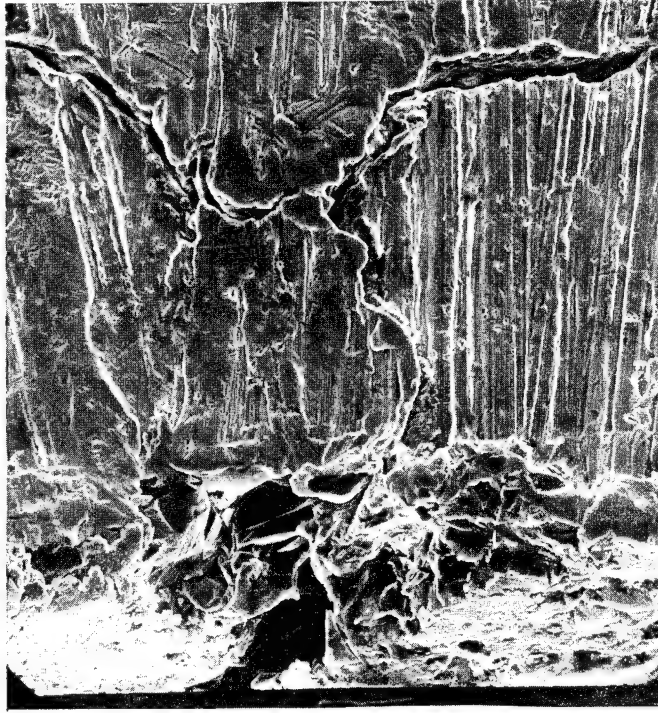


#4 Failed in Grip

Figure 77 Failed Fatigue Specimen



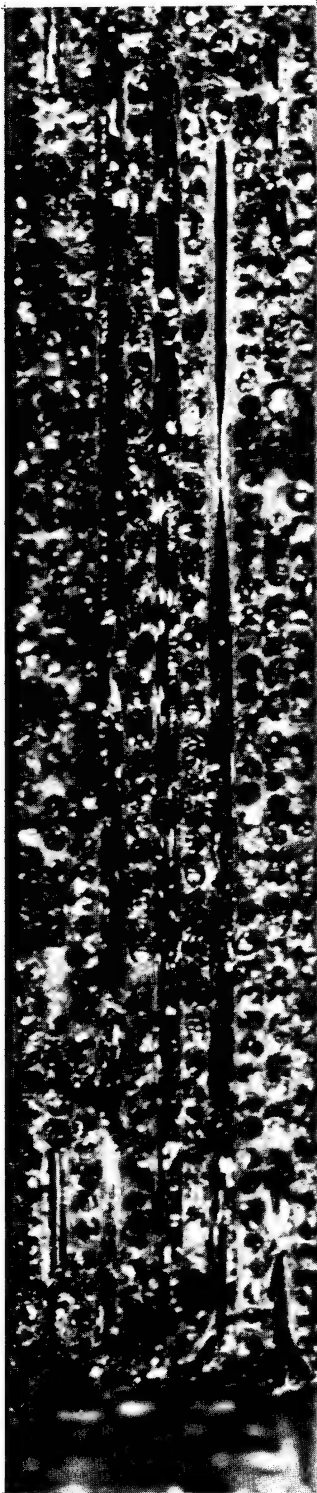
20.6 x



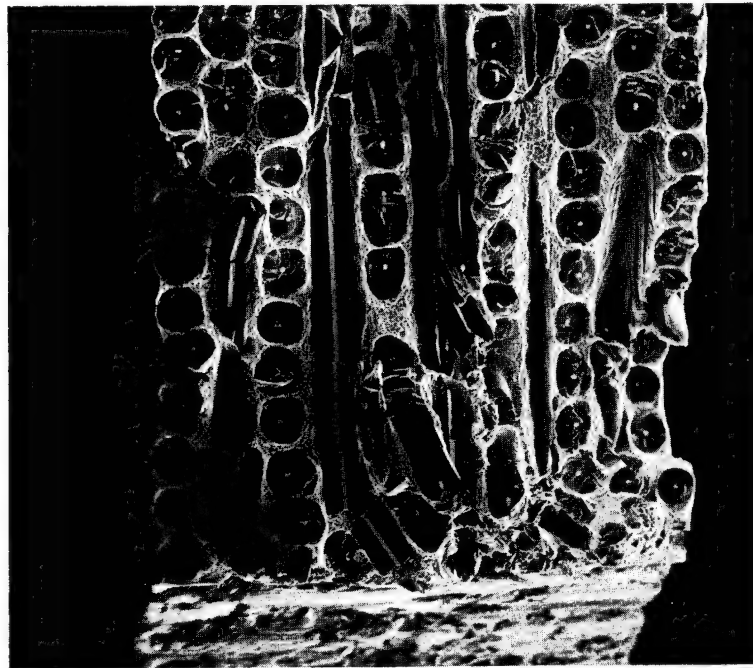
200 x

LOAD  
DIRECTION

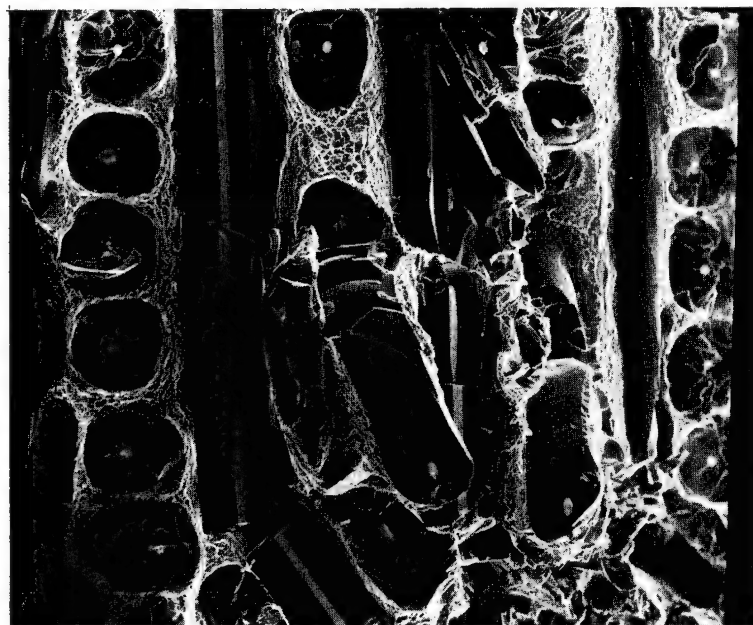
Figure 78 Fatigue Crack at Edge of Hole in Fatigue Specimen



20 x

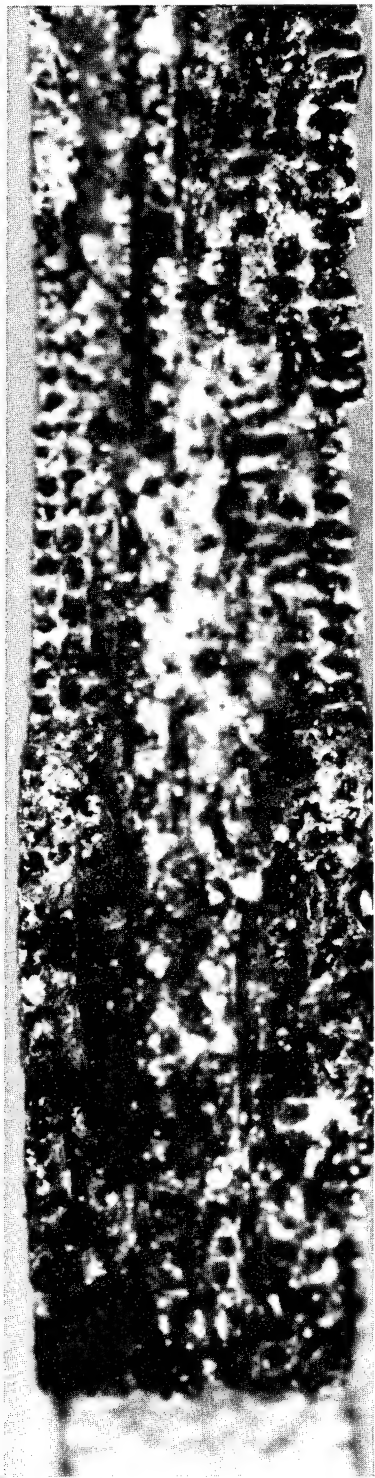


36 x

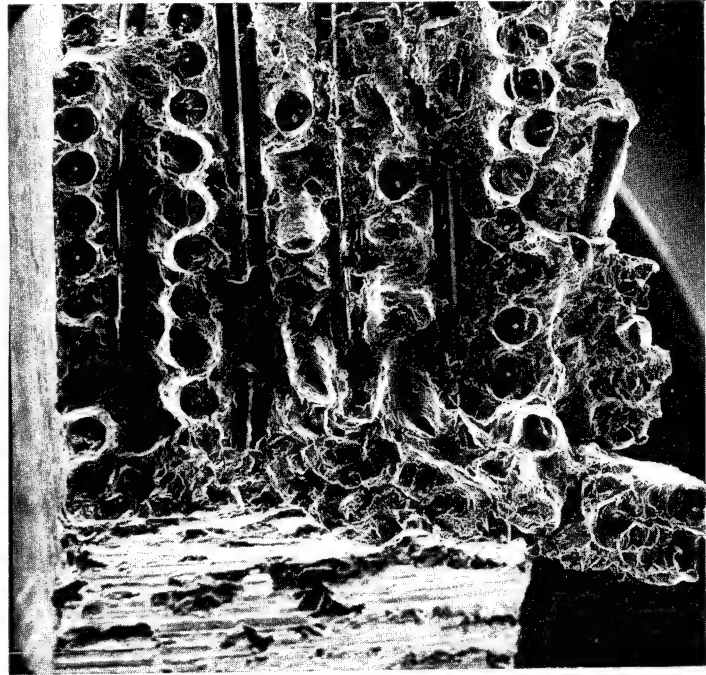


72 x

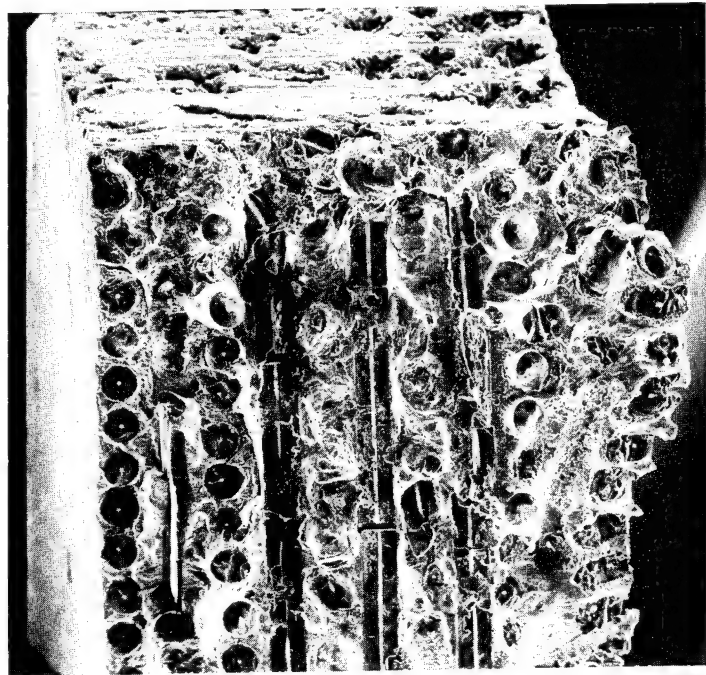
Figure 79 SEM Pictures of Fatigue Specimen 2 Tested Staticly in Tension to Failure



19.2 x



32 x



32 x

Figure 80 SEM Pictures of Fatigue Specimen 3. (failed on the 2,362,000th cycle of a Maximum Alternating Tensile Stress of 242.8MPa (35,222 psi))

$R = 0.1$      $K_t = 2.52$

Boron/Aluminum Laminate (11 plies)

$90^\circ, 45^\circ, 90^\circ, 0^\circ, -45^\circ, 0^\circ, -45^\circ, 0^\circ, 90^\circ, 45^\circ, 90^\circ$

Ti-8Al-1Mo-1V, REF: Fig 5.3.2.2.8(b) Mil-Hdbk-5B

Annealed Titanium (Comm Pure)  $F_{ty} = 55.2 \text{ GPa}$  (80,000 psi)

Derived from Ti-8Al-1Mo-1V

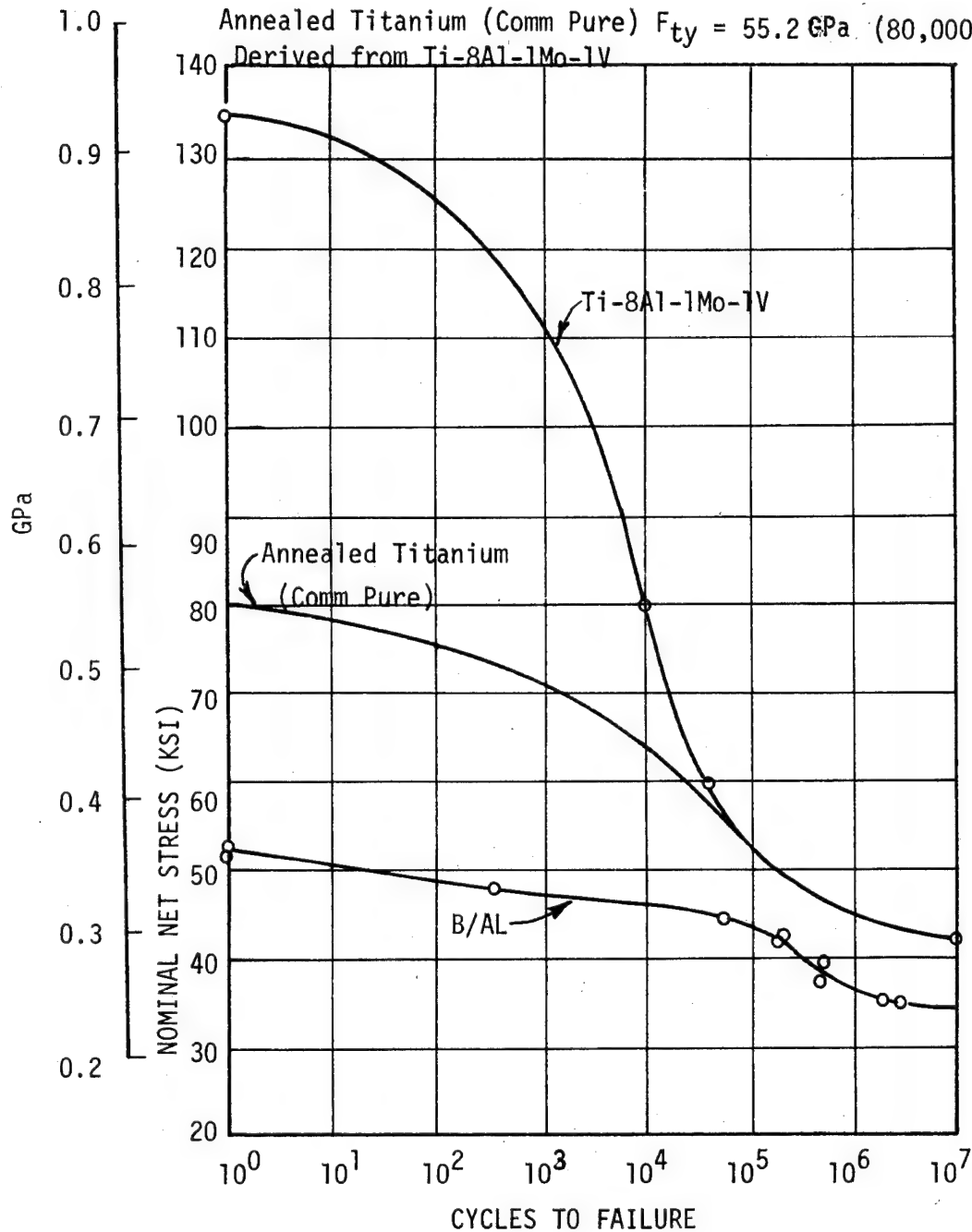


Figure 81 Fatigue Properties Comparison

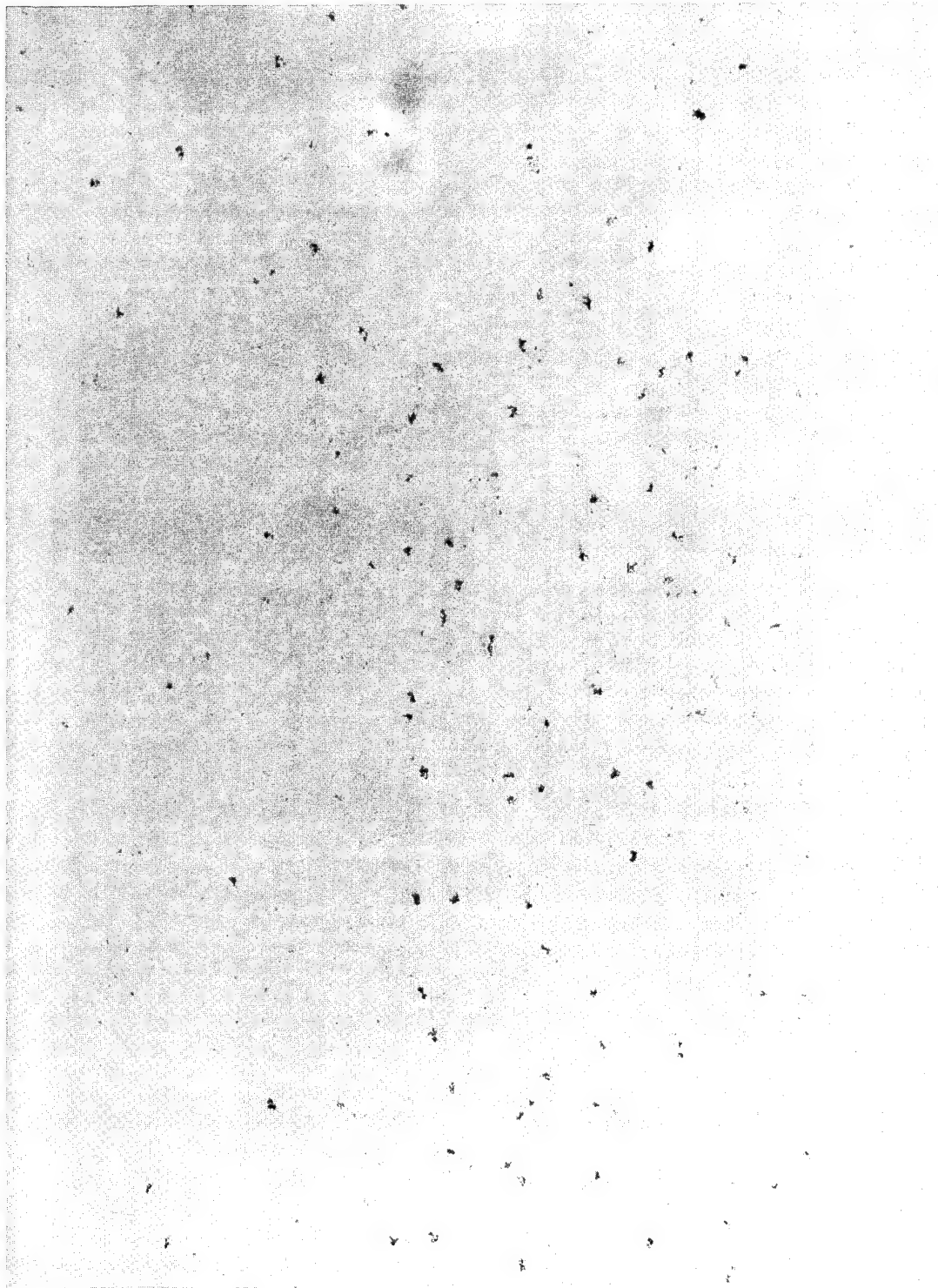


Figure 82 Surface Blemishes on Second Boron/Aluminum Aft Pylon Skin

---



Figure 83 Boron/Aluminum Aft Pylon Skin-Edges and Corner Trimmed and Holes Punched

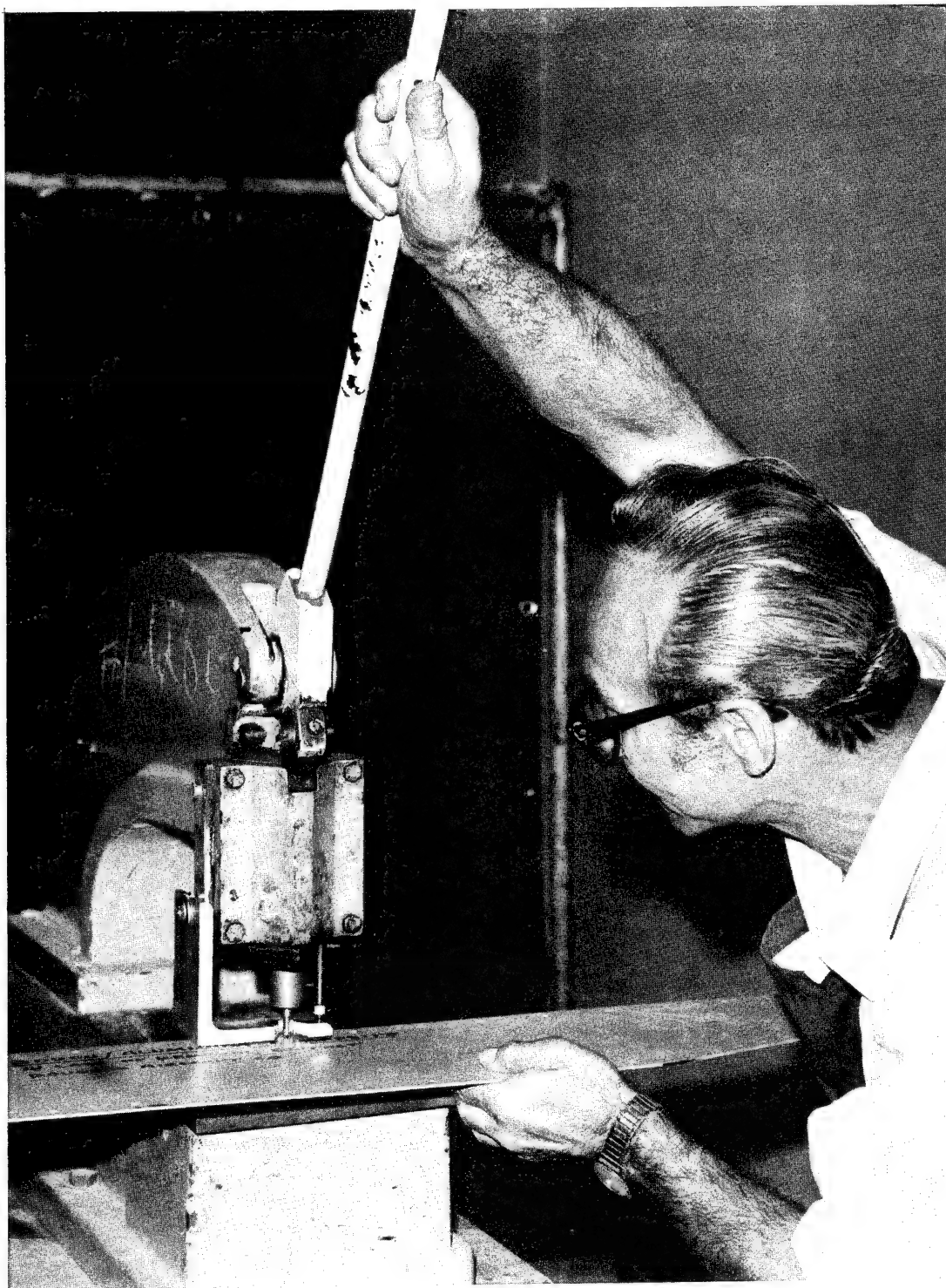


Figure 84    Punching Holes in Boron/Aluminum Skin

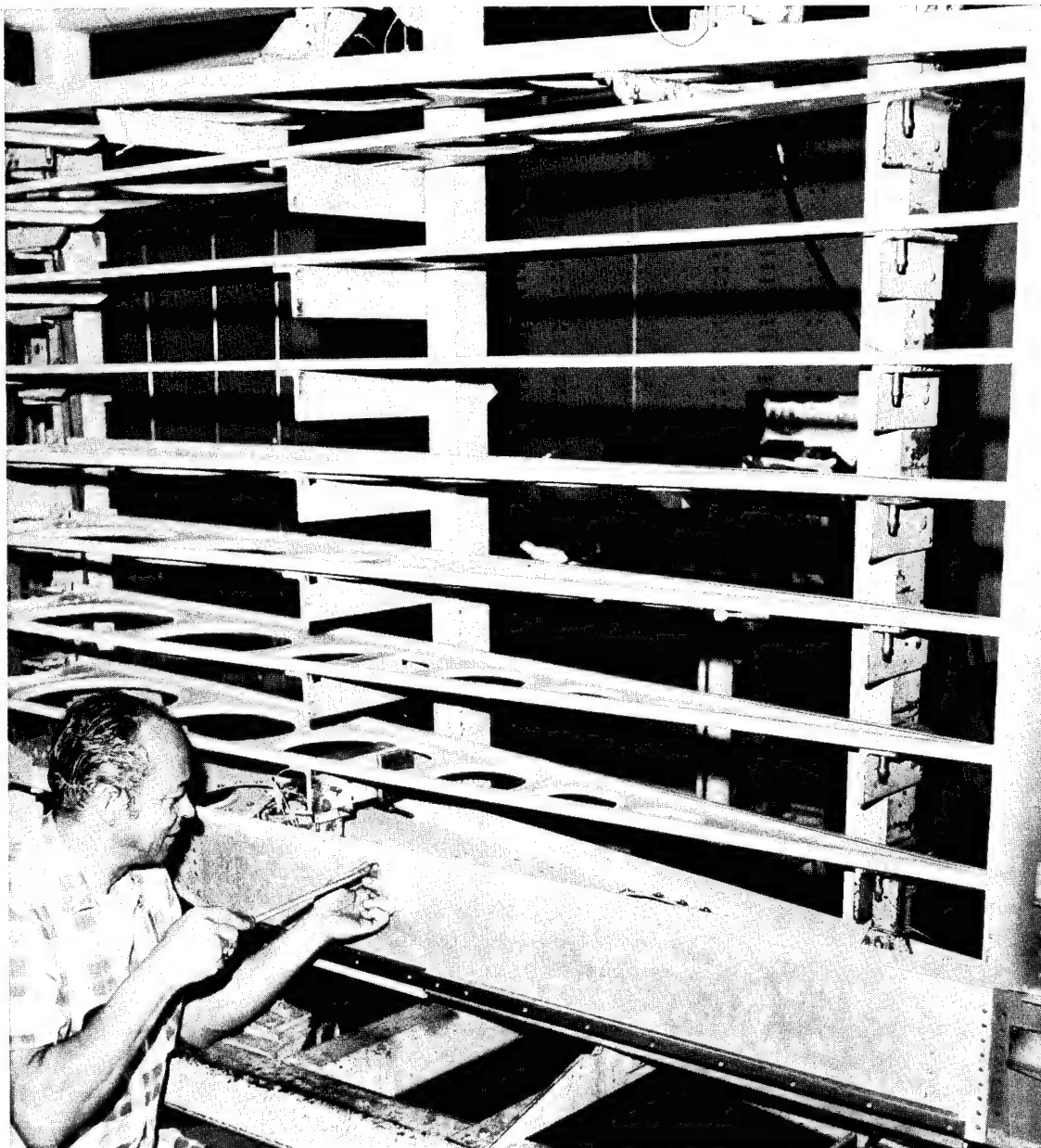


Figure 85 Installation of the Boron/Aluminum Skin Onto the Substructure

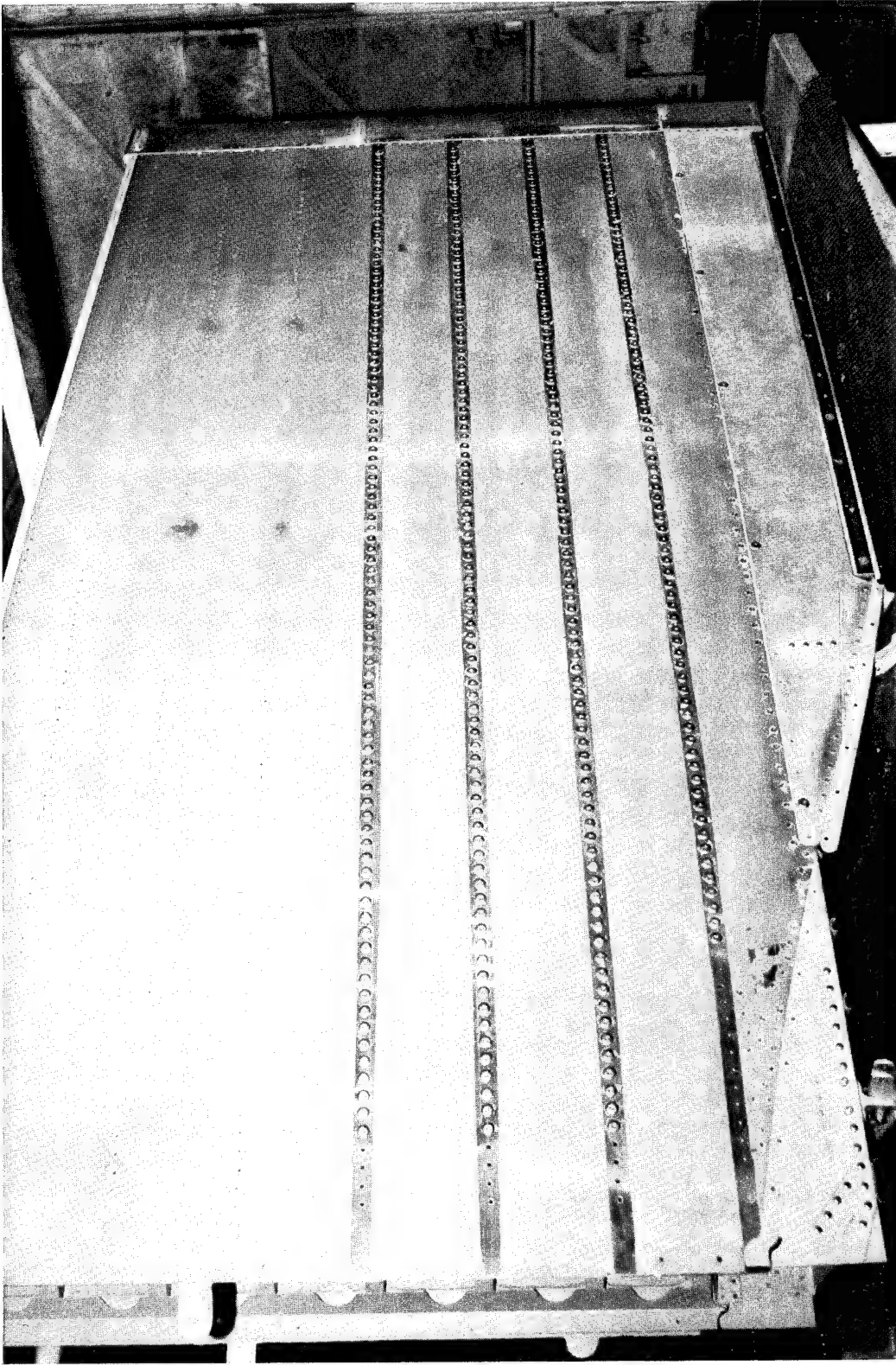


Figure 86 Installation of the Aluminum Upper Skins Onto the Substructure

APPENDIX A

MATERIAL PROCUREMENT DIFFUSION BONDED  
BORON/ALUMINUM COMPOSITE SHEETS

## APPENDIX A - MATERIAL PROCUREMENT DIFFUSION BONDED BORON/ALUMINUM COMPOSITE SHEETS

Material shall meet the following requirements:

### 1) Material

The material shall be furnished as composite flat sheet formed by diffusion bonding boron filaments and aluminum alloy foil such that the filaments are solidly embedded in the aluminum alloy matrix.

The boron filaments shall be 0.1422mm (0.0056 inch) diameter and shall meet the requirements of MMS-583, Class C. The aluminum alloy shall be 6061. The finished product shall be furnished in the as-fabricated condition.

### 2) Composition

The composition of the composite sheet shall be 45 volume percent (minimum) boron filament, the balance being aluminum alloy.

### 3) Composite Construction and Quantities

All panels shall be constructed such that the boron filaments are oriented as shown in Figure A1. All panels shall have a ply orientation pattern of 90°, 45°, 90°, 0°, -45°, 0°, -45°, 0°, 90°, 45°, and 90°. Ply orientations are defined in Figure A1 with the 90° orientation lying in a direction parallel to the fibers in the first ply.

Panels A through J (10 panels) shall consist of 11 total plies, and be 2.032mm (0.080 inch) thick.

### 4) Sizes

Panels A through F shall be 29.21 x 57.15cm (11 1/2 x 22 1/2 inch). Panels G through J shall be 172.72 x 20.32cm (68 x 8 inch). (NOTE: The 90° orientation is always parallel to the second dimension).

### 5) Filament and Ply Alignment

All filaments comprising a single ply shall be laid parallel one to another within one degree of the long axis of the ply.

All plies of a given orientation shall be laid down such that the fibers are parallel within one degree of the required nominal orientation. Cross-ply in the completed panel shall be oriented such that they are within one degree of the designated orientation.

6) Dimensional Tolerances

All dimensional tolerances shall be specified in FED-STD-245 as applicable to 6061 aluminum sheet.

7) Mechanical Properties

The material shall exhibit the following target mechanical properties:

	0° Orientation	90° Orientation
Tensile ultimate strength	393 MPa (57,000 psi)	503.3MPa (73,000 psi)
Tensile Modulus of Elasticity	162 GPa (23.5x10 <sup>6</sup> psi)	168.9 GPa (24.5x10 <sup>6</sup> psi)

Tests shall be conducted in either the 0° or 90° orientations, in accordance with ASTM E8. Rectangular specimens may be used in lieu of reduced section specimens. A minimum of two tests per pressing shall be conducted in order to certify that the target mechanical properties have been met. The test specimens shall be cut from the panels to be delivered. The test specimens representing Panels G, H, I, and J shall be tested in the 90° orientation. (NOTE: Material for performing these tests has not been included in the sizes shown in Figure A1 and therefore, the fabricated width would have to be greater to accommodate a row of tensile QC coupons).

8) Nondestructive Inspection

A through-transmission ultrasonic inspection shall be performed and a C-scan generated of two panels (each from separate pressing) from A through F by the supplier per attached instructions. Other inspections shall be performed as necessary by the supplier to ensure that the material complies with the workmanship requirements.

9) Identification

All panels shall be appropriately marked to indicate panel identification.

10) Workmanship Requirements

The material shall be of uniform quality and condition, free from exposed filaments, protruding filament ends, and burrs.

The surfaces shall be free from cracks, folds, wrinkles, laps, edge delaminations, foreign objects and other defects which would adversely affect the serviceability of the material. Light scratches, heat marks, indentations or other surface defects which can be removed without exceeding material specifications shall not be cause for rejection.

The material shall be essentially free from internal voids, delamination, crossed filament, filament misalignment and foreign matter.

## 11) Responsibility for Inspection and Testing

The supplier is responsible for the performance of all inspection and test requirements specified herein. The supplier may use his own facilities or any commercial laboratory acceptable to McDonnell Douglas Corporation. McDonnell Douglas Corporation reserves the right to repeat any or all of the inspections set forth herein and reject any material which does not conform to the prescribed requirements.

### NDI METHODS FOR A1/B PANELS

Ultrasonic C-Scan Inspection - Composite specimens shall be ultrasonically C-scanned for voids or delaminations. Immersion ultrasonic methods employing an X-Y bridge scanner and facsimile paper recorder shall be used. Inspection may be conducted at 5.0 to 10.0 MHz whichever is most applicable for the thickness of part being tested. Search units shall be short or medium focused elements, 1.27 to 1.91cm (1/2 to 3/4 inch) diameter. The panels are to be tested using through transmission plate methods. Panels should be as flat as possible prior to ultrasonic inspection. The amplitude of the ultrasonic signal shall be set to 80% of vertical saturation over the best area of each panel. The amplitude gate shall be set around the transmitted signal for through-transmission (ie; 40% amplitude or less). The mode shall be set so areas with amplitudes above 40% will record on the paper.

Place a reference marker (lead tape or steel button approximately 6.35mm (1/4 inch) diameter or X-ray penetrometer) on the upper left hand surface of the part to be tested so that the location of discontinuities in the part can be correlated with indications on the facsimile recordings, where the part dimensions preclude the scanning and recordings of the entire part in one C-scan recording, overlap reference markers shall be imaged on two adjacent C-scan recordings. The reference marker shall be in the same positions for both C-scan inspections.

C-scan facsimile recordings are to be shipped with specimens and are to be identifiable to each specimen. The specimen identification, date, inspection technique, and each unit size and frequency shall be indicated on the facsimile recording. Location of all reference markers shall also appear on the specimen surface.

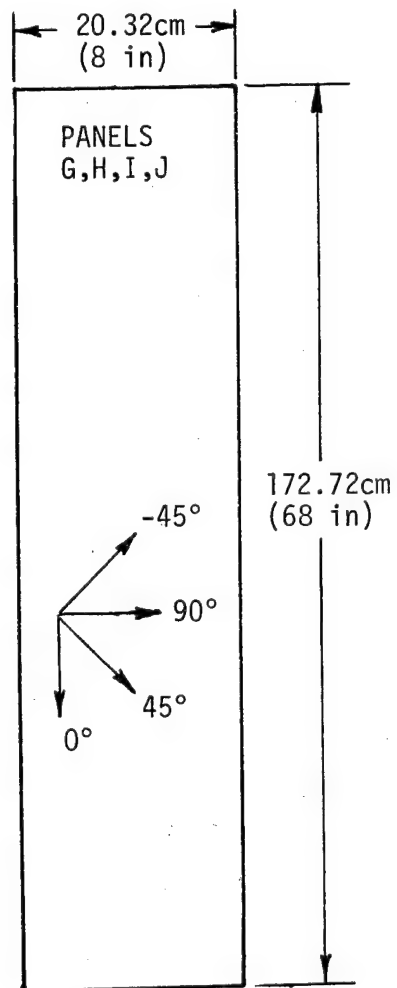
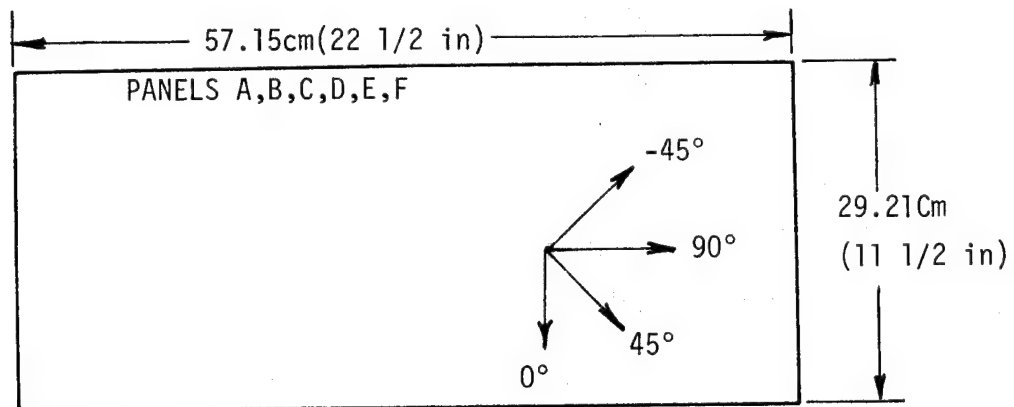
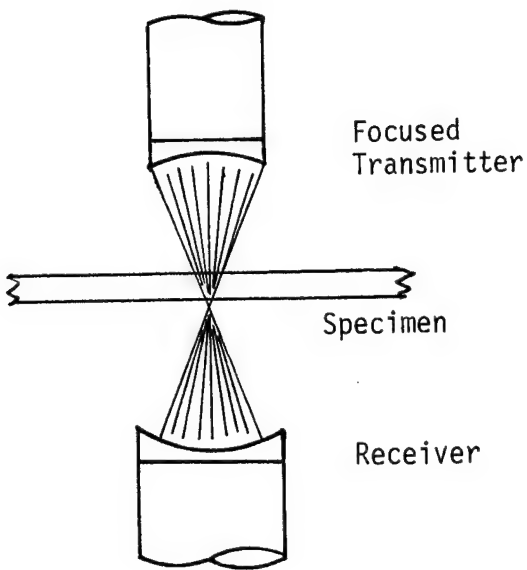
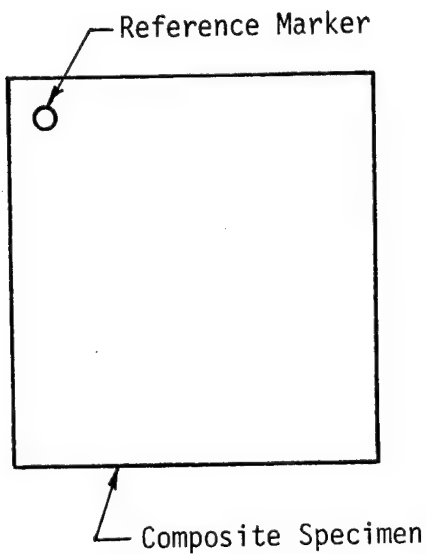
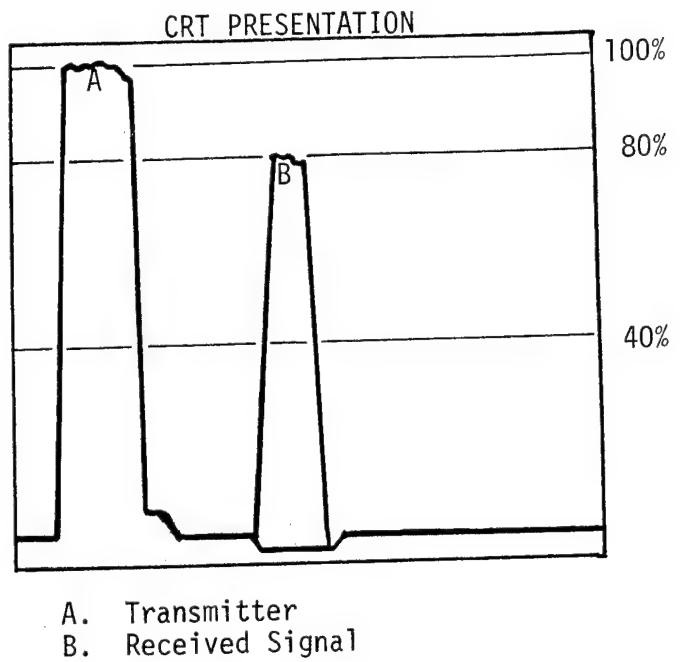


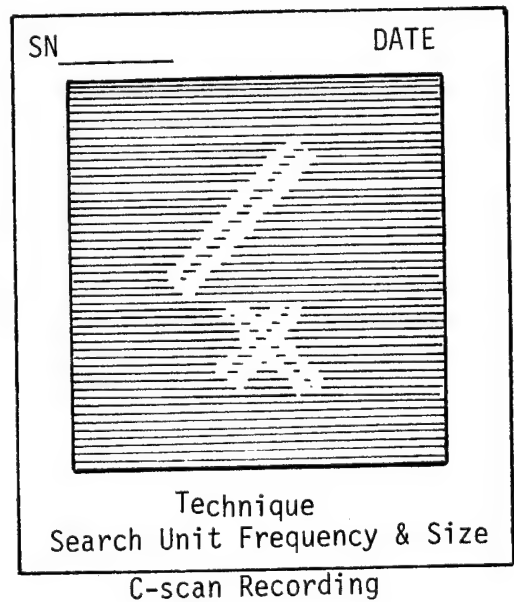
Figure A1 Panel Description



A. Thru-Transmission



Reference Marker  
Defects (50%  
Signal Loss)



B. Part and Representative C-scan  
Recording, Ultrasonic C-scan  
Inspection of Composite Specimens

APPENDIX B

DPS 3.67 - 67 HOLE PREPARATION

AND TRIMMING OF BORON/ALUMINUM

DOUGLAS PROCESS STANDARD  
DPS 3.67-67 HOLE PREPARATION  
AND TRIMMING OF BORON/ALUMINUM

A. SCOPE AND USE

This Process Standard provides the instructions and requirements for preparation of attachment holes and edge trimming of boron/aluminum composite sheet. It shall be used only when specified on Engineering Rework Drawing AVB7129.

B. APPLICABLE SPECIFICATIONS

DPS 3.02 - Identification of Parts and Assemblies  
DPS 4.025- Dissimilar Materials Protection  
DPS 4.710- Minimum Fabrication Practices for Metals

C. MATERIALS AND SPECIAL EQUIPMENT

DPM NO.	MATERIAL NAME	SPECIFICATION OR PRODUCT SOURCE
5126	Paper Abrasive Silicon Finishing Fastcut Finishing Paper	Carborundum Company Los Angeles, Ca (1)
5417	Lubricant, DAC Lube Stick	Kerns United Company
5739	Lubricant Metalworking Oil, Cut, Solvent, Cimcool Five Star	Cincinnati Milling Products Div, Los Angeles, Ca
-	Tap Magic Cutting Fluid	The Steco Corporation Little Rock, Ar
-	Punches-HSS Steel, with Prick Tip	DAC Stock Items
-	Reamers-HSS Multiple Flute Reamers	DAC Stock Items
-	Punch Press-Diacro #2 Bench Press, Manually Operated, with Punch Adapter-Whitney-Jensen "Junior" Hand Punch	DAC Stock Items

(DPM's are Douglas stock numbers for internal company use only).

FOOTNOTE: (1) Contact Douglas buyer for alternate approved products or sources.

D. HOLE PREPARATION REQUIREMENTS

- Holes shall be punched (maximum material thickness 2.286mm(.090 in) to final size with a Diacro #2 bench press, manually operated, with punch adapter or Whitney-Jensen "Junior" hand punch.
- To minimize hole distortion and allow the boron fibers to shear free of burrs, punch shall be manually operated rather than machine driven to slow down punch speed.

#### D. Continued

3. Punches shall be checked frequently for wear. To minimize wear, apply DAC lub stick (DPM 5417) around the outer periphery of entry point on the male die.
4. Holes that are undersize due to punch wear can be reamed to final size with multiple flute type reamers.
5. Punches shall be kept sharp to prevent undersize holes and protruding burrs.
6. Tap magic cutting fluid shall be applied on reamer when holes necessitate reaming.
7. Reamer shall be operated at 350 to 500 rpm. A continuous 50-65cm/min (20-25 in/min) feed rate shall be applied during the ream operation to reduce premature dulling of reamer.
8. Edge of holes (protruding burrs) shall be deburred with silicone-carbide paper or a steel mill file.
9. Refer to DPS 4.025 for dissimilar materials protection.

#### E. EDGE TRIMMING REQUIREMENTS

1. Trimming shall be accomplished with a diamond impregnated cutting wheel, operated at 1500 to 2000 rpm. Do not operate at slower speeds.
2. Metalworking lubricant (DPM 5739) shall be mixed at a ratio of one part lubricant to 30 parts water and shall be used to flood the wheel/work interface to prevent heat build-up and diamond sparking.
3. Part to be trimmed shall be set-up within the milling machine coolant tray. Coolant must be contained within the tray to avoid abrasive injury to machine sliding surfaces. Clamp part down to prevent distortion.
4. Appearance of as-trimmed edges should be clean and not exceeding maximum of 0.762mm (0.030 inch) protruding burrs on both top and bottom edges. Burrs shall be removed with a mill type file. (Reference DPS 4.710). Burrs protruding above 0.762mm (0.030 inch) indicates wheel is not cutting properly, and work should be corrected.
5. To retain material identification, parts shall be labeled immediately after edge trim per DPS 3.02.

APPENDIX C

MANUFACTURING PLAN FOR  
BORON/ALUMINUM AFT PYLON SKIN  
AVB7097-30

## Fabrication and Assembly of Boron/Aluminum Aft Pylon Skin AVB7097-30

### General Plan

A skin of 6Al-4V titanium is presently used on production DC-10 aircraft in the aft pylon structure over the #2 engine. The skin is subjected to high temperatures during service. The object of this program is to substitute a skin of boron/aluminum material for the titanium to determine the long-term effects of actual service conditions on the boron/aluminum. The skins will be removed from the aircraft after five years of service for analysis and evaluation. A total of four parts will be fabricated, with one part installed on each of three separate production DC-10 aircraft and one part sent to NASA as a spare.

The intent of the Manufacturing Plan is to provide an outline of fabrication and assembly steps similar to the planning papers normally used at Douglas but with further explanation about correct techniques and tools required to produce the parts.

### General Machining and Hole Preparation

Boron/aluminum composite material requires special cutting and hole preparation processing to produce high quality components with maximum strength potentials. These mechanical operations have been documented in a Douglas Process Standard (DPS 3.67-67) and Manufacturing Engineering-Research and Development memos. The most important aspects of cutting and hole preparation are summarized as follows:

- 1) All cutting of boron/aluminum shall be accomplished with the Accurate Diamond Tool Company, sintered diamond slotted wheel operating at a minimum of 1524SMPM (5000 SFPM) (1500 rpm for 35.56cm (14 inch) diameter wheel). The wheel/work interface shall be flooded with Cimcool 5 Star coolant at approximately 30:1 water-coolant concentration.
- 2) As the products of the cut are extremely abrasive, the special coolant pumping system, work piece holding tray and the tooling department #8 horizontal mill have been designated for boron/aluminum use exclusively.
- 3) Hole generation shall be accomplished by punching to full-size using special punches in the Manufacturing Development Center with the Diacro #2 manual punch press. All punches have a conical tip to pick up transfer punch indentations for accurate hole locations. High speed steel (HSS) reamers shall be used on the boron/aluminum to bring hole diameters to drawing requirements when less than 0.127mm (0.005 inch) undersize. A lubricant such as Tap Magic shall be used during reaming operations.

### Fabrication of Skin AVB7097-30

- 1) Boron/aluminum sheet 2.032mm (0.080 inch) thick, 20.32 x 172.72cm (8 x 68 inch) long shall be supplied by outside sources to the Manufacturing Development Center. This material shall be completely diffusion bonded and ready for layout and subsequent trimming to final net dimensions. An existing steel template, AFB70972-29,-30, shall be used to mark part

profile and to locate all attachment holes by transfer punching through 6.35mm (0.250 inch) diameter tooling holes. Light scribe lines shall be made through prussion blue marking dye to provide guidelines for trimming without damaging the part.

- 2) Each part shall be cut in the horizontal mill using the impregnated diamond wheel specified previously. Dowel pins positioned on the cutting bed plate shall be used as stops to align cut edges accurately, maintaining continuity on interrupted cuts. A total of four straight cuts shall be made on each part. The corner radius shall be generated by hand grinding the part to scribe lines using a silicone-carbide wheel.
- 3) The modified Diacro manual punch has been setup with full-sized punches and dies sized with 0.051mm (0.002 inch) diameter clearance. The work-piece shall be placed under the punch so transfer punch indentations can be aligned with the conical tip on the punch. Every hole shall be produced with a lubricated punch which reduces friction and prevents aluminum build-up on the punch.
- 4) Burrs on the exit side of the hole shall be removed by lightly touching the hole edge with a diamond impregnated reamer with 90° included angle bevels on the reamer end. Reamer speed shall be 400-500 rpm.
- 5) After edge trimming and hole punching, the part will be ready for fabrication inspection prior to installation on the aircraft subassembly.

#### Assembly Procedures

- 1) The boron/aluminum skin shall be positioned on the titanium substructure and clamped in place. Preliminary tooling holes shall be drilled along the periphery of the skin from previously punched holes. Drill bushings fitted into the full-size attachment holes in the boron/aluminum skin shall be used to assure accurate alignment of holes. Standard Cleco clamps shall be installed to secure the skin to the substructure during drilling of pilot holes in the titanium details.
- 2) Number 30 pilot holes shall be drilled into the titanium from each of the skin holes, using the boron/aluminum skin as a drill template.
3. The boron/aluminum skin shall then be removed from the titanium substructure. All holes shall be opened to full-size per drawing requirements by drilling and reaming with conventional tools.
- 4) The skin shall be repositioned on the substructure and mechanical attachments shall be installed from the forward end of the structure working aft.

The boron/aluminum skin (LH side) shall be installed on the substructure before the RH side titanium skin to permit accessibility for nut installations. The standard RH titanium skin (AVB7097-29) shall then be installed per normal production practice.

- 5) AVB7097-30 is fabricated as a flat skin. The pylon assembly has a slight curvature to which the skin will conform. No separate forming operations shall be performed.